Physics Copy **B-31**

WT-1454

OPERATION
PLUMBBOB

NEVADA TEST SITE

MAY–OCTOBER 1957

Project 30.7

TEST OF GERMAN UNDERGROUND PERSONNEL SHELTERS

CIVIL EFFECTS TEST GROUP
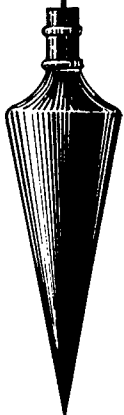
20011105 053

NOTICE

This report is published in the interest of providing information which may prove of value to the reader in his study of effects data derived principally from nuclear weapons tests.

This document is based on information available at the time of preparation which may have subsequently been expanded and re-evaluated. Also, in preparing this report for publication, some classified material may have been removed. Users are cautioned to avoid interpretations and conclusions based on unknown or incomplete data.

Hot Topic Documents

1. homeland defense

2. terrorism

3. anti-terrorism

4. urban warfare

5. chemical warfare

6. biological warfare

7. middle east

8. etc.

Report to the Test Director

TEST OF GERMAN UNDERGROUND PERSONNEL SHELTERS

By

Edward Cohen

and

A. Bottenhofer

Approved by: H. J. JENNINGS
Director
Program 30

Approved by: R. L. CORSBIE
Director
Civil Effects Test Group

Ammann & Whitney
New York, New York
July 1960

ABSTRACT

The objective of Project 30.7 was to investigate the predicted behavior of German underground personnel shelters, equipment, and certain instrumentation. Data obtained will be used for evaluation and improvement of present design criteria.

Nine reinforced-concrete underground shelters, designed by German engineers, were tested at the 170-, 155-, 110-, 78-, 26-, 11.5-, and 7.2-psi overpressure ranges as determined from average blast-line instrumentation measurements.

Reinforcing steel, doors, and ventilation equipment were received from West Germany and were incorporated in the shelters.

Preshot and postshot precise location surveys were made to determine the total lateral and vertical motions of the structure as a result of the blast.

Blast instrumentation used in the shelters and entranceways consisted of U. S. Wiancko pressure gauges, Carlson earth-pressure gauges, Ballistic Research Laboratories (BRL) self-recording pressure gauges, and dynamic pressure gauges. Free-field measurements were recorded along the blast line using U. S. self-recording and electronic pressure gauges and German self-recording pressure gauges. Structural response was recorded by BRL deflection and acceleration gauges, SR-4 strain gauges, and Waterways Experiment Station scratch gauges.

Radiation measurements were taken using U. S. gamma-radiation film dosimeters, gamma-radiation chemical dosimeters, neutron detectors, telemetering gamma dosimeters, and German gamma chemical dosimeters.

Mice were used as biological specimens in environmental tests in seven of the nine structures tested. In addition to the environmental tests, a series of tests was performed in the nine structures to check for the possible occurrence of dust in the shelters as a consequence of nuclear explosions.

Ground shock spectra were recorded under Project 1.9 for free field conditions and for the interior of a shelter.

An experiment was included to investigate the transmission of ground shock acceleration to a simulated body. This test recorded the shock-absorbing characteristics of a commercial product (Ensolite) manufactured by the United States Rubber Company.
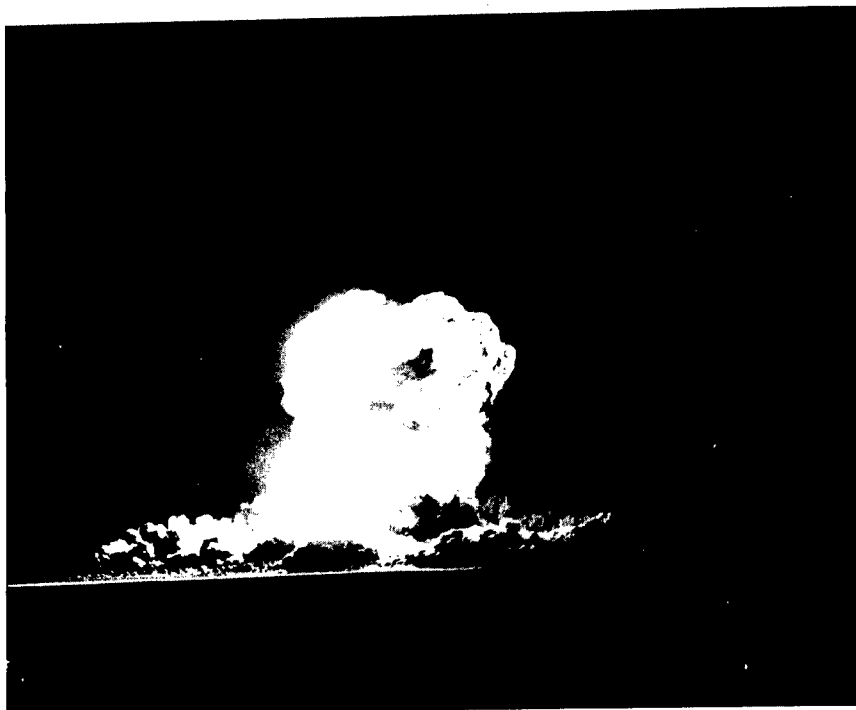
PREFACE

The policy of the U. S. Government of furnishing the governments of friendly nations with unclassified information on nuclear effects, through NATO and elsewhere, has led to the participation of the West German Government, acting through their U. S. representatives, in the 1957 Nevada continental test series, Operation Plumbbob, at the Nevada Test Site. The invitation to participate in the test was extended by the Federal Civil Defense Administration (FCDA) in response to a request from the West German Government. Their participation was correlated by, and under the sponsorship of, FCDA.

Test information will be made available to the West German Government in accordance with the procedures and limitations imposed by the security regulations of the United States Atomic Energy Commission (USAEC). It was expected that the information obtained would be of interest and value also to the FCDA and other agencies of the U. S. Government.

The West German Government engaged the firm of Ammann & Whitney, Consulting Engineers, as their agent to pursue the outlined program to its completion here in the United States. The services of Ammann & Whitney included developing the contract drawings and maintaining liaison with FCDA, including financial arrangement, allocating and arranging for equipment to measure blast pressure, radiation and structural response, receiving the equipment from Germany and arranging for its shipment to the Test Site, providing field supervision during construction, and inspecting and reporting the test results in accordance with USAEC and FCDA requirements.

Edward Cohen, senior author, was in charge of the work for Ammann & Whitney and served as Project Officer. Anton Bottenhofer served as Assistant Project Officer.

The structures of Project 30.7, which consisted of nine German shelters, were tested in the Smoky shot of Operation Plumbbob at 5:30 a.m. on the morning of Aug. 31, 1957. The device used was a 43-kt nuclear device mounted on a 700-ft steel tower. The test was located in area T2C of Yucca Flats at the Nevada Test Site.

ACKNOWLEDGMENTS

CONTENTS

CONTENTS (Continued)

CONTENTS (Continued)

ILLUSTRATIONS

CHAPTER 1

ILLUSTRATIONS (Continued)

ILLUSTRATIONS (Continued)

ILLUSTRATIONS (Continued)

ILLUSTRATIONS (Continued)

ILLUSTRATIONS (Continued)

ILLUSTRATIONS (Continued)

TABLES

TABLES (Continued)

Chapter 1

INTRODUCTION

1.1 OBJECTIVE

The main objective of this test was to observe the behavior under blast conditions of protective structures of German design built with German materials to determine the relative efficiency of different types of construction and to obtain information for the improvement of these structures and the development of design criteria for future protective structures.

Data on strains, deflections and deformations, pressures, soil displacements, and radioactivity were obtained from German instrumentation and from extensive supplemental instrumentation provided by U. S. agencies. Physical characteristics and structural behavior were determined by observation and inspection.

1.2 GENERAL INFORMATION

1.2.1 Scope

This project included three types of underground cast-in-place concrete personnel shelters: (1) type A rectangular shelter, designed for an overpressure of 132 psi; (2) type A cylindrical shelter, designed for 132 psi, and (3) type C rectangular shelter, designed for 14.7 psi.

Nine structures were built, four type A rectangular shelters, two type A circular shelters, and three type C rectangular shelters.

The architectural drawings of the shelters are shown in Figs. 1.1 to 1.3.

1.2.2 Location

The shelters were constructed at the following predicted peak overpressure levels:

1 type A rectangular (designated RAa)   264.6 psi.
1 type A rectangular (designated RAb))
1 type A circular (designated CAa)   } 198.5 psi.
1 type A rectangular (designated RAc))
1 type A circular (designated CAb)   } 132.3 psi.
1 type A rectangular (designated RAd)   88.2 psi.
1 type C rectangular (designated RCa)   29.4 psi.
1 type C rectangular (designated RCb)   14.7 psi.
1 type C rectangular (designated RCc)   7.4 psi.

See Fig. 1.4 for maximum recorded overpressures.

1.2.3 Orientation

The entrances of the structure were oriented as shown in Fig. 1.4. This orientation placed the direction of the entrance stairs radial to Ground Zero (GZ). It was expected that this orientation would provide minimum reflected pressures on the main blast door.

1.3 DESCRIPTION OF STRUCTURES

1.3.1 Type A Rectangular

The type A rectangular shelter is designed for 25 persons. The general over-all dimensions are 13 ft 9 in. wide by 35 ft 5 in. long by 11 ft $5\frac{1}{2}$ in. high. The shelter consists of the entrance stairs and ramp, a vestibule, the main shelter body, an exit chamber, an emergency-exit tunnel, a vertical exit shaft, and a ventilation shaft (Figs. 1.5 to 1.12).

The entrance consists of a 4-ft 7-in.-wide stair on one side and a ramp on the other, each ramp being 19 ft 8 in. long and leading to a common landing in front of the shelter (Figs. 1.5 to 1.7). The stairway and ramp walls and slabs are $11\frac{3}{4}$ in. thick. Entrance from the landing into the vestibule is through a 2-ft $10\frac{1}{2}$-in. by 6-ft $1\frac{3}{4}$-in. opening, which is closed on the exterior side by means of a steel arch type blast door.

The vestibule, 6 ft $6\frac{3}{4}$ in. by 4 ft 11 in. by 7 ft $6\frac{1}{2}$ in. high, provides an air lock for entry into the main chamber (Fig. 1.8). Entrance is through a 2-ft $10\frac{1}{2}$-in. by 6-ft $1\frac{3}{4}$-in. opening, which is closed by a gastight fire door..

The main body of the shelter has a floor area 9 ft 10 in. by 13 ft $1\frac{1}{2}$ in. and is 7 ft $6\frac{1}{2}$ in. high (Figs. 1.9 to 1.11). The walls, floor slab, and roof slab are 1 ft $11\frac{1}{2}$ in. thick. The roof slab has a 4-ft earth cover for radiation protection.

An emergency exit is provided through an exit chamber at the opposite end of the shelter. The exit chamber is entered through a 2-ft $1\frac{3}{4}$-in. by 2-ft $9\frac{1}{2}$-in. gastight fire door. The chamber is 2 ft $11\frac{1}{2}$ in. by 3 ft $3\frac{1}{4}$ in. by 7 ft $6\frac{1}{2}$ in. high. Access from the exit chamber into the emergency-exit tunnel is through a 2-ft $1\frac{3}{4}$-in. by 2-ft $9\frac{1}{2}$-in. opening provided with a blast door on the exterior side. This tunnel, 7 ft long, has a cross section of 2 ft $7\frac{1}{2}$ in. by 5 ft 3 in., with $11\frac{3}{4}$-in.-thick walls, roof, and floor slab. It leads to a vertical shaft, 2 ft $7\frac{1}{2}$ in. square with $11\frac{3}{4}$-in.-thick walls, which provides access to grade above.

Adjacent to the exit chamber is a 4-ft 11-in.-square reinforced-concrete air-intake stack (Fig. 1.12), extended to a grade level. This stack provides filtered air for the protected ventilation system of the structure, which normally operates during blast conditions.

The filtered-air system was not placed in operation during this test.

1.3.2 Type A Circular

The type A circular shelter consists of a protected entranceway, a vestibule, the main body of the shelter (25 persons), an exit chamber, and a combination emergency exit and ventilation shaft (Figs. 1.13 to 1.20).

The over-all length of the cylinder is 44 ft $7\frac{1}{2}$ in. The vestibule and the main chamber are of circular cross section, with an interior radius of 4 ft $1\frac{1}{4}$ in. and 1-ft $3\frac{3}{4}$-in.-thick walls (Figs. 1.13 and 1.14). Radiation protection is provided by 5 ft 3 in. of earth cover over the shelter.

The shelter is entered by means of a covered stair with $11\frac{3}{4}$-in.-thick walls, stair slab, and roof slab (Fig. 1.15). Entrance into the vestibule is through a 2-ft $10\frac{1}{2}$-in. by 6-ft $1\frac{3}{4}$-in. steel arch type blast door (Figs. 1.16 and 1.17). Entrance from the vestibule to the main chamber is through a 2-ft $10\frac{1}{2}$-in. by 6-ft $1\frac{3}{4}$-in. gastight fire door. At the rear of the shelter, the exit chamber can be entered through a 2-ft $1\frac{3}{4}$-in. by 2-ft $9\frac{1}{2}$-in. gastight fire door, and from this chamber access is made to the exit shaft through a 2-ft $1\frac{3}{4}$-in. by 2-ft $9\frac{1}{2}$-in. blast door (Fig. 1.18). Exit to the grade above is provided by this shaft, which has $11\frac{3}{4}$-in.-thick walls and a 2-ft $\frac{1}{2}$-in.-square opening at the top, which is closed by a steel cover or grating (Figs. 1.19 and 1.20).

Adjacent to the exit shaft is the filtered-air intake chamber (Fig. 1.18), which provides protected ventilation during blast conditions.

1.3.3 Type C Rectangular

The type C rectangular shelter (25 persons) is also of reinforced concrete. The over-all dimensions, excluding the emergency tunnel, are 20 ft 4 in. by 17 ft $8\frac{1}{2}$ in. by 6 ft $6\frac{3}{4}$ in. high.

The shelter consists of the double entranceway (ramp and stair) leading to a common landing, the entrance vestibule, the main body, the exit chamber, and the emergency-exit tunnel and exit shaft (Figs. 1.21 to 1.27).

The entrance stair and ramp are similar to those of the type A rectangular shelter (Figs. 1.5 to 1.7). Entrance into the vestibule is through a 2-ft $10\frac{1}{2}$-in. by 6-ft $1\frac{3}{4}$-in. blast door. The vestibule is 4 ft $3\frac{1}{4}$ in. by 3 ft $3\frac{1}{2}$ in. by 6 ft $6\frac{3}{4}$ in. (Fig. 1.22). Entrance from the vestibule into the main chamber is through a 2-ft $7\frac{1}{2}$-in. by 6-ft $6\frac{3}{4}$-in. opening (no fire door is provided for this type structure).

The main chamber is 10 ft 6 in. by 13 ft $1\frac{1}{2}$ in. by 6 ft $6\frac{3}{4}$ in. high (Figs. 1.22 to 1.25). The walls, floor slabs, and roof slab are $11\frac{3}{4}$ in. thick. Radiation protection is provided by 3 ft of earth cover.

An opening (with no door) at the rear of the shelter provides access to the 4-ft $3\frac{1}{4}$-in. by 3-ft $3\frac{1}{2}$-in. exit chamber, from which entrance can be gained to the 7-ft-long emergency-exit tunnel through a 2-ft $1\frac{3}{4}$-in. by 2-ft $9\frac{1}{2}$-in. blast door (Fig. 1.26). The emergency tunnel has a cross section of 2 ft $7\frac{1}{2}$ in. by 5 ft 3 in., with $11\frac{3}{4}$-in. thick walls and slabs.

Exit from the end of the tunnel to the grade above is through a 2-ft $7\frac{1}{2}$-in.-square vertical shaft, which is closed by a hinged cover or grating to prevent debris from falling into the shaft.

Adjacent to the exit chamber is the filtered-air intake chamber, which is 4 ft $3\frac{1}{4}$ in. by 2 ft $7\frac{1}{2}$ in. by 6 ft $6\frac{3}{4}$ in. high. Figure 1.27 is the above-ground view of the combination emergency-exit and air-intake shaft.

1.3.4 Ventilation

The ventilation for all three types of shelters is similar. Although the structures were designed for the use of two systems (natural and filtered air), only the filtered-air system was provided in this test. With this system the air enters the four 2-in. pipes passing through the air-intake stack at the ground surface. The air passes down and through a 3-ft 4-in. depth of double-washed coarse sand. The filtered air is then pumped into the main chamber of the structure by a manually or electrically operated air pump located 3 ft $7\frac{1}{2}$ in. above the floor slab (Fig. 1.24). In the shelters that have a gastight door between the main chamber and antechamber (type A, rectangular and circular), the foul air is exhausted at the entrance end of the main chamber by a manually operated exhaust valve (Figs. 1.8, 1.9, and 1.13). Once the foul air is in the vestibule (antechamber), it is removed from the structure by means of an overpressure flap valve through the exterior wall into the entranceway.

The quantity of air entering the shelter can be regulated during either manual or electrical operation. A calibrated flowmeter indicates to an operator the quantity of air passing through the pump. When the flow indicator is held steady at its center position, the quantity being drawn in is 750 liters/min. A flow greater than this exceeds the functional capacity of the coarse-sand filter.

For electrical operation of the air pump, assuming the speed of the motor to be constant, the quantity of air is manually regulated by a hinged throttling valve. When the air pump is operated manually, the throttling valve is placed in the fully open position (Auf), and the quantity of air is regulated by the person turning the handle.

In the fully closed position (Zu), the throttling valve and cast-iron pump case do not seat perfectly and some leakage is possible. However, this leakage is of no consequence since the valve is used only as a means of regulating the quantity of air passing through the pump.

During the test all throttling valves were left fully open. The manually operated exhaust valves in the four type A rectangular and two type A circular shelters were left open 1 cm. All overpressure flap valves operated freely and were in a closed position for the test.

1.3.5 Doors

The main blast doors of the structures are of two types. The main entrance doors of the type A rectangular and the type A circular shelters consist of a plate curved inward with tubular members across to act as struts to take the compressive forces when the curved plates of the door are put into tension by the blast loads (Figs. 1.16 and 1.17).

The second type blast door, used for the main entrance of the type C shelter and a smaller size for the emergency exits of all the structures, is a flat plate with horizontal stiffeners (Fig. 1.26).

Although placed at various pressure levels, the blast doors for the type A rectangular and the type A circular structures were designed for an overpressure of 220 psi. The blast doors for the type C rectangular structure were designed for an overpressure of 66 psi. The vertical and horizontal emergency-exit blast doors were designed for 147 and 13 psi, respectively.

The fire doors are made of two flat plates, with a fire-resistant material between (Fig. 1.8). The whole assembly is $1\frac{1}{8}$ in. thick. These doors were previously tested to resist a temperature of 1100°C for a period of 2 hr.

All doors, both blast and fire, are made gastight by rubber-tubing gaskets.

Recesses left in the concrete to receive the frame anchorages permitted the installation of the door frames after the structural concrete was placed. Doors were manufactured by Mannesmann-Stahlblechbau, West Germany.

1.4 THEORY

The German shelters were designed by German engineers in accordance with German codes[1] and criteria.[2,3] To duplicate, to as great a degree as possible, the conditions that would prevail for structures constructed in Germany, the specifications and drawings were developed in accordance with German construction practices. The reinforcing bars, ventilation equipment, and doors were shipped to the Nevada Test Site from West Germany. A shortage of reinforcing bars developed during construction, and comparable U. S. steel was substituted.

The structures were designed for static loading conditions. The equivalent loads assumed were equal to one-third the peak incident overpressure and were considered to be uniformly distributed on the exterior walls, roof, and floor slabs so as to cause maximum working stresses. The working loads considered in the design are given in Table 1.1.

The minimum material specifications and allowable design stresses were as follows:
Concrete: f_c, 4260 psi (cube strength); and f_c, 1420 psi (allowable design stress).
Steel: minimum yield stress, 31,300 psi; ultimate stress, 47,500 to 71,200 psi; minimum elongation before breaking, 15 per cent; and allowable design stress, 20,000 psi.

The structures were designed for either an 80-kt device at an explosion height of 1550 ft or a 5-Mt device at a height of 4140 ft. (A postshot dynamic analysis of the roof slab of shelter RAa is included as Appendix C of this report.)

The thickness of earth cover above the roof slab of the main shelter was so proportioned that the attenuated radiation present in the structure was equal to 25 r. The attenuation factor used in the design was computed from "Effects of Atomic Weapons."[4]

REFERENCES

1. German Code of Standards, D.I.N. 1045.
2. Herman Leutz, Aufgaben des baulichen Luftschutzes, Ziviler Luftschutz, December 1956.
3. Herman Leutz, Grundsätzliches zu den Richtlinien fur Schutzraumbauten, Bundes Baublatt.
4. Samuel Glasstone (Ed.), "The Effects of Atomic Weapons," Superintendent of Documents, U. S. Government Printing Office, Washington, D. C., 1950.

TABLE 1.1—DESIGN LOADS

	Peak overpressure, psi	Equivalent static loads	
		Direct load, psi	Rebound, psi
Type A, rectangular	132.5	44	5
Type A, circular	132.5	44	5
Type C, rectangular	14.7	5	1.7
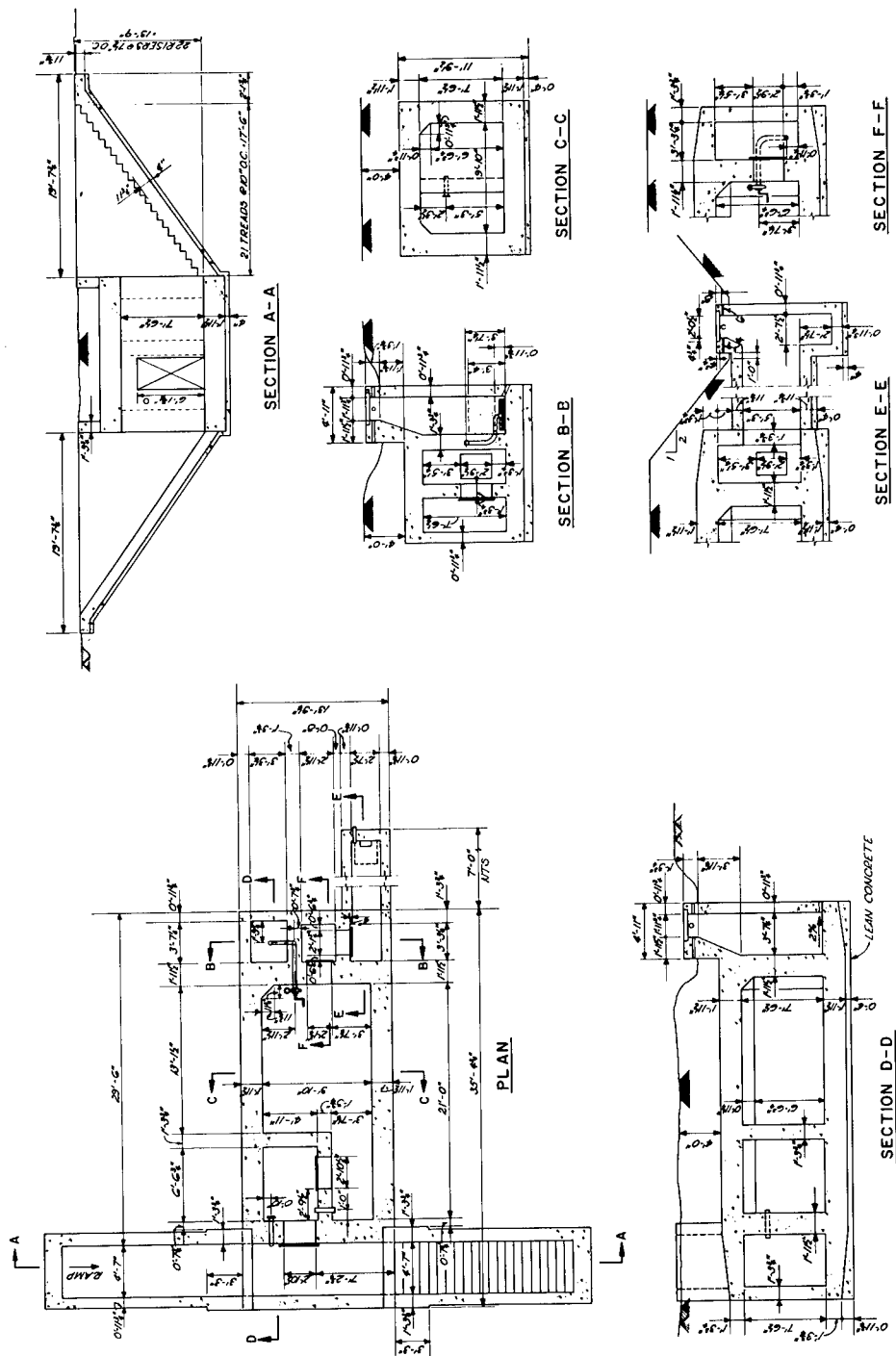
Fig. 1.1— Architectural layout for type A rectangular shelter.
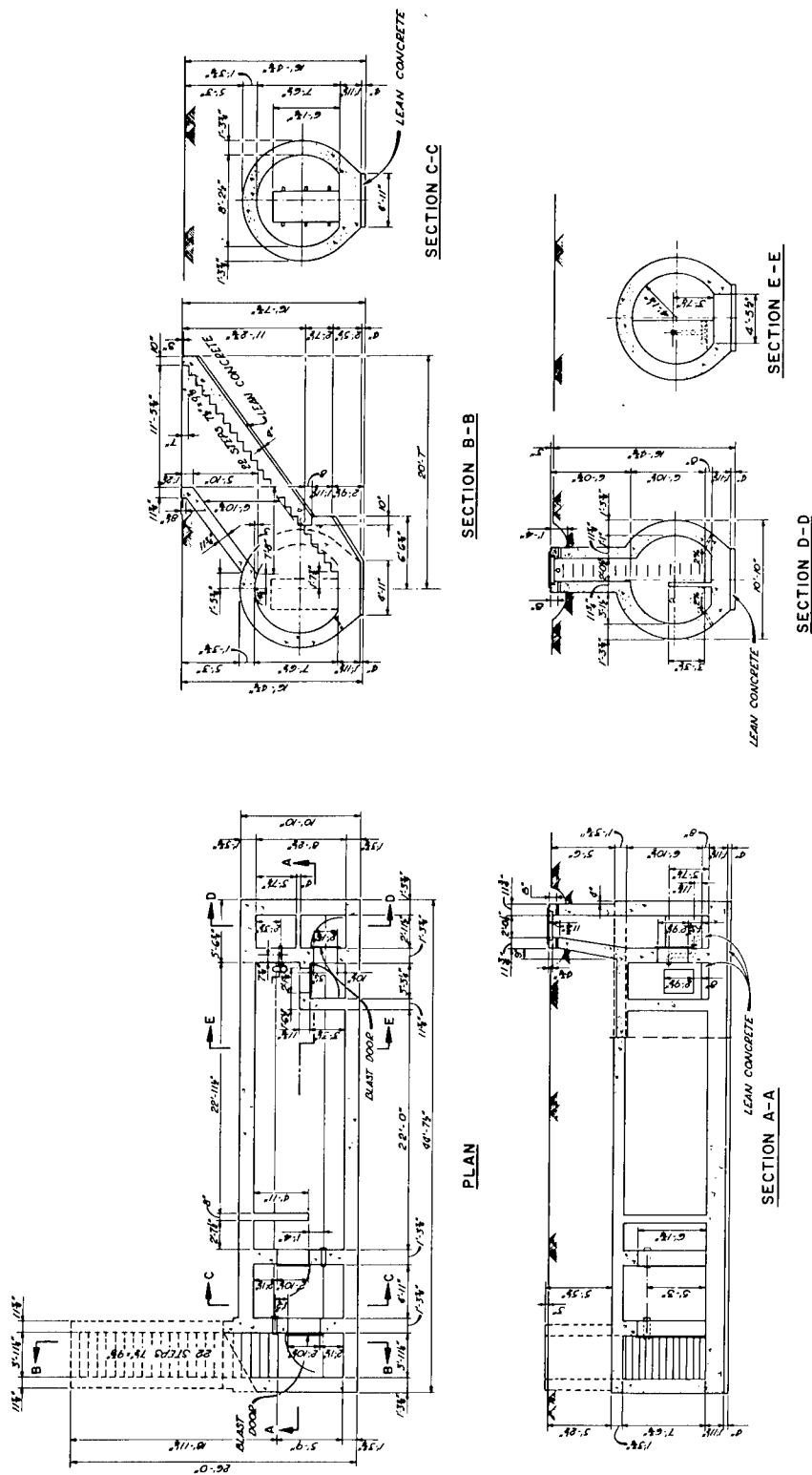
Fig. 1.2—Architectural layout for type A circular shelter.

Fig. 1.3—Architectural layout for type C rectangular shelter.
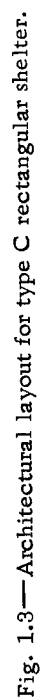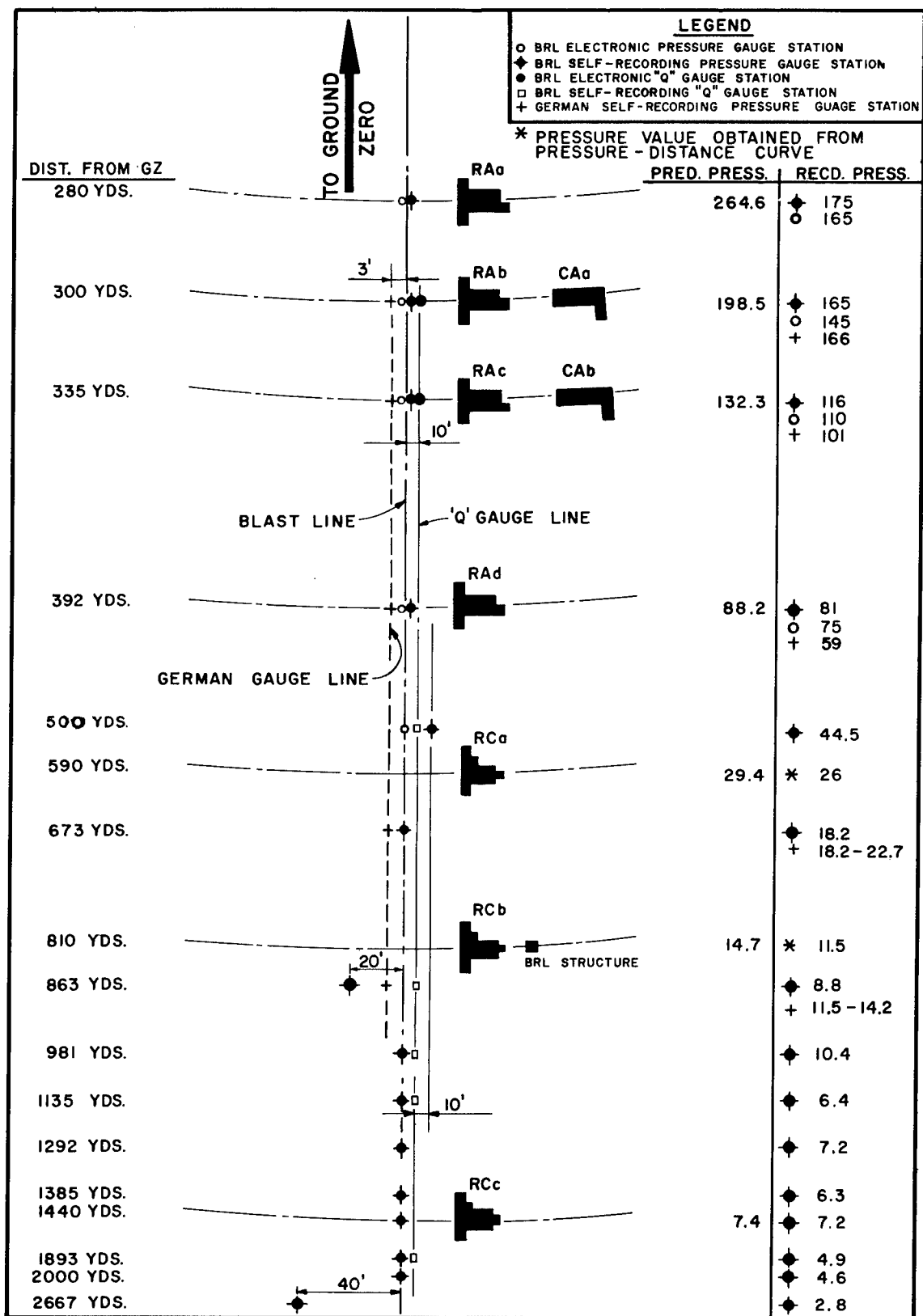
Fig. 1.4—Location and orientation of structures, project 30.7.
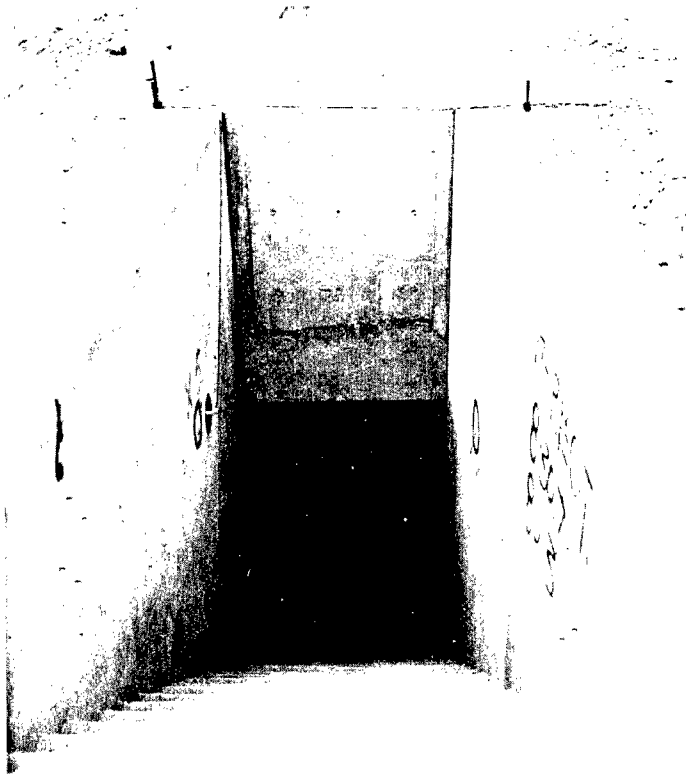
Fig. 1.5 — Entrance facing away from GZ (structure RA).
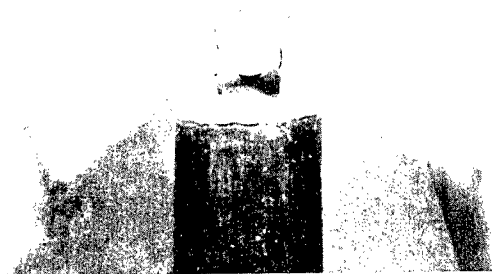
Fig. 1.6 — Entrance facing GZ (structure RA).
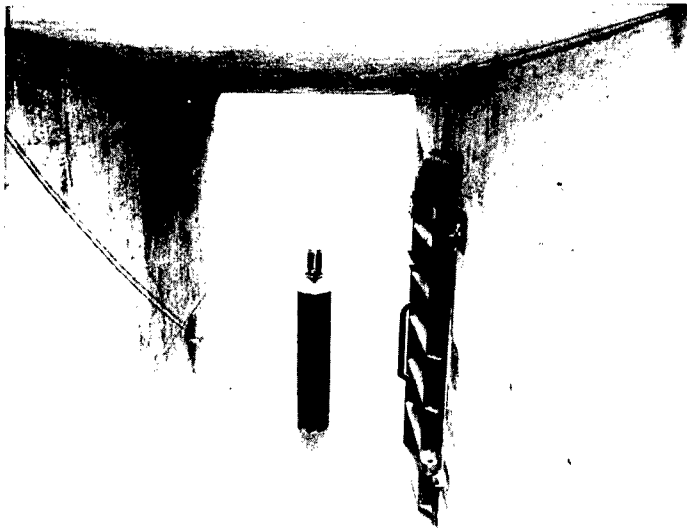
Fig. 1.7—Entrance landing (structure RA).
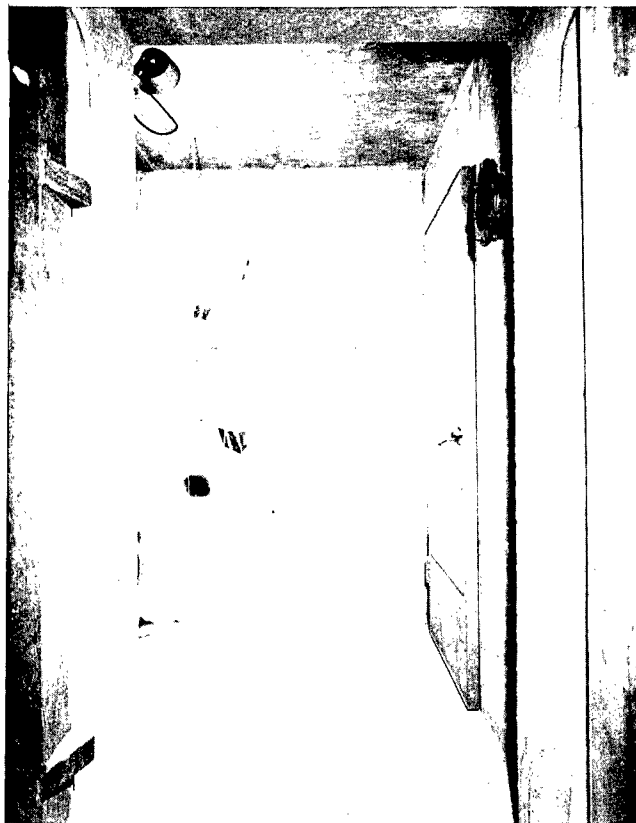
Fig. 1.8—Vestibule (structure RA).
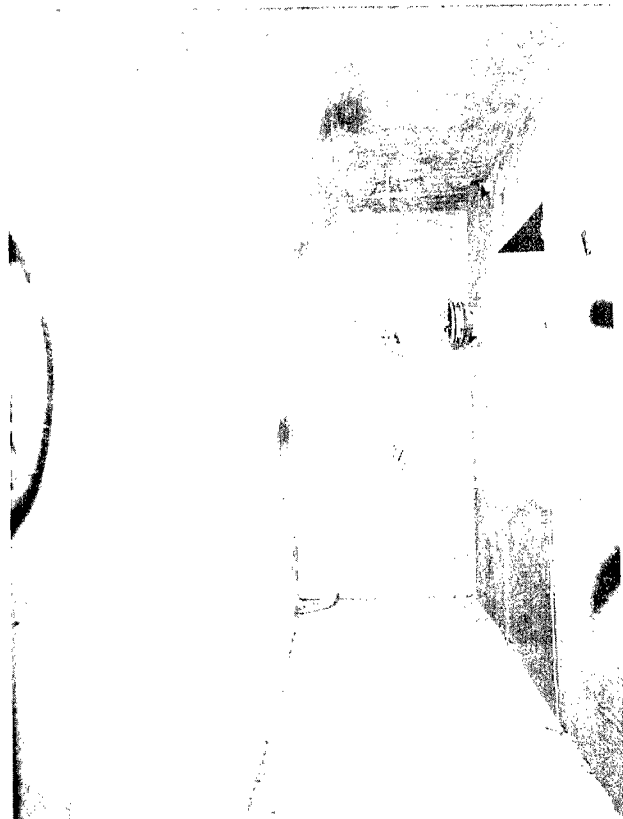
Fig. 1.9—Main chamber adjacent to vestibule (structure RA).
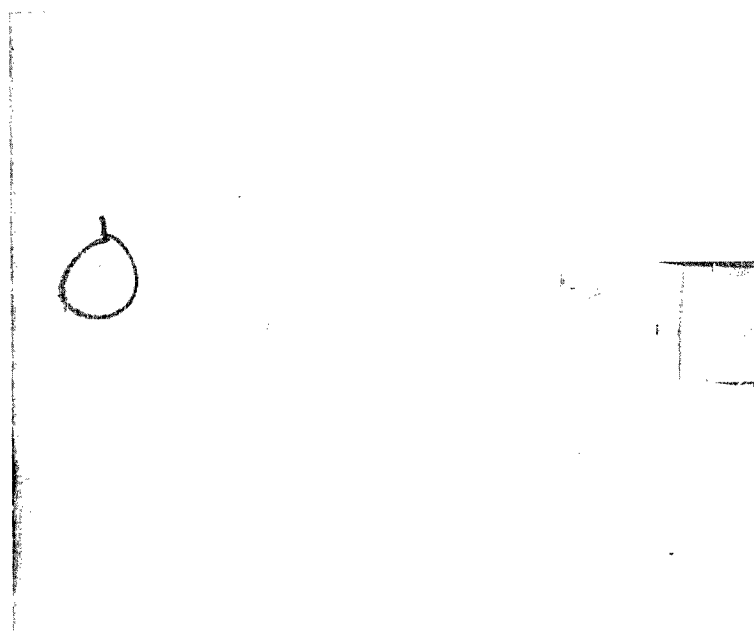
Fig. 1.10—Main chamber (structure RAd).

Fig. 1.11—Main chamber (structure RAb).
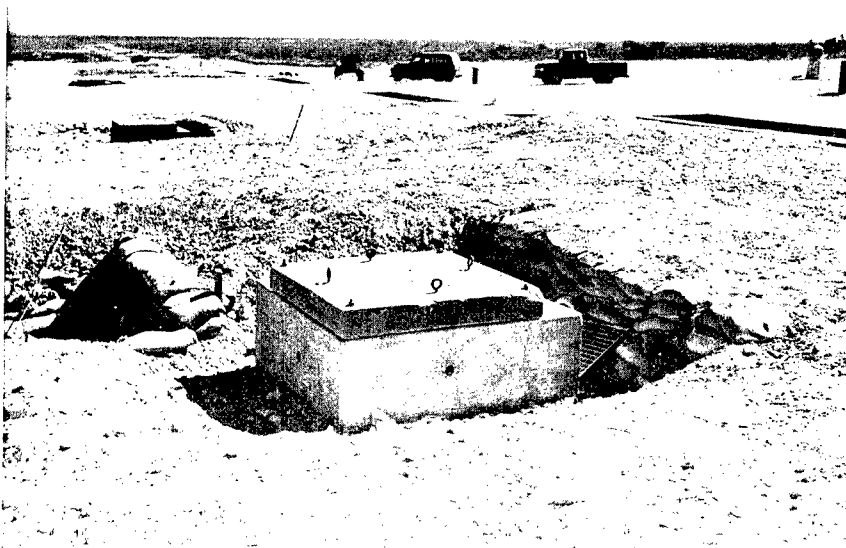
Fig. 1.12—Above-ground section of vent stack (structure RA).

Fig. 1.13—Looking into main chamber from vestibule (structure CA).
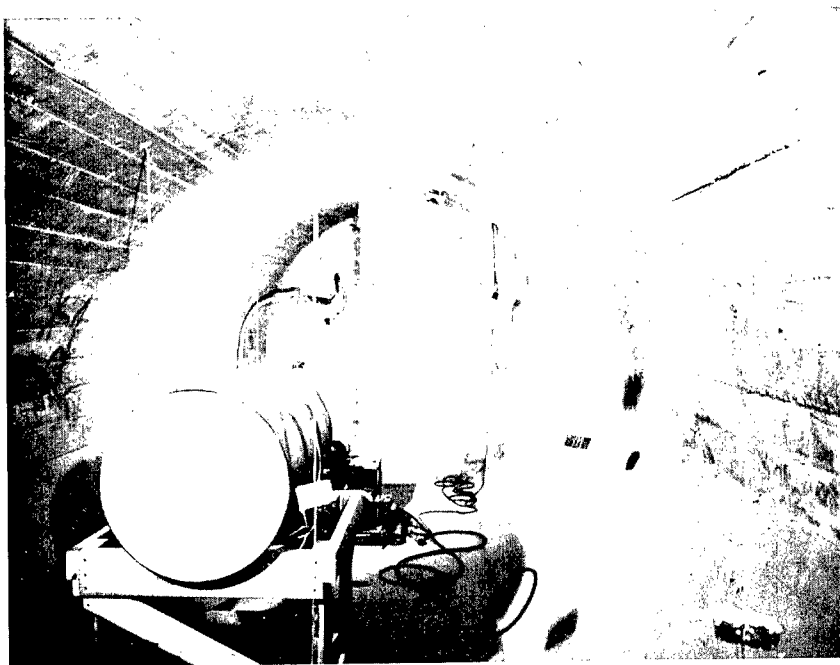
Fig. 1.14—Forward view of main chamber (structure CA).
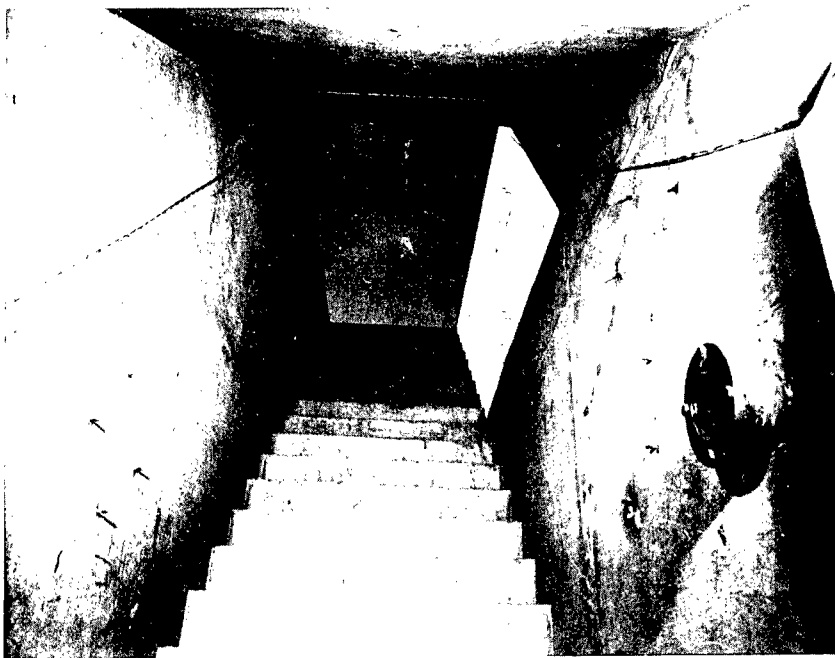
Fig. 1.15—Main entrance (structure CA).

Fig. 1.16—Interior view of main blast door (structure CA).

Fig. 1.17—Exterior view of main blast door (structure CA).
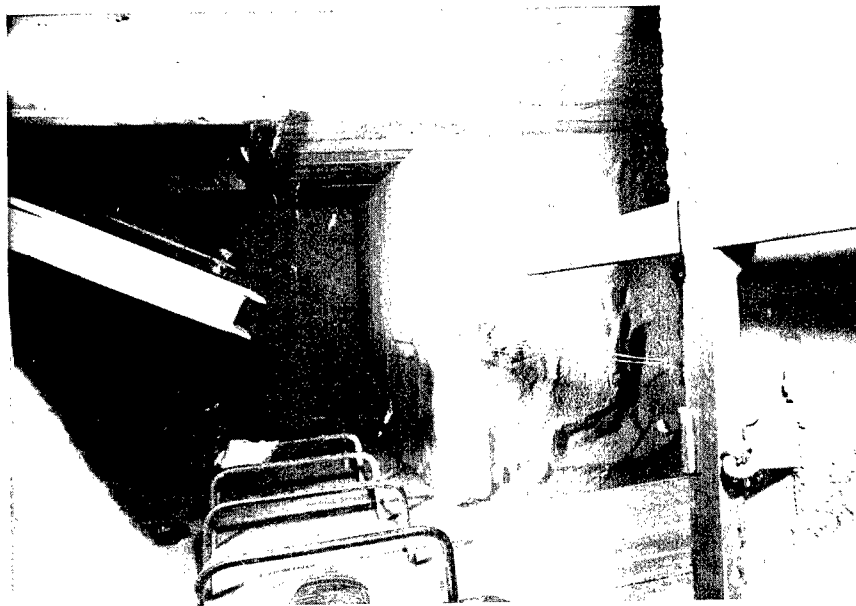
Fig. 1.18—Emergency exit blast door (structure CA).

Fig. 1.19—Emergency exit shaft (structure CA).
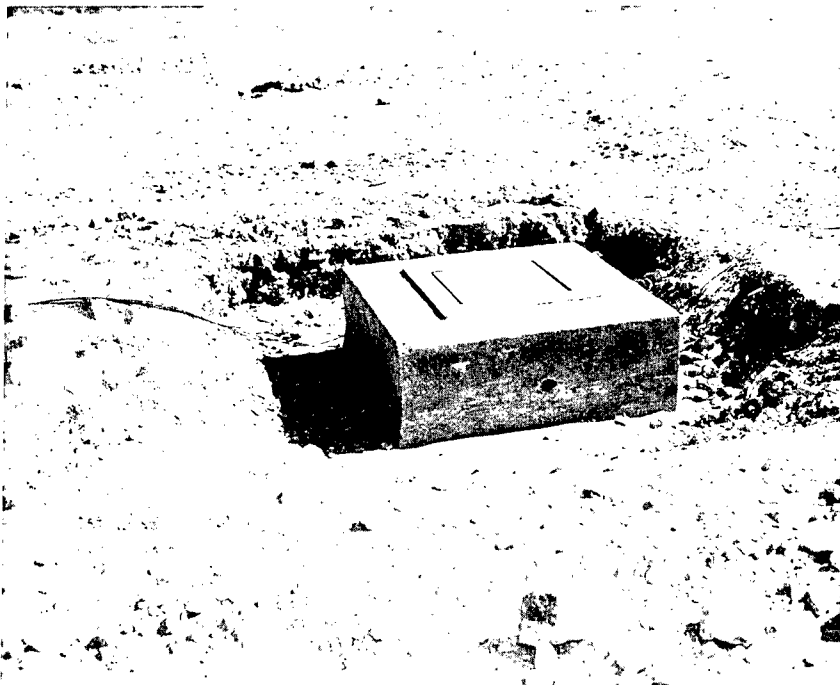
Fig. 1.20—Above-ground section of exit shaft (structure CA).

Fig. 1.21—Vestibule (structure RC).
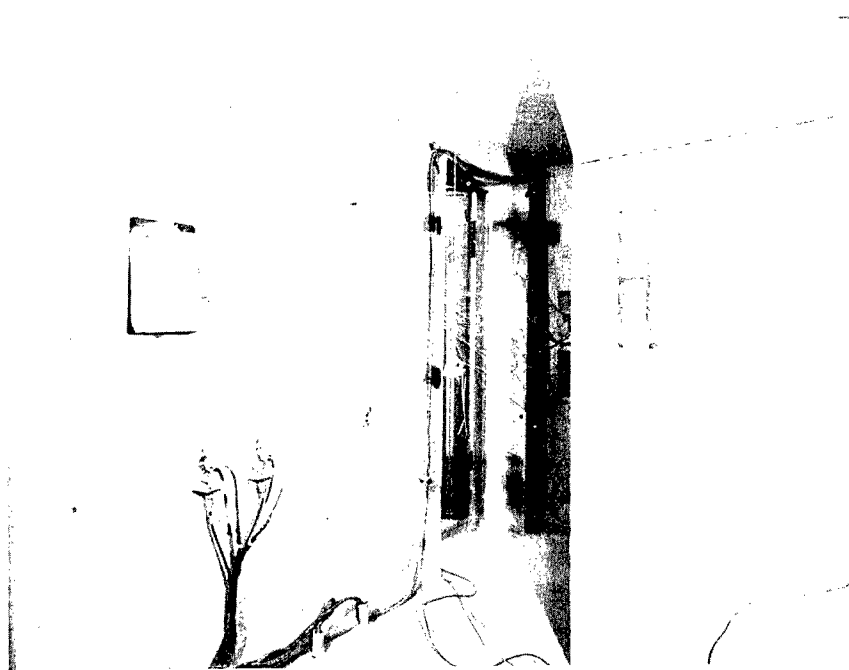
Fig. 1.22—Interior view of vestibule (structure RC).
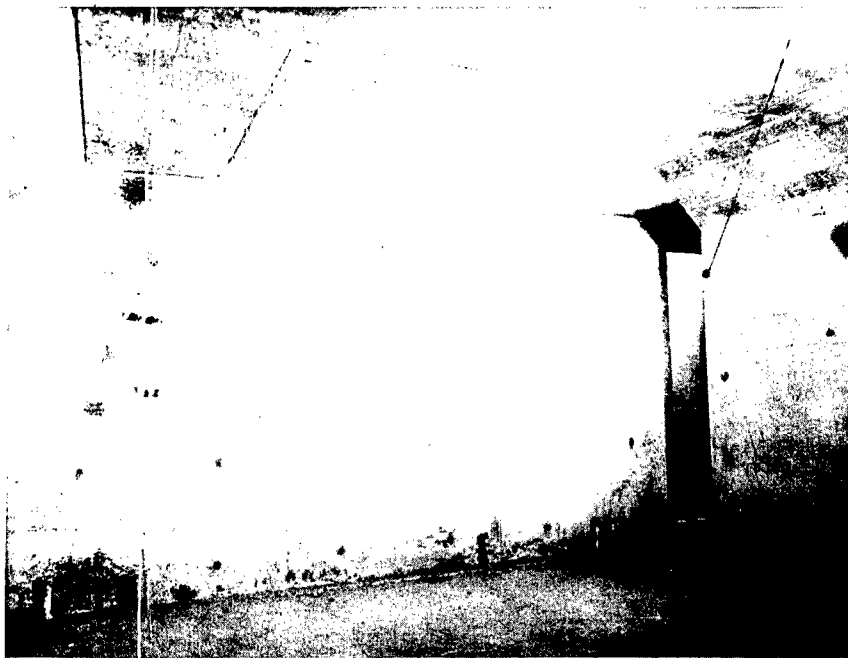
Fig. 1.23—Forward view of main chamber (structure RC).

Fig. 1.24—Rear view of main chamber (structure RC).
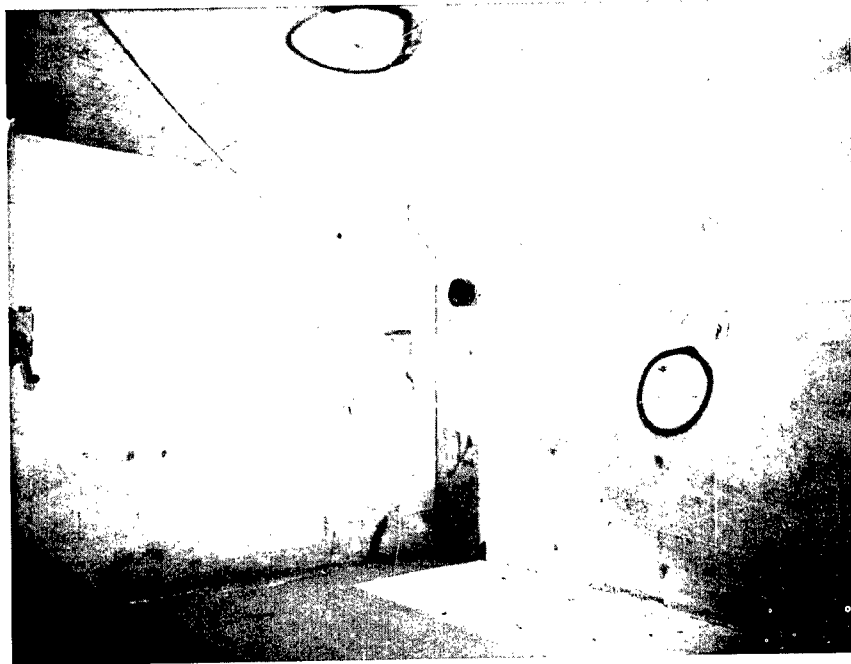
Fig. 1.25—Rear view of main chamber (structure RC).
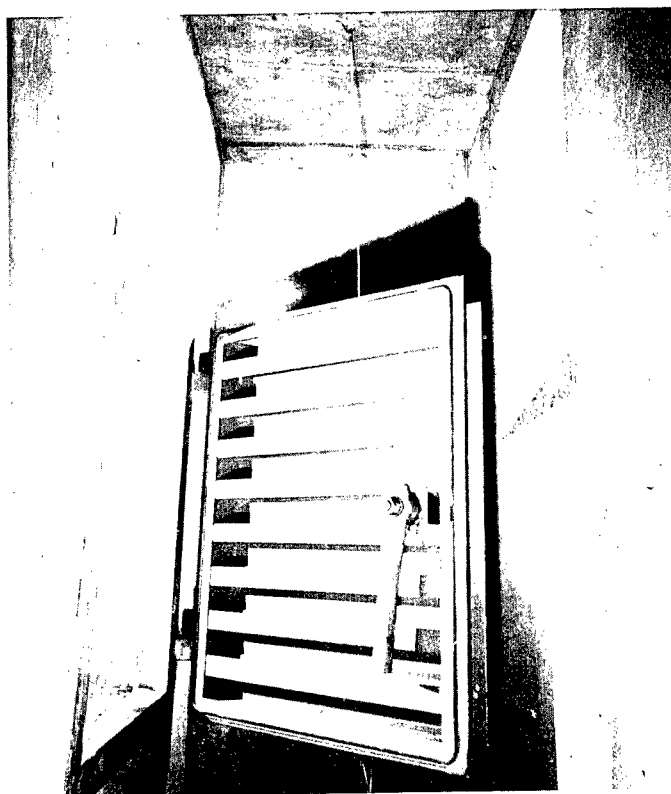
Fig. 1.26—Emergency-exit blast door (structure RC).
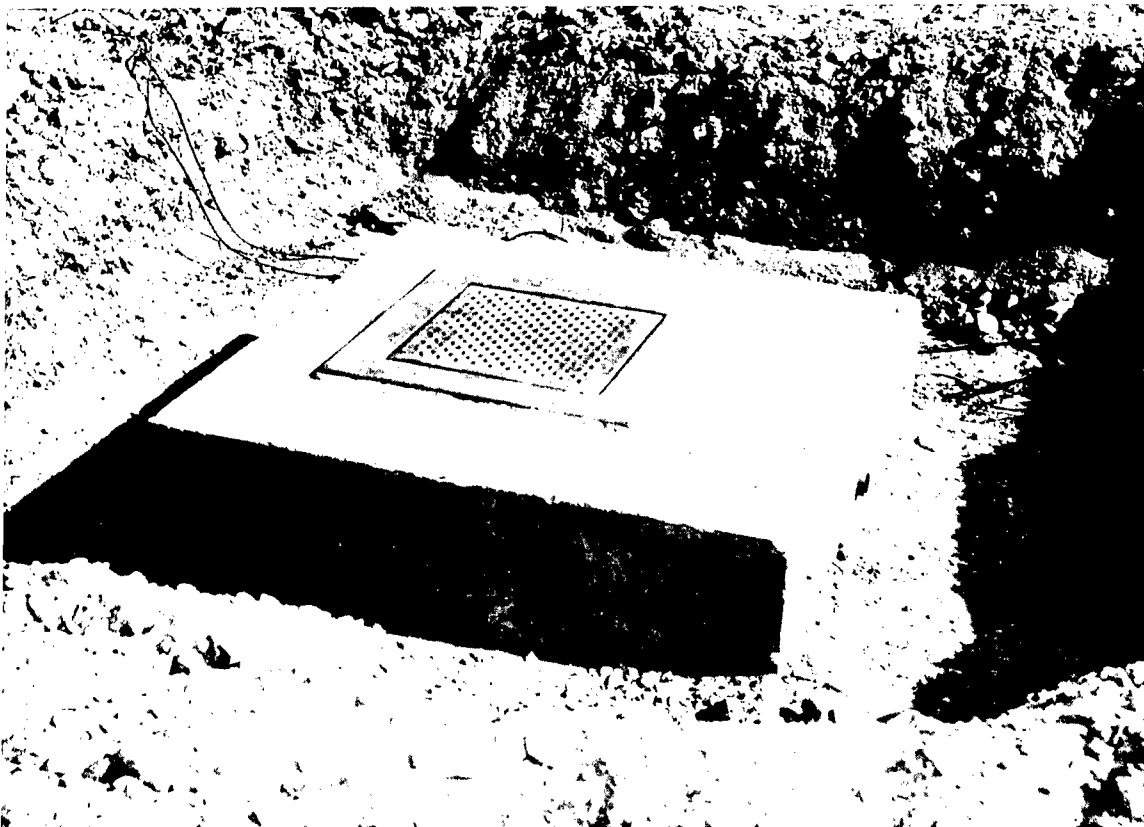
Fig. 1.27—Above-ground view of the emergency-exit shaft and vent stack (structure RC).

Chapter 2

PROCEDURE

2.1 SURVEYS

Preshot and postshot high-order field surveys of the horizontal and vertical coordinates of survey points, designated Y_1, Y_2, etc., were required to allow a determination of the absolute and relative lateral and vertical movements of the structures during the blast.

A second set of survey points, X_1, X_2, etc., was located in the structures to allow a determination of the relative lateral or horizontal movement of component parts of the structures.

The locations of these survey points are shown in Figs. 2.1 to 2.3.

2.2 INSTRUMENTATION

2.2.1 General

The major portion of the instrumentation used in the structures of Project 30.7 was U. S. equipment. The U. S. instrumentation, as provided by the Federal Civil Defense Administration (FCDA), recorded blast pressure, radiation, and structural-response variations. In addition to this equipment, supplemental pressure instrumentation supplied by the West German Government was incorporated in the test.

2.2.2 U. S. Pressure Instrumentation

The U. S. pressure instruments installed in the structures of Project 30.7 consisted of Wiancko electronic pressure gauges, Carlson electronic earth-pressure gauges, Ballistic Research Laboratories (BRL) self-recording pressure-time gauges, and BRL electronic and self-recording dynamic pressure gauges. The pressure instrumentation was installed in the structures by members of Project 30.5c.

The number, type, and location of the pressure instrumentation are tabulated in Table 2.1, and locations are shown in Figs. 2.4 to 2.12.

In addition to the instrumentation in the structures, U. S. blast-line pressure data are available for determining both the free-field surface overpressures and the dynamic pressures to which the structures were subjected.

The blast-line instrumentation and the maximum overpressures recorded are indicated in Fig. 1.4.

The instrumentation description and test results have been extracted from the Project 30.5c report, WT-1536, and are more fully described therewith.

2.2.3 German Pressure Instrumentation

Five self-recording pressure gauges, supplied by the West German Government, were used in the test. These gauges were so positioned along the blast line that their postshot results could be checked by U. S. instrumentation. The locations of the German gauges and corresponding U. S. gauges are shown in Fig. 1.4.

2.2.4 Structural Response

Structural response of the structures was recorded by BRL displacement and acceleration gauges and SR-4 strain gauges. These gauges were provided by FCDA and were installed by Project 30.5c.

Scratch gauges, supplied by the FCDA, were also used to determine relative deflections of structure RAa. The gauges consisted of two separate sections of metal tubing, each having a steel base and a universal-joint connection between the tubing and the base. One tube was of a larger diameter than the second. The smaller tube was placed inside the larger section, which had a pointer-spring type assembly mounted on it. A mark was inscribed on the smaller of the two tubes when there was a differential settlement between the bases of the gauge. The length of the scratch indicated the amount of deflection of the member on which the gauge was mounted.

The locations of the structural-response instruments are tabulated in Table 2.1 and shown in Figs. 2.4 to 2.12.

2.2.5 Radiation Instrumentation

Radiation measurements were made with U. S. gamma-radiation film dosimeters, gamma-radiation differential chemical dosimeters, and neutron detectors and with gamma-radiation differential chemical dosimeters supplied by the West German Government. Also included for gamma-radiation measurements were two dual-unit telemeters. One of the units was placed in structure RAc, and the other was located on the blast line at a predicted pressure level of 88 psi. The telemetering instruments act as remote radiation detectors, transmitting gamma-time records to a central receiving station.

Five gamma-radiation differential chemical dosimeters were placed along the blast line (Fig. 1.4) as a part of the radiation program.

The installation of all radiation-recording instruments, including the German equipment, was performed by Projects 30.5c, 39.9, and 39.1a.

The placement of the radiation-detection equipment in the structures is shown in Fig. 2.13.

2.3 GROUND SHOCK SPECTRA

2.3.1 General

Displacement spectra of ground shocks produced by nuclear devices, from which the velocity and acceleration spectra can be derived, were obtained by Project 1.9, which participated in shots Smoky, Whitney, Galileo, Charleston, and Stokes. A ground-shock response spectrum is a convenient method for interpreting free-field earth motions with regard to the relative effects in a structure or the effects on equipment within a structure placed in the soil. A response spectrum can be used to describe the behavior of a simple dynamic system as a function of its frequency.

2.3.2 Theory

A ground-shock spectrum is a plot of the maximum responses of single-degree-of-freedom systems (reed gauges) vs. the natural frequencies of the systems. The response is due to ground-induced motion of the reed-gauge base and is measured in the tests as peak instantaneous displacement. Acceleration and velocity spectra are derived from the measured displacement spectra. The mathematical relations given below are the bases for the response spectra.

Figure 2.14 illustrates a single-degree-of-freedom spring-mass system (neglecting damping); (a) shows the system at rest, and (b) shows the system in motion in the x direction as a result of an acceleration of the base.

The general differential equation of motion for a system having an acceleration input is

$$\ddot{\mu} + \omega^2 \mu = \ddot{x}$$

where $\mu = x - y$ = the displacement of the mass relative to the base

  x = displacement of the base

  y = displacement of the mass

  ω = undamped natural circular frequency of a spring-mass system

The dots denote differentiation with respect to time.

The system responses have the following relations:[1]

$$\mu_{max} = D, \text{ the displacement (response) spectrum}$$
$$\omega\mu_{max} = V, \text{ the velocity (response) spectrum}$$
$$\omega^2\mu_{max} = A, \text{ the acceleration (response) spectrum}$$

The displacement-response system (D) consists of the recorded values of the maximum displacement of the various masses relative to their bases for a number of spring-mass systems covering a range of frequencies. The acceleration-response spectrum (A) consists of the maximum absolute accelerations of the mass systems. The velocity spectrum is composed, not of the actual peak velocities of the masses relative to their bases but of pseudo relative velocities that are nearly the same as the peak relative velocities. The velocity spectrum is useful, however, in the determination of the upper bound of the strain energy in structures.

2.3.3 Instrumentation

Twelve shock gauges and protecting canisters were used in the tests. The shock gauge is a completely self-contained mechanical unit requiring no electronic or communication channels. Essentially, it consists of 10 masses attached to cantilever springs mounted on two sides of a vertical plate (Fig. 2.15). The natural frequencies of the spring-mass system are approximately 3, 10, 20, 40, 80, 120, 160, 200, 250, and 300 cycles/sec.

Peak responses to the shock input for each spring-mass system are obtained on polished, smoked record plates, which are marked by the movement of a stylus attached to each mass.

The gauge is protected by a cylindrical canister 2 ft in diameter and approximately 2 ft deep. Figure 2.16 shows the two canisters as they were placed in structure RAc. Transmission of shock input to the gauge (either in the vertical or horizontal direction) is secured by bolting the gauge in the desired position to the 1-in. baseplate of the canister.

Vertical and radial gauges to record free-field effects were placed approximately 1 ft below the ground surface at various distances from GZ during shots Smoky, Whitney, Galileo, Charleston, and Stokes. During shot Smoky one radial and one vertical gauge were placed in the underground rectangular structure of Project 30.7 at the 1005-ft range (Fig. 2.16). The canisters were bolted to the floor slab of the structure. One radial and two vertical gauges were placed adjacent to the structure; a distance of 5 feet was used between gauges.

2.4 ACCELERATION TEST

A test was performed under the direction of Project 30.5 to ascertain the effects on the human body of the acceleration of a structure subjected to blast loads:

In structure RAc concrete blocks were cast around concrete-filled rubber boots. The boots and blocks had a weight approximately equal to that of the average human. Three pairs of boots were mounted on three different types of flooring: (1) three 1-in.-thick layers of Ensolite cemented together; (2) one 1-in. layer and one $\frac{1}{2}$-in. layer of Ensolite cemented together, and (3) the existing concrete floor of the structure. The instrumentation used in the test included one Wiancko accelerometer mounted on each of the three blocks and two accelerometers mounted on the floor. The instruments mounted on the floor were arranged to measure both vertical and horizontal acceleration of the structure. One displacement gauge was used on the block that was located on the $1\frac{1}{2}$-in.-thick pad of Ensolite.

The location and details of the Ensolite test equipment are shown in Fig. 2.17, and a view of the test is given in Fig. 2.16.

2.5 BIOLOGICAL TEST

2.5.1 General

Under the direction of Projects 33.5 and 33.6, internal environmental biological tests were performed in the structures of Project 30.7. The objectives of these tests were (a) to determine the effect of environment on biological specimens (mice) occupying the shelters during a nuclear explosion and (b) to determine the existence and origin of dust resulting from a nuclear detonation, which would be a potential hazard to personnel located in structures.

In general, the biological test consisted of a sample of 20 mice; one sample was placed in each of seven of the nine structures tested. The test objectives were twofold: (1) to place the specimens in the shelters and to follow their mortality rate over a 60-day period postshot and (2) if possible, in case of death, to relate the cause of death to a specific environmental factor.

The dust-accumulation test consisted in placing one or more of the same and/or different types of dust accumulators in the structures for exposure during the detonation. The purposes of the study were to (a) obtain samples of postshot dust appearing in the structures as a consequence of the nuclear explosion, (b) establish, if possible, the sources of postshot dust, i.e., whether particles arose from preexisting dirt on the floor or actually spalled from the ceiling, wall, and floor slab as a result of the explosion, and (c) establish the particle sizes of the preshot and postshot dust.

The biological-test description and results, as accumulated in this report, have been abstracted from the reports of Projects 33.5 and 33.6, ITR-1447 and WT-1507, respectively.

2.5.2 Environmental Test of Mice

(a) *Animals.* The animals used in the study were mice of the RAP strain. Body weights were between 20 and 25 g, and ages averaged approximately six weeks. In addition to the sample used in each structure, two samples were kept as controls. Each sample of 20 mice was placed in a wire-mesh cage approximately 9 by 15 by 9 in. (see Fig. 2.18). The cages contained copious amounts of food (Purina Laboratory Chow) and two water bottles. In the event the blast were to jar the water bottles from the cage, each cage had sliced raw potatoes to act as a source of moisture. Control tests had shown that animals under these circumstances could survive for four days unattended.

(b) *Locations.* The cages were placed in seven of the nine structures tested. The cages in structures RAa, RAc, RAd, RCa, RCb, and RCc were placed on the floor slab near the corner of the main chamber formed by the walls facing GZ and the antechamber. In structure CAb the cage was located between the gasoline generator and the gasoline storage tank. The cages in all seven structures were secured to the floor by an elastic band stretched across the top of the cage and anchored to the floor slab.

The location of the mice is shown in Fig. 2.19.

(c) *Time of Placement.* The animals were placed in the structures three and four days before the shot. Each day thereafter the food and water supply was replenished up to, and including, the day before the shot.

2.5.3 Dust-accumulation Test

(a) *Dust Collectors.* Two types of dust collectors were utilized in the study. These collectors consisted of sticky-tray fallout collectors and motor-driven air samplers.

(b) *Sticky-tray Fallout Collectors (Types B, C, and D).* Two types of sticky-tray collectors were used during the study. The first type consisted of sticky paper (8 by 9 in.) mounted by masking tape to the top of either aluminum trays (12 by 12 in.) or $\frac{1}{16}$-in.-thick plates of galvanized sheet metal ($9\frac{1}{2}$ by $10\frac{1}{2}$ in.). The top of the sticky paper was protected by two rectangular pieces of paper, each covering half the sticky surface. The paper protector was removed when exposure of the tray was desired. The sticky-resin trays, which were the second type used, were prepared by coating one side of the aluminum trays with an alkyl resin put in a solution of toluene (1 part resin to 4 parts toluene). The coating operation was done with an

atomizer of the type commonly employed to spray nasal passages. Dummy trays were taped over the resin collectors to protect them during transportation and installation.

The sticky-tray collectors were broken down into two additional classifications, namely, type B (paired sticky-paper trays) and type C (single sticky-paper trays). Type B sticky-paper trays were placed in the nine structures for preshot controls. These control trays, which recorded the preshot dust accumulation, were removed from the shelter at the time the structures were finally prepared for the detonation. The sticky sides of two trays were placed face to face to trap the collected dust between the two layers of transparent material. At the time of removal of the control trays, two experimental type B trays were uncovered so that the postshot dust accumulation could be recorded. In addition, single sticky-paper trays (type C) were installed in the structures that had been coated with fluorescent dye. The single sticky-paper trays, when not in use, were protected by dummy aluminum trays, which were taped over them.

Single resin trays (type D) were installed in the structures that had been coated with fluorescent dye. As in the case of the type C trays, the resin trays were protected by aluminum tray covers.

The fluorescent dye was used to establish the source of postshot dust. A 0.1 per cent solution of fluorescein-sodium, placed in a 50/50 water-alcohol solution, was applied with ordinary paint rollers. The floors of structures RAa, CAb, RAd, and RCb were covered to avoid contamination of the floor dirt with the dye.

At the time the dust collectors were placed, a sample of dirt was scraped from the floor of each structure to establish the character of the shelter dirt which existed preshot.

The control sticky-paper trays, as previously mentioned, were broken into two categories, dirty and clean. Twelve dirty control trays were placed in the structures, as indicated in Table 2.2. These trays were placed in the structures 14 days before the test, at which time dust on the floor was disturbed by swatting the floor with a piece of cardboard. The 12 control trays were removed the day following their placement, at which time 3 additional clean trays were placed. The clean trays were uncovered three days before the test and removed two days later.

All experimental dust collectors (types B, C, and D) were exposed in the structures from one to three days before the test.

(c) *Air Sampler (type E)*. A high-volume automatic air sampler was installed in structure CAb (circular at 132 psi) to check the concentration of dust particles suspended in the air at different times after the blast.

This instrument is equipped with a $\frac{1}{2}$-hp motor, which operates a suction pump that draws approximately 15 cu ft/min through a Whatman No. 41 filter paper. The volume of air sampled depends upon the particular filter employed and the amount of dust which has accumulated on it during its operation. The air flow rate used for calculations is the mean of the initial and final flow rates as determined by a Fischer and Porter Flowrator.

The sampler consists of two basic units: the motor and pump unit and the filter magazine unit. The latter accommodates eight $3\frac{3}{8}$-in.-diameter filters, which cycle sequentially according to a preset sampling interval. Initiation of sampling is also controlled by a preset timer.

For this test two samplers using Whatman No. 41 filter paper as the filter medium were employed. The first instrument was set so that each of the eight filters was exposed for a period of $1\frac{1}{2}$ hr; after 12 hr, the instrument having run its cycle, the operation would cease. The second instrument was set so that it would run continuously on one filter until the power supply failed.

The air sampler, with its power supply, was installed in the structure six days before the test. Several preshot tests were run on the equipment to determine whether or not the generator air supply was sufficient. The sampler operated during shot time test, but, under a prolonged test two days before the shot, the air supply was found to be insufficient. Even though the sampler was unlikely to function properly, it was started 6 hr before the test.

The samplers used in the test by Project 33.5 and the description of their operation were obtained from Program 37 through the cooperation of K. H. Larsen.

(d) *Location.* Two experimental sticky-paper trays (type B) were placed in each of the nine structures tested. Structures RAa, RAd, CAb, and RCb had one sticky-paper tray (type C) and one resin tray (type D), in addition to the type B trays. These structures, which contained the type C and D collectors, were also coated with fluorescent dye. Both air samplers, along with their gasoline-generator supply, were located in structure CAb.

The number and type of dust collectors are given in Table 2.2, and their locations are shown in Fig. 2.19.

REFERENCE

1. Y. C. Fung and M. V. Barton, "Some Characteristics and Uses of Shock Spectra," Report AM No. 6-14, The Ramo-Wooldridge Corporation, California, Oct. 15, 1956.

TABLE 2.1 — LOCATION AND NUMBER OF U. S. INSTRUMENTS*

Structure	Predicted overpressure, psi	Electronic gauges						Self-recording		
		Pressure (P)	Pressure (P_t)	Dynamic pressure (Q)	Deflection (D)	Acceleration (A)	Strain (S)	Dynamic pressure ($\overline{Q}$)	Pressure ($\overline{P}$)	Scratch gauges
RAa	264.6							1	7	4
RAb	198.5	5	4	1	3	1	4		9	
RAc	132.3				1	5		1	8†	
RAd	88.2							1	5	
CAa	198.5	4	3		2	1	1		5	
CAb	132.3								6†	
RCa	29.4	5	4	1	4	1	3		6	
RCb	14.7							1	6	
RCc	7.4							1	4	

*P, Carlson pressure gauges
P_t, Wiancko pressure gauges
Q, electronic dynamic pressure gauges
D, BRL deflection gauges

A, acceleration gauges
S, SR-4 strain gauges
$\overline{Q}$, self-recording dynamic pressure gauges

$\overline{P}$, self-recording pressure gauges
†One very-low-pressure gauge included

TABLE 2.2—NUMBER AND TYPE OF DUST COLLECTORS*

Structure	No. and type of experimental collectors				No. and type, type B control collectors		Remarks
	B	C	D	E	No.	Type*	
RAa	2	1	1		1	C	Dye-treated 11 days before test
RAb	2				1	C	
RAc	2				1	C	
					1	C_1	
RAd	2	1	1		1	C	Dye-treated 11 days before test; vacuumed 1 day before test
CAa	2				1	C	
CAb	2	1	1	2	1	C	Dye-treated 11 days before test; vacuumed 1 day before test
RCa	2				1	C	
					1	C_1	
RCb	2	1	1		1	C	Dye-treated 11 days before test; vacuumed 2 days before test
RCc	2				1	C	Vacuumed 1 day before test
					1	C_1	

*Control collectors: C, dirty control; C_1, clean control.
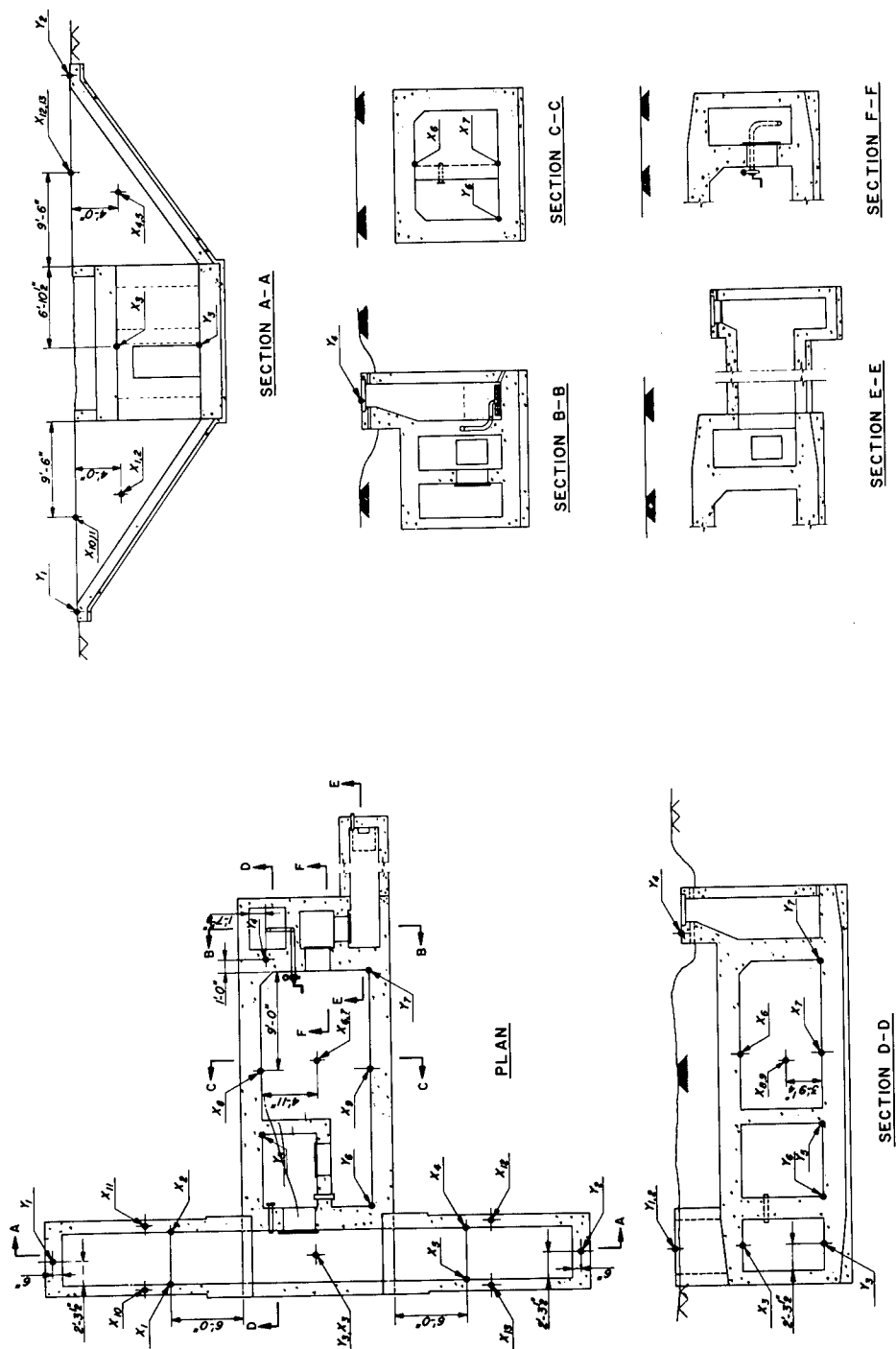
Fig. 2.1—Type A rectangular shelter, survey points.
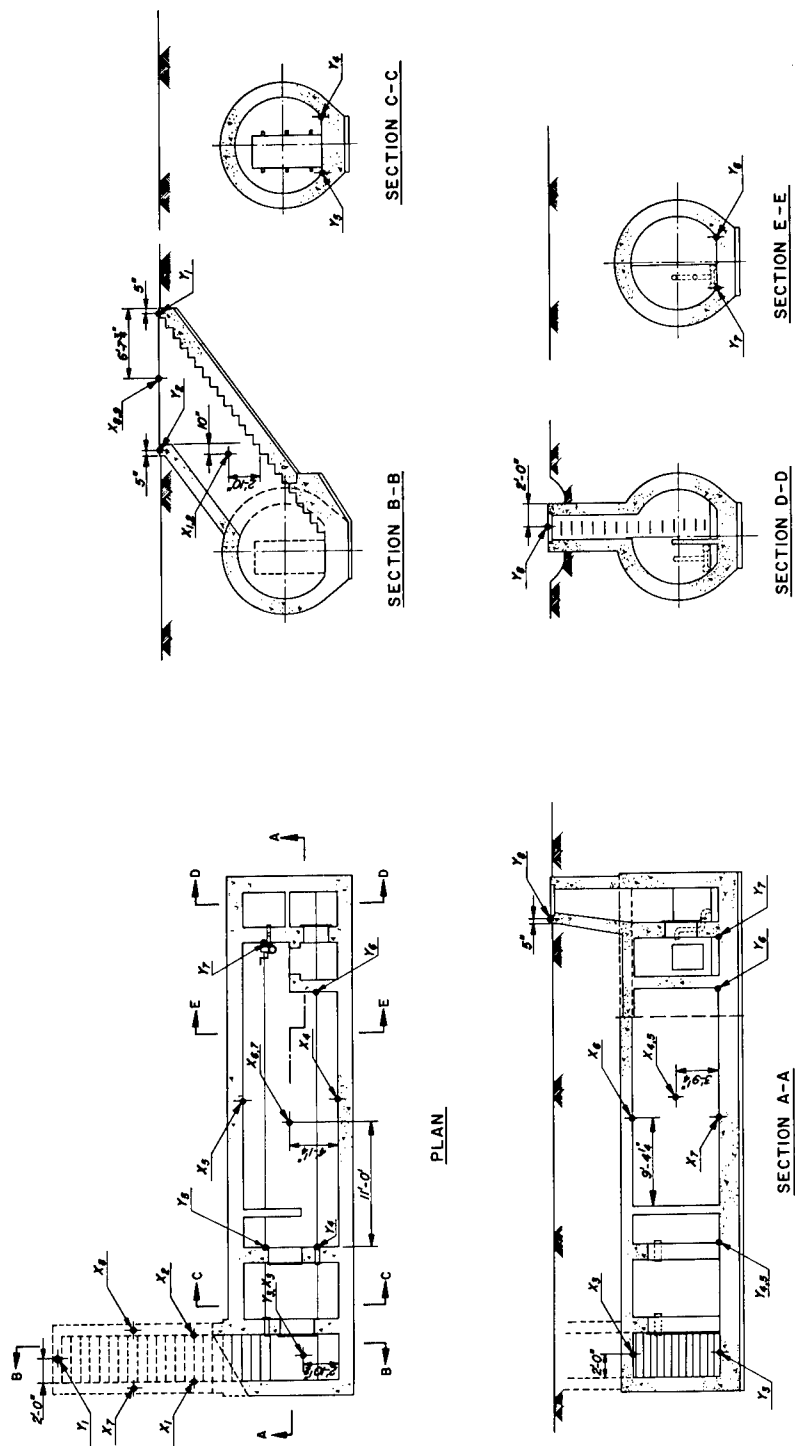
Fig. 2.2—Type A circular shelter, survey points.
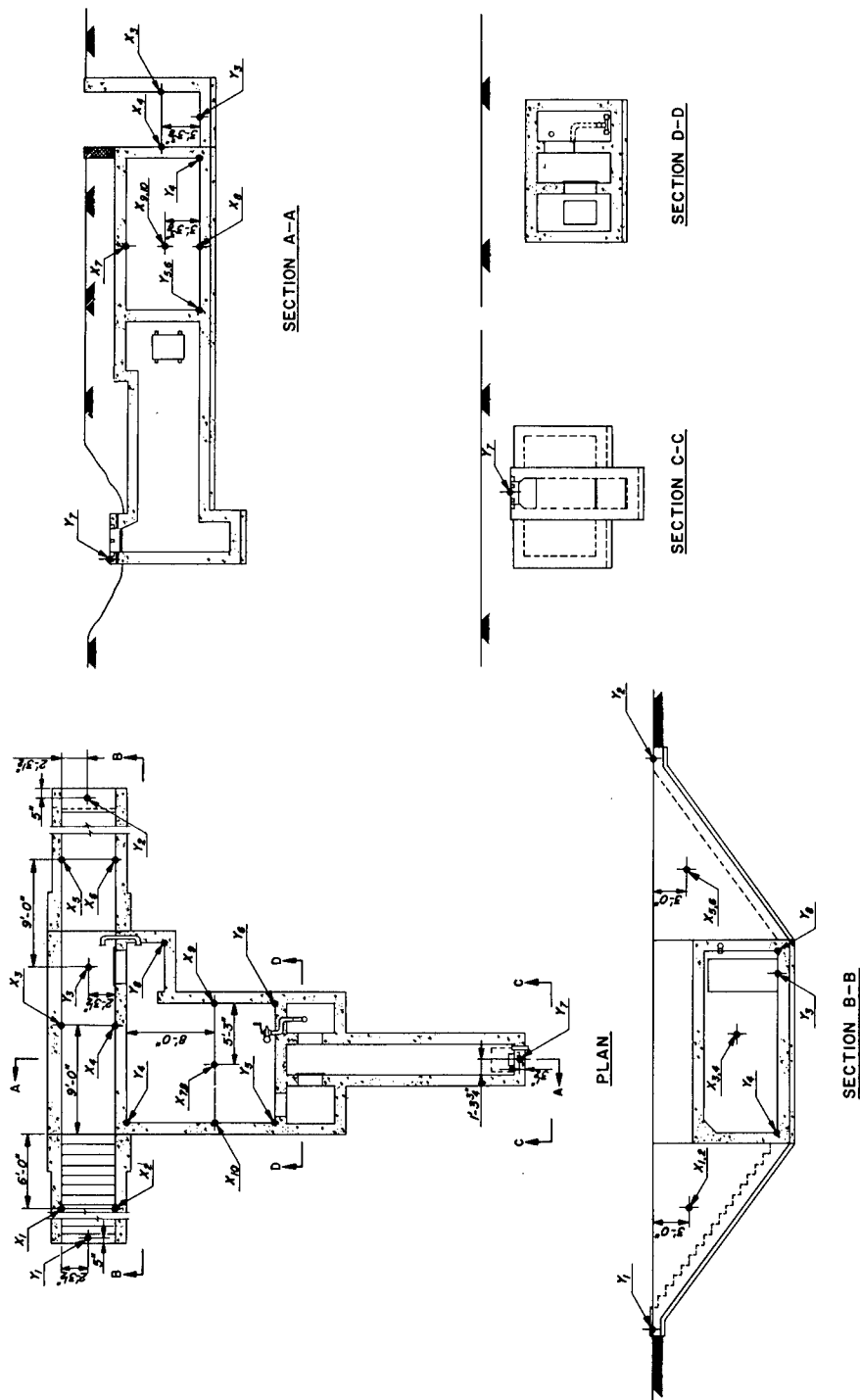
Fig. 2.3—Type C rectangular shelter, survey points.
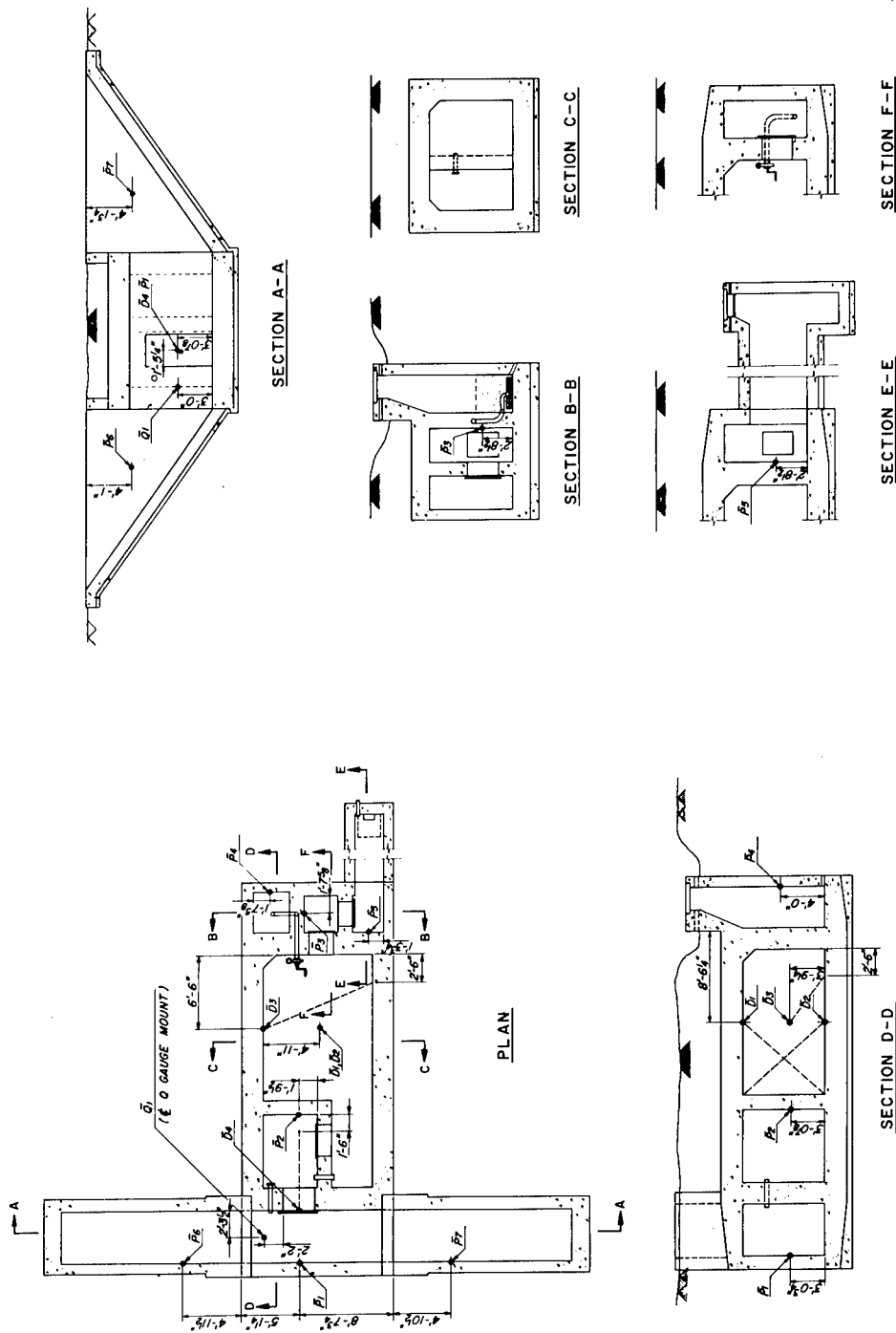
Fig. 2.4—Instrumentation layout for type A rectangular shelter (structure RAa).

50

Fig. 2.5—Instrumentation layout for type A rectangular shelter (structure RAb).

Fig. 2.6 — Instrumentation layout for type A rectangular shelter (structure RAc).

Fig. 2.7—Instrumentation layout for type A rectangular shelter (structure RAd).
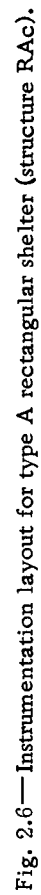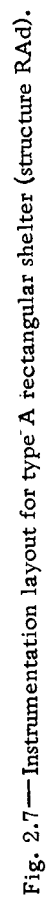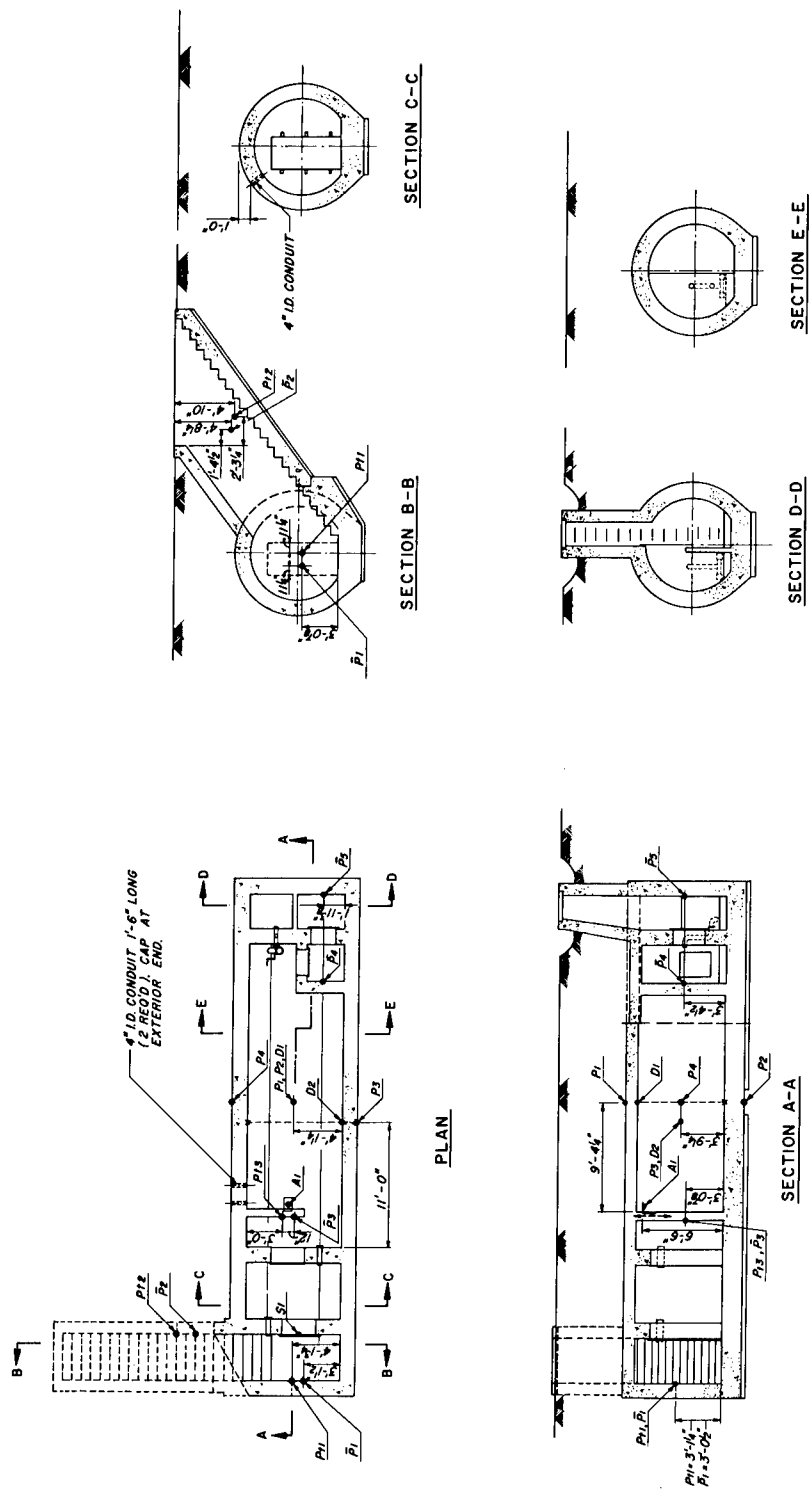
Fig. 2.8—Instrumentation layout for type A circular shelter (structure CAa).
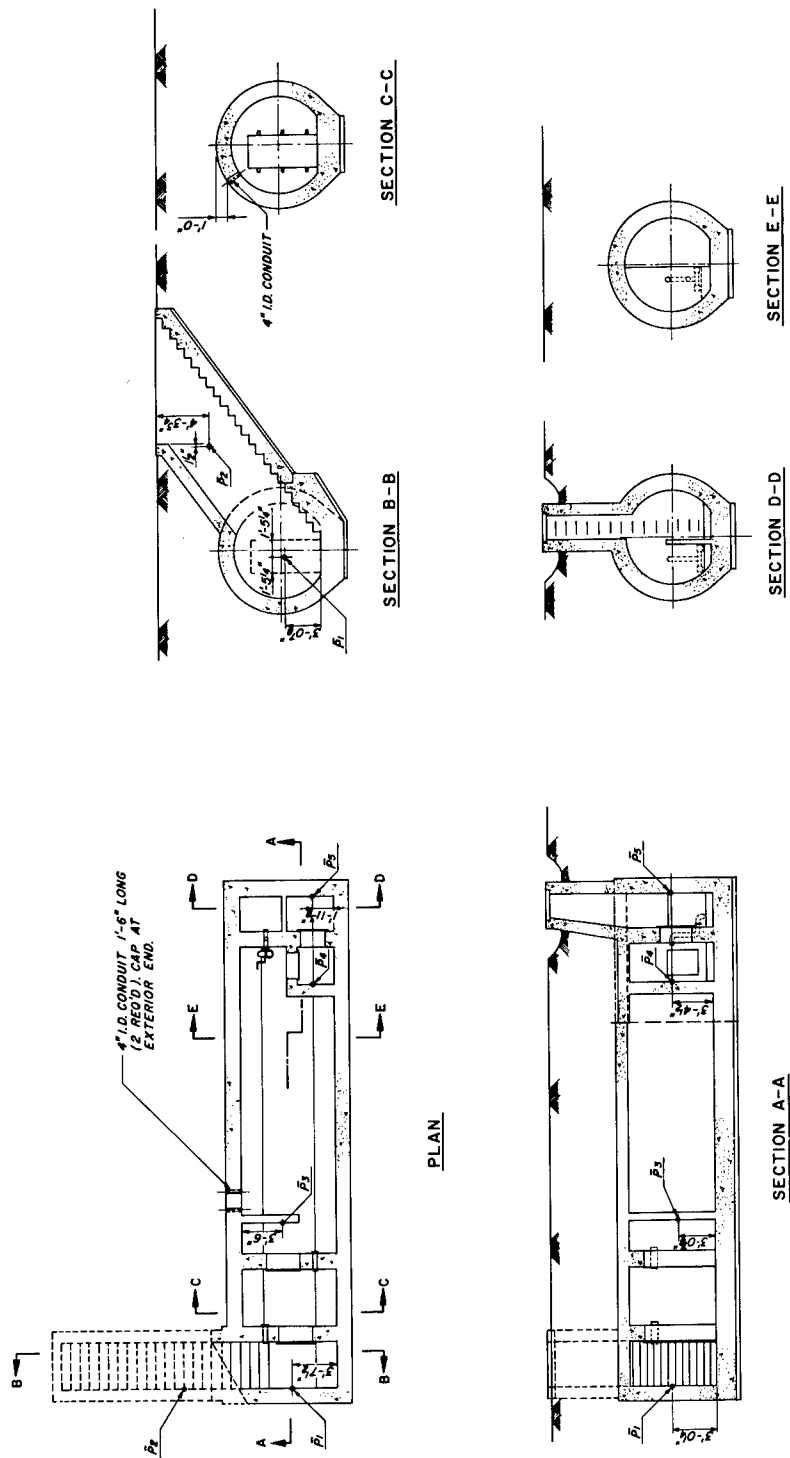
Fig. 2.9 — Instrumentation layout for type A circular shelter (structure CAb).

Fig. 2.10—Instrumentation layout for type C rectangular shelter (structure RCa).
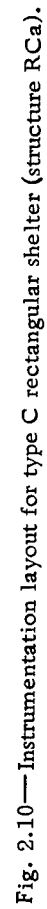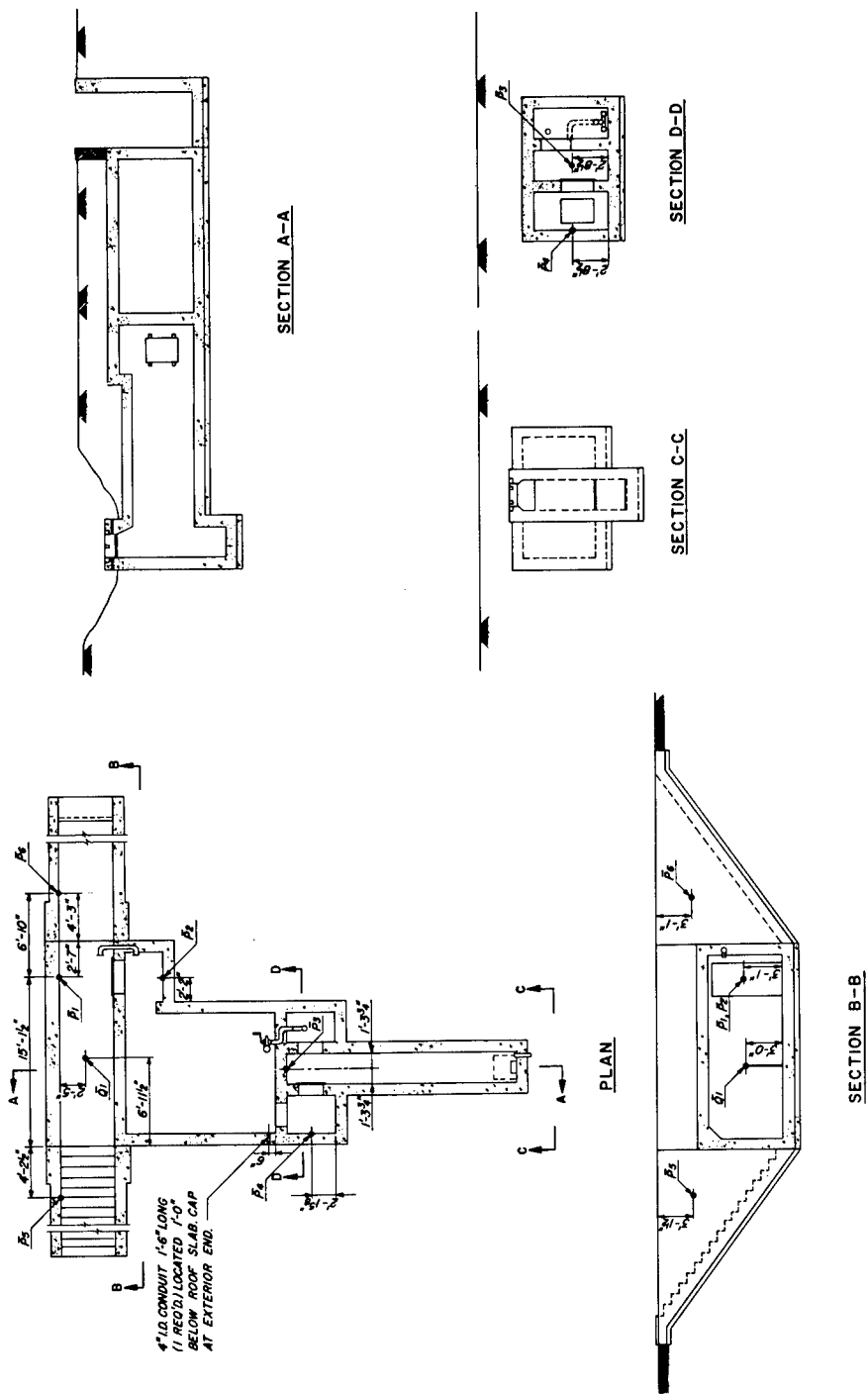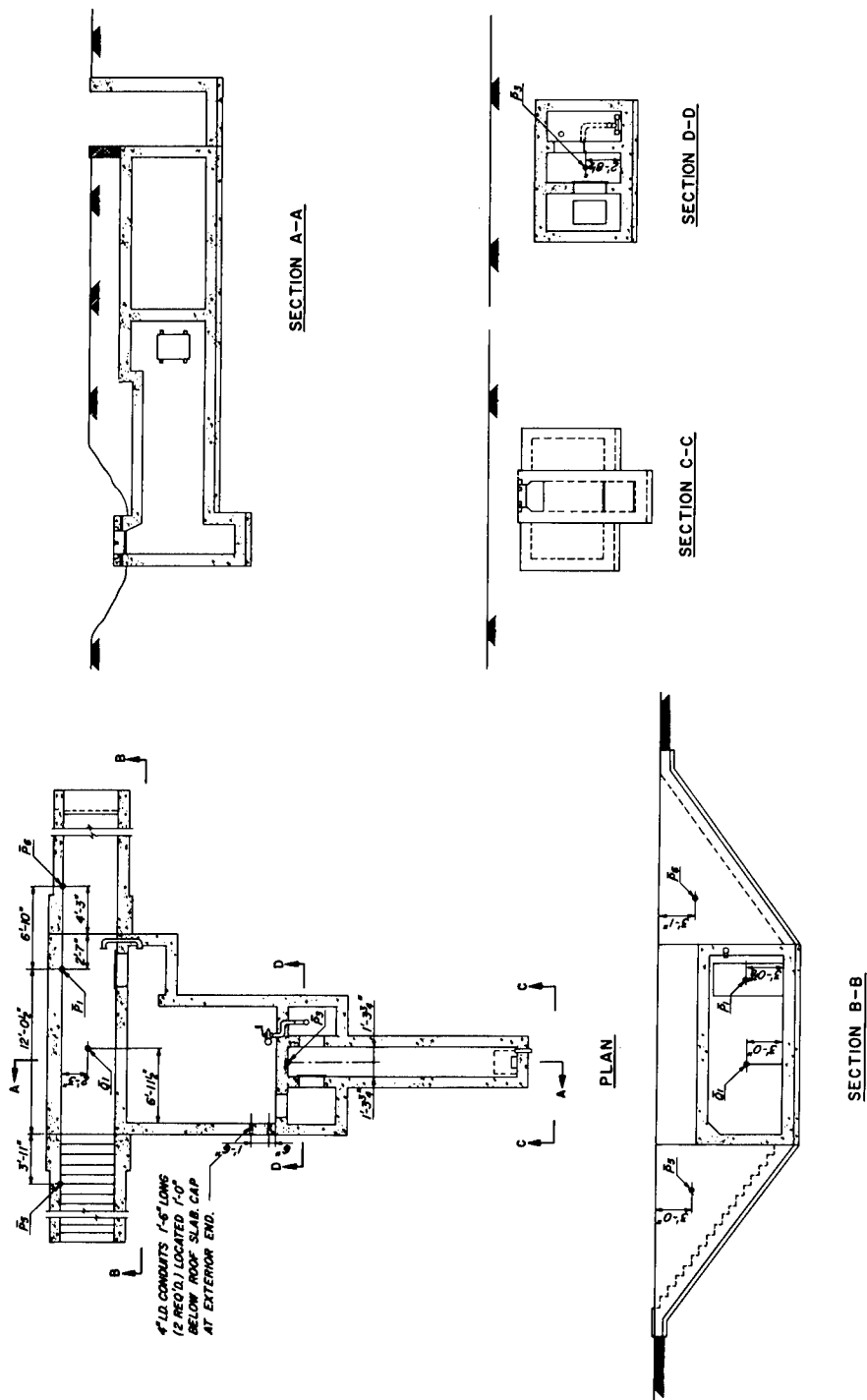
Fig. 2.11—Instrumentation layout for type C rectangular shelter (structure RCb).

57

Fig. 2.12—Instrumentation layout for type C rectangular shelter (structure RCc).

LEGEND
• EG & G FILM BADGES - 3 FT. HT.
△ EG & G FILM BADGES - 3 & 5 FT. HT.
▲ EG & G FILM BADGES
◙ SULFUR & GOLD DETECTORS
   STRUCTURES RAc and CAb only

NOTE:
   ALL EG & G FILM BADGES
SHOWN ON PLAN HAVE SAME
NUMBERS FOR EACH STRUCTURE
OF TYPE SHOWN.

RECTANGULAR   TYPE - A
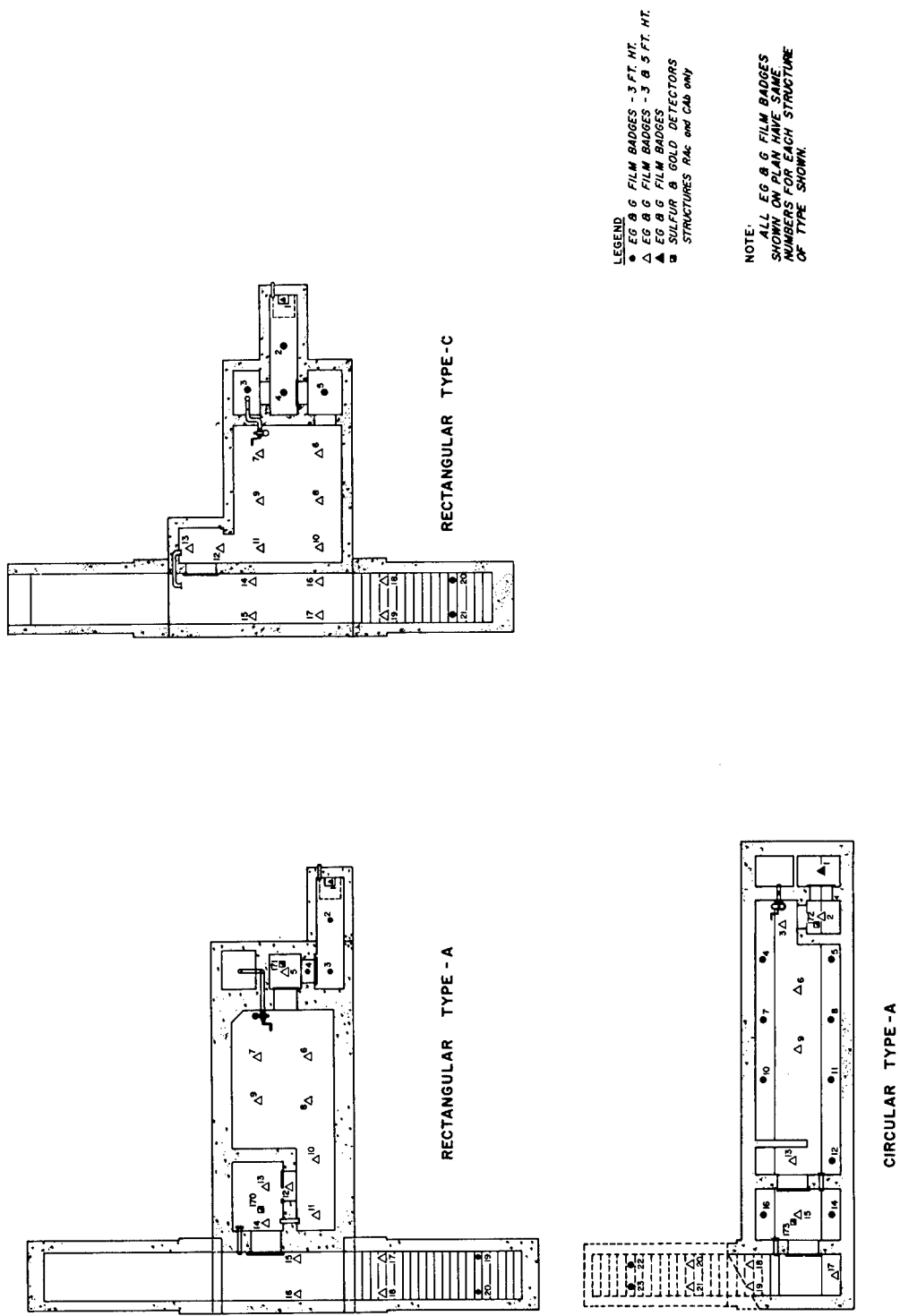
CIRCULAR   TYPE-A

Fig. 2.13—Location of radiation-detection equipment.

59
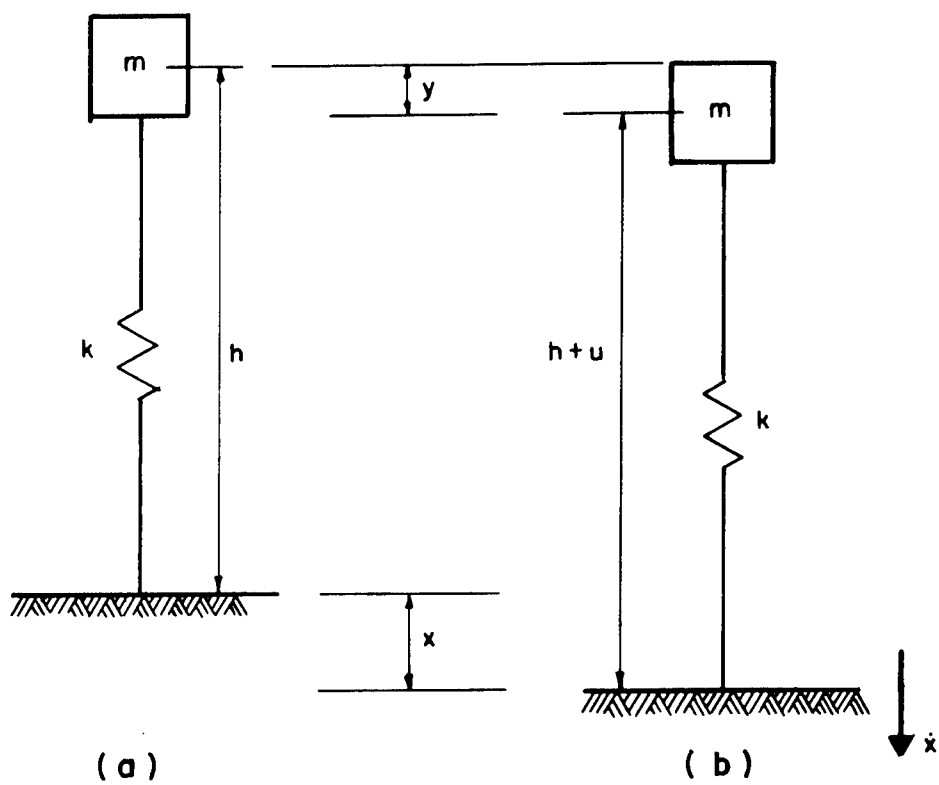
Fig. 2.14—Single-degree-of-freedom spring-mass system.
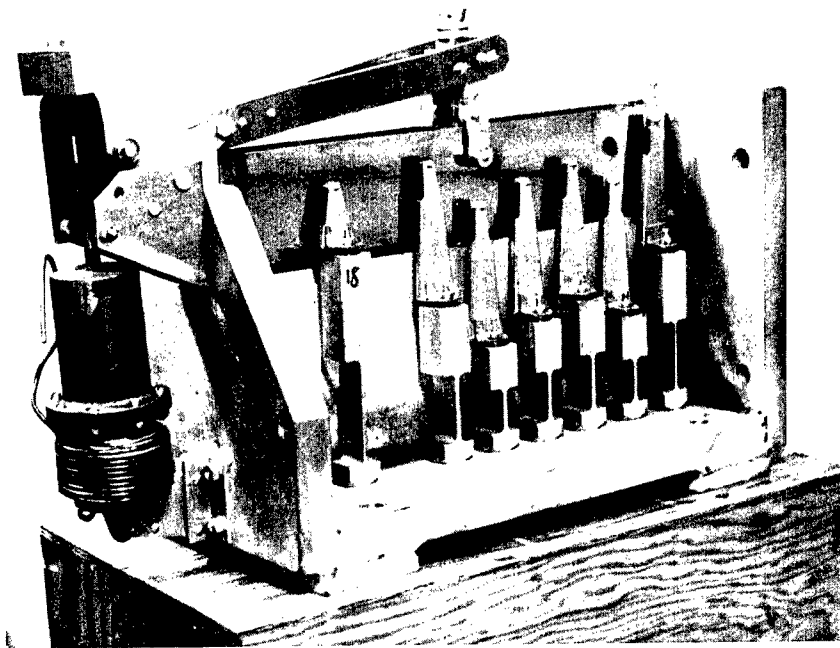
Fig. 2.15—Shock gauge.
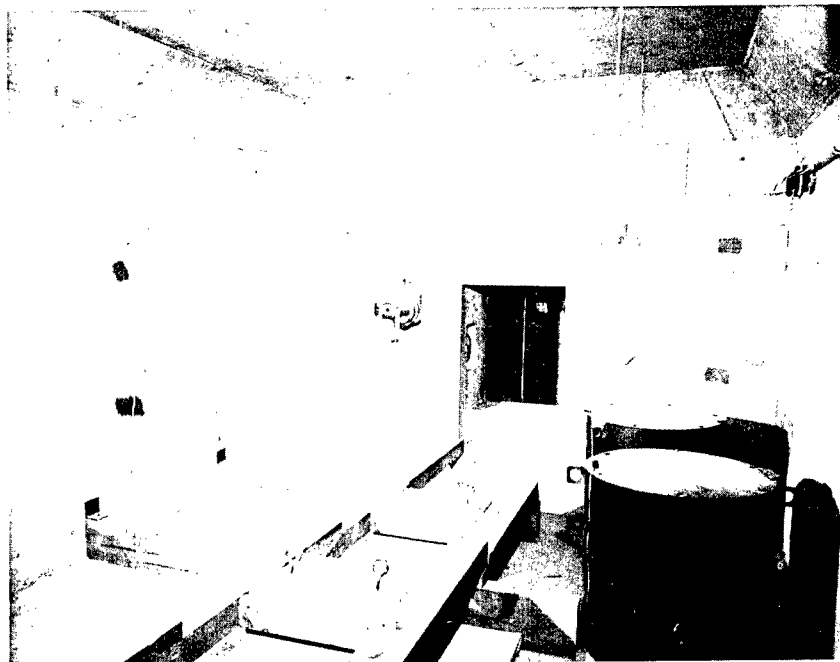
Fig. 2.16—Shock-gauge canisters and Ensolite test equipment.

Fig. 2.17—Layout of acceleration test.
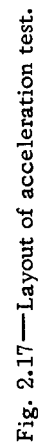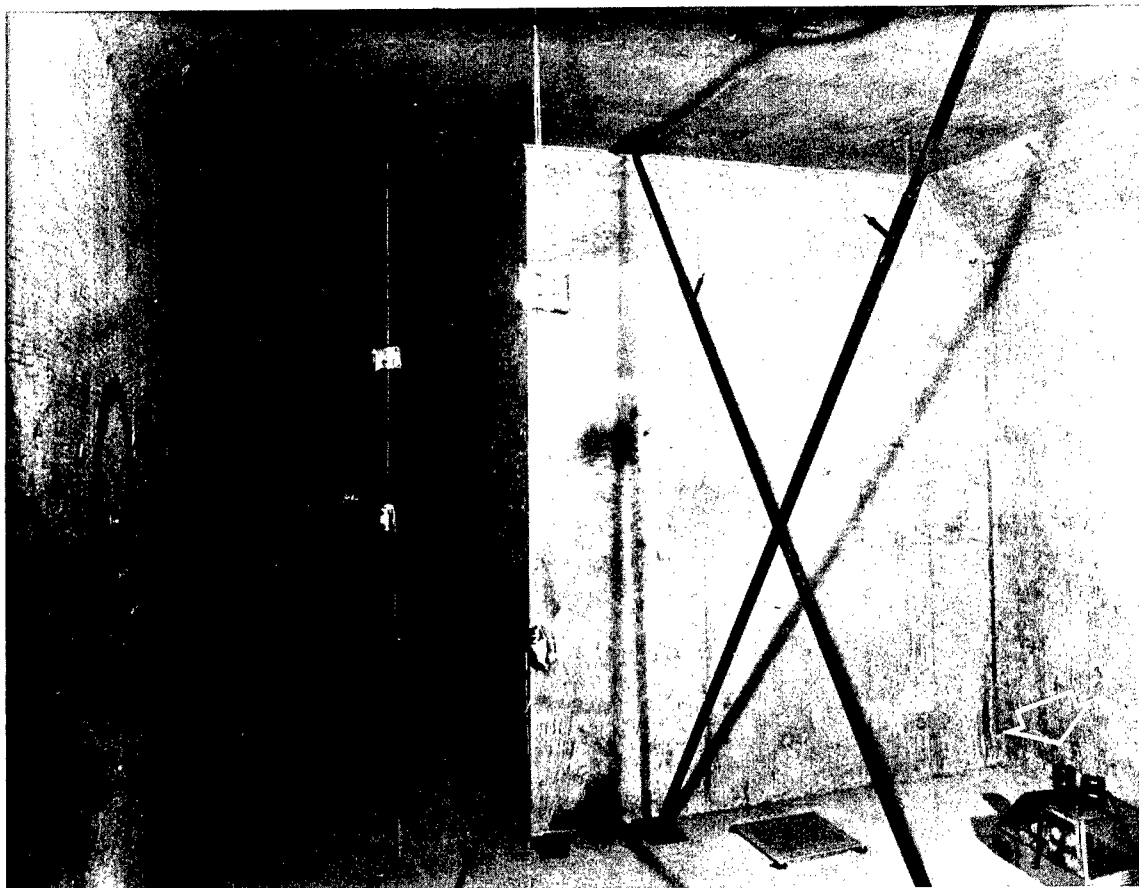
Fig. 2.18—Mouse cage.

RECTANGULAR TYPE-C

RECTANGULAR TYPE - A

CIRCULAR TYPE - A

GENERATOR

GASOLINE BARREL

AIR SAMPLERS
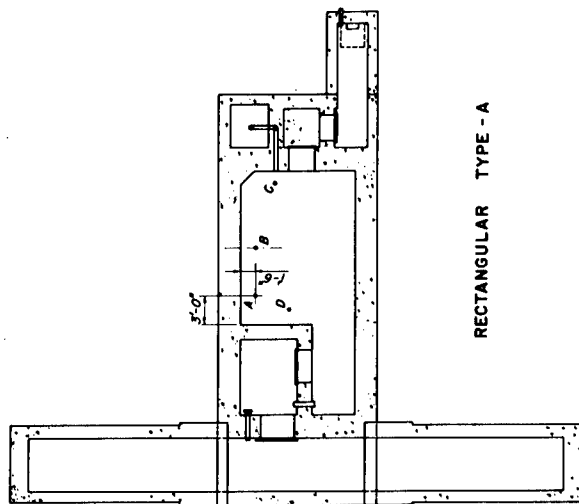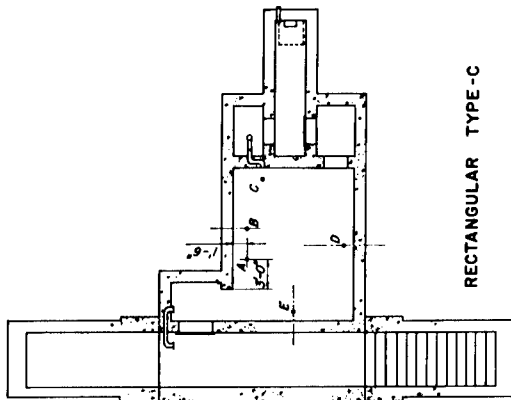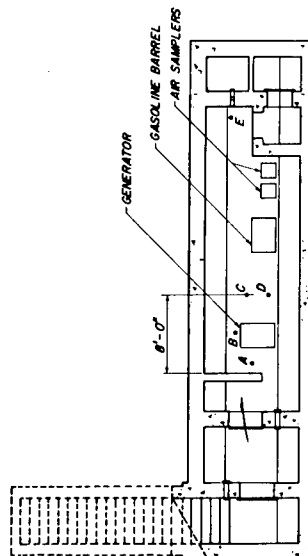
BIOLOGICAL TEST SPECIMENS

SHELTER	SPECIMEN LOCATIONS				
	A	B	C	D	E
RAa	△	—	□□	⊠	—
RAb	—	⊞	□□	—	—
RAc	△	□□	—	—	—
RAd	⊞	□□	⊠	⊞	—
CAa	—	□□	△	—	⊠
CAb	⊞	—	△	□□	—
RCa	△	—	—	□	⊞
RCb	△	—	⊠	□□	—
RCc	△	—	□	—	□

LEGEND
□ STICKY TRAY COLLECTORS (PAIRED)
⊠ STICKY TRAY COLLECTORS (SINGLE)
⊞ RESIN COLLECTORS
△ ANIMAL CAGE

NOTE:
AIR SAMPLERS, GASOLINE BARREL
AND GENERATOR LOCATED IN
SHELTER CAa

Fig. 2.19—Location of biological specimens.

Chapter 3

BLAST RESULTS

3.1 Structural Blast Damage

3.1.1 Rectangular Concrete Shelter (Structure RAa)

(a) *Entranceways*. In the ramp entrance facing GZ separations formed at the intersections of the interior and exterior walls with the ramp slab. The interior wall was pulled away from the slab 7 in. at the bottom and $\frac{1}{16}$ in. at the top of the ramp. The intersection of the ramp and exterior wall was similar to that at the interior wall; that is, the crack varied from 4 to 7 in. near the bottom to zero inches at the top of the ramp. Bowing of the interior wall into the backfill was produced at the quarter-height along the contraction joint. A $\frac{1}{16}$- to $\frac{1}{2}$-in. vertical crack was formed near the bottom of the ramp. This crack terminated at a laminated area located at the mid-height of the wall. There was spalling on both sides at the upper section of the crack. Cracks varying from $\frac{1}{16}$ to $\frac{3}{8}$ in. in width, perpendicular to the plane of the ramp, were located approximately 2 ft on center along the length of the wall. The majority of these cracks ran the full height of the wall. A crack starting at a chipped-out section located at the intersection of the end of the roof slab and the interior wall ran diagonally toward the top of the wall. The section of the wall above this crack was deflected back into the fill. The exterior wall damage was similar to that described for the interior wall. A chipped section of the exterior ramp wall was located approximately 4 ft above the landing at the contraction joint. A horizontal crack, with spalling on both sides, above this section produced a $\frac{1}{2}$-in. bow in this wall. There were numerous diagonal cracks perpendicular to the plane of the ramp located approximately 2 to 3 ft on center in the upper two-thirds of wall. These cracks varied in size from $\frac{1}{32}$ to 1 in. in width. The top of the parapet located above the landing roof slab that faces GZ was deflected into the backfill 6 in. at the intersection of the exterior wall and 1 ft at the interior wall. The corners of the parapet and side walls were chipped, and the reinforcement was exposed.

A 3-in. crack in the landing floor slab ran from the contraction joint at the bottom of the ramp along the center line of the slab to the Q-gauge mount. There it became a 2-in. crack, running diagonally to the exterior wall. A $1\frac{1}{2}$- to 2-in. crack was located along the intersection of the floor slab and the exterior wall. The crack was continuous the full length of the landing. The roof slab had a continuous longitudinal 1-in. crack along its center line. Two diagonal cracks $\frac{1}{16}$ in. in width branched off the main crack, one terminating at the interior wall and the other at the exterior wall. A $\frac{3}{8}$-in. crack was produced along the intersection of the roof slab and the exterior wall. The exterior wall was badly damaged, having a longitudinal crack located at the mid-height of the wall. Spalling of 2 to 3 in. on each side was observed along its entire length.

In the entrance away from GZ, bowing separations were produced along the intersection of the stairs and the two walls. The separation of the interior wall varied from $2\frac{1}{2}$ in. at the bottom to $4\frac{1}{2}$ in. at the three-quarter point from the bottom and back to 3 in. at the top of the stairs. The exterior wall had a separation of $\frac{3}{4}$ in. at the bottom and 2 in. at the top of the

stairs. The exterior wall had several $\frac{1}{32}$-in. cracks perpendicular to the plane of the stairs located in the upper section of the entrance. The interior wall had a spalled crack located at its quarter point which started at the contraction joint, ran parallel to the stairs, and ended above the sixth riser from the bottom. At the intersection of the top end of the roof slab and the interior wall was a chipped-out section of the wall. This section had two $\frac{3}{32}$-in. cracks leading out from it and running parallel to the stairs.

The interior surfaces of the ramp, stairs, and the landing were completely scoured by the blast. Debris covered the entire entrance.

(b) *Antechamber.* No damage was noted in the walls, roof, and floor slab of the antechamber.

(c) *Main Chamber.* Hairline cracks were formed at the intersection of the roof slab and the haunches along the rear and side walls of the main chamber. The intersection of the walls located at points A, B, and C of Fig. 3.1 had continuous hairline cracks the full height of the walls. Diagonal hairline cracks were formed at the four corners of the door opening located at point D. Numerous transverse and longitudinal hairline cracks were produced on the floor slab of the main chamber. No cracks were present in the floor slab of the main chamber adjacent to the main seal door.

The crack patterns for structure RAa are shown in Figs. 3.1 to 3.3. Appendix C contains the postshot dynamic analysis of the roof slab of shelter RAa. The analysis indicates that only minor cracking was expected under the applied blast load.

(d) *Exit Chamber.* As in the main chamber, diagonal cracks were formed at the four corners of the door opening located at point E, Fig. 3.1. No structural damage was evident in the roof and floor slabs.

(e) *Exit Tunnel and Shaft.* The tunnel and shaft themselves had no visible cracks. There was a $\frac{1}{16}$- to $\frac{1}{8}$-in. lateral separation at the contraction joint between the exit tunnel and the main structure. The tunnel was displaced 1 in. vertically upward at the opening from the main structure. An area approximately 1 ft square had spalled in the tunnel roof slab adjacent to the contraction joint. Debris was strewn the full length of the tunnel and was piled 3 ft above the tunnel floor directly under the exit hatch.

(f) *Doors.* All doors, with the exception of the horizontal emergency-exit hatch cover, were undamaged by the blast. The grout pockets holding the door frame anchors were all sound except for the top pocket on the latch side of the large sealed door, which was cracked around the edges of the grout pocket.

The emergency-exit hatch cover was blown down into the exit tunnel and deposited opposite the small blast door. The exit hatch cover showed no other damage except straightening of the hinge support straps. The releasing mechanism was also undamaged.

(g) *Ventilation.* The overpressure flap valve was closed before the test and was found closed after the test. There was no sign of damage to the valve or hinge assembly or to the manually operated exhaust valve inside the shelter.

Inspection showed the manually operated ventilator to be in good working condition, except that some leakage was noted. On the "Zu" (closed) setting, the flow-indicator plug rises slowly to the top of the graduated tube when the handle is turned rapidly. However, it is doubtful if leakage, in addition to that noted in Sec. 1.3.4, was caused by the blast.

The results of the blast are shown in Figs. 3.4 to 3.24.

3.1.2 Rectangular Concrete Shelter (Structure RAb)

(a) *Entranceways.* In the entrance facing GZ the separation of the ramp from the interior wall varied in size from hairline near the top to $2\frac{1}{2}$ in. at the bottom of the ramp. The exterior wall and ramp slab intersection had a similar crack that varied from hairline near the top to 2 in. at the bottom. A transverse crack was located at the one-third point up the ramp. The interior ramp wall had a laminated section located near the roof slab. An additional laminated area was formed at the intersection of the ramp and this wall. Both laminated areas had $\frac{1}{16}$-in.

cracks along their top edges. A $\frac{1}{16}$- to $\frac{1}{8}$-in. vertical crack was located at a point midway up the ramp. Spalling was evident along both edges of this crack. Two vertical $\frac{1}{8}$- and $\frac{1}{4}$- to $\frac{3}{8}$-in. cracks were located in the upper third of this wall. There were several $\frac{1}{32}$-in. cracks in the wall. Numerous vertical and diagonal $\frac{1}{32}$- to $\frac{1}{8}$-in. cracks were present along the face of the exterior wall. A chipped section of the wall was located at the contraction joint between the ramp and landing. The top of the parapet located above the landing roof slab was deflected 3 in. into the backfill.

On the ramp side of the landing a $1\frac{1}{2}$-in. crack was formed at the center line of the floor slab. The crack ran to the center of the landing. A $\frac{3}{4}$-in. crack branched from this crack and ran next to the Q-gauge mount, at which point it became a 1-in. crack and continued to the first riser of the entrance away from GZ. The intersection of the roof slab and the exterior wall had a continuous $1\frac{1}{2}$-in. crack along the entire length of the landing. The exterior wall had several $\frac{1}{32}$- and $\frac{3}{32}$-in. cracks located midway along the landing. There was also a $\frac{1}{16}$-in. horizontal crack $3\frac{1}{2}$ ft above the floor slab of the landing on the GZ end of the wall which ran to the $\frac{3}{32}$-in. vertical crack. Sections of these exterior walls at the contraction joint of the entrance facing GZ were chipped out by the blast.

Continuous separations were observed along the intersection of both walls and the stair in the entrance facing away from GZ. At the interior wall the crack varied from 1 in. at the bottom to 2 in. at the mid-height of the stairs and then decreased to $\frac{3}{4}$ in. at the top. The exterior wall separation was similar but varied in size from $\frac{1}{8}$ in. at the bottom to $1\frac{1}{2}$ in. at the mid-height and back to $\frac{1}{2}$ in. at the top of the stairs. The interior wall had a laminated section located adjacent to the edge of the landing roof slab. The laminated area had a $\frac{1}{32}$-in. horizontal crack that ran toward the top of the stairs. The exterior wall had a vertical $\frac{1}{32}$-in. crack located above the sixth riser from the bottom of the stairs. Several $\frac{1}{64}$- and $\frac{1}{32}$-in. cracks were also present in this wall.

(b) *Antechamber*. The walls and roof were not damaged. The floor slab had one hairline to $\frac{1}{16}$-in. crack running from the rear wall of the antechamber to a point located midway between the main door opening.

(c) *Main Chamber*. The section of main chamber adjacent to the gastight door had several $\frac{1}{32}$-in. cracks in its floor slab. The roof and walls of this section received no structural damage. The roof slab of the main room in the structure had diagonal hairline cracks that started at a strain-gauge block out at the center of the room and ran toward the four corners. A longitudinal crack, hairline in width, was located along the center line of the slab. Hairline cracks were developed at the intersection of the haunch and the roof slab along the rear and both side walls of the room. Cracks were formed along the intersection of walls at points A and B of Fig. 3.25. Also, at the gastight door opening, located at point C of Fig. 3.25, diagonal cracks were formed leading out from the four corners of the door opening. Numerous transverse and longitudinal cracks were produced in the floor slab, their sizes varying from $\frac{1}{32}$ to $\frac{1}{16}$ in.

The crack patterns for structure RAb are shown in Figs. 3.25 to 3.27.

(d) *Exit Chamber*. The opening located at point D of Fig. 3.25 had diagonal cracks leading from its four corners. No damage was observed in the roof or floor slabs.

(e) *Exit Tunnel and Shaft*. No cracking was found in the vertical exit shaft or the exit tunnel. The contraction joint between the emergency exit tunnel and the main part of the shelter was opened $\frac{1}{8}$ to $\frac{1}{4}$ in., with spalling at the joint of the tunnel walls and roof slab. There was a vertical dislocation between the tunnel and shelter, the tunnel being $\frac{3}{4}$ in. higher.

(f) *Doors*. The only door showing any damage was the emergency-exit hatch cover. As in structure RAa, the bent steel hinge straps again were straightened out and allowed the hatch cover to be pushed into the emergency-exit tunnel. The hatch cover was deposited on the floor of the exit tunnel at the edge of the pit and was buried under 3 ft of debris. The hatch operating mechanism and the hatch frame were undamaged.

The grout under the frame of the main blast door was blown into the antechamber by the overpressure, but this door and the remaining blast door and two gastight doors were in good working order.

67

(g) *Ventilation*. The ventilation system was in working condition and had the same settings after the test as before. That is, the overpressure flap valve was closed and was working easily, the manually operated exhaust valve was open 1 cm, and the ventilator was on "Auf" (open). As in structure RAa, there again was some small leakage in the mechanically operated ventilator when it was set on "Zu" (closed) and turned rapidly. The cast-iron flange of the ventilator assembly, which bolts to the projecting intake pipe from the sand filter, was broken at the time of initial assembly and not during the test.

The blast damage incurred by structure RAb is shown in Figs. 3.28 to 3.32.

3.1.3 Rectangular Concrete Shelter (Structure RAc)

(a) *Entranceways*. The entrance facing GZ had cracks formed along the intersection of the ramp slab and both walls. The separation of the interior wall from the slab varied from hairline at the ground surface to $\frac{3}{8}$ in. at the bottom of the ramp. The exterior wall and slab separation varied from $\frac{1}{32}$ in. at the surface to $\frac{1}{2}$ in. at the bottom. The interior wall developed two $\frac{1}{32}$-in. cracks at its mid-height. These cracks were located near the lower portion of the ramp. The wall at the construction joint deflected into the backfill $\frac{3}{8}$ in. at its base and $2\frac{1}{2}$ in. at the top of the parapet. There were no cracks in the exterior wall, but at the contraction joint the wall deflected into the backfill zero inches at its base and $1\frac{7}{8}$ in. at the top of the parapet. The top of the parapet located above the landing roof slab was pushed $1\frac{1}{2}$ in. into the backfill.

The roof slab over the landing had a $\frac{1}{8}$-in. continuous crack along its intersection with the exterior wall. A $\frac{1}{16}$-in. crack developed; it started at the edge of the roof slab on the opposite side of the landing from GZ, continued along the center line of the slab for three-quarters of its length, then turned diagonally toward the exterior wall. The interior wall of the landing had a vertical $\frac{1}{32}$-in. crack running its full height. The crack was located at the center of the landing.

Both walls in the entrance away from GZ separated from the stairs at their intersection. The crack along the stairs and the interior wall varied from $\frac{1}{4}$ in. at the bottom tread to $\frac{3}{4}$ in. at the mid-height of the stairs and to $\frac{1}{8}$ in. at the top riser. The exterior wall and stair separation varied from hairline at the bottom to $\frac{3}{8}$ in. at mid-height and to $\frac{1}{4}$ in. at the top riser. The interior wall had a laminated area located at the intersection of the wall and the roof slab. The top of the laminated area was bounded by a $\frac{1}{32}$-in. crack. Several additional $\frac{1}{32}$-in. cracks and one $\frac{1}{16}$-in. crack were located near the laminated section. The exterior wall had three $\frac{1}{32}$-in. cracks and one $\frac{1}{4}$-in. crack located near the contraction joint in the upper half of the wall.

(b) *Antechamber*. The walls, roof, and floor slab received no structural damage from the blast.

(c) *Main Chamber*. One longitudinal hairline crack started at the center of the chamber roof slab and ran to the interior corner of the antechamber. There were several diagonal cracks branching off this longitudinal crack. Diagonal cracks, starting at the center of the chamber, ran toward the two rear corners of the room. There were hairline to $\frac{1}{16}$-in. longitudinal cracks produced in the floor slab. The center portion of the slab could not be investigated owing to the presence of the Ensolite test equipment. Cracks were formed at the intersection of the walls as located by points A, B, and C of Fig. 3.33. Diagonal cracks were present at the four corners of the door opening at the rear of the chamber, point D.

The crack patterns for structure RAc are shown in Figs. 3.33 to 3.35.

(d) *Exit Chamber*. No cracking was evident in the roof and floor slabs. Cracks were formed at the four corners of the opening in the wall at point E, Fig. 3.33.

(e) *Exit Tunnel and Shaft*. The tunnel and shaft themselves had no visible cracks. At the contraction joint between the main structure and the tunnel, a $\frac{1}{2}$ in. lateral displacement occurred. The tunnel floor was displaced vertically $\frac{3}{4}$ in. above the floor of the main structure. Debris was piled $2\frac{1}{2}$ ft above the floor of the tunnel below the exit shaft. Sand bags that were used to reinforce the sloped ground surface at the exterior end of the shaft were found broken open and hanging from the climbing rungs in the shaft.

(f) *Doors.* All doors, with the exception of the horizontal exit-shaft hatch cover, were un-damaged by the blast. The hatch cover was found at the edge of the pit below the shaft. It had been completely covered with debris. The anchor straps for the hatch cover had been straight-ened out by the force of the cover being pushed away from it.

The grout pockets for holding the doors were found upon inspection to be sound, but the grout under the main blast-door frame was blown into the antechamber by the pressure wave.

(g) *Ventilation.* The overpressure flap valve was closed before the test and remained closed after the test. There was no sign of damage to the valve or hinge assembly or to the manually operated exhaust valve inside the shelter.

Inspection showed the manually operated ventilator to be in good working condition except that some leakage was noted on the "Zu" (closed) setting. The flow-indicator plug rises slowly to the top of the graduated tube when the handle is turned rapidly. However, it is doubtful if leakage in addition to that noted in Sec. 1.3.4, was caused by the blast.

The results produced by the blast loading are as shown in Figs. 3.36 to 3.53.

3.1.4 Rectangular Concrete Shelter (Structure RAd)

(a) *Entranceways.* In the entrance facing GZ there was a separation of the interior wall from the ramp slab varying from $\frac{1}{32}$ in. near the top of the entrance to $\frac{1}{16}$ in. at the bottom. The exterior wall was also separated from the ramp, the size of the cracks varying from $\frac{1}{8}$ in. at the top to $\frac{1}{4}$ in. at the bottom of the ramp. There was a chipped-out section of the interior wall located at its intersection with the edge of the roof slab over the landing. The deflection of the wall into the backfill at the contraction joint varied from zero inches at the ramp to $\frac{3}{8}$ in. at the bottom of the roof slab. The exterior wall had a $\frac{1}{64}$-in. vertical crack located near the upper end of the ramp.

A $\frac{1}{16}$-in. crack was present along the intersection of the exterior wall and the roof slab of the landing.

The separation of the stairs in the entrance away from GZ from the interior wall varied from hairline at the bottom riser to $\frac{1}{8}$ in. at the top of the stairs. The exterior wall separation varied from $\frac{1}{8}$ in. at the bottom to $\frac{3}{8}$ in. at the mid-height and back to $\frac{1}{8}$ in. at the top of the stairs. The interior wall had a $\frac{1}{32}$-in. diagonal crack running from the intersection of the edge of the roof and the wall to a point located at the top of the seventh riser from the bottom of the stairs. No deflection of this wall into the backfill was apparent. The exterior wall deflection at the contraction joint varied from zero inches at the bottom to $\frac{3}{4}$ in. at the underside of the roof slab.

The crack patterns for structure RAd are shown in Figs. 3.54 to 3.56.

(b) *Antechamber.* No damage to the walls, roof, or floor slabs was apparent in the ante-chamber.

(c) *Main Chamber.* The main chamber received no structural damage from the blast.

(d) *Exit Chamber.* The walls, roof, and floor slab of the exit chamber appeared to be in the same condition before and after the test.

(e) *Exit Tunnel and Shaft.* No cracks were evident in the shaft or tunnel. The contraction joint between the main structure and the exit tunnel had a lateral separation of about $\frac{3}{8}$ in. No vertical movement was apparent at this joint. One of the climbing rungs in the exit shaft was deformed. Sand and debris filled the pit at the bottom of the shaft to a depth of approximately 9 in.

(f) *Doors.* The only door showing any damage was the emergency-exit hatch cover. The bent steel hinge straps were straightened out, allowing the cover to be pushed into the emer-gency-exit tunnel. The hatch-operating mechanism and the hatch frame were undamaged.

(g) *Ventilation.* The overpressure flap valve was closed before the test and remained closed after the test. There was no sign of damage to the valve or hinge assembly or to the manually operated exhaust valve inside the shelter.

69

Inspection showed the manually operated ventilator to be in good working condition, except that some leakage was noted on the "Zu" (closed) setting. The flow-indicator plug rises slowly to the top of the graduated tube when the handle is turned rapidly. However, it is doubtful if leakage, in addition to that noted in Sec. 1.3.4, was caused by the blast.

The results produced by the blast loading are shown in Fig. 3.57.

3.1.5 Circular Concrete Shelter (Structure CAa)

(a) *Entranceway.* The single entranceway, which faced away from GZ, had a $\frac{1}{32}$-in. crack down the center line of the sloping roof slab over the stairs. This crack started at the free end of the roof slab and continued past the contraction joint to $1\frac{1}{2}$ ft past the crown of the cylindrical section.

A $\frac{1}{32}$- to $\frac{1}{16}$-in. crack ran along the center line of the stairs from the fifth riser from the top to the contraction joint at the sixth riser from the bottom. Another $\frac{1}{32}$-in. crack ran from the fifth tread from the bottom to the floor of the landing along the intersection of the exterior wall and the stairs. At the intersection of the exterior wall and the stairs, there was a $\frac{1}{64}$-in. crack that started at the eighth riser from the top and ran to the top riser. It continued diagonally from the intersection of the exterior wall and the top tread as a $\frac{1}{16}$-in. crack across the horizontal portion of the wall. A similar $\frac{1}{32}$-in. crack started at the other end of the top tread and ran diagonally across the top of the interior retaining wall to its outside face.

At the bottom of the vertical contraction joint in the retaining walls, there was a $\frac{3}{8}$-in. separation of the exterior walls and a $\frac{1}{4}$-in. separation of the interior. The joints were closed at the top. Differential vertical movement was apparent. The portion of the sloping roof slab above the contraction joint was $\frac{3}{16}$-in. lower than the corresponding section toward the cylinder.

The corner formed by the sloping roof slab and the interior wall from the contraction joint to top of slope had a hairline crack. This crack extended up to the top of the parapet portion of the sloping roof slab at its intersection with the interior wall and ran diagonally toward the cylinder to the edge of the wall. This diagonal crack was $\frac{1}{32}$ in. wide.

The floor slab of the landing had a $\frac{1}{32}$- to $\frac{1}{16}$-in. crack perpendicular to the plane of the door across the entire width. A similar hairline crack was present near the crown of the roof slab.

There was also a vertical hairline crack 1 ft from, and parallel to, the upstairs side of the main blast door. This crack started at the top recess on the far side of the door frame from GZ and continued to the floor. The grout in this anchor pocket was loosened.

The crack patterns for structure CAa are shown in Figs. 3.58 to 3.60.

(b) *Antechamber.* The only visible damage in the chamber between the large blast door and large gastight doors was a continuation of the longitudinal cracks along the center line of the floor slab and crown. In this chamber the crack in the floor slab was $\frac{1}{32}$ in. wide and the crack in the crown was hairline.

(c) *Main Chamber.* In the main chamber the crack in the floor slab, which began at the end of the cylinder, continued as a $\frac{1}{32}$-in. longitudinal crack down the center line of the floor for practically the full length of the cylinder. Approximately 5 ft from the exit end of this cylinder, this crack became $\frac{1}{64}$ in. wide. There was also a similar, but narrower, crack in the crown of the roof slab for the entire length of the main chamber.

The wall of the cylinder away from GZ had three cracks, hairline in width, starting at the intersection of the cylinder with the floor slab and running up to a point about 30 deg from the crown on the side away from GZ. These cracks were approximately at the center and quarter points of the length of the unstiffened wall. Two 6-in.-long vertical hairline cracks were also found in the wall facing GZ around the middle diameter at the center of span of the wall.

(d) *Exit Chamber.* No damage to the walls, floor slab, or cylinder was noted in this chamber.

(e) *Exit Shaft.* At the intersection of the vertical exit shaft with the cylinder, a $\frac{1}{32}$- to $\frac{1}{64}$-in. horizontal crack had run around the shaft, except on the end wall. About 6 in. above this

intersection, there was a $\frac{1}{64}$-in. crack on the wall facing GZ. On the walls toward and away from GZ, at about their mid-height, another fine crack was noted.

The hatch cover was deposited on the top of the sand in the filter chamber. The top climbing rung was bent down by the hatch cover. No other damage was noted.

(f) *Doors*. With the exception of the emergency-exit hatch cover, all doors were in place and in good operating condition. The hardened grout under the bottom angles of the door frame of the main blast door was blown in by the overpressure. This debris dented the large seal door where it hit. The sheet-metal skin of the door was unbroken.

As in structure RAa, the hinge straps for the emergency-exit hatch cover were again bent straight, and the cover was blown in and deposited as noted above. There was no damage to the door operating mechanism.

(g) *Ventilation*. After the test the overpressure flap valve was found jammed in an open position with no signs of structural damage. The manually operated exhaust valve was in its preshot condition and, as in the other structures, the ventilator was set on "Auf" (open) and working with some leakage when set on "Zu" (closed) and turned rapidly.

The damage that resulted from the blast wave is shown in Figs. 3.61 to 3.72.

3.1.6 Circular Concrete Shelter (Structure CAb)

(a) *Entranceway*. There was a $\frac{1}{32}$-in. crack along the sloped portion of the entrance roof slab. This crack started at the upper end of the slab and continued to a point located at the contraction joint above the sixth riser from the bottom of the stairs. A $\frac{1}{64}$-in. crack started at the contraction joint and ran down the lower portion of the slab. The crack branched out into two separate $\frac{1}{64}$-in. cracks above the landing. A separation was present along the entire length of the intersection of the entrance roof slab and exterior wall; it varied from hairline to $\frac{1}{64}$ in. in width. There was approximately $\frac{1}{8}$ in. of lateral movement of the entrance away from the structure at the contraction joint. There was a $\frac{1}{2}$-in. spalled area on each side of the contraction joint along the roof slab. The stairs had a crack located along their center line ranging in size from $\frac{1}{64}$ in. at the seventh riser from the top to $\frac{1}{16}$ in. at the contraction joint. The interior wall was separated from the stairs by a crack that started at the top riser as $\frac{1}{16}$ in. wide and decreased to hairline in nature at the contraction joint. The separation of the exterior wall from the stairs started at the top riser as a $\frac{1}{64}$-in. crack and continued down to the eleventh riser from the top, where it was hairline in size.

The exterior wall had two $\frac{1}{64}$-in. cracks that were perpendicular to the plane of the stairs and were located above the eighth and ninth risers from the top. Several similar cracks were located on the interior wall opposite the above-described cracks.

The ceiling and floor slab of the landing had longitudinal cracks that ran from the exterior wall to points located above and below the center line of the blast door, respectively. The sizes of the floor and roof slab cracks were hairline and $\frac{1}{64}$ in. in width, respectively.

The crack patterns for structure CAb are shown in Figs. 3.73 to 3.75.

(b) *Antechamber*. The cracks in the floor and crown that were present in the landing also continued into the antechamber with their same widths. No transverse separations were evident in this section of the structure.

(c) *Main Chamber*. At the center line of the floor slab in the main chamber, a $\frac{1}{32}$-in. longitudinal crack started at the large gastight door and continued to the rear wall of the structure. This crack decreased to $\frac{1}{64}$ in. in width in the rear portion of the room. The cracks in the landing and antechamber are believed to be a continuation of this separation. Several $\frac{1}{64}$-in. transverse cracks were produced in the floor slab. The crown of the structure had a crack similar to that found in the floor except for the size, which is hairline.

The wall of the cylinder away from GZ had three hairline cracks. These cracks started at the intersection of the cylinder and the floor slab and ran up to a point about 30 deg from the crown on the side away from GZ.

(d) *Exit Chamber*. No damage to the walls, floor slab, or cylinder was noted in this chamber.

(e) *Exit Shaft*. The below-ground portion of the shaft was undamaged. That part of the shaft which extends above the surface had horizontal $\frac{1}{16}$-in. cracks on the four faces of the walls located 8 in. below the top of the shaft. The concrete around the hatch cover frame was badly spalled.

The hatch cover was deposited on the floor at the bottom of the pit below the shaft. The sand at the rear of the filter was scooped out to a depth of approximately 1 ft and deposited on the floor.

(f) *Doors*. With the exception of the emergency-exit hatch cover, all doors were in place and in good operating condition. The hinge straps for the emergency-exit hatch cover were again bent straight, and the cover was blown in and deposited as noted. There was no damage to the door operating mechanism. Again, the grout under the main blast door frame had been blown into the antechamber. However, as for structure CAa, the door was dented, but the sheet-metal face was not torn.

(g) *Ventilation*. The overpressure flap valve was found in an open position after the test. The manually operated exhaust valve was removed so that the exhaust pipe for the generator could pass through the duct for the valve.

The results of the blast are shown in Figs. 3.76 to 3.81.

3.1.7 Rectangular Concrete Shelter (Structure RCa)

(a) *Entranceways*. There was no physical damage to the ramp slab and only minor damage to the interior and exterior retaining walls facing GZ. Several $\frac{1}{64}$-in. and hairline cracks approximately 6 to 9 in. long were noted on the retaining walls. The contraction joints in the walls located at the bottom of the ramp were opened $\frac{1}{32}$ to $\frac{3}{32}$ in., with $\frac{1}{8}$ to $\frac{1}{4}$ in. of spalling on the interior wall joint. At the top of the parapet wall by this joint, a piece 9 by 4 by 3 in. deep was chipped out of the top of the parapet wall, and in the ramp slab a crack of from $\frac{1}{64}$ to $\frac{1}{32}$ in. was present. At the intersection of the exterior ramp wall and the ramp slab there was a hairline crack extending approximately three-quarters of the way up the ramp.

A $\frac{1}{16}$-in. separation along the entire length of the contraction joint, located between the parapet wall above the main structure roof slab adjacent to the landing, was observed.

The contraction joint between the stairs and landing walls away from GZ was opened $\frac{3}{32}$ in. at the bottom and zero at the top. At the intersection of the stairs and the interior and exterior retaining walls a hairline crack was opened the entire length of the stairs. As in the entrance facing GZ, 6- to 9-in.-long cracks ranging from $\frac{1}{64}$ in. to hairline were found starting at the upper edge of both walls. Spalling of $\frac{1}{8}$ to $\frac{1}{4}$ in. on each side was also noted at the contraction joint between the shelter and interior stair retaining wall.

The parapet wall and the interior ramp retaining wall appeared to have been displaced $\frac{1}{16}$ in. inward at their respective intersections with the main structure.

The crack patterns for structure RCa are shown in Figs. 3.82 to 3.84.

(b) *Antechamber*. There was no damage to the walls of the antechamber, except that at the corners formed by the various walls perpendicular to one another (points A, B, and C, Fig. 3.82) there were vertical hairline cracks the entire length of the intersection.

The floor slab had a $\frac{1}{32}$-in. diagonal crack from the inside corner nearest GZ to the center of the chamber. This crack continued perpendicular to the plane of the door, terminating at the center line of the main blast door. Two other $\frac{1}{32}$-in.-wide cracks, approximately 6 in. long, ran parallel to the rear wall.

On the roof slab there was a $\frac{1}{64}$-in. longitudinal crack running from approximately the center line of the blast door to the rear wall. This crack ran through the lintel beam over the main blast door and extended up the exterior face of the front wall to the contraction joint. Hairline cracks at the intersection of the roof slab with all walls were noted.

(c) *Main Chamber*. Diagonal cracks starting at the center of the roof slab and extending out toward the four corners were observed. At their origin these cracks were $\frac{1}{64}$ in.; they became hairline in width at 6 in. to 3 ft away from their starting point. The intersection of the haunch away from GZ and the roof slab had a hairline crack that continued around the rear

wall of the main chamber at the roof slab. All interior joints between the walls had vertical hairline cracks the full height of the wall, as shown by points D, E, and F, Fig. 3.82.

In the floor slab $\frac{1}{32}$-in. diagonal cracks, similar to those in the roof slab, were formed. Random longitudinal and transverse cracks, parallel to the front wall and the two walls perpendicular to the blast line, were also noted.

Located at the opening leading to the exit chamber, $\frac{1}{64}$-in. diagonal cracks were formed at the corners of the opening nearest GZ; at the other two corners there were hairline diagonal cracks. No other cracking of the walls was noted.

(d) *Exit Chamber.* Diagonal $\frac{1}{64}$-in. cracks, located at the four corners of the opening between the exit chamber and tunnel, were formed.

(e) *Exit Tunnel and Shaft.* The contraction joint between the emergency exit tunnel and the main structure was opened $\frac{1}{16}$ in. Approximately 9 in. from the top of the joint on the side away from GZ, a $\frac{1}{64}$-in. crack started in the wall of the main structure and continued up to the roof slab at a 45 deg. angle. There was no apparent vertical displacement between the sections on either side of the joint.

(f) *Doors.* All doors, including the emergency-exit hatch cover, were in good operating condition.

(g) *Ventilation.* The overpressure flap valve was found in an open position after the test. The mechanical ventilator worked on "Auf" (open), but some leakage was noted on "Zu" (closed).

The blast damage produced in structure RCa is shown in Figs. 3.85 to 3.91.

3.1.8 Rectangular Concrete Shelter (Structure RCb)

(a) *Entranceways.* The ramp slab and its intersections with the interior and exterior retaining walls showed no evidence of cracking. In each wall there were two cracks from $\frac{1}{64}$ in. to hairline in width, starting at the top of the wall and running vertically downward for 6 to 9 in. The contraction joints in the walls located at the bottom of the ramp were opened $\frac{1}{32}$ to $\frac{1}{64}$ in.

Along the entire length of the contraction joint located between the parapet wall above the main structure and the roof slab there was a separation of from $\frac{1}{64}$ in. to hairline. At the upper corner (away from GZ) of the grouted door anchorage recess, there was a hairline crack that ran diagonally up the face of the wall to the above contraction joint. The grout in the anchor recess was loose and could be moved slightly.

The contraction joint between the stairs and the landing retaining walls away from GZ was opened $\frac{1}{32}$ to $\frac{1}{64}$ in. There were no cracks at the intersection of the stairs with either the interior or exterior retaining walls. In the interior stair retaining wall there were five vertical hairline cracks some 6 to 9 in. long. These cracks started at the top of the wall above the fifth, seventh, tenth, thirteenth, and fifteenth treads from the bottom of the stairs. In the exterior ramp retaining wall there were three $\frac{1}{64}$-in. to hairline cracks starting at the top of the wall above the sixth, eighth, and tenth treads.

The crack patterns for structure RCb are shown in Figs. 3.92 to 3.94.

(b) *Antechamber.* The rear wall of the antechamber had a vertical hairline crack from the roof to the floor slab. This crack was located about one-third the distance from the wall nearest GZ to the main chamber and is indicated by point C, Fig. 3.92. Parallel to this crack, and about 6 in. farther from GZ, was another 9-in.-long hairline crack extending down from the roof slab. At the corners formed by the wall nearest GZ and the two adjoining walls (points A and B, Fig. 3.92), vertical hairline cracks the entire length of the corner were found.

There were no cracks in the floor slab.

On the roof slab the only crack to be seen was a hairline crack which started at the center line of the lintel beam over the blast door, ran up to the roof slab, and continued around at the intersection of the roof slab and various walls to the main chamber.

(c) *Main Chamber.* On the roof slab there were two transverse hairline cracks. The first crack originated at the center of the survey point X-7 and ran about 3 ft toward the wall near-

est GZ. There it split, one branch continuing transverse to about 6 in. from the top of the haunch and the other branch running on a diagonal toward the rear of the structure to the top of the haunch. On the side of the survey point away from GZ, the crack continued to the top of the haunch and down the haunch to the top of the wall. At the top of the haunch the crack had two additional branches that ran diagonally down the haunch to the top of the wall.

The second transverse crack was parallel to the main branch of the above-described crack but $1\frac{1}{2}$ ft nearer the front wall of the structure. It ran from the bottom of the haunch on the side away from GZ to about $1\frac{1}{2}$ ft away from the top of the haunch on the opposite wall; there it split, with both branches running diagonally to the top of the haunch nearest the entrance to the antechamber. Another diagonal crack branched from the main transverse stem and ran toward the corner formed by the front wall and the wall away from GZ. It stopped at the top of the haunch and continued along the intersection of the top of the haunch and roof slab to the rear corner. Another crack ran along the intersection of the roof slab and the rear wall.

A longitudinal crack, perpendicular to, and originating at, the center of the forward transverse crack, ran to the front wall of the structure. There it intersected a crack along the corner formed by the front wall and the roof slab. At all interior corners in the main chamber there were vertical cracks running the full height of the wall (points D, E, and F, Fig. 3.92). These cracks, as well as all others in the roof slab, were hairline in width.

In the floor slab there were random transverse longitudinal and diagonal cracks. A longitudinal $\frac{1}{64}$-in. crack started at approximately the center point of the floor and terminated about 3 ft away from the rear wall. Perpendicular to this crack at its origin was a $\frac{1}{64}$-in. transverse crack, which ran to the base of the wall toward GZ. It extended about 1 ft past the longitudinal crack toward the wall away from GZ. A $\frac{1}{64}$-in. longitudinal crack $2\frac{1}{2}$ ft long ran parallel to, and about 1 ft away from, the wall nearest GZ at the entrance end of the wall.

Parallel to the wall away from GZ, at about its center, there were three $\frac{1}{64}$-in.-wide cracks about 2 ft long. There were a number of $\frac{1}{64}$-in. diagonal cracks which ran toward the corner formed by the wall away from GZ and the rear wall at a point about 4 ft out from either wall.

Near the corner formed by the front wall and the wall away from GZ there was a $\frac{1}{32}$-in. crack parallel to the front wall. From this transverse crack there were two short longitudinal cracks which branched off perpendicular and ran toward the front wall.

(d) *Exit Chamber.* Diagonal cracks were formed at the corners of all the openings in the wall. No structural damage was observed in the roof and floor slab of the exit chamber.

(e) *Exit Tunnel and Shaft.* The contraction joint between the emergency-exit tunnel and the main structure had a hairline crack continuous around the walls, roof, and floor slab. There was no apparent vertical movement of the joint.

(f) *Doors.* All doors, including the emergency-exit hatch cover, were in good operating condition.

(g) *Ventilation.* The overpressure flap valve was found in an open position after the test. The mechanical ventilator worked on "Auf" (open), but some leakage was noted on "Zu" (closed).

The blast results are shown in Figs. 3.95 to 3.98.

3.1.9 Rectangular Concrete Shelter (Structure RCc)

(a) *Entranceways.* Cracks were not formed in the ramp slab or at its intersections with either wall in the entrance facing GZ. The interior ramp wall had two vertical $\frac{1}{64}$-in. cracks starting at the top of the wall and running approximately 1 ft toward the ramp. They were located mid-way up the sloped portion of the entrance. No cracks were apparent in the exterior wall. The contraction joints at the bottom of the ramp were open approximately $\frac{1}{32}$ in.

The joint above the roof slab running the full length of the landing was separated, varying in size from hairline at the entrance away from GZ to $\frac{1}{64}$ in. above the blast door.

One vertical crack was present in the interior stair wall facing away from GZ. The contraction joints at the bottom of the stairs were open $\frac{1}{32}$ in.

The crack patterns for structure RCc are shown in Figs. 3.99 to 3.101.

(b) *Antechamber.* No cracks were apparent in the walls, roof, or floor slab of the antechamber.

(c) *Main Chamber.* The roof slab had hairline cracks along its intersection with the haunch on both longitudinal walls. The rear wall and roof slab intersection had a $\frac{1}{64}$-in. separation on the GZ half of the structure. Both rear corners of the main chamber had vertical hairline cracks the full height of the wall, as indicated by points A and B, Fig. 3.99. Numerous longitudinal $\frac{1}{64}$-in. cracks were located in the floor slab near the wall facing GZ. There were several additional $\frac{1}{64}$-in. cracks at the center of the floor slab.

(d) *Exit Chamber.* As in the case of structures RCa and RCb, short diagonal hairline cracks were formed at the corners of the openings in the walls. No damage could be observed in the roof and floor slab.

(e) *Exit Tunnel and Shaft.* A hairline crack was formed around the contraction joint between the main structure and the tunnel. No vertical movement was observed in the tunnel.

(f) *Doors.* All doors, including the emergency-exit hatch cover, were in operating condition after the test.

(g) *Ventilation.* The overpressure flap valve was found in a closed position after the test. The mechanical ventilation worked on "Auf" (open), but some leakage was observed in the "Zu" (closed) position.

3.2 INSTRUMENTATION TEST RESULTS

3.2.1 U. S. Pressure Instrumentation

The peak results of the pressure instrumentation provided by the FCDA and evaluated by members of Project 30.5c, are shown in Tables 3.1 to 3.4. The pressure-time curves for the instrumentation provided in the structures are shown in Figs. 3.102 to 3.105.

The results of the peak measurements of the blast-line pressure instrumentation located between structure RAa and 2667 yd from GZ are tabulated in Tables 3.5 and 3.6 and are shown in Fig. 1.4. In addition to the tabulated peak-pressure data as indicated above, the pressure-distance curves for peak side-on and corrected dynamic pressures that resulted along the blast line are given in Fig. 3.106. The pressure-time curves for the self-recording dynamic pressure gauges located at 500, 863, 981, and 1135 yd from GZ are indicated in Fig. 3.107. The definitions of the ordinate symbols for Figs. 3.105 and 3.107 are as follows:

$\Delta p_p^{*\prime}$ = total head pressure as measured
$\Delta p^\prime$ = side-on pressure as measured
$q_c^{*\prime}$ = dynamic pressure as measured
q^* = dynamic pressure (corrected)
M^* = Mach number

Figure 3.108 indicates the pressure-time curves for the electronic incident air-pressure (Wiancko) gauges that were located at 280, 300, 335, and 392 yd from GZ and the self-recording incident-pressure gauges at 280, 300, and 392 yd from GZ. The average pressure at the particular distance from GZ is as noted on the curve. Pressure-time curves for the self-recording incident-pressure gauges located at distances of 500, 863, 981, 1135, 1292, 1385, 1440, 1893, 2000, and 2667 yd from GZ are given in Fig. 3.109.

The pressure results obtained from the test are more fully defined by Project 30.5c, report WT-1536.

3.2.2 German Pressure Instrumentation

The results of the pressure measurements obtained from the five German gauges located near the blast line are summarized in Table 3.7. A full description of the results of these in-

struments is given by Project 30.5c in report WT-1536. Figures 3.110 to 3.116 show the condition of these gauges after recovery from their field locations.

3.2.3 Structural Response

The blast results of the structural-response equipment, as given in Table 2.1, are as indicated in Tables 3.8 to 3.10. No reliable data were obtained from the deflection gauges. Owing to the small magnitude of the deflections, the gauges themselves produced large errors. Figures 3.117 and 3.118 show the strain-time and acceleration-time curves, respectively, for the gauges within structures RAb and CAa. The complete results of the deflection, acceleration, and SR-4 strain gauges are given by Project 30.5c, report WT-1536.

3.2.4 Radiation Instrumentation

The results of the gamma film dosimeters are given in Figs. 3.119 to 3.121. The values of the radiation dosages as given in these figures are average values of several dosimeters located near the indicated values. These values indicate the total gamma-radiation dosage accumulated over an approximate 52-hr period. The total dose-distance curve for the gamma film dosimeters located along the blast line is given in Fig. 3.122. Table 3.11 indicates the results obtained by Project 39.1 from gamma-radiation chemical dosimeters placed along the blast line.

Three of the four sulfur and gold detectors placed in the German structures (Fig. 2.13) gave reliable results. In structure RAc, detector No. 170 gave readings of 3.362×10^9 and 2.317×10^{12} for the sulfur and gold-cadmium difference, respectively. In the exit chamber of the same structure detector No. 171 gave readings of 1.103×10^8 and 7.421×10^{10}. Of the two detectors placed in structure CAb only No. 173 was recovered. The readings obtained from this detector were 2.295×10^8 and 7.147×10^{11}. All readings are given in neutrons per square centimeter.

The results are fully defined by Projects 39.1, 39.1a, and 39.9 in reports WT-1500, WT-1466, and WT-1509, respectively.

3.3 GROUND SHOCK SPECTRA

Peak-displacement responses to shock of single-degree-of-freedom systems (reed gauges) of various natural frequencies are presented in Table 3.12 for shots Smoky, Whitney, Galileo, Charleston, and Stokes. As this table indicates, peak displacement of reed gauges of known frequencies was recorded near the surface in the free-field and in a shelter (structure RAc).

These records show that the horizontal (radial) measurements are generally less than one-half the vertical measurements. The horizontal displacements recorded in the shelter are approximately the same as those for the free-field gauges adjacent to the structure. However, the vertical displacements in the shelter were considerably less than the free-field measurements, indicating attenuations in the vertical direction. In all cases high accelerations are associated with high frequencies, and high displacements are associated with low frequencies.

Figures 3.123 and 3.124 are plots of vertical (Fig. 3.123) and horizontal (Fig. 3.124) displacements vs. frequency recorded at shots Smoky, Whitney, and Galileo for near-surface free-field values and values recorded inside the shelter during shot Smoky. This plot indicates that the data follow a consistent pattern.

3.4 ACCELERATION TEST

The results of the acceleration test, or Ensolite experiment, which are designed to investigate the transmission of structural acceleration to the blocks, indicated that acceleration was reduced by a factor of 3.

The peak acceleration and deflection values are indicated in Table 3.13. Figure 3.125 indicates the acceleration-time and displacement-time curves obtained from this test.

3.5 BIOLOGICAL TEST RESULTS

3.5.1 Environmental Test of Mice

(a) *General.* The mice were recovered from the seven structures two days after the test.

Upon recovery and examination of the mice, if death had occurred, the body and spleen weights were recorded, and the entire organism was fixed in buffered formalin. Average weights of the surviving animals for each location were taken daily by getting the total weight for each group and dividing by the number in the group.

(b) *Mortality.* The immediate mortality of the mice was confined to structure CAb. All the mice were found dead upon recovery. The cause of death was attributed to carbon monoxide poisoning produced by the gasoline generator that operated the air sampler. The cause of death was determined by a pathologist.

The location, number, time of recovery after the test, and time of death of the mice that died between their recovery and 20 days after the test are given in Table 3.14. The table also includes the 20 mice of structure CAb.

3.5.2 Dust-accumulation Test

(a) *General.* The experimental sticky-paper trays were recovered from the structures two days after the test. Table 3.15 indicates the type of collector and the times of exposure and recovery.

(b) *Paired Sticky-paper Collectors (Type B).* After recovery of the type B collectors, the transparent paper was stripped from the trays. At this time they were inspected and photographed.

Inspection and photographing of the samples revealed a definite variation in size and number of gross particles captured during the test in relation to the location from GZ of the various structures of the RA type. This variation, a decrease of particle size and number as the distance of the structure increased from GZ, is indicated in the experimental collector results shown in Figs. 3.126 to 3.129. Figure 3.130 is a photograph of a typical laboratory control collector before exposure to contamination.

Inspection of the trays revealed considerable amounts of very fine dust which was not evident from the photographs of the collectors of structures RAb, RAc, and RAd. The presence in the structures of this dust, which differed from the preshot contamination of the shelters, after the test was believed to be attributed to the fact that all conventional means of entrance remained airtight after the blast. In addition to the above-described source of the dust, small amounts of similar fine dust were found in the ventilation equipment when it was removed after the test.

The sticky-paper trays that were recovered from the RC structures produced minimum results. The variation, as clearly defined in the RA structures, was not fully evident in these structures. The photographic results of the type B collectors of the RC structures are shown in Figs. 3.131 to 3.133.

In the CA structures the variation of particle size and number, similar to that which occurred in the RA structures, clearly defined the location of the structures from GZ. Even though structure CAb was vacuum cleaned before the test, whereas structure CAa remained in its preshot condition, more hard concrete particles were found on the trays of the latter structure than were found in the former structure. The photographic data obtained from the CA structures are shown in Figs. 3.134 and 3.135.

(c) *Single Sticky-paper (Type C) and Sticky-resin (Type D) Collectors.* Upon recovery of the type C and D collectors, the tray contents were illuminated with ultraviolet light. The exposure to the light revealed no fluorescent particles. The trays were then placed over a beaker of hot glycerine to activate the fluorescent dye. Upon reexamination of the trays under an ultraviolet light, small fluorescent particles became visible to the naked eye. These particles varied in number from 20 to 50 for the various structures tested. The structures farther

away from GZ indicated more fluorescent particles on the trays than those structures closer to the detonation. It has been theorized that this phenomenon may have resulted from the thinner thickness of the members and earth cover of the structures farther away.

(d) *Air-sampler Collector (Type E).* Unfortunately the sampler was not in operation during the test. From the condition of the structure after the test, it appears that the air supply for the gasoline generator was insufficient. Therefore no results could be obtained from the test.

TABLE 3.1— CARLSON EARTH-PRESSURE
GAUGE MEASUREMENTS

Structure	Gauge No.	Peak value, psi	Remarks
RAb	P-1	167.0	Good record
	P-2	214.0	Good record
	P-3		Bad record
	P-4	14.0	Good record
	P-5	240.0	Good record
CAa	P-1	133.0	Good record
	P-2	282.0	Poor record
	P-3	38.0	Good record
	P-4	22.0	Good record
RCa	P-1	12.6	Good record
	P-2	16.6	Good record
	P-3	11.3	Good record
	P-4	13.9	Good record
	P-5		No record

TABLE 3.2— WIANCKO AIR-PRESSURE GAUGE
MEASUREMENTS

Structure	Gauge No.	Peak value, psi	Remarks
RAb	Pt-1	125.0	Good record
	Pt-2		Poor record
	Pt-3	140.0	Good record
	Pt-4	165.0	Good record
CAa	Pt-1		Questionable record
	Pt-2	85.0	Poor record
	Pt-3		Questionable record
RCa	Pt-1	12.6	Good record
	Pt-2		Questionable record
	Pt-3	19.0	Good record
	Pt-4	10.4	Good record

TABLE 3.3— ELECTRONIC AND SELF-RECORDING
DYNAMIC PRESSURE GAUGE MEASUREMENTS

Structure	Gauge No.*	Peak value, psi	Remarks
RAa	$\overline{Q}$ (T)		No records: gauge
	$\overline{Q}$ (S)		nose 30 ft from mount
RAb	Q (D)	230.0	Good record
	Q (S)		Poor record
RAc	$\overline{Q}$ (T)		Questionable record
	$\overline{Q}$ (S)	167.3	Poor record
RAd	$\overline{Q}$ (T)	79.0	Questionable record
	$\overline{Q}$ (S)	76.5	Questionable record
RCa	Q (D)		No record
	Q (S)	13.4	Good record
RCb	$\overline{Q}$ (T)	22.0	Poor records: gauges
	$\overline{Q}$ (S)	17.1	stopped
RCc	$\overline{Q}$ (T)	8.1	Poor record
	$\overline{Q}$ (S)	7.8	Poor record

*Q, electronic gauge; $\overline{Q}$, self-recording gauge; (T), total pressure = side-on plus dynamic; (S), side-on; (D), dynamic.

TABLE 3.4— BRL SELF-RECORDING PRESSURE
GAUGE MEASUREMENTS

Structure	Gauge No.	Peak value, psi	Remarks
RAa	$\overline{P}$-1	155.0	Good record
	$\overline{P}$-2		No record
	$\overline{P}$-3		No pressure
	$\overline{P}$-4	28.2	Peak pressure
	$\overline{P}$-5	96.0	Good record
	$\overline{P}$-6	195.0	Good record
	$\overline{P}$-7	190.0	Good record
RAb	$\overline{P}$-1	143.0	Good record
	$\overline{P}$-2	3.5	Peak pressure
	$\overline{P}$-3	2.15	Good record
	$\overline{P}$-4	12.6	Good record
	$\overline{P}$-5	68.0	Good record
	$\overline{P}$-6	250.0	Good record
	$\overline{P}$-7	245.0	Good record
	$\overline{P}$-8	110.0	Good record
	$\overline{P}$-9	150.0	Good record
RAc	$\overline{P}$-1	75.0	Good record
	$\overline{P}$-2	2.2	Peak pressure
	$\overline{P}$-3	1.7	Good record
	$\overline{P}$-4	14.3	Good record
	$\overline{P}$-5	38.5	Good record
	$\overline{P}$-6	150.0	Good record
	$\overline{P}$-7	110.0	Good record
	VLP-7	0.2	Peak pressure
RAd	$\overline{P}$-1	50.0	Good record
	$\overline{P}$-4	14.1	Good record
	$\overline{P}$-5	32.0	Good record
	$\overline{P}$-6	112.0	Good record
	$\overline{P}$-7	70.0	Good record

TABLE 3.4 — (Continued)

Structure	Gauge No.	Peak value, psi	Remarks
CAa	$\overline{P}$-1	107.0	Good record
	$\overline{P}$-2	96.0	Good record
	$\overline{P}$-3		No pressure inside
	$\overline{P}$-4	3.0	Peak pressure
	$\overline{P}$-5	62.0	Good record
CAb	$\overline{P}$-1	104.0	Good record
	$\overline{P}$-2	100.0	Good record
	$\overline{P}$-3		No record
	$\overline{P}$-4	1.9	Good record
	$\overline{P}$-5	60.0	Good record
	VLP	0.19	Good record
RCa	$\overline{P}$-1	17.0	Good record
	$\overline{P}$-2	0.87	Questionable record
	$\overline{P}$-3		No record
	$\overline{P}$-4	0.44	Questionable record
	$\overline{P}$-5	21.5	Good record
	$\overline{P}$-6	17.5	Good record
RCb	$\overline{P}$-1	4.6	Good record
	$\overline{P}$-2		No record
	$\overline{P}$-3	1.9	Good record
	$\overline{P}$-4	0.3	Peak pressure
	$\overline{P}$-5	20.0	Good record
	$\overline{P}$-6	10.5	Good record
RCc	$\overline{P}$-1	7.1	Good record
	$\overline{P}$-3	1.7	Good record
	$\overline{P}$-5	10.0	Good record
	$\overline{P}$-6	5.2	Good record

TABLE 3.5—BLAST-LINE MEASUREMENTS OF PEAK OVERPRESSURE

Distance from GZ, yd	Type of gauge	Peak pressure, psi	Remarks
280	Self-recording	175.0	Poor record
	Electronic	165.0	Good record
300	Self-recording	165.0	Good record
	Electronic	145.0	Good record
	German	166	Peak pressure
335	Self-recording	116.0	Peak only
	Electronic	110.0	Good record
	German	101	Peak pressure
392	Self-recording	81.0	Good record
	Electronic	75.0	Good record
	German	59	Peak pressure
500	Self-recording	44.5	Good record
590		26.0	From pressure-distance curve
672	Electronic	18.2	Peak only
	German	18.2, 22.7	Peak pressure
810		11.5	From pressure-distance curve
863	Self-recording	8.8	Good record
	German	11.5, 14.2	Peak pressure
981	Self-recording	10.4	Good record
1135	Self-recording	6.4	Good record
1292	Self-recording	7.2	Good record
1385	Self-recording	6.3	Good record
1440	Self-recording	7.2	Good record
1893	Self-recording	4.9	Good record
2000	Self-recording	4.6	Good record
2667	Self-recording	2.8	Good record

TABLE 3.6—BLAST-LINE MEASUREMENTS
OF PEAK DYNAMIC PRESSURE

Structure	Distance from GZ, yd	Max. dynamic pressure* (corrected), psi
RAa	280	360.0
RAb and CAa	300	320.0
RAc and CAb	335	280.0
RAd	392	230.0
RCa	590	74.0
RCb	810	28.0
RCc	1440	1.5

* Taken from Fig. 3.106.

TABLE 3.7—GERMAN PEAK-PRESSURE GAUGE MEASUREMENTS

Location from GZ, yd	Gauge No.	Paper diaphragm type	Smallest hole size perforated	Peak pressure, psi	Pressure meter		Remarks
					Membrane No.	Displacement, mm	
300	FW–E700 MD2	White	No. 9 (both)	166	MDI-3 MDI-4	26.6 64.9	Filled with sand and stones. Both dosimeters cut, one of the halves missing. Only one No. 8 hole slit. All spacer tubes intact. Protective shield indicates severe sand-blasting.
335	FW–E700 MD1	White	No. 7 (both)	101	MDI-1 MDI-2	13.7 20.5	Filled with sand and stones. Dosimeters dented badly. MDI-1 assembly very loose in upper plate. Protective shield gone. All spacer tubes sheared.
392	FW–E700 MD3	Yellow	No. 11 (both)	59	MDI-5 MDI-6	12.6 24.2	Filled with sand and stones. One dosimeter severed, both dented. One No. 12 hole punctured by sand (pin hole). Shield gauge and one spacer tube sheared.
672	FW–E700 MD4	Yellow	Nos. 6 and 7 (one each)	18.2 22.7	MDI-7 MDI-8	9.6 16.0	Filled with sand and stones. MDI-8 assembly loose. Sand apparently punctured holes, Nos. 6, 8, 9, and 10 in size. Protective shield gone. All spacer tubes sheared.
863	FW–E700 MD5	Yellow	Nos. 4 and 5 (two each)	11.5 14.2	MDI-9 MDI-10	11.4 4.0	Sand and stones in holes. Both No. 5 holes apparently punctured by sand. One No. 7 and one No. 8 with pin-hole puncture. One spacer tube sheared.

TABLE 3.8 — SCRATCH-GAUGE MEASUREMENTS

Gauge No.	Member	Angle of gauge to member	Length of scratch, in.	Deflection of member, in.
$\bar{D}$-1	Roof	49°	0.07	0.053
$\bar{D}$-2	Floor	49°	0.10	0.076
$\bar{D}$-3	Wall	69°	0.08	0.075
$\bar{D}$-4	Door	63°	0.46*	

*Includes thickness of rubber gasket.

TABLE 3.9 — ACCELERATION GAUGE MEASUREMENTS

Structure	Gauge No.	Peak value, g*	Remarks
RAb	A-1	−14.5 +8.5	Good record
CAa	A-1	−11.5 +9.5	Good record
RCa	A-1	+1.6	Questionable record

*Upward direction is (+).

TABLE 3.10 — SR-4 STRAIN-GAUGE MEASUREMENTS

Structure	Gauge No.	Peak values, (in./in.) $\times 10^{-3}$*	Remarks
RAb	S-1	+0.33 −0.04	Good record
	S-2	−0.38	Good record
	S-3	−0.80	Good record
	S-4	+1.80 −1.50	Good record
CAa	S-1	−0.46	Partial record
RCa	S-1		No record
	S-2		No record
	S-3		Questionable record

*Positive (+) = tension; negative (−) = compression.

TABLE 3.11—BLAST-LINE GOAL-POST DATA*

Range, yd	Slant range (D), yd	D^2	Dose, r	RD^2
400	466			Lost
600	649			Lost
800	841			Lost
1000	1034			Lost
1200	1229	1.51×10^6	2870	4.33×10^9
1400	1426	2.03×10^6	2235	4.54×10^9
1500	1525	2.33×10^6	1700	3.96×10^9
1600	1623	2.63×10^6	1480	3.89×10^9
1700	1722	2.97×10^6	1420	4.22×10^9
1800	1821	3.32×10^6	1150	3.82×10^9
1900	1920	3.69×10^6	1325	4.89×10^9
2000	2019	4.08×10^6	1000	4.08×10^9

* Not plotted, results contaminated by fallout, recovery D + 3 days.

TABLE 3.12—DISPLACEMENT SHOCK SPECTRUM

Radial direction*				Vertical direction*			
f, cycles/sec	D, in.	f, cycles/sec	D, in.	f, cycles/sec	D, in.	f, cycles/sec	D, in.
Gauge 1		Gauge 3		Gauge 2		Gauge 4	
2.56		2.66	0.199	2.56	0.710	2.74	0.516
8.82	0.137	8.87	0.0260	8.82	0.569	9.66	0.440
22.0	0.0318	22.2	0.0248	22.0	0.101	20.4	0.165
36.0	0.0451	36.5	0.0093	36.0	0.0498	32.8	0.0633
90.0	0.0231	92.0	0.0074	90.0	0.0385	88.0	0.0560
134	0.0056	132	0.0018	131	0.0128	133	0.0309
184	0.0121	176	0.0017	179	0.0088	185	0.0154
228	0.0027	224	0.0020	209	0.0030	220	0.0066
269	0.0065	279		268	0.0027	265	0.0026
339		312		303	0.0033	293	0.0012

Shot Stokes, surface, 33-psi overpressure

Radial direction*				Vertical direction*			
Gauge 5				Gauge 6			
2.72	2.25			2.54	1.62		
9.37	0.453			8.72	0.906		
22.3	0.113			21.9	0.336		
36.9	0.0451			37.0	0.0744		
95.0	0.0185			92.0	0.0167		
138	0.0101			138	0.0099		
184	0.0099			185	0.0034		
234	0.0041			246	0.0051		
285	0.0022			280	0.0039		
296	0.0031			363	0.0038		

Shot Smoky, inside shelter, 116-psi overpressure

TABLE 3.12— (Continued)

Radial direction*				Vertical direction*			
f, cycles/sec	D, in.	f, cycles/sec	D, in.	f, cycles/sec	D, in.	f, cycles/sec	D, in.

Shot Smoky, surface, 116-psi overpressure

Gauge 9				Gauge 7		Gauge 8	
2.55	1.95			2.60	5.45	2.53	4.53
9.12	0.359			8.56	1.52	8.82	1.46
22.4	0.189			22.4	0.845	22.6	0.525
33.9	0.131			37.4	0.254	37.1	0.205
93.0	0.0227			91.0	0.132	93.0	0.103
107	0.0149			132	0.0673	137	0.0450
181	0.0107			187	0.0221	180	0.0199
203	0.0042			238	0.0106	236	0.0122
293	0.0055			280	0.0112	294	0.0055
357	0.0027			335	0.0066	328	0.0066

Shot Galileo, surface, 130-psi overpressure

Gauge 11				Gauge 10		Gauge 12	
2.35	0.653			2.48	4.10	2.47	4.25
8.63	0.377			8.26	0.946	8.23	1.22
22.5	0.164			22.7	0.320	21.0	0.475
36.5	0.0453			37.1	0.314	35.0	0.280
95.0	0.0349			94.0	0.140	94.0	0.121
138	0.0184			138	0.0441	136	0.0267
186	0.0103			187	0.0446	178	0.0442
237	0.0032			234	0.0098	229	0.0161
294	0.0046			272	0.0139	300	0.0121
317	0.0029			365	0.0046	339	0.0053

Shot Whitney, surface, 146-psi overpressure

Gauge 4†				Gauge 3†			
2.74	1.60			2.66	3.10		
9.66	0.260			8.87	1.47		
20.4	0.119			22.2	0.788		
32.8	0.0834			36.5	0.348		
86.0	0.0187			92.0	0.141		
134	0.0118			132	0.0992		
185	0.0088			176	0.0402		
220	0.0064			227	0.0090		
269	0.0026			284	0.0152		
314	0.0054			330	0.0080		

TABLE 3.12— (Continued)

Radial direction*				Vertical direction*			
f, cycles/sec	D, in.	f, cycles/sec	D, in.	f, cycles/sec	D, in.	f, cycles/sec	D, in.

Shot Charleston, surface‡

Gauge 5 (20-psi overpressure)		Gauge 9 (18-psi overpressure)		Gauge 6 (20-psi overpressure)		Gauge 8 (18-psi overpressure)	
2.72	0.263	2.55	0.265	2.54		2.53	0.728
9.37	0.111	9.12	0.0838	8.72	0.280	8.82	0.368
22.3	0.0900	22.4	0.0691	21.9	0.221	22.6	0.194
36.9	0.0404	33.9		37.0		37.1	0.0828
95.0	0.0190	93.0	0.0096	92.0	0.0246	93.0	0.0208
138	0.0100	107	0.0050	138	0.0093	137	0.0048
184	0.0014	181	0.0023	185	0.0062	180	0.0025
234	0.0030	203	0.0020	246	0.0023	236	0.0015
285	0.0026	293	0.0019	280	0.0023	294	0.0015
296	0.0020	357	0.0009	363	0.0007	328	0.0016

Gauge 11 (15-psi overpressure)				Gauge 10 (15-psi overpressure)		Gauge 12 (12-psi overpressure)	
2.35	0.879			2.48	0.407	2.47	0.492
8.63	0.262			8.26	0.163	8.23	0.177
22.5	0.195			22.7	0.0726	21.0	0.207
36.5	0.0804			37.1	0.0231	35.0	0.0786
95.0	0.0246			94.0		94.0	0.0193
138	0.0033			138		136	0.0101
186	0.0020			187		178	0.0053
237	0.0019			234		229	0.0005
294	0.0011			272		300	
317	0.0007			365	0.0009	339	0.0006

*f, natural frequency; D, peak displacement.

† Canister tops were about 18 in. below ground level in hard ground. Two other gauges bolted to concrete pads in the same vicinity were knocked loose, and the data were lost.

‡ Tangential direction for gauge 7 (20-psi overpressure): insignificant displacement.

87

TABLE 3.13— ENSOLITE EXPERIMENT DATA (STRUCTURE RAc)

Location of gauge	Direction of measurement	Measurement	Gauge No.	Maximum value*
Boot (3-in. Ensolite)	Vertical	Acceleration	A-1	+3.1 g −2.1 g
Boot (concrete floor)	Vertical	Acceleration	A-2	+9.8 g −2.2 g
Boot ($1\frac{1}{2}$-in. Ensolite)	Vertical	Acceleration	A-3	+3.7 g −1.8 g
Concrete Floor	Vertical	Acceleration	A-4	−6.6 g +4.8 g
Concrete Floor	Horizontal	Acceleration	A-5	+2.8 g −1.8 g
Boot ($1\frac{1}{2}$-in. Ensolite)	Vertical	Deflection	D-1	−1.5 in. +0.65 in.

* Horizontal positive (+) acceleration−movement of floor slab toward GZ. Vertical positive (+) acceleration−movement of floor slab upward.

TABLE 3.14— MORTALITY RESULTS OF BIOLOGICAL TEST

Structure	Time of recovery, days after the test	Number and time of death
RAa	2	1 on 1 day after recovery; 1 on 14 days after recovery
RAc	2	None
RAd	2	None
CAb	2	20 before recovery
RCa	2	None
RCb	2	None
RCc	2	None

TABLE 3.15— EXPOSURE AND RECOVERY OF DUST COLLECTORS*

Structure	Dust collector	Day of final preparation of structure	Day exposed or recovered			
			Control collectors		Experimental collectors	
			Exposed	Recovered	Exposed	Recovered
RAa	B	D-1	D-14	D-13	D-3	D+2
	C				D-3	D+2
	D				D-3	D+2
RAb	B	D-1	D-14	D-13	D-3	D+2
RAc	B	D-1	D-14	D-13	D-1	D+2
	B		D-3	D-1		
RAd	B	D-1	D-14	D-13	D-3	D+2
	C				D-3	D+2
	D				D-3	D+2
CAa	B	D-1	D-14	D-13	D-3	D+2
CAb	B	D-1	D-14	D-13	D-1	D+2
	C				D-1	D+2
	D				D-1	D+2
	E				D-1	D+12
RCa	B	D-1	D-14	D-13	D-1	D+2
	B		D-3	D-1		
RCb	B	D-1	D-14	D-13	D-1	D+2
	C				D-1	D+2
	D				D-1	D+2
RCc	B	D-1	D-14	D-13	D-1	D+2
	B		D-3	D-1		

* D—, days before test; D +, days after test.
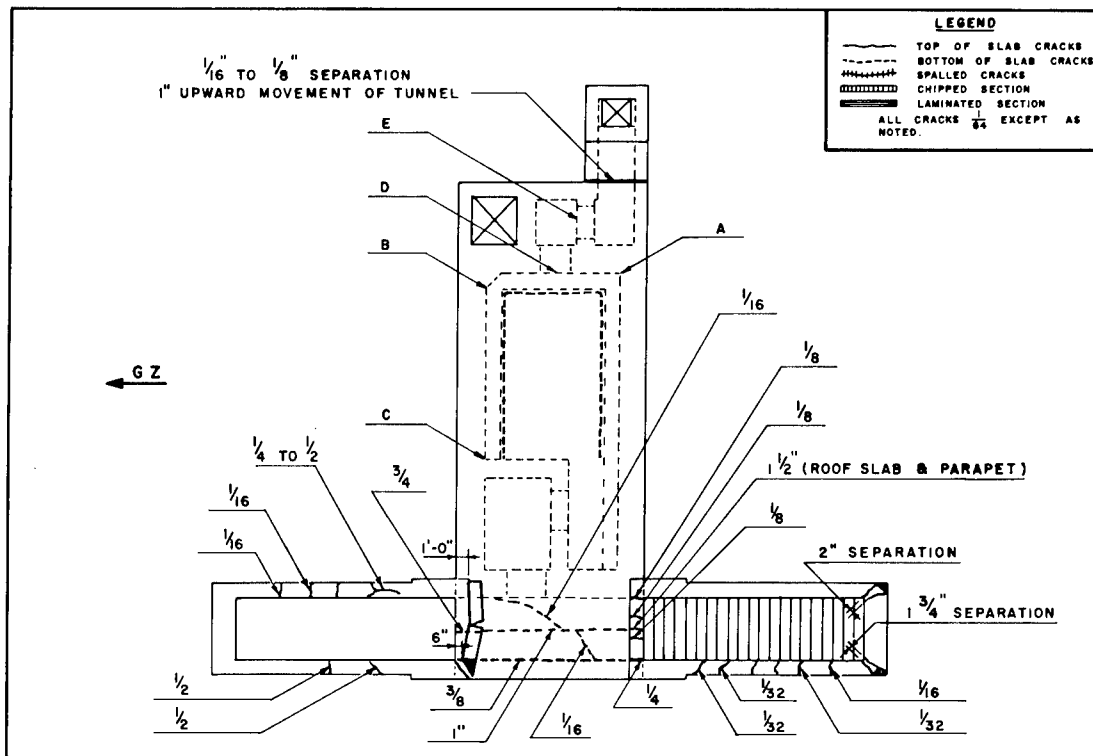
Fig. 3.1—Roof-slab crack pattern (structure RAa).
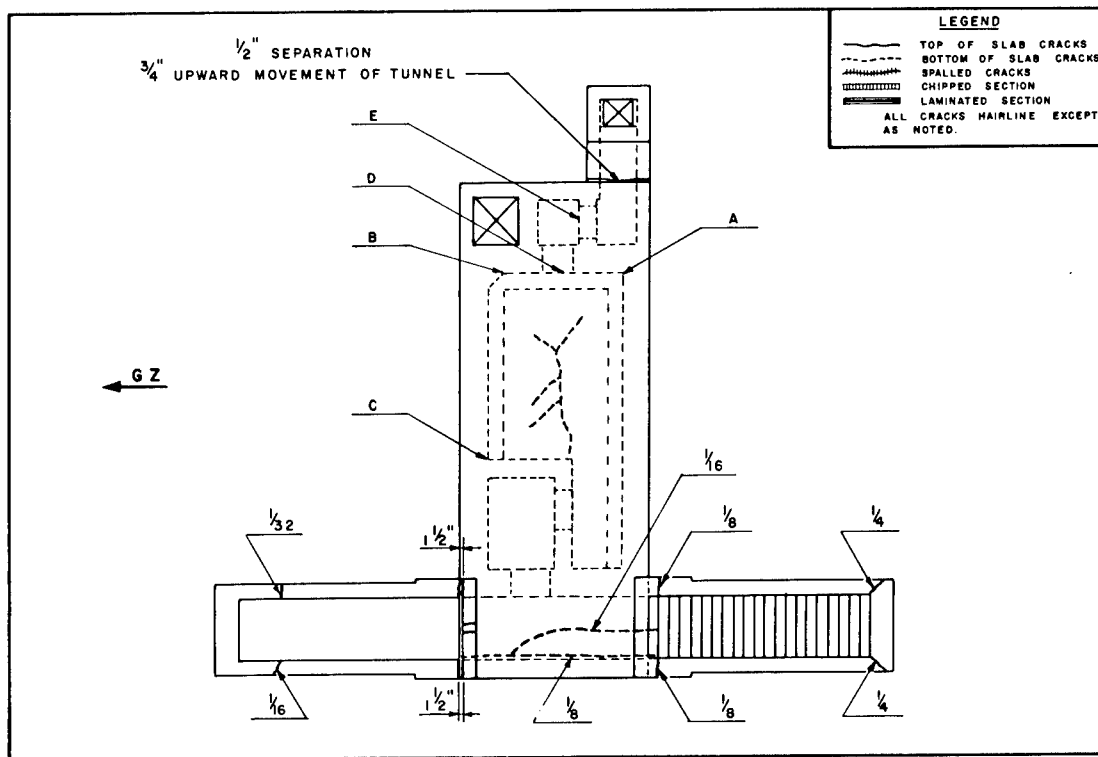
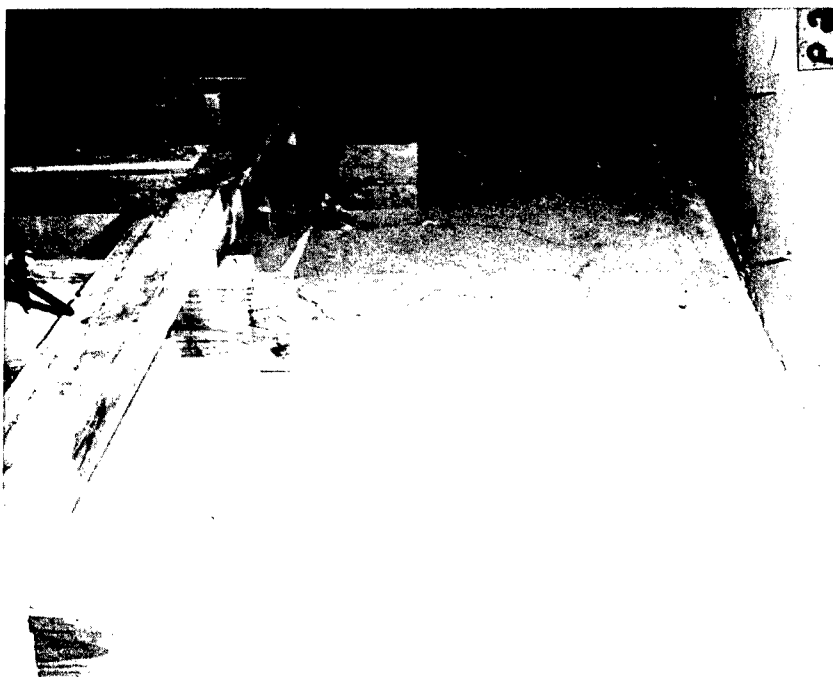

Fig. 3.2—Floor-slab crack pattern (structure RAa).
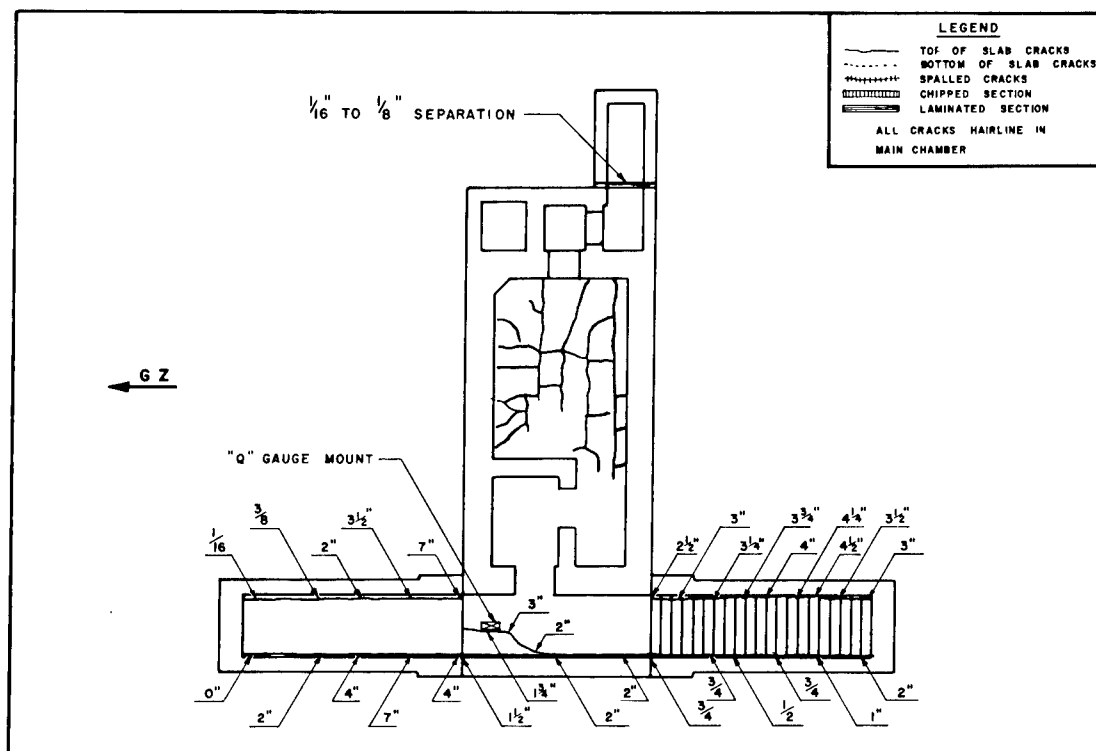
Fig. 3.3—Entrance crack pattern (structure RAa).
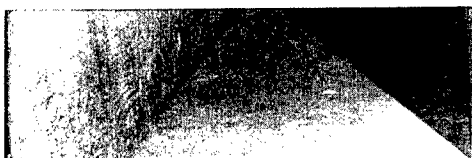
Fig. 3.4—Floor slab of main chamber looking toward the main entrance (structure RAa).
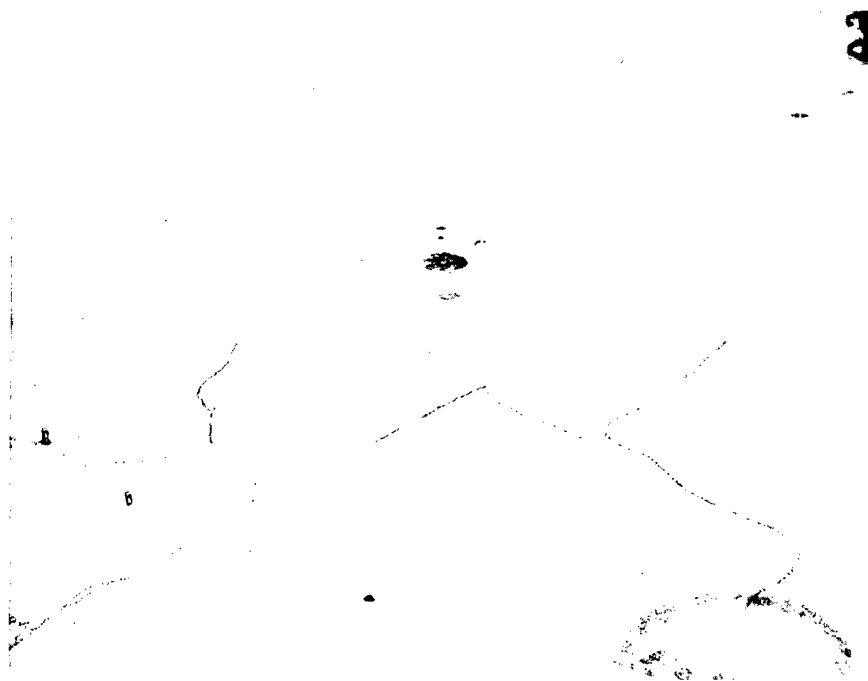
Fig. 3.5—Floor slab of main chamber looking toward the emergency exit (structure RAa).

Fig. 3.6—Center of main-chamber roof slab (structure RAa). Note survey point X-6.

Fig. 3.7—Bottom of emergency-exit shaft (structure RAa). Note debris and sand bags in shaft.
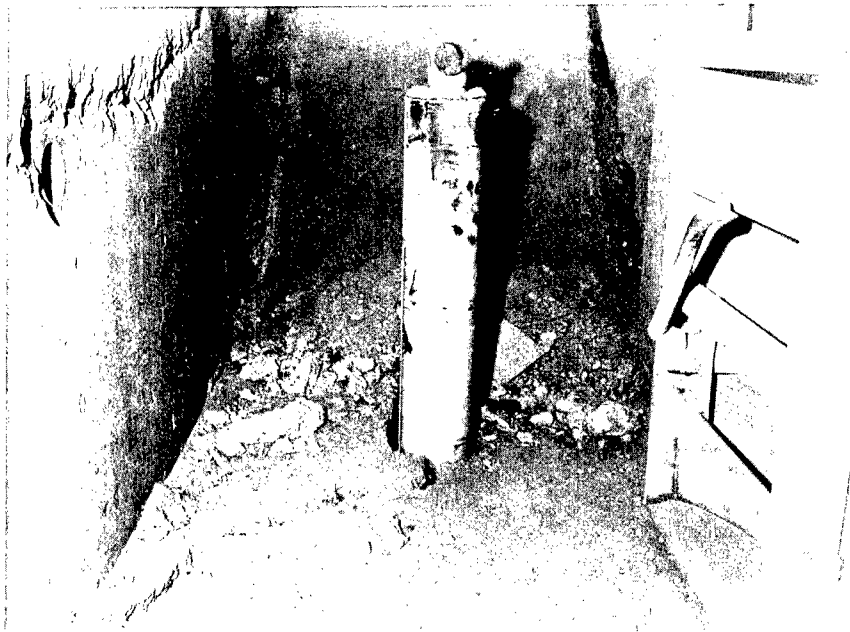
Fig. 3.8—Landing floor slab looking toward GZ (structure RAa). Note debris at bottom of ramp before cleaning.

Fig. 3.9—Cracks along center of landing roof slab and at intersection with exterior wall (structure RAa).

Fig. 3.10—Looking up stairs away from GZ (structure RAa).
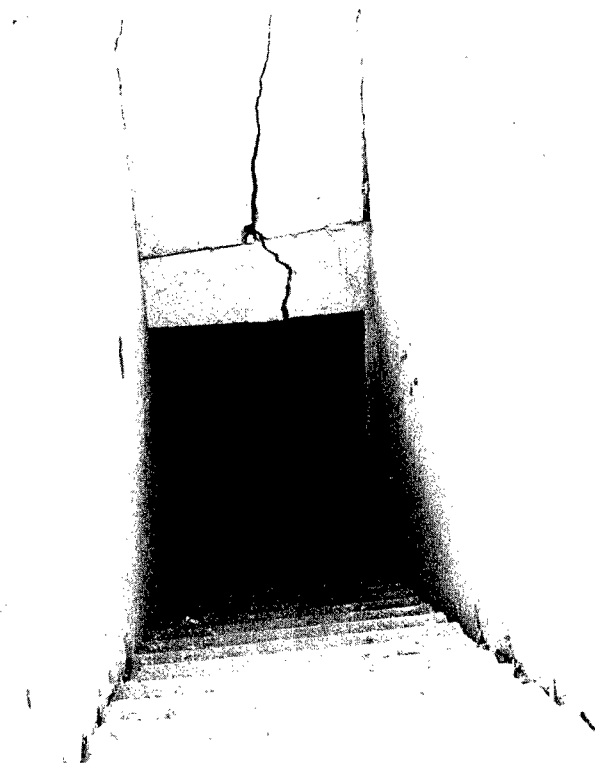
Fig. 3.11—Cracks in parapet wall and end of landing roof slab at entrance facing away from GZ (structure RAa).
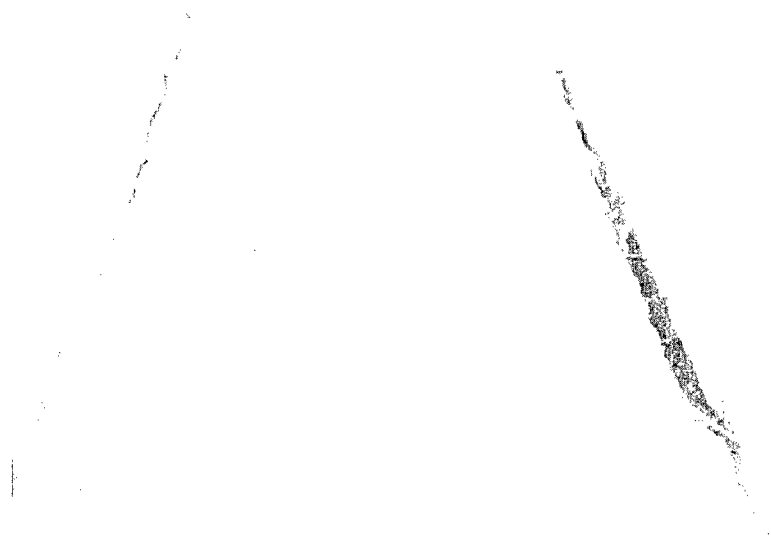
Fig. 3.12—Details of separations between ramp slab and interior and exterior walls facing toward GZ (structure RAa).
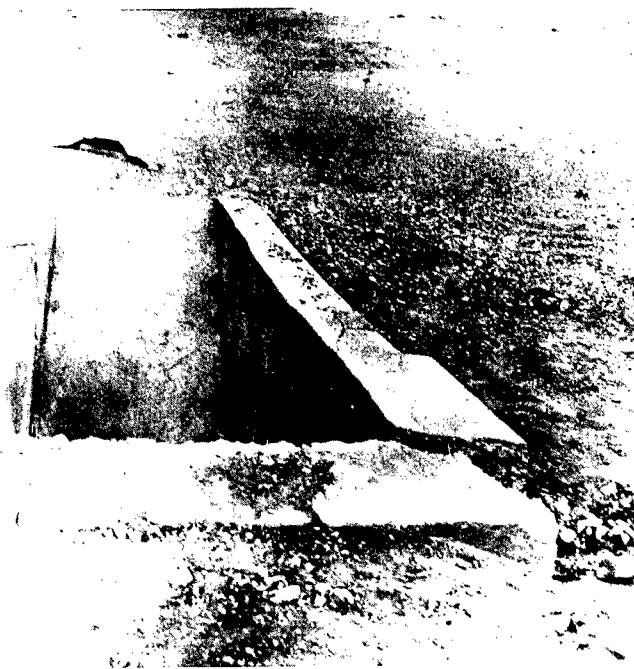
Fig. 3.13—Blast damage to ramp walls of entrance facing GZ (structure RAa).
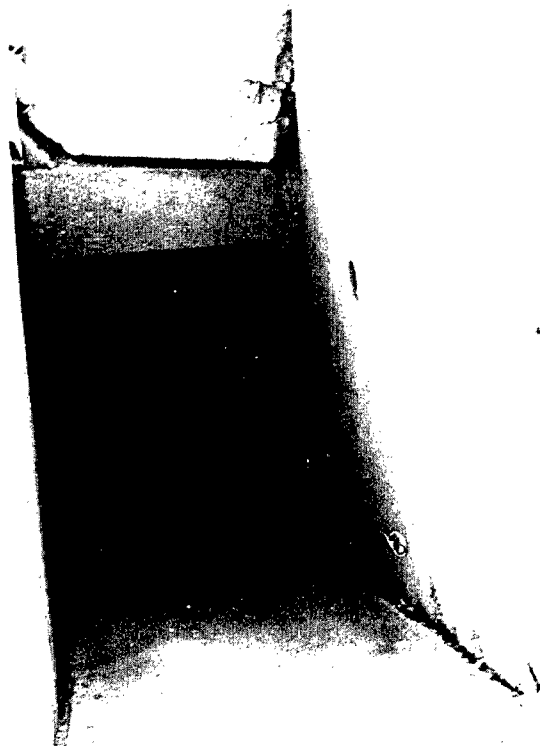
Fig. 3.14—Blast damage of parapet wall, exterior wall, and ramp on entrance facing toward GZ (structure RAa).

Fig. 3.15—Blast damage at intersection of interior wall and parapet wall facing toward GZ. (structure RAa).

Fig. 3.16 — Detail of cracks and spalled and laminated area in interior wall at contraction joint at entrance facing toward GZ (structure RAa).

Fig. 3.17 — Detail of crack at intersection of exterior wall and parapet wall facing toward GZ (structure RAa).
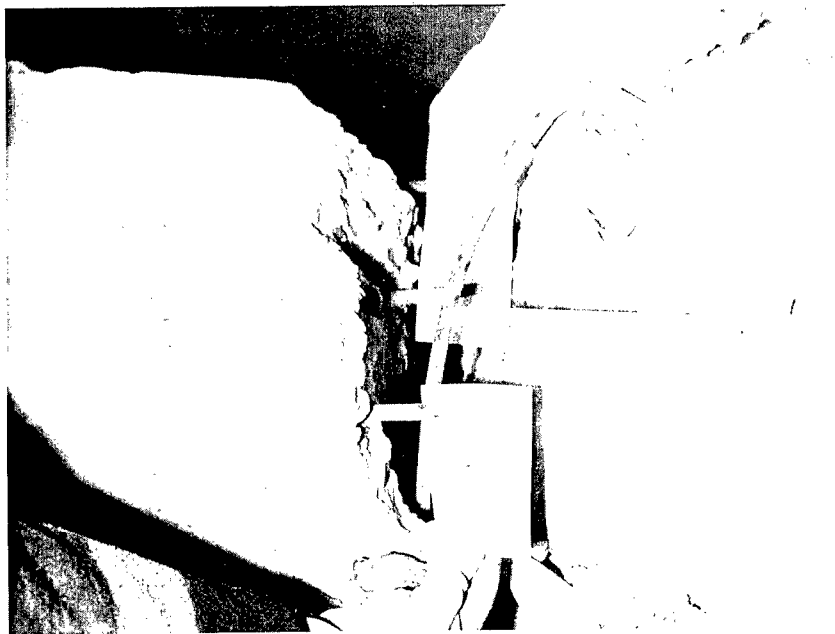
Fig. 3.18—Detail of necked-down reinforcement at intersection of exterior wall and parapet wall facing toward GZ (structure RAa).
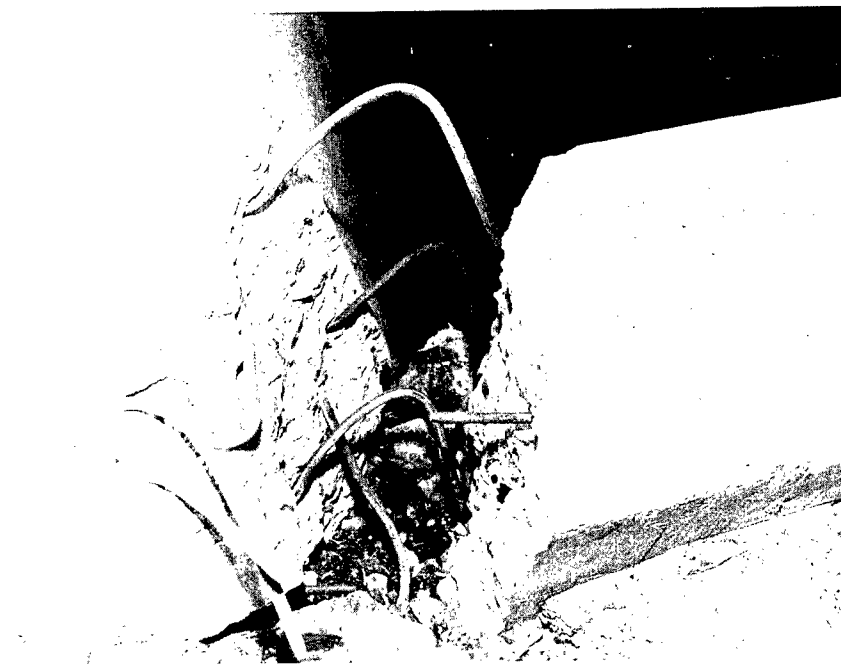
Fig. 3.19—Detail of crack at intersection of interior wall and parapet wall facing toward GZ (structure RAa).

Fig. 3.20—Detail of necked-down reinforcement torn from parapet at interior wall (structure RAa).

Fig. 3.21—Detail of necked-down reinforcement torn from interior wall at parapet (structure RAa).

Fig. 3.22—Detail of exposed reinforcement after chipping at corner of interior wall and parapet facing toward GZ (structure RAa).
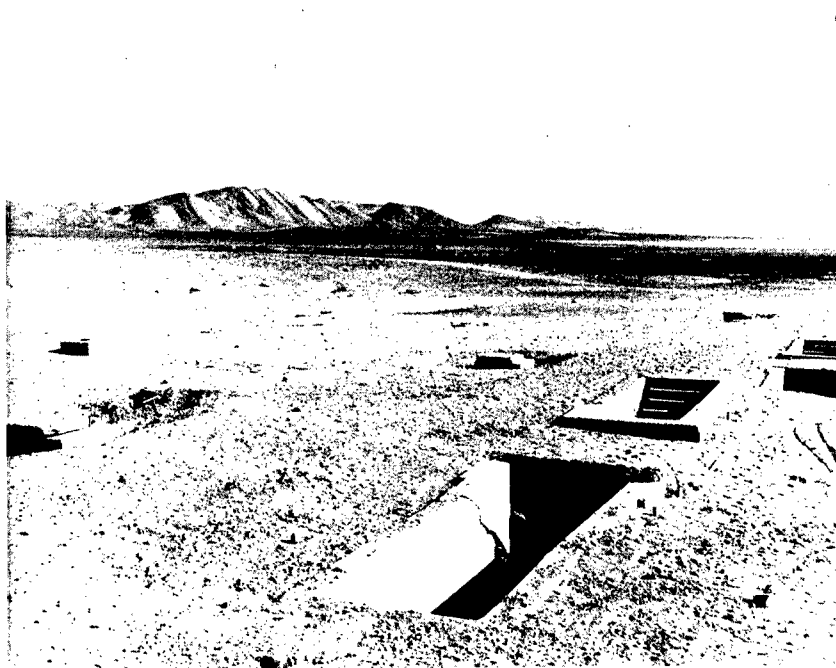
Fig. 3.23—Above-ground portion of ventilation shaft and main entrance (structure RAa).

Fig. 3.24—Emergency-exit shaft (structure RAa).
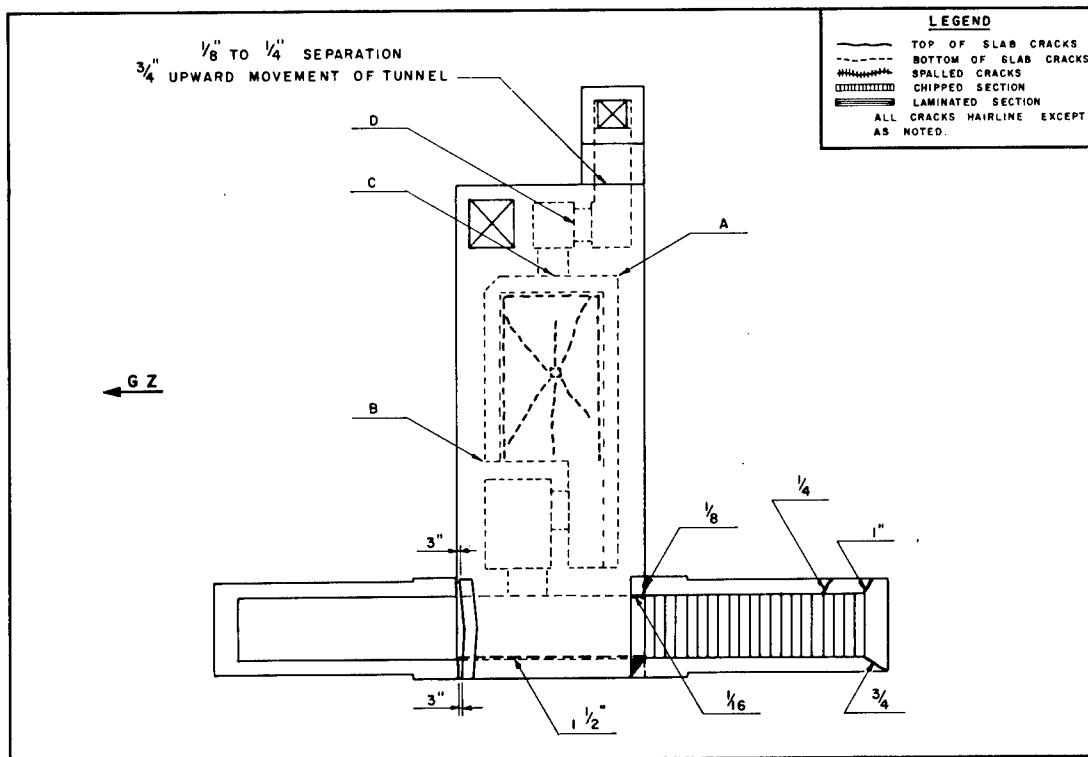
Fig. 3.25—Roof-slab crack pattern (structure RAb).
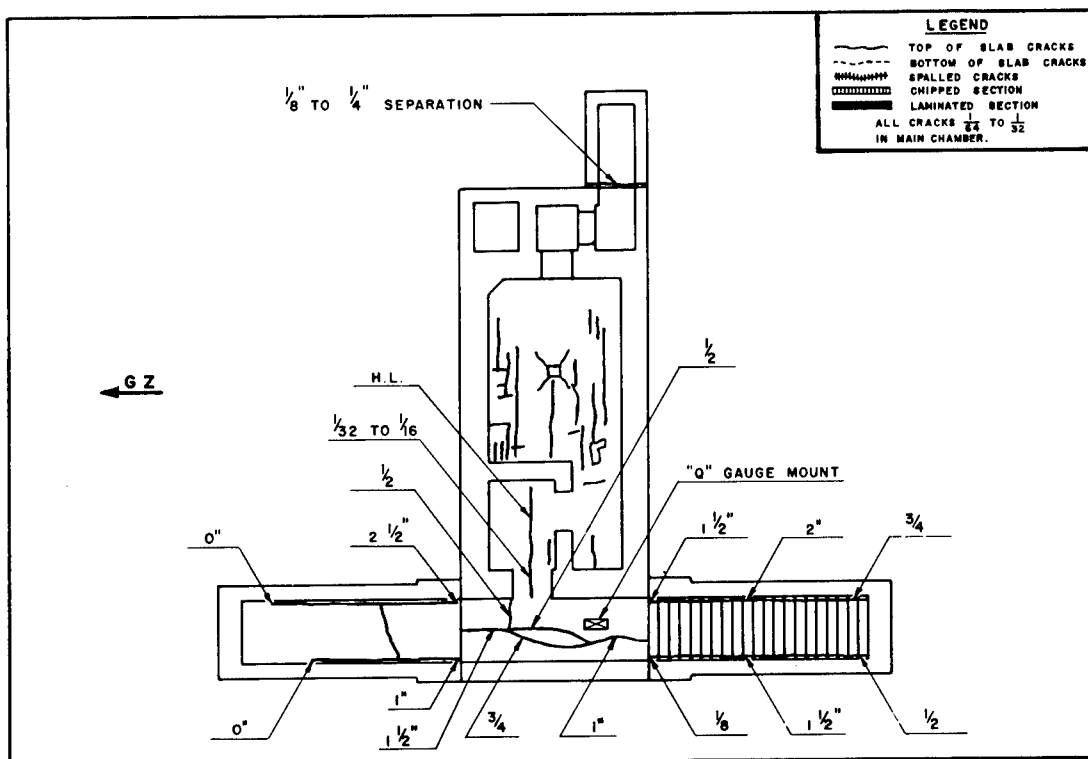
Fig. 3.26—Floor-slab crack pattern (structure RAb).

Fig. 3.27—Entrance crack pattern (structure RAb).
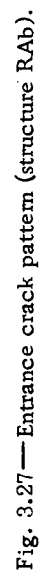
Fig. 3.28—Cracks in floor slab of main chamber, looking toward main entrance (structure RAb).

Fig. 3.29—Cracks, strain-gauge recess, and survey point in roof slab of main chamber (structure RAb).
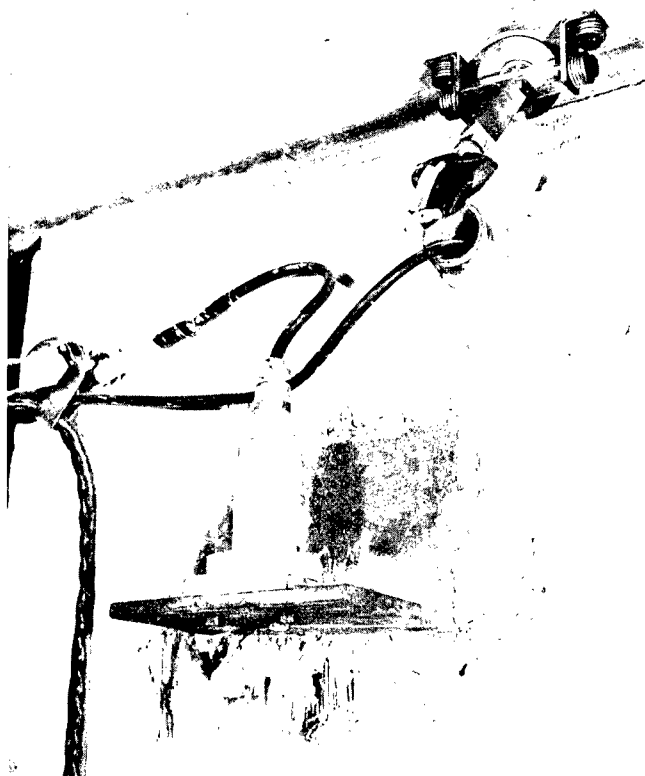
Fig. 3.30—Close-up of accelerometer and displacement gauge tie point (structure RAb).
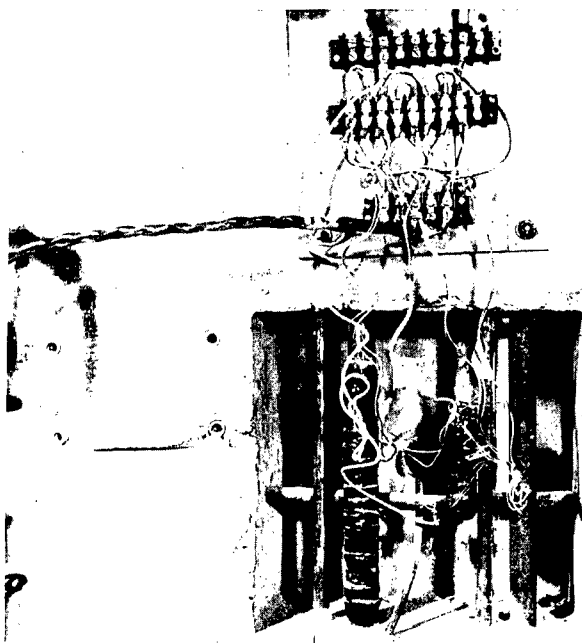
Fig. 3.31—Close-up of strain gauge in side wall of main chamber (structure RAb).
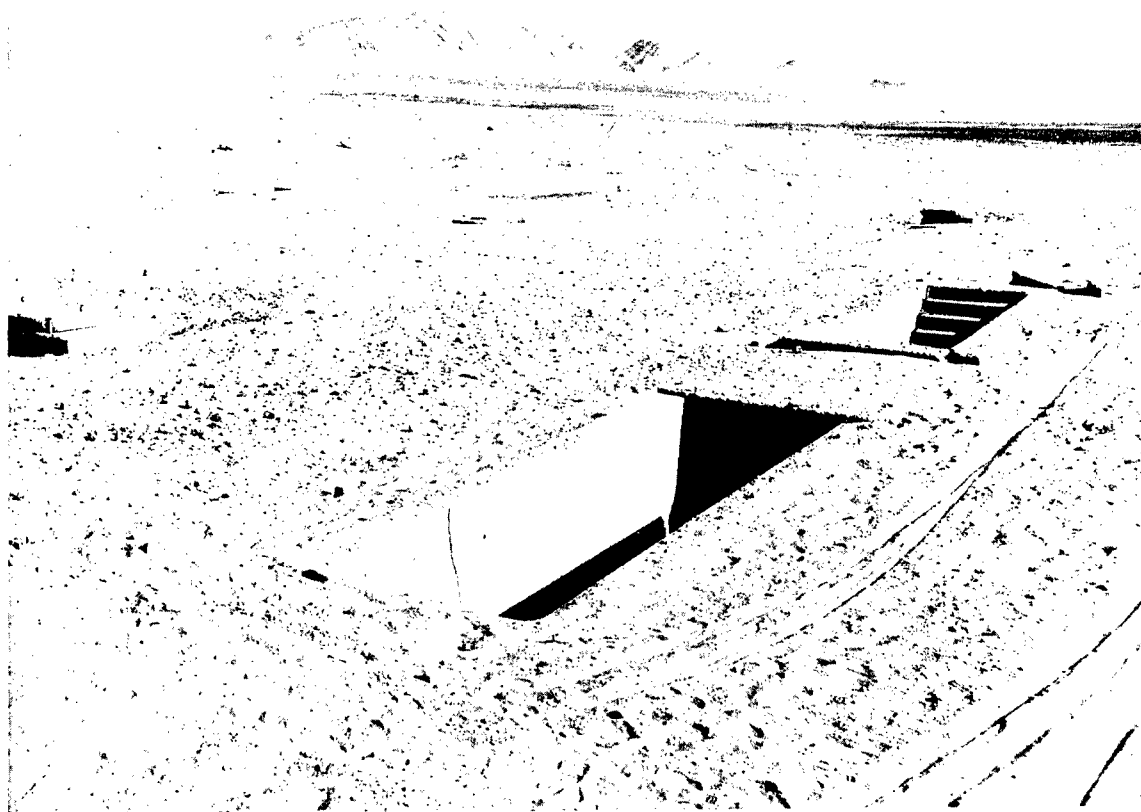
Fig. 3.32—Above-ground portion of ventilation shaft and main entrance (structure RAb).

LEGEND

	TOP OF SLAB CRACKS
	BOTTOM OF SLAB CRACKS
	SPALLED CRACKS
	CHIPPED SECTION
	LAMINATED SECTION
	ALL CRACKS HAIRLINE EXCEPT AS NOTED.

Fig. 3.33—Roof-slab crack pattern (structure RAc).

LEGEND

	TOP OF SLAB CRACKS
	BOTTOM OF SLAB CRACKS
	SPALLED CRACKS
	CHIPPED SECTION
	LAMINATED SECTION
	ALL CRACKS HAIRLINE TO $\frac{1}{16}$ IN MAIN CHAMBER

Fig. 3.34—Floor-slab crack pattern (structure RAc).
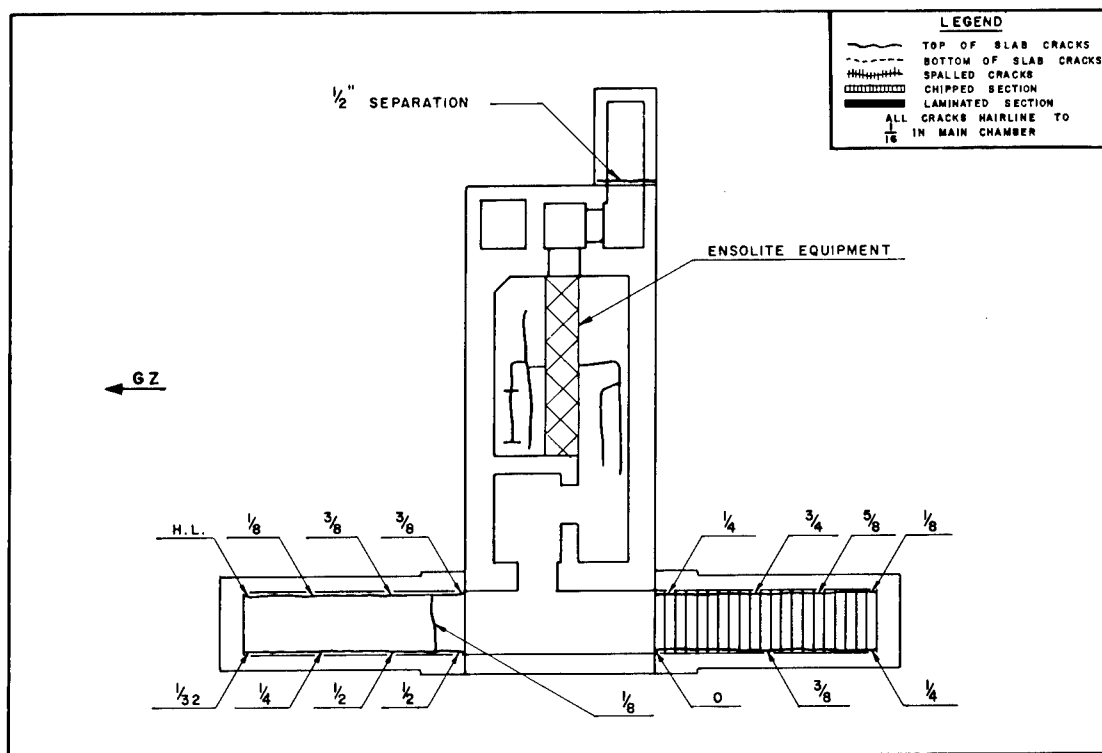
Fig. 3.35—Entrance crack pattern (structure RAc).
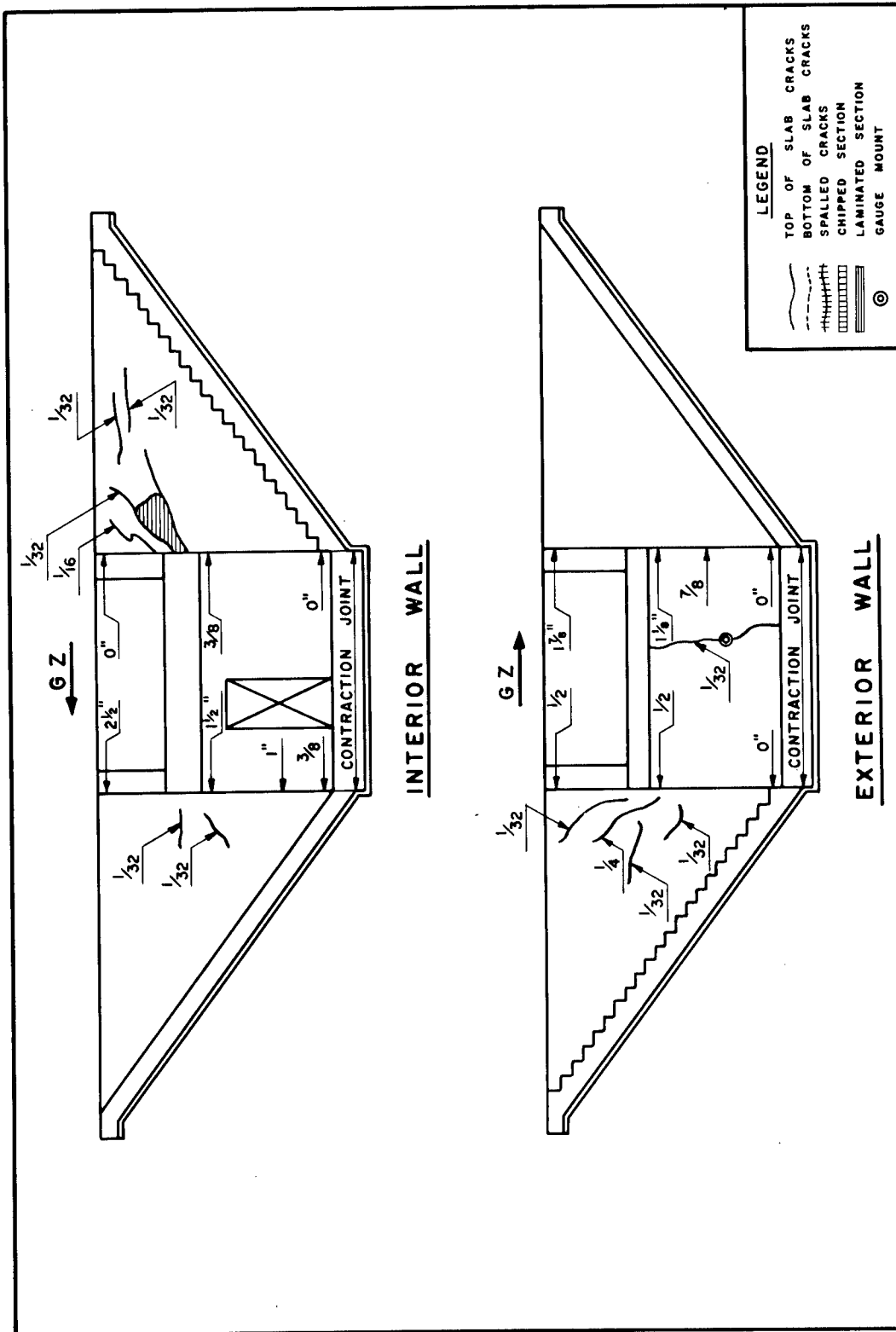
Fig. 3.36—Floor of main chamber (structure RAc).
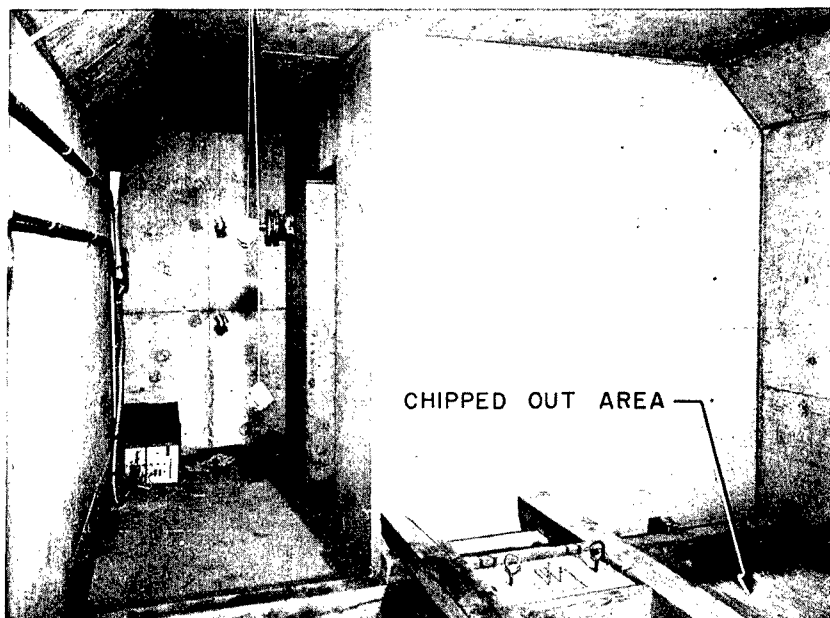
CHIPPED OUT AREA

Fig. 3.37—Forward section of main chamber, indicating general location of chipped-out area (structure RAc).
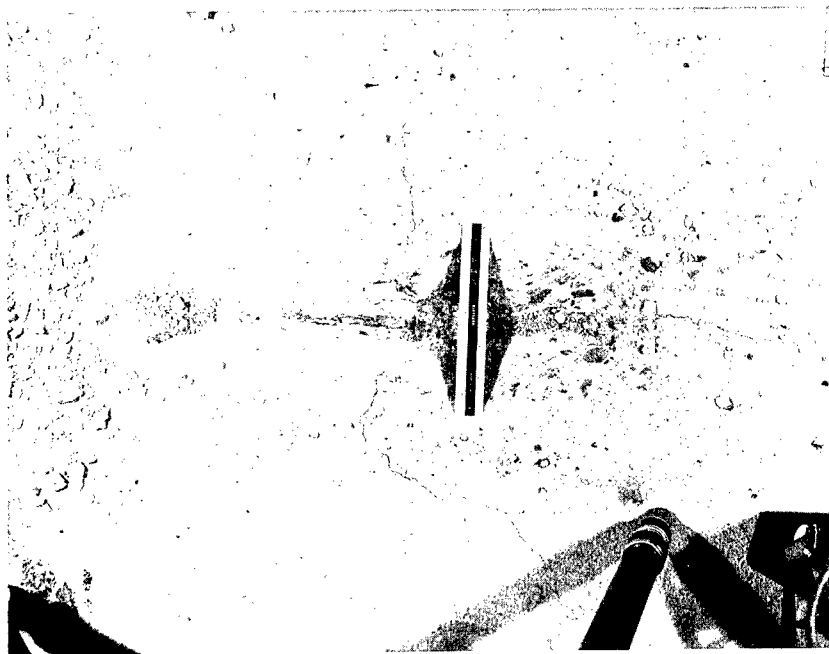
Fig. 3.38—Over-all view of chipped-out section with associated crack pattern (structure RAc).
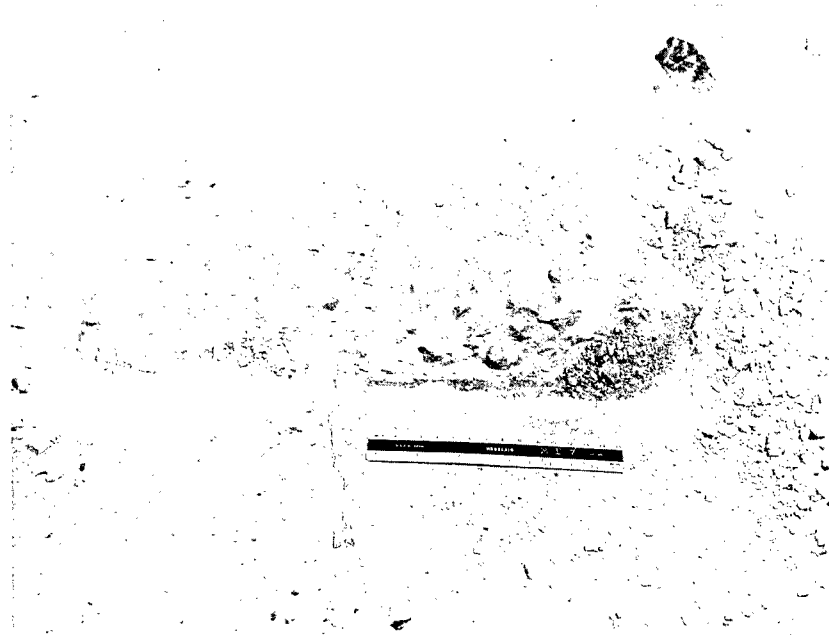
Fig. 3.39—Detail of end of chipped-out section facing toward the main entrance (structure RAc).

Fig. 3.40—Detail of end of chipped-out section facing toward the main entrance (structure RAc).
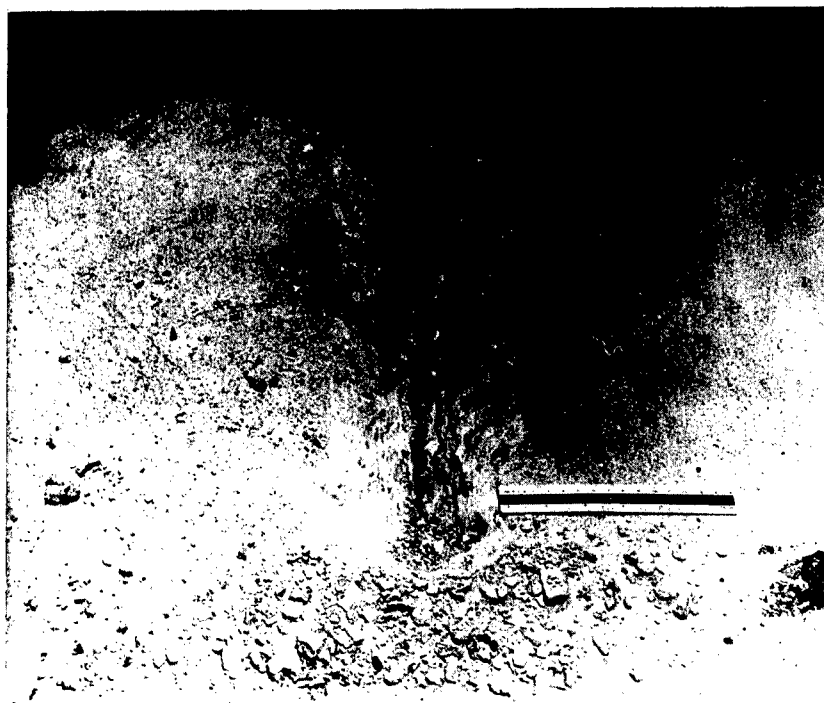
Fig. 3.41—Detail of end of chipped-out section facing toward the emergency exit (structure RAc).
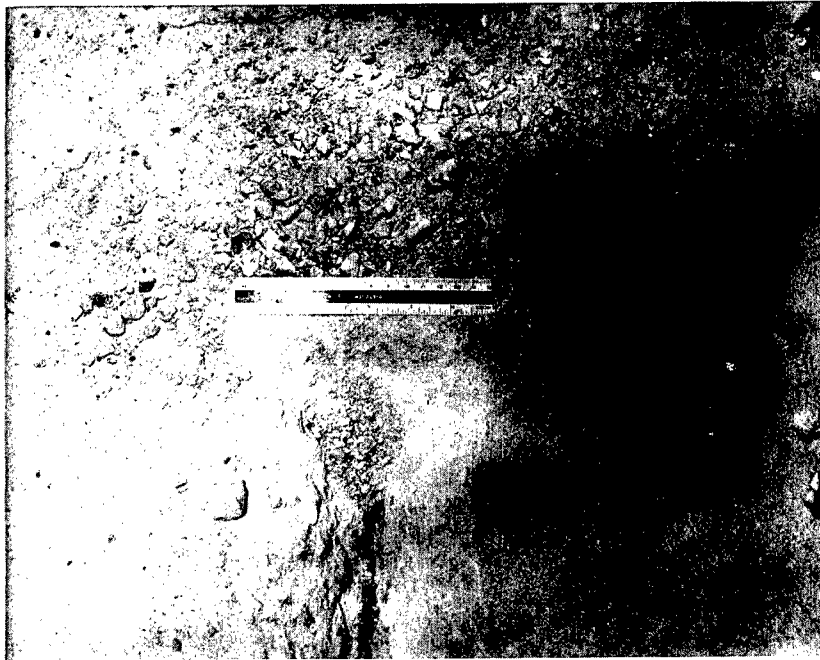
Fig. 3.42—Detail of end of chipped-out section facing toward the emergency exit (structure RAc).

Fig. 3.43—Cracks in roof slab of main chamber (structure RAc).

Fig. 3.44—Bottom of emergency-exit shaft (structure RAc). Note debris and sandbags in shaft.
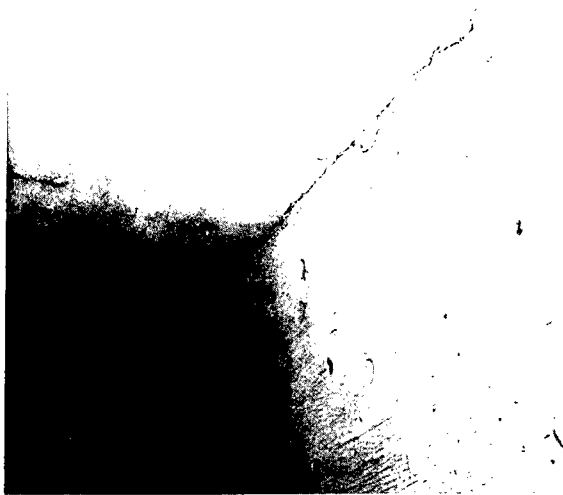
Fig. 3.45—Cracks in roof slab over landing, looking away from GZ (structure RAc).
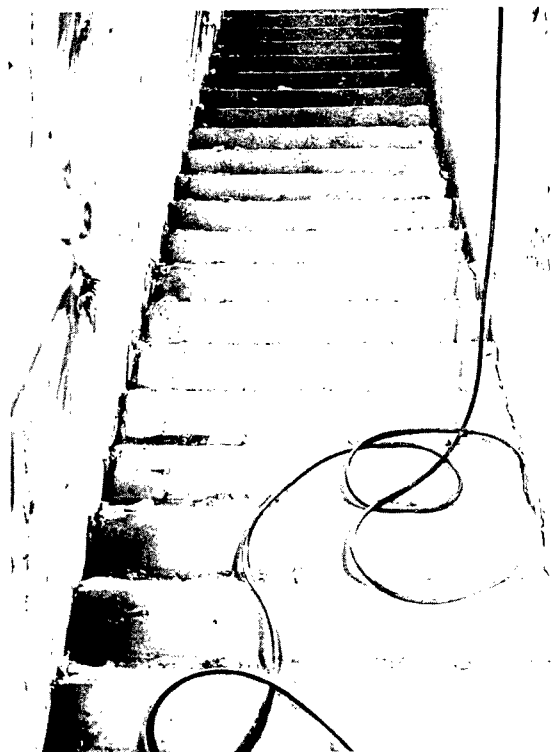
Fig. 3.46—Looking up stairs facing away from GZ, showing
separations between stairs and interior and entrance walls
(structure RAc).
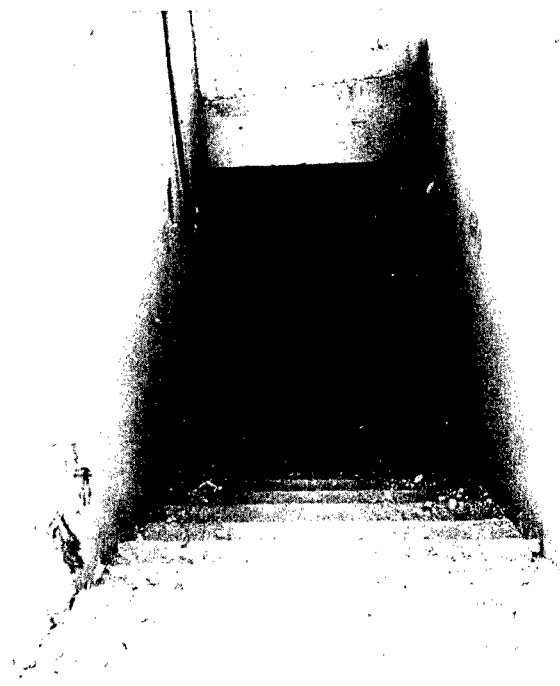
Fig. 3.47—Looking down entrance facing away from GZ, showing
cracks between parapet wall and interior and exterior walls
(structure RAc).
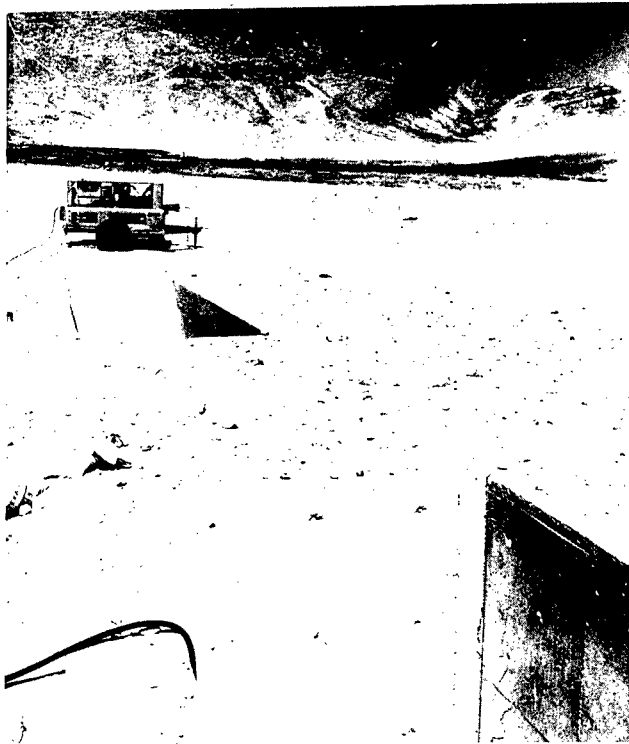
Fig. 3.48—Detail of cracks at intersection of parapet wall and
interior wall and entrance facing away from GZ (structure RAc).
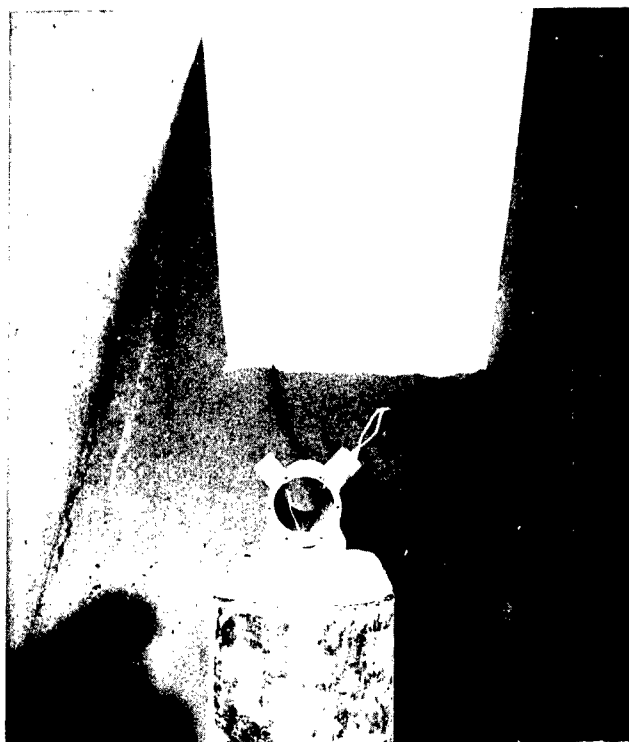
Fig. 3.49—Looking up entrance toward GZ, after cleaning
(structure RAc).

Fig. 3.50—Looking down entrance toward GZ, showing separation of parapet wall from interior and exterior walls and bowing of ramp wall (structure RAc).
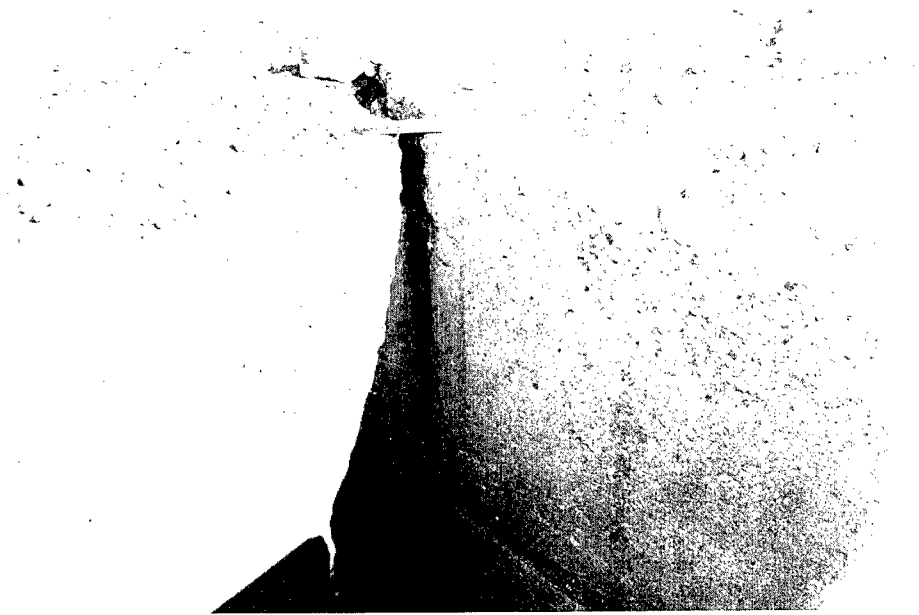
Fig. 3.51—Detail of separation between interior wall and parapet wall of entrance facing toward GZ (structure RAc).
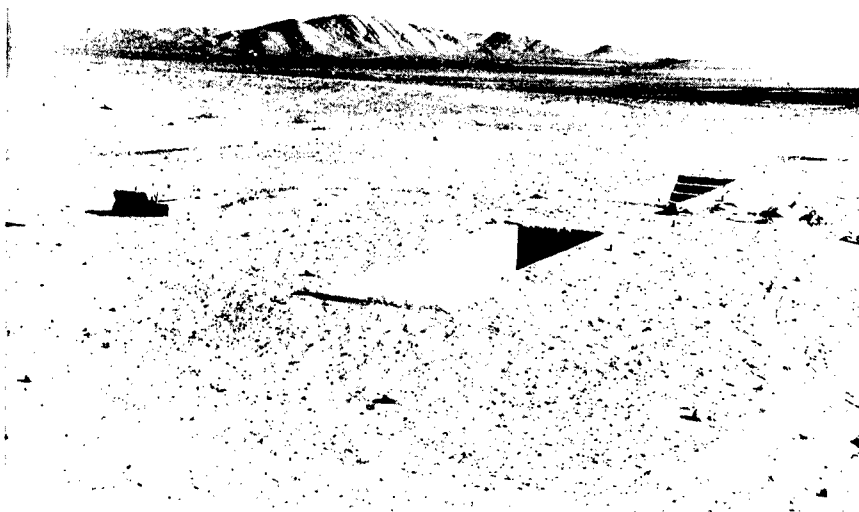
Fig. 3.52—Above-ground portion of ventilation shaft and main entrance (structure RAc).
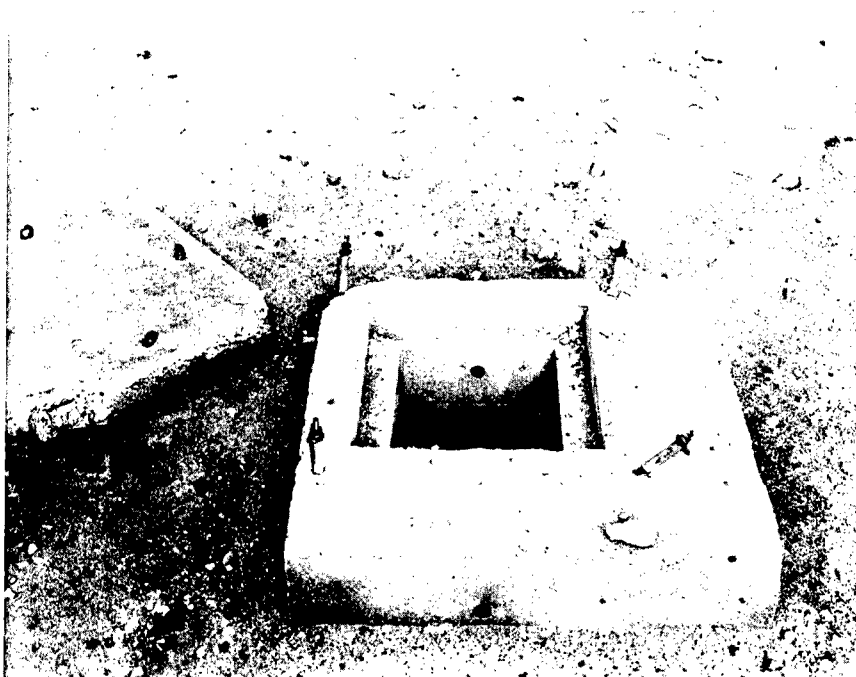
Fig. 3.53—Detail of exposed portion of ventilation shaft after cover was removed (structure RAc).
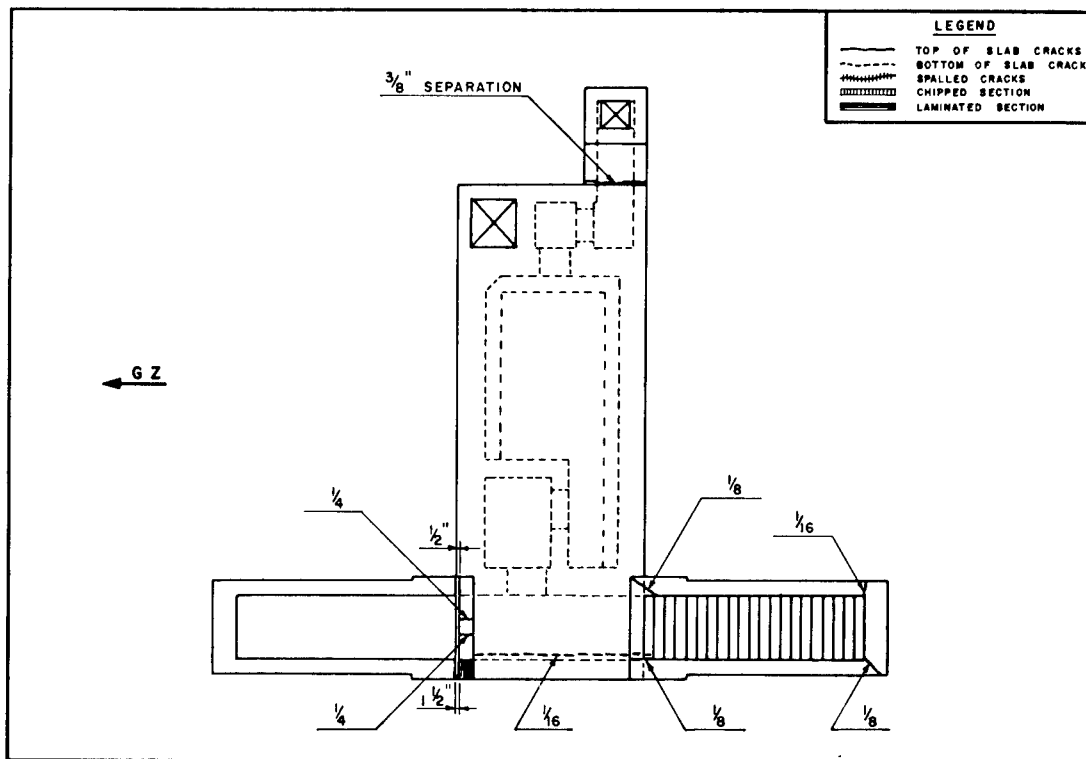
Fig. 3.54—Roof-slab crack pattern (structure RAd).
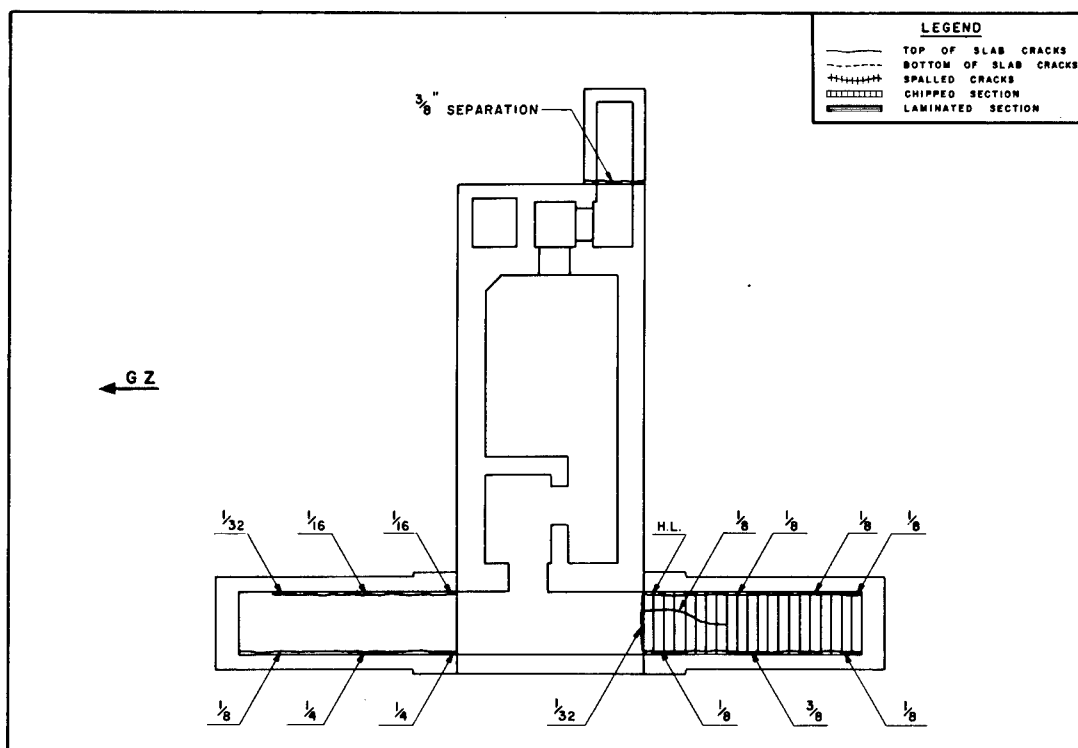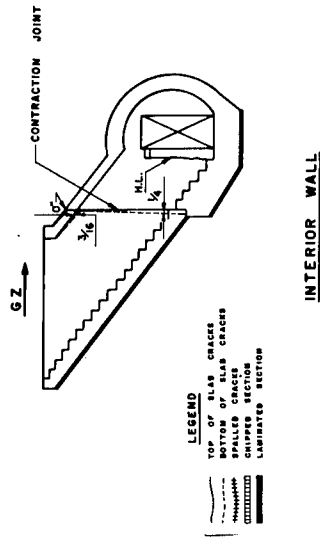

Fig. 3.55—Floor-slab crack pattern (structure RAd).

119

LEGEND

TOP OF SLAB CRACKS
BOTTOM OF SLAB CRACKS
SPALLED CRACKS
CHIPPED SECTION
LAMINATED SECTION

GZ

INTERIOR WALL

GZ

EXTERIOR WALL

Fig. 3.56—Entrance crack pattern (structure RAd).
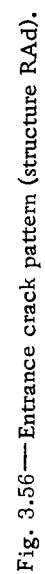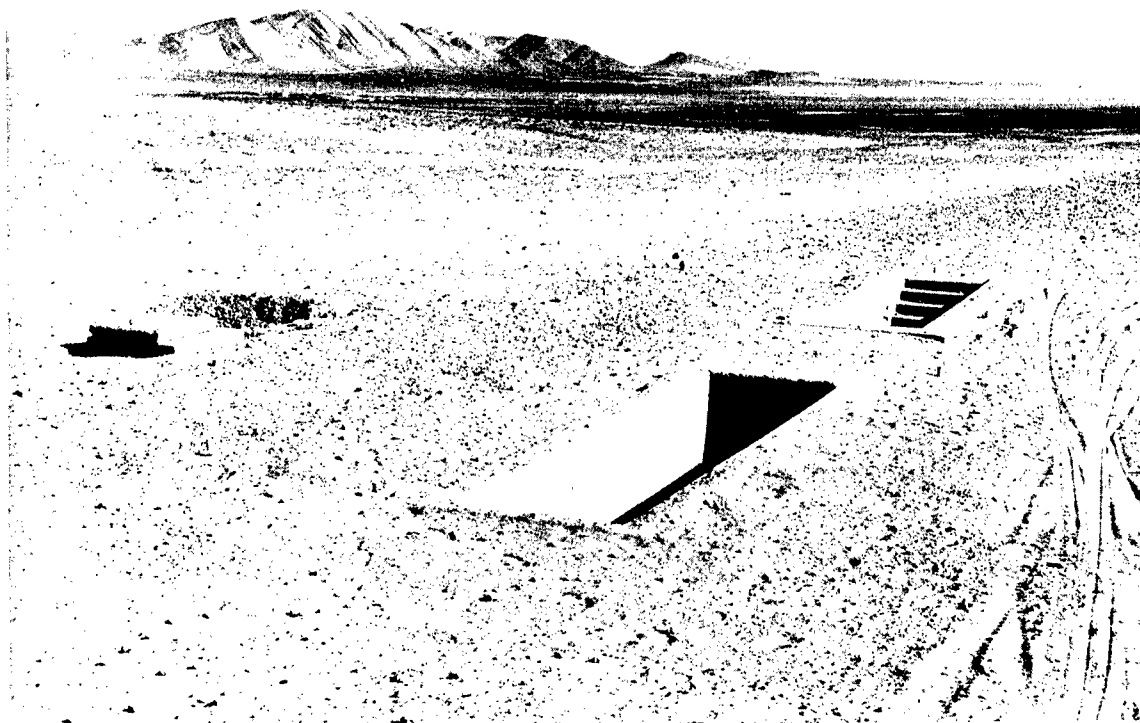
Fig. 3.57—Above-ground portion of ventilation shaft and main entrance (structure RAd).

LEGEND
TOP OF SLAB CRACKS
BOTTOM OF SLAB CRACKS
SPALLED CRACKS
CHIPPED SECTION
LAMINATED SECTION

INTERIOR WALL

CONTRACTION JOINT

LEGEND
TOP OF SLAB CRACKS
BOTTOM OF SLAB CRACKS
SPALLED CRACKS
CHIPPED SECTION
LAMINATED SECTION

EXTERIOR WALL

CONTRACTION JOINT

Fig. 3.60—Entrance crack pattern (structure CAa).

LEGEND
TOP OF SLAB CRACKS
BOTTOM OF SLAB CRACKS
SPALLED CRACKS
CHIPPED SECTION
LAMINATED SECTION

Fig. 3.58—Roof-slab crack pattern (structure CAa).

LEGEND
TOP OF SLAB CRACKS
BOTTOM OF SLAB CRACKS
SPALLED CRACKS
CHIPPED SECTION
LAMINATED SECTION

Fig. 3.59—Floor-slab crack pattern (structure CAa).

122

Fig. 3.61—Over-all view of chipped-out section with associated crack pattern (section CAa).
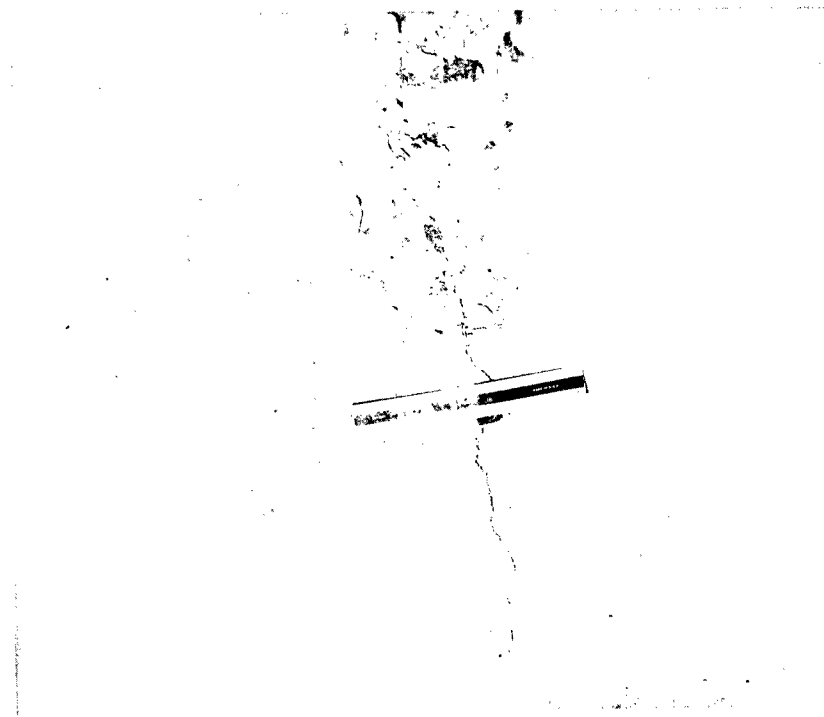
Fig. 3.62—Detail of end of chipped-out section facing toward the emergency exit (structure CAa).
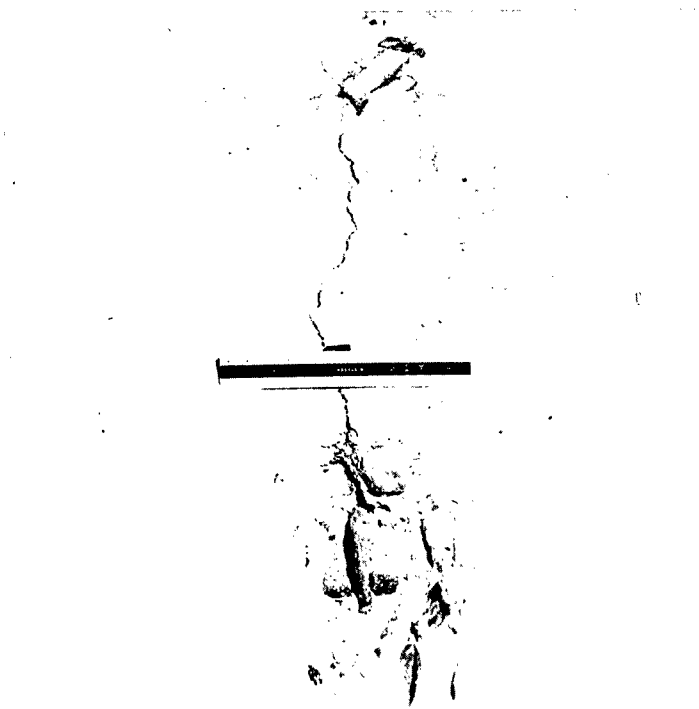
Fig. 3.63—Detail of end of chipped-out section facing toward the main entrance (structure CAa).
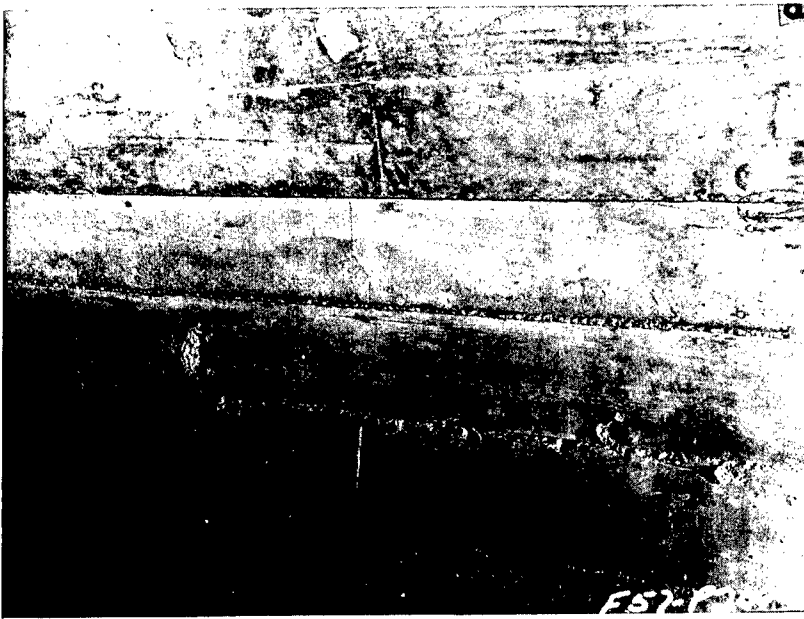
Fig. 3.64—Crack in the main chamber at approximately the center of the side facing toward GZ (structure CAa).

Fig. 3.65—Crack in side of main chamber facing away from GZ (between displacement gauge tie point and Carlson gauge) (structure CAa).
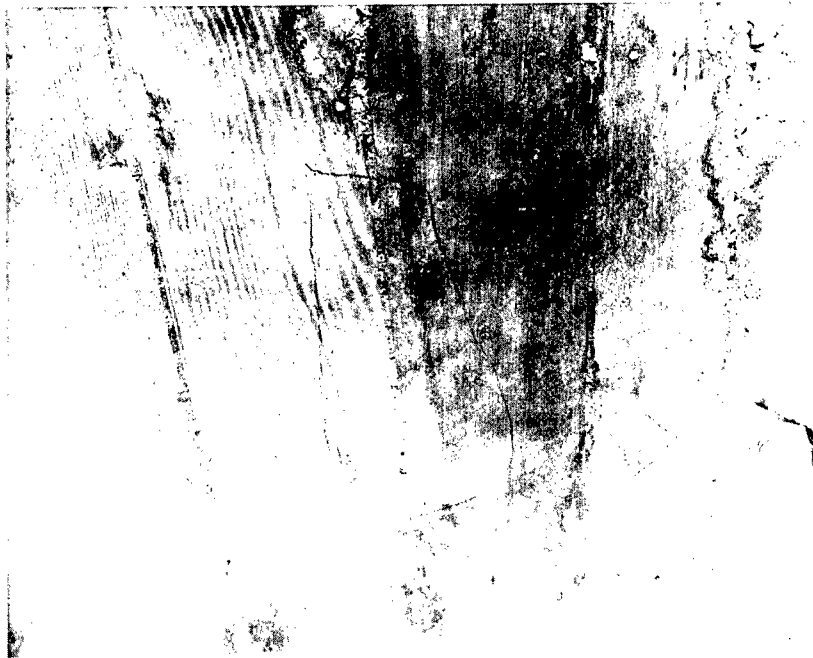
Fig. 3.66—Detail of crack in center of ceiling (structure CAa).

Fig. 3.67—Emergency-exit shaft from chamber between small blast and gastight doors (structure CAa).
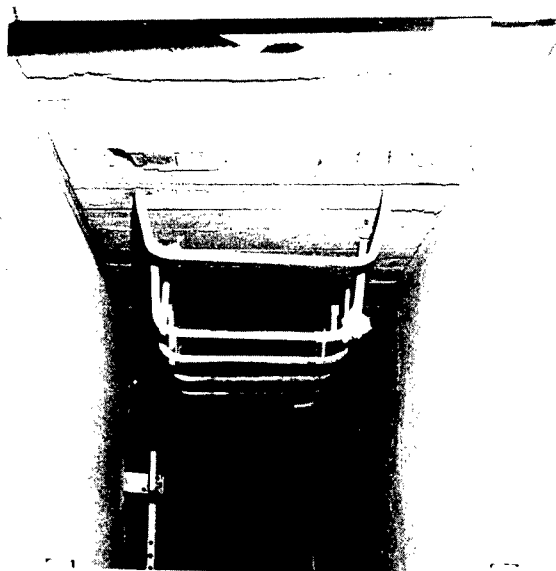
Fig. 3.68—Emergency-exit shaft (structure CAa). Note bent climing rungs and straightened hinge strap.

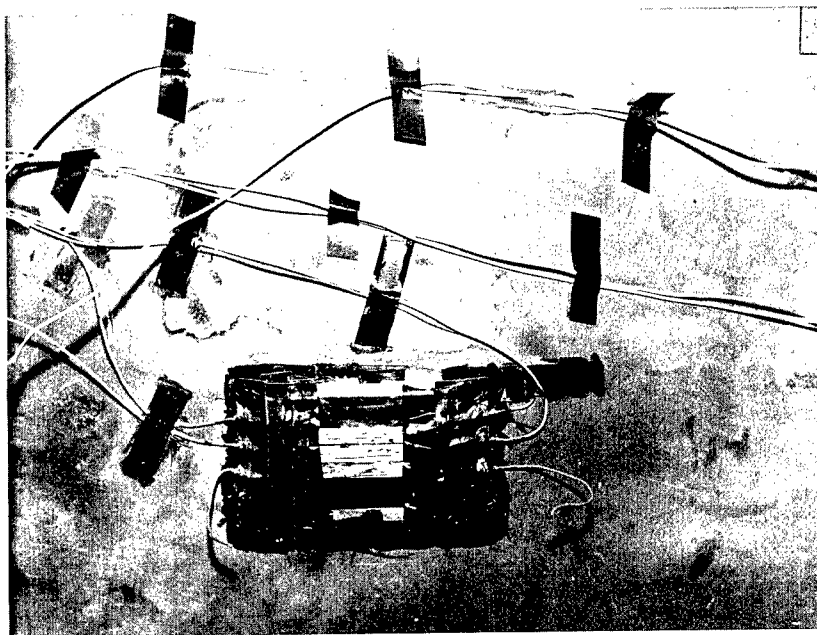Fig. 3.69—In-place detail of open antiblast flap valve (structure CAa).

Fig. 3.70—Detail of strain gauges on main blast door (structure CAa).

Fig. 3.71—Looking up stairs facing away from GZ (structure CAa). Note crack running up stairs and separation of construction joint.

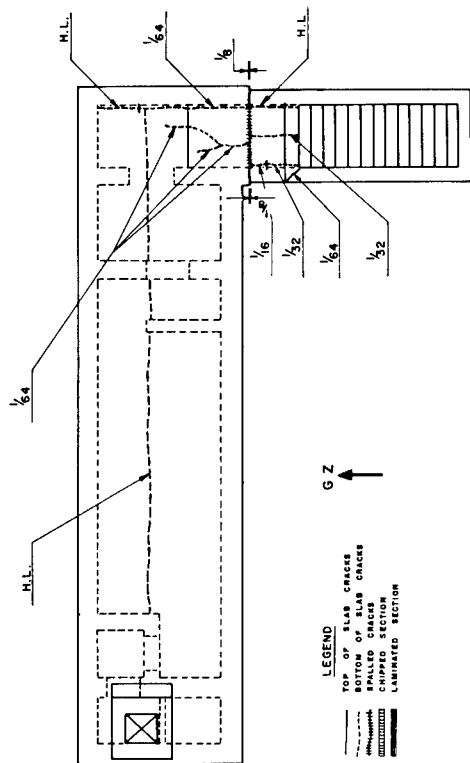Fig. 3.72—Above-ground portion of main entrance and emergency-exit shaft (structure CAa).

CONTRACTION JOINT

INTERIOR WALL

G Z

$\frac{1}{32}$
$\frac{1}{16}$

LEGEND

TOP OF SLAB CRACKS
BOTTOM OF SLAB CRACKS
SPALLED CRACKS
CHIPPED SECTION
LAMINATED SECTION
ALL CRACKS ⫫ TO H.L.
EXCEPT AS NOTED.

G Z

H.L.

$\frac{1}{64}$

CONTRACTION JOINT
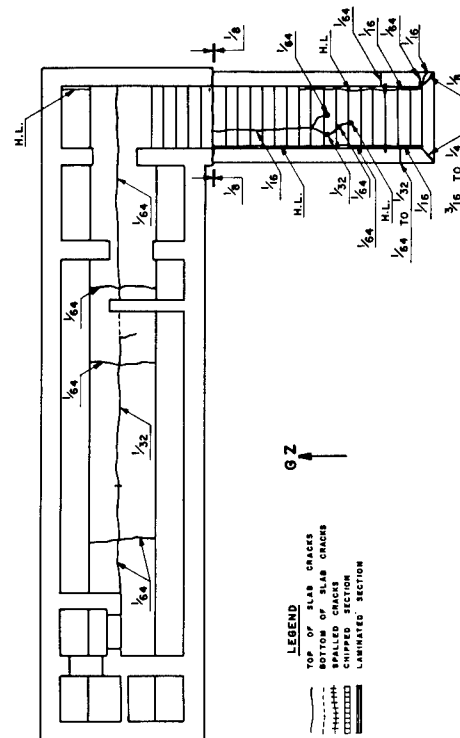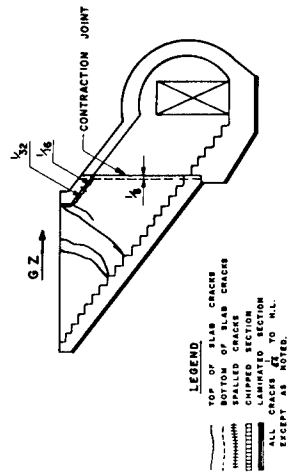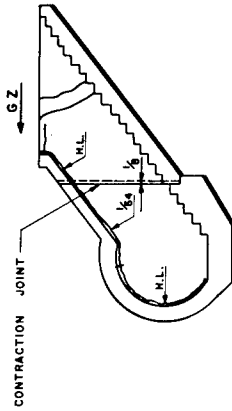
EXTERIOR WALL

H.L.

Fig. 3.75—Entrance crack pattern (structure CAb).

H.L.

$\frac{1}{64}$

$\frac{1}{16}$

H.L.

$\frac{1}{16}$
$\frac{1}{32}$
$\frac{1}{64}$
$\frac{1}{32}$

$\frac{1}{64}$

H.L.

G Z

LEGEND

TOP OF SLAB CRACKS
BOTTOM OF SLAB CRACKS
SPALLED CRACKS
CHIPPED SECTION
LAMINATED SECTION

Fig. 3.73—Roof-slab crack pattern (structure CAb).

$\frac{1}{8}$
$\frac{1}{64}$
H.L.
$\frac{1}{16}$
$\frac{1}{64}$
$\frac{1}{16}$

H.L.

$\frac{1}{8}$

$\frac{1}{16}$

$\frac{1}{8}$
$\frac{1}{16}$
$\frac{1}{32}$
$\frac{1}{64}$
H.L. TO $\frac{1}{32}$
$\frac{3}{16}$ TO $\frac{1}{4}$
$\frac{1}{64}$

$\frac{1}{64}$

$\frac{1}{64}$

$\frac{1}{32}$

$\frac{1}{64}$

G Z

LEGEND

TOP OF SLAB CRACKS
BOTTOM OF SLAB CRACKS
SPALLED CRACKS
CHIPPED SECTION
LAMINATED SECTION

Fig. 3.74—Floor-slab crack pattern (structure CAb).

129

Fig. 3.76—Side of main chamber facing toward GZ (structure CAb). Note cracks by survey point X-4 and horizontal cold joint.
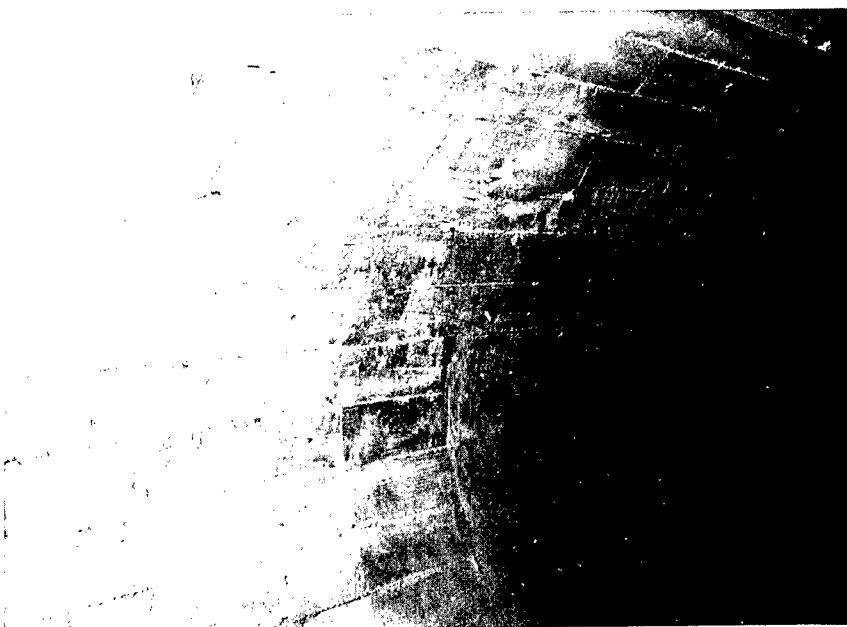

Fig. 3.77—Side of chamber facing away from GZ (structure CAb). Note survey point X-5, cracks, and horizontal cold joint.

Fig. 3.78—Looking into emergency-exit shaft from chamber between small blast and gastight doors (structure CAb). Note climbing rungs deformed by blown-in match cover.
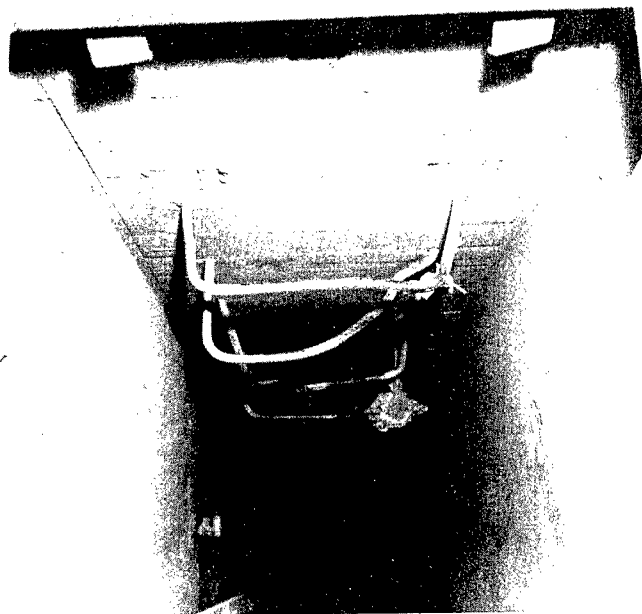

Fig. 3.79—Emergency-exit shaft (structure CAb). Note bent climbing rungs and straightened hinge straps.
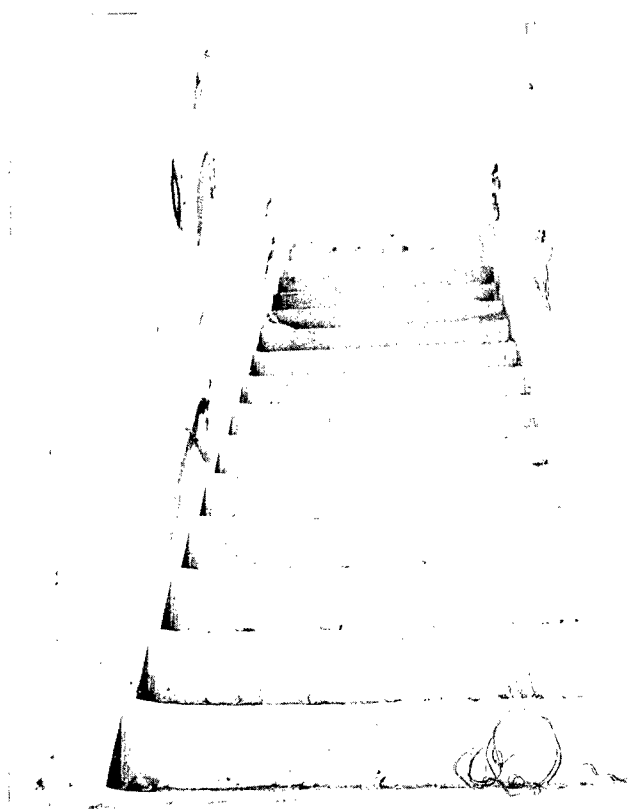
Fig. 3.80—Looking up stairs facing away from GZ (structure CAb). Note crack running up stairs.
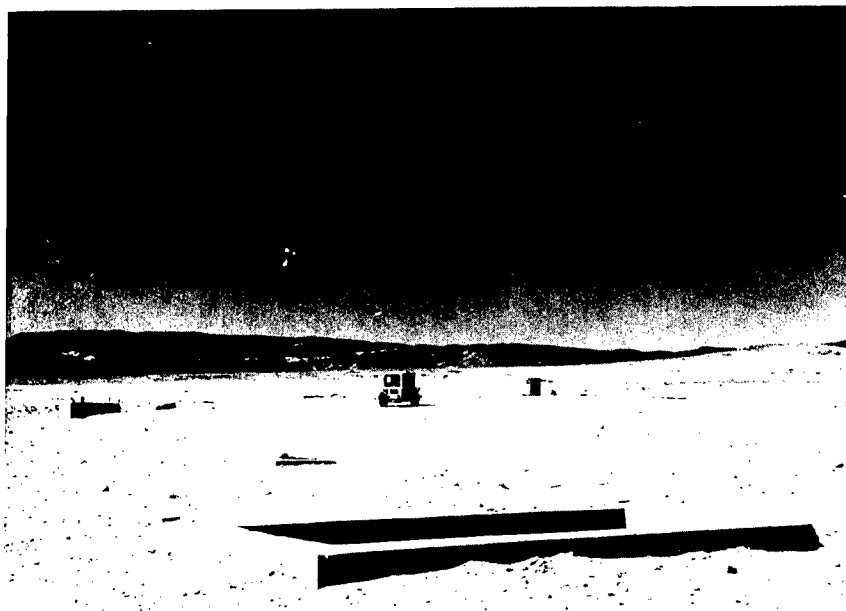
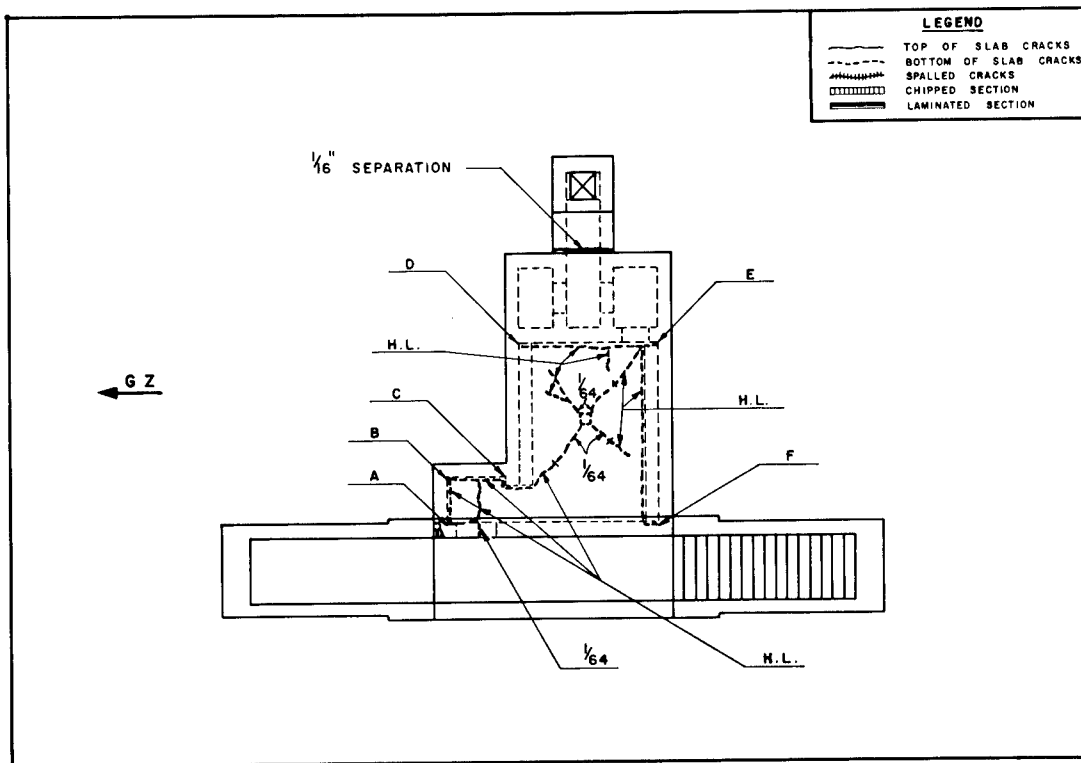Fig. 3.81—Above-ground portion of main entrance and emergency-exit shaft (structure CAb).

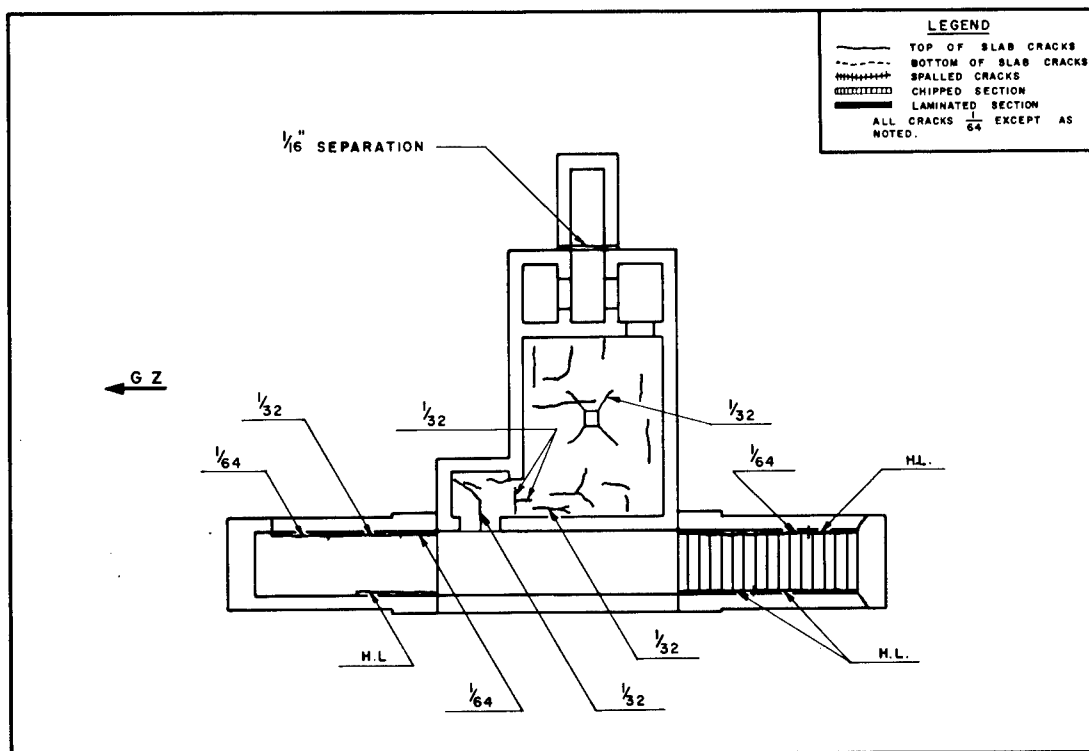Fig. 3.82—Roof-slab crack pattern (structure RCa).

Fig. 3.83—Floor-slab crack pattern (structure RCa).

133

Fig. 3.84—Entrance crack pattern (structure RCa).

134

Fig. 3.85—Cracks in floor slab of main chamber looking toward emergency-exit corner of wall nearest GZ (structure RCa).
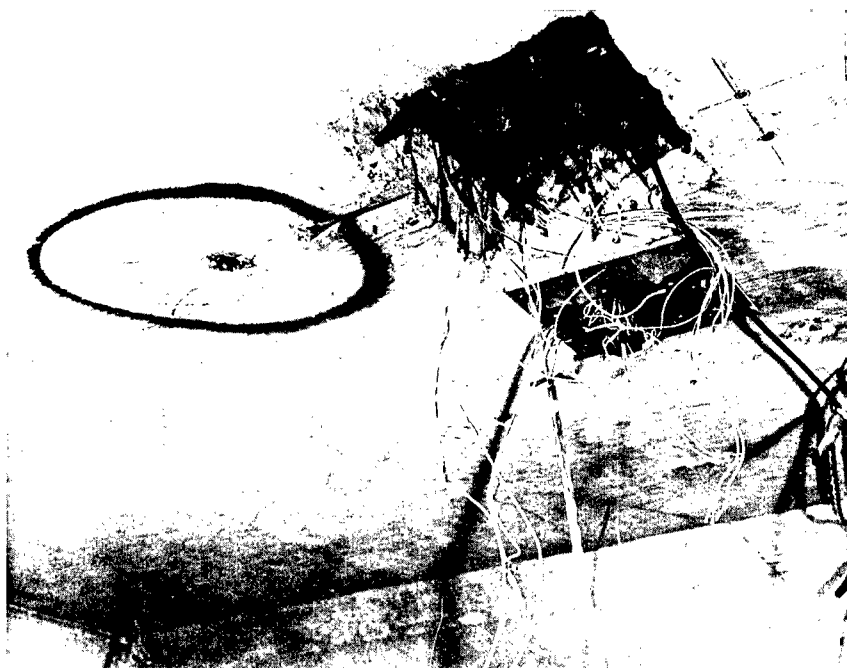

Fig. 3.86—Cracks in roof slab of main chamber, looking toward emergency-exit end of wall facing away from GZ (structure RCa).
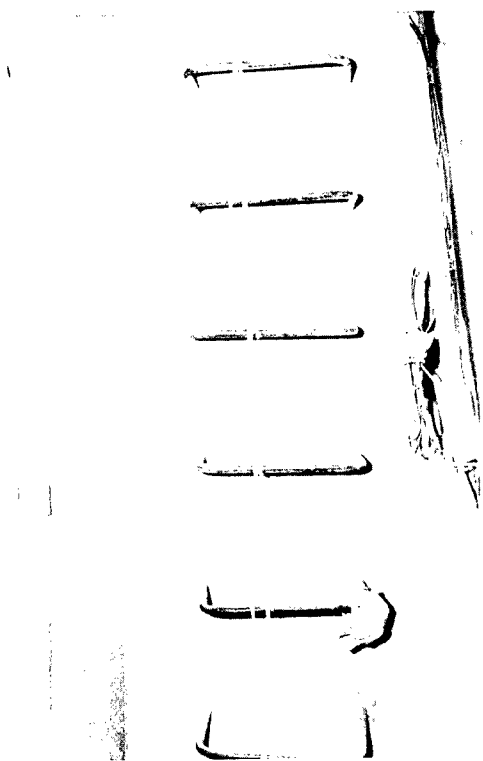
135

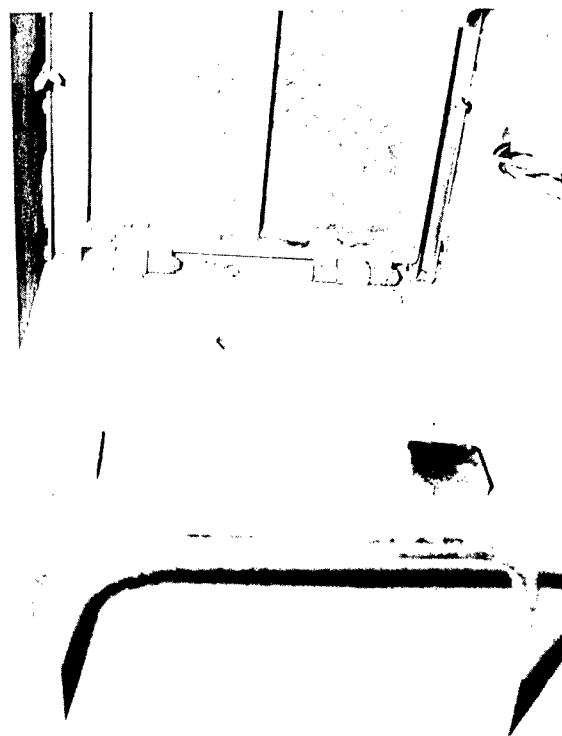Fig. 3.87—Rear end of emergency-exit shaft (structure RCa).

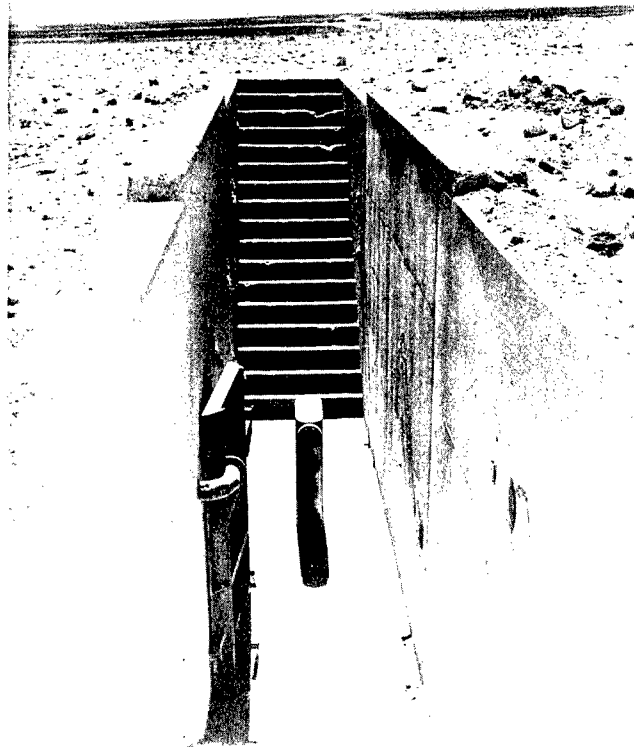Fig. 3.88—Interior view of top of emergency-exit shaft (structure RCa).

Fig. 3.89—View of main entrance after cleaning away debris, looking away from GZ (structure RCa).

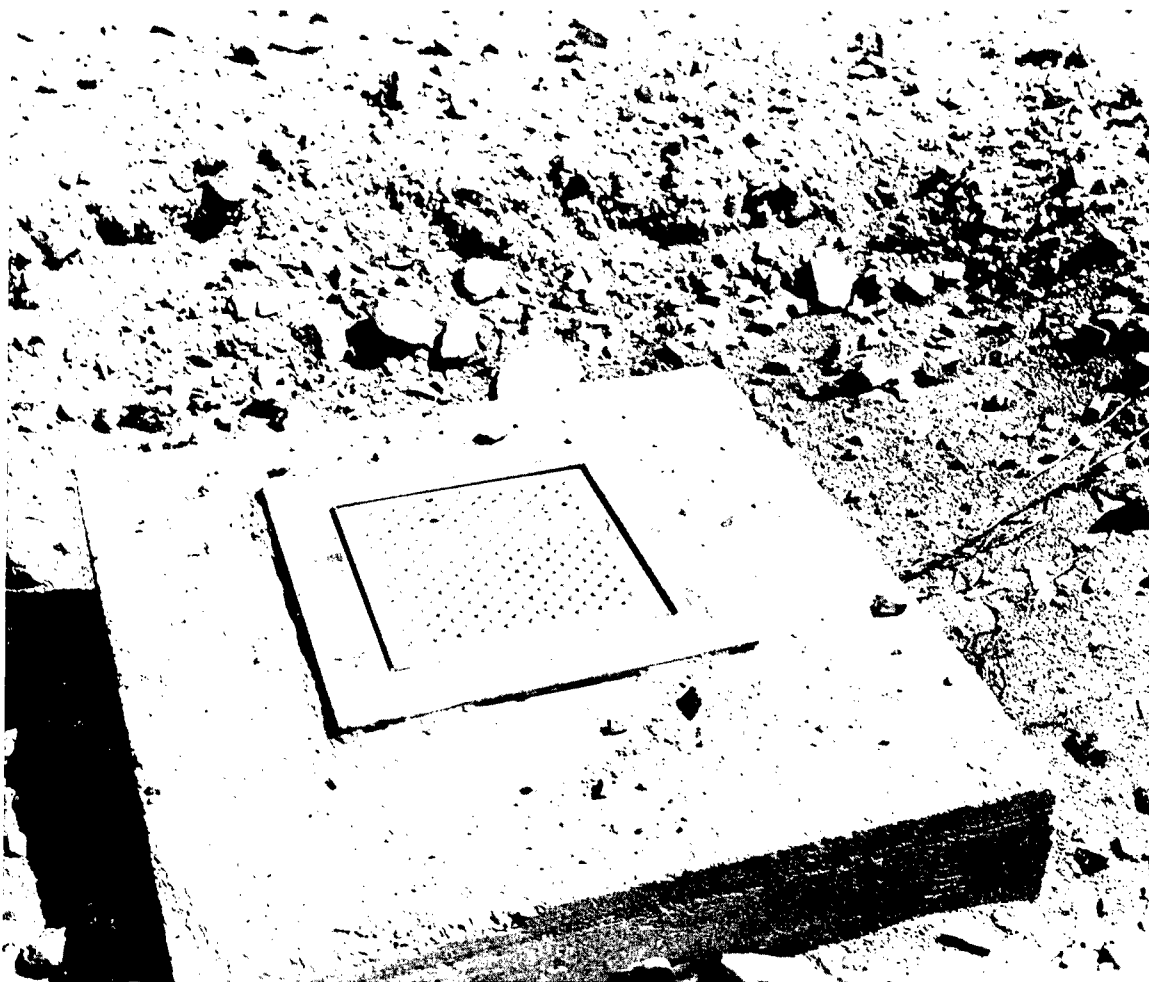Fig. 3.90—Detail of chipped-out section at GZ end of parapet wall (structure RCa).

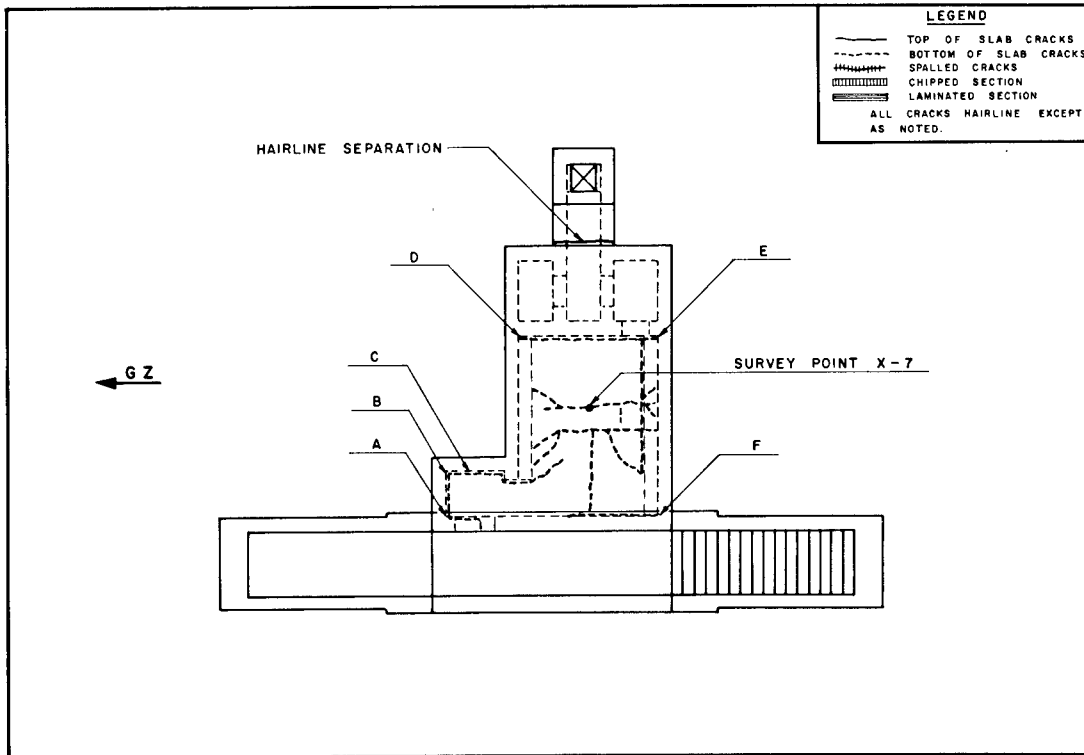Fig. 3.91—Exterior view of emergency-exit shaft and cover (structure RCa).

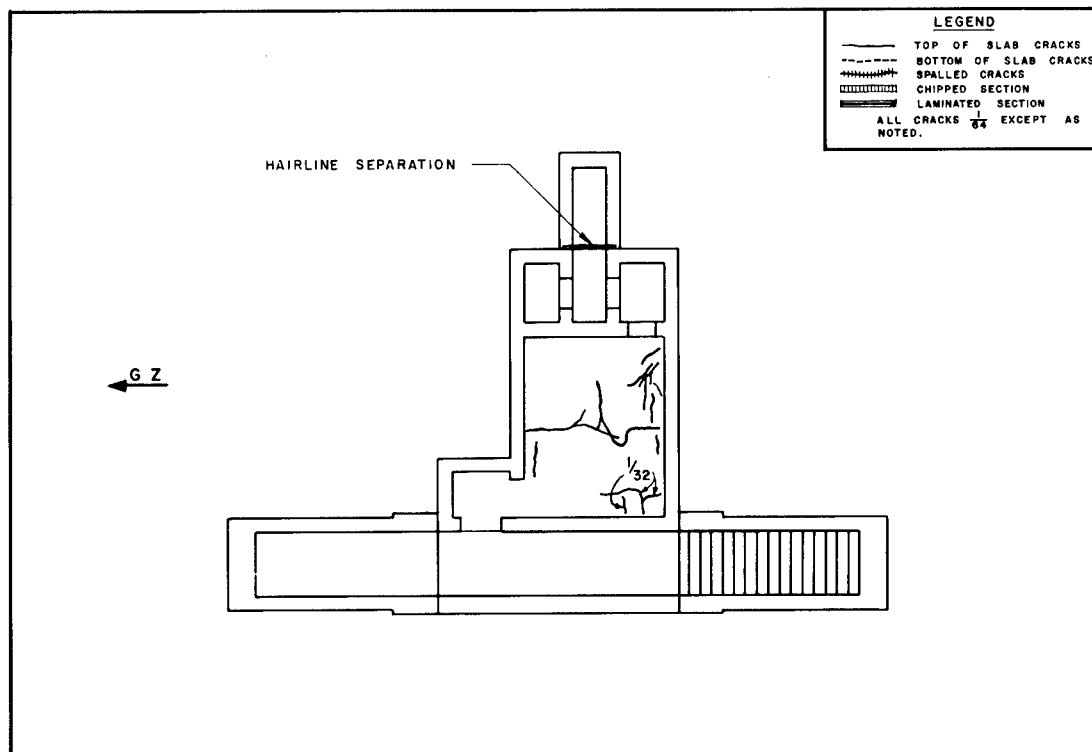Fig. 3.92—Roof-slab crack pattern (structure RCb).

Fig. 3.93—Floor-slab crack pattern (structure RCb).

139

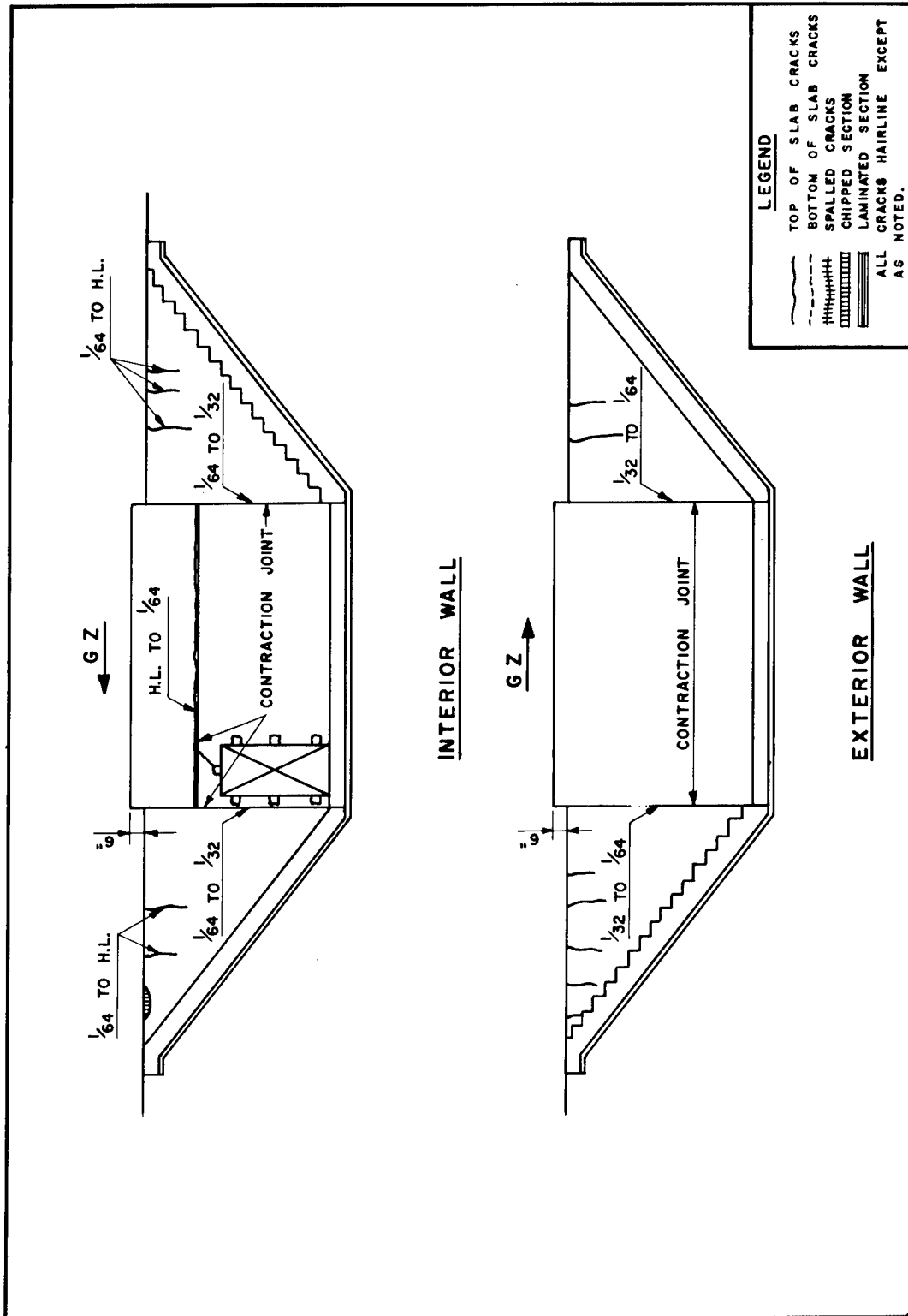Fig. 3.94—Entrance crack pattern (structure RCb).

Fig. 3.95—Cracks in floor slab of main chamber, looking toward GZ wall by main entrance end (structure RCb).

Fig. 3.96—Cracks by center of roof slab (structure RCb). Note survey point X-7.

Fig. 3.97—Cracks in haunch and wall of main chamber facing away from GZ (structure RCb).
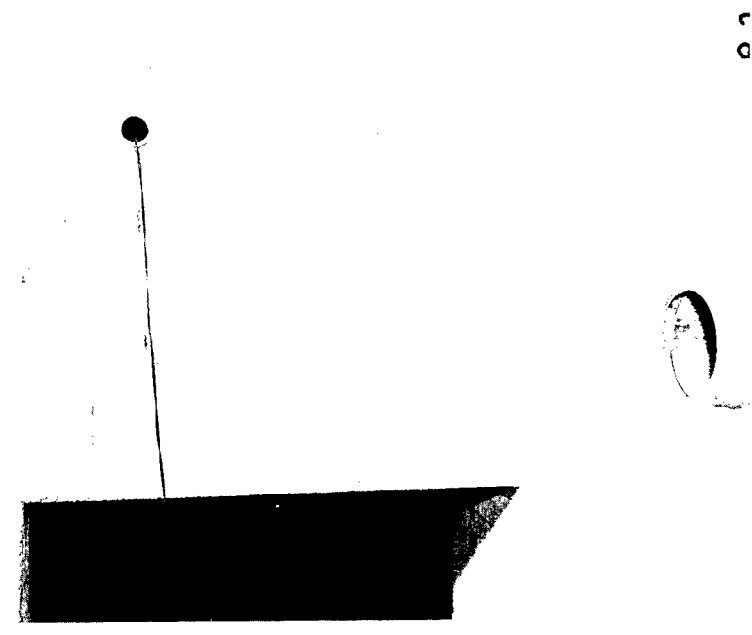
Fig. 3.98—Diagonal cracks above entrance to exit chamber (structure RCb).
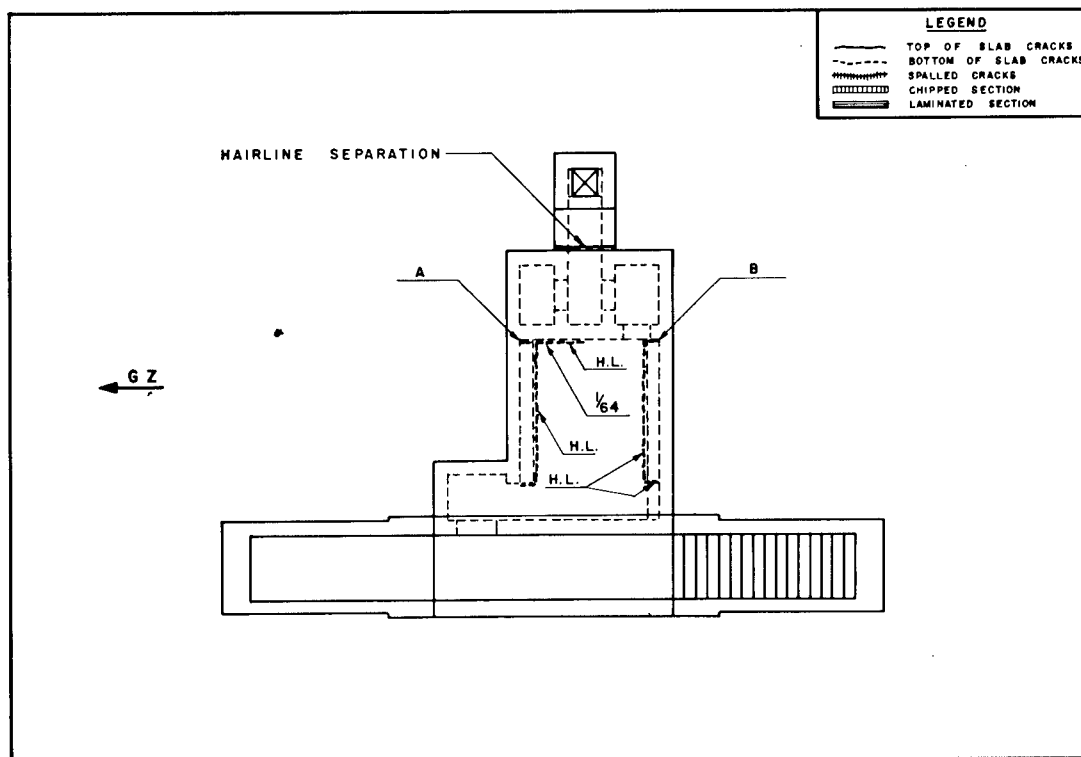
Fig. 3.99—Roof-slab crack pattern (structure RCc).
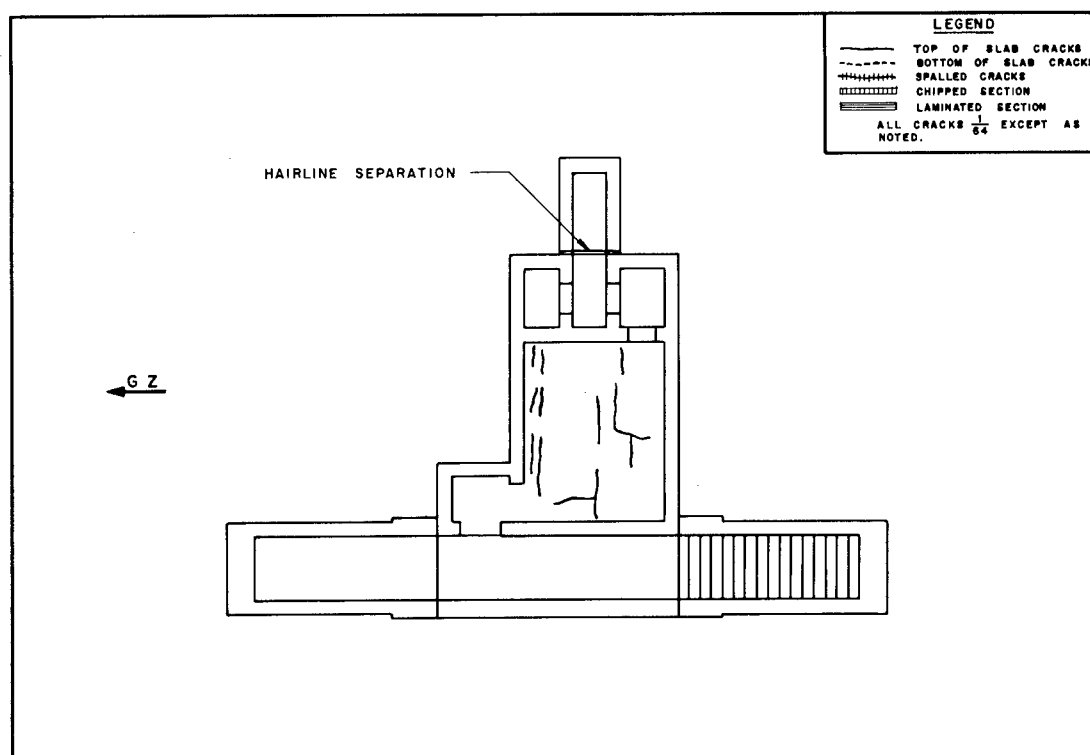
Fig. 3.100—Floor-slab crack pattern (structure RCc).

143

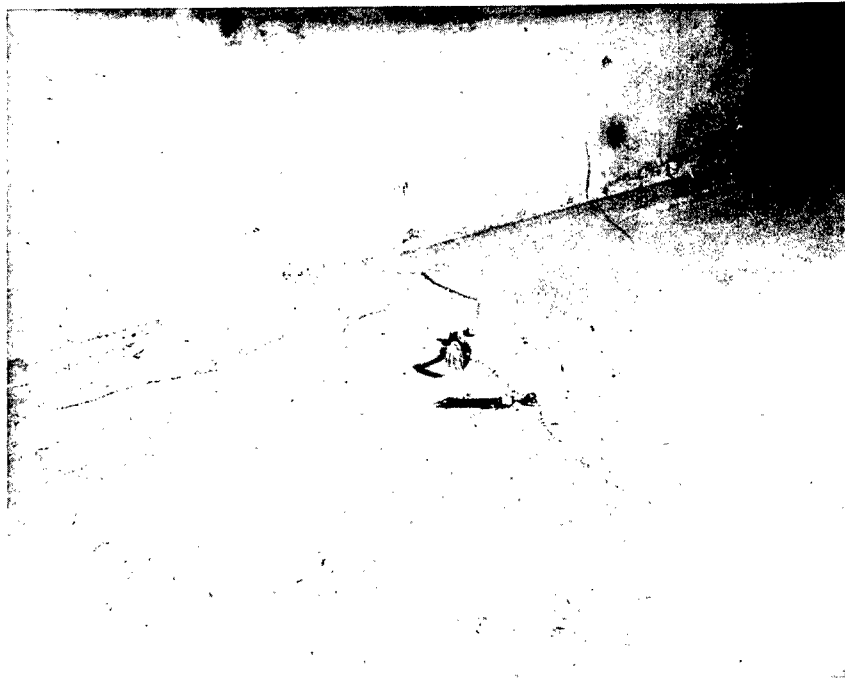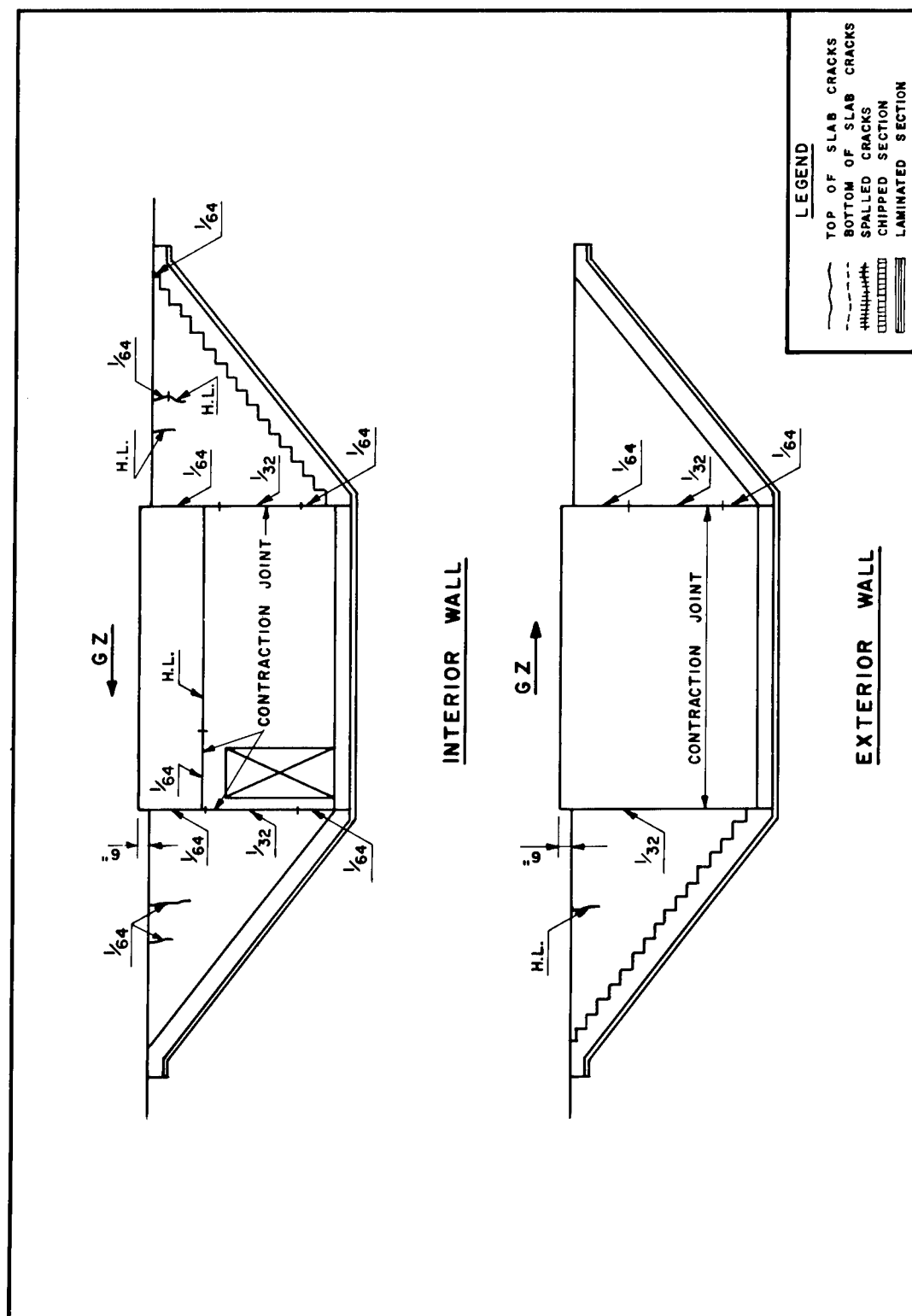Fig. 3.101—Entrance crack pattern (structure RCc).
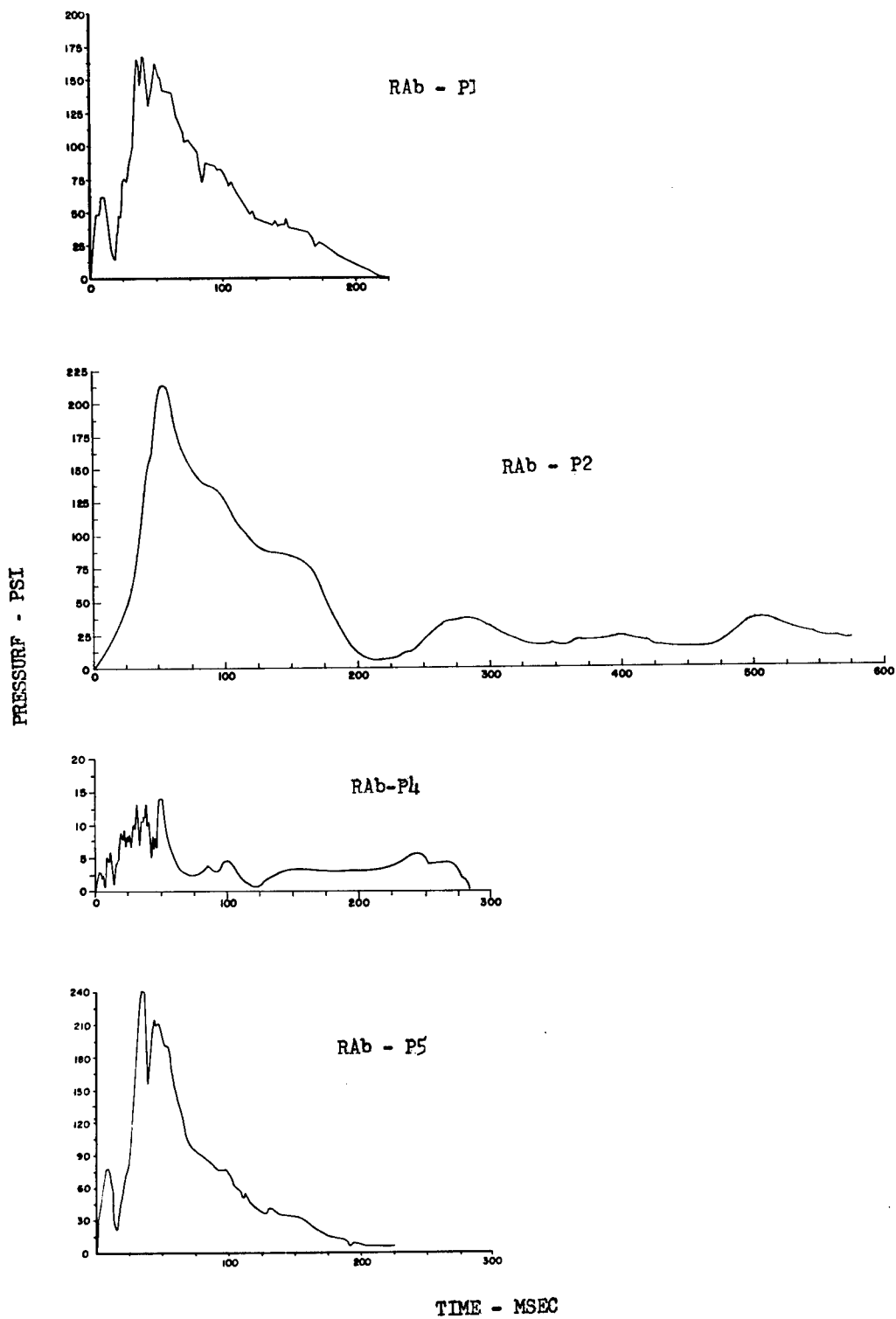
Fig. 3.102—Pressure-time; Carlson earth-pressure gauge records.

CAa - P1

CAa - P2

CAa - P3

CAa - P4

PRESSURE - PSI

TIME - MSEC

Fig. 3.102—(Continued)

146

RCa-P1

RCa - P2

RCa - P3

RCa - P4

PRESSURE - PSI

TIME - MSEC

Fig. 3.102—(Continued)

147
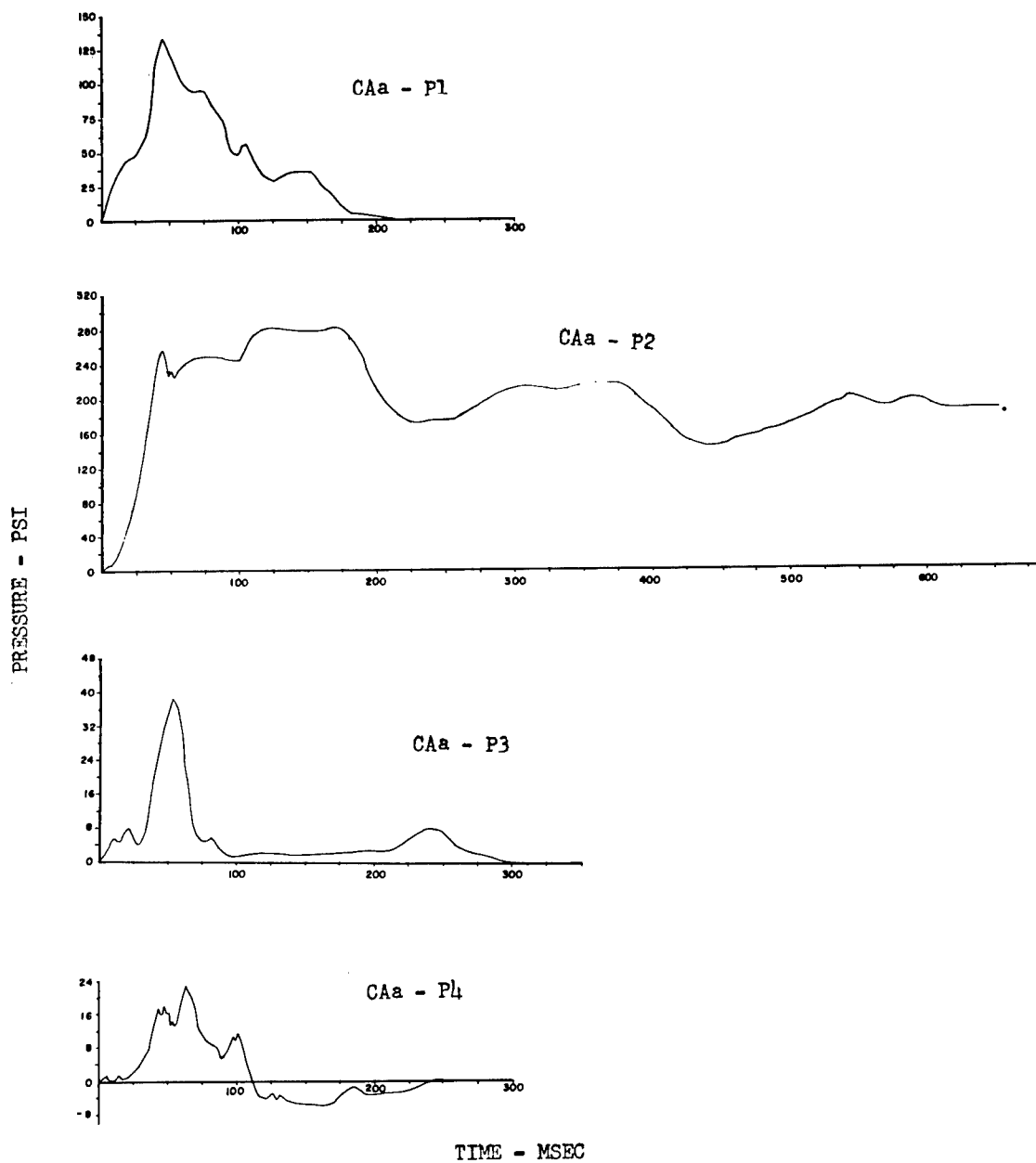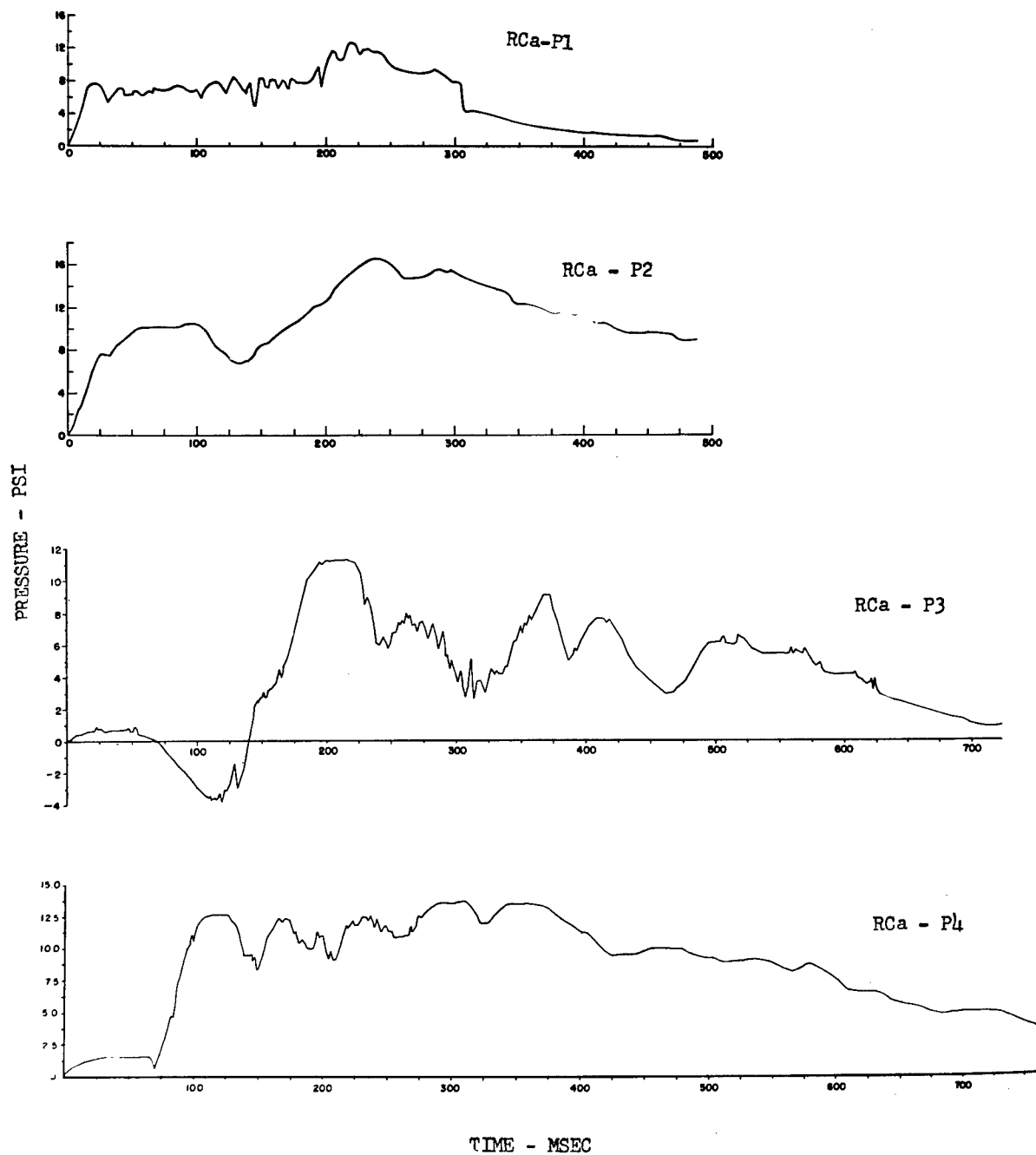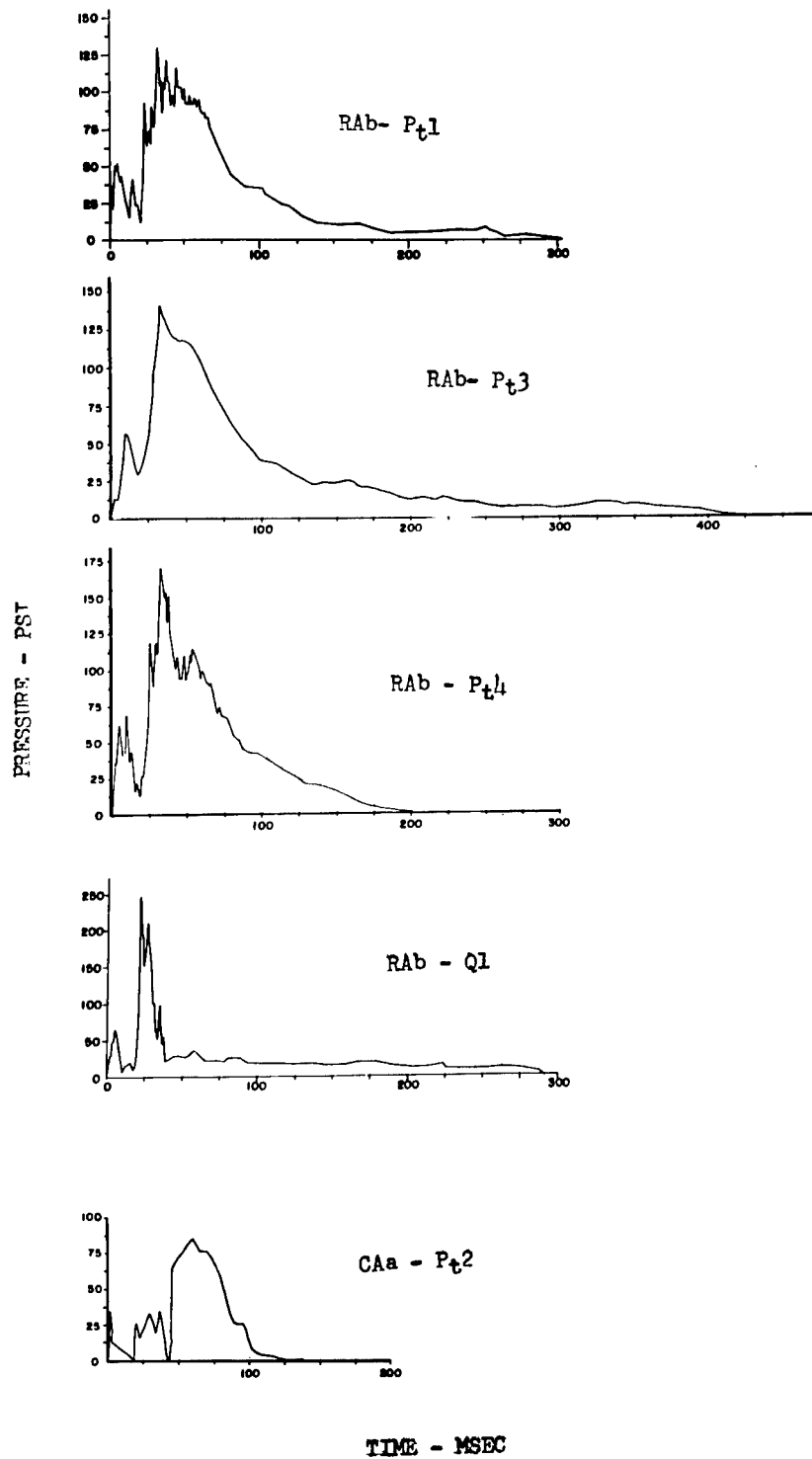
Fig. 3.103—Pressure-time; electronic incident- and dynamic-pressure gauge records.

RCa - P_t1

RCa - P_t3

RCa - P_t4

RCa - Q1

PRESSURE - PSI

TIME - MSEC
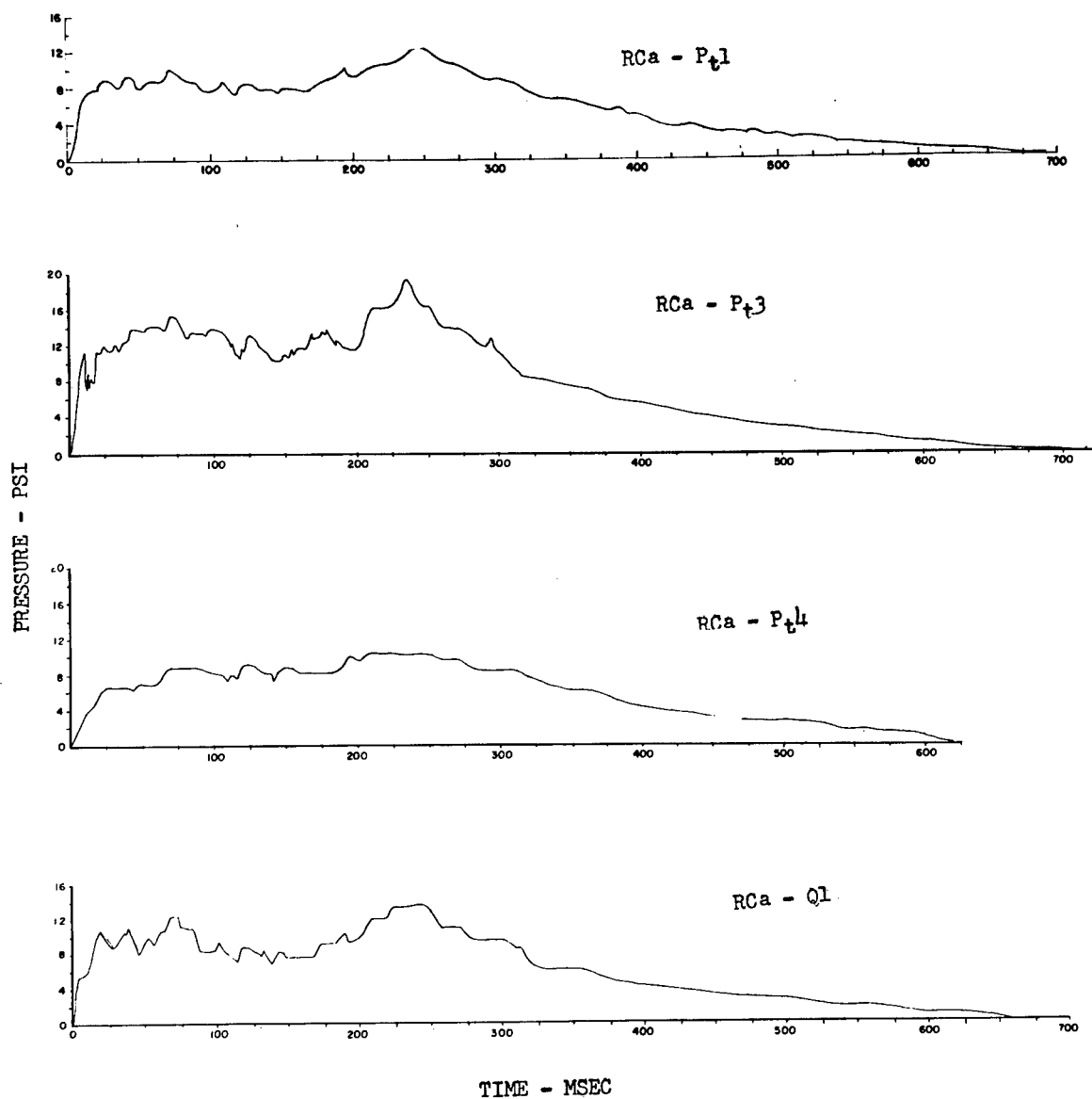
Fig. 3.103—(Continued)

149
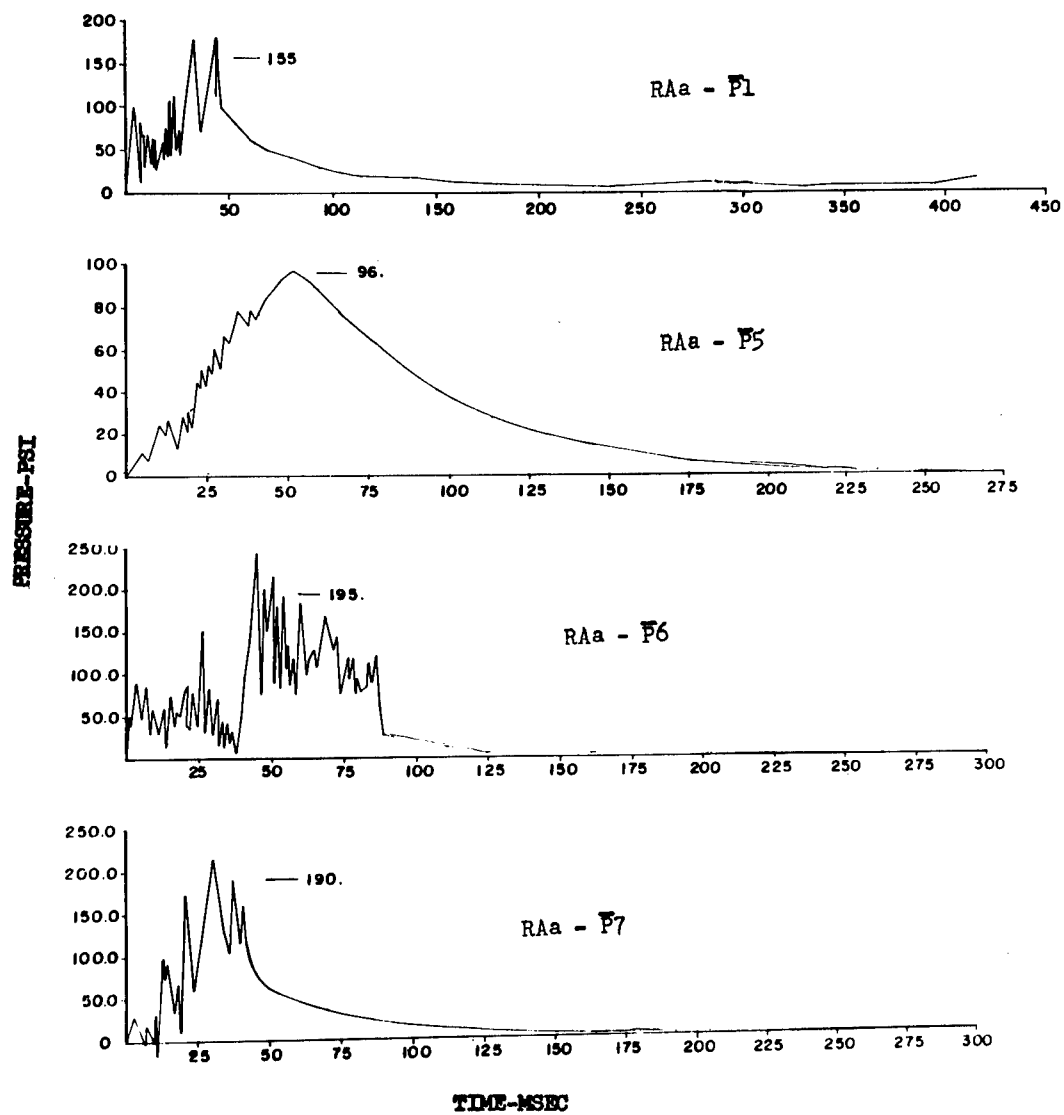
Fig. 3.104—Pressure-time; BRL self-recording pressure gauge records.
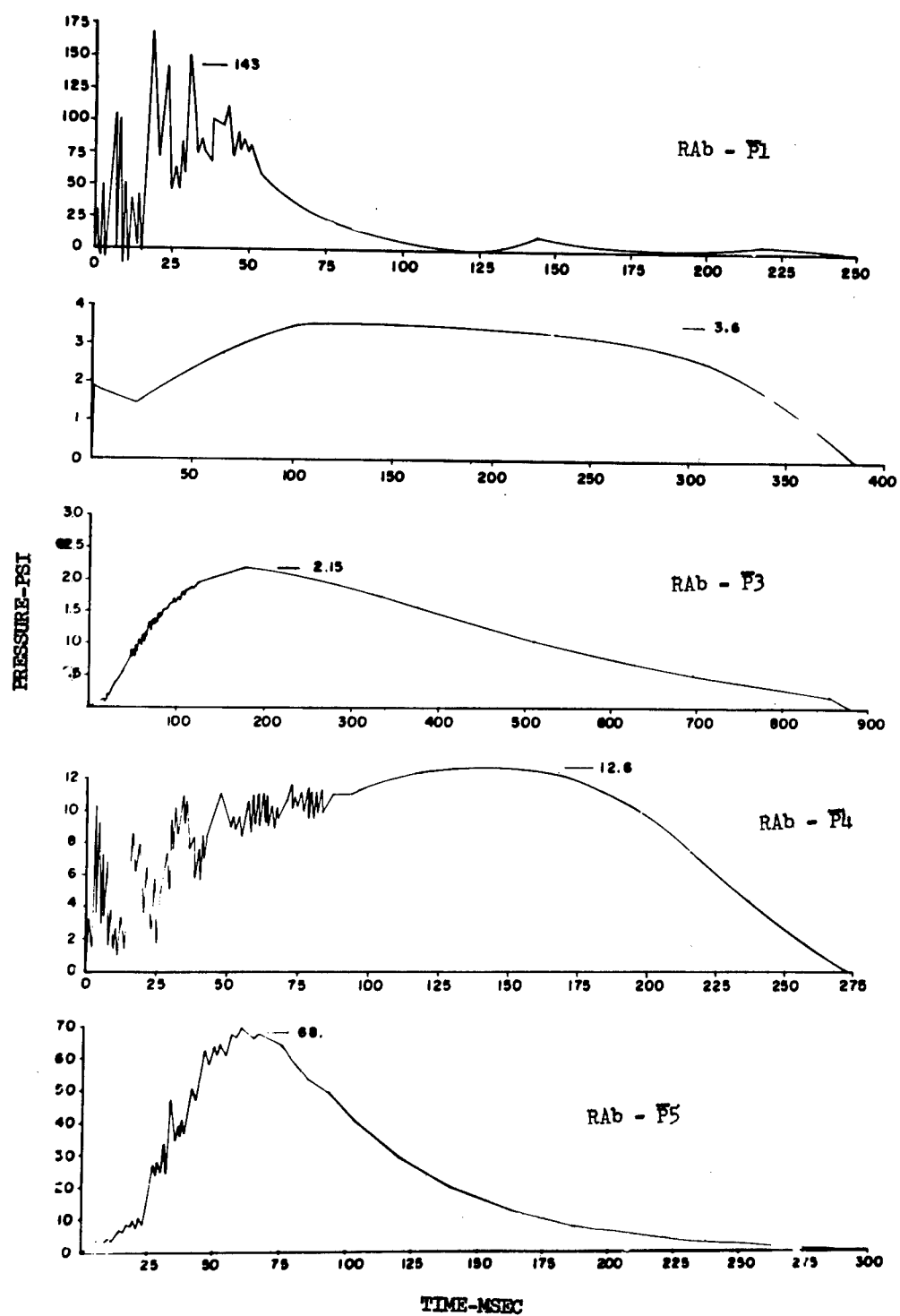
Fig. 3.104 — (Continued)
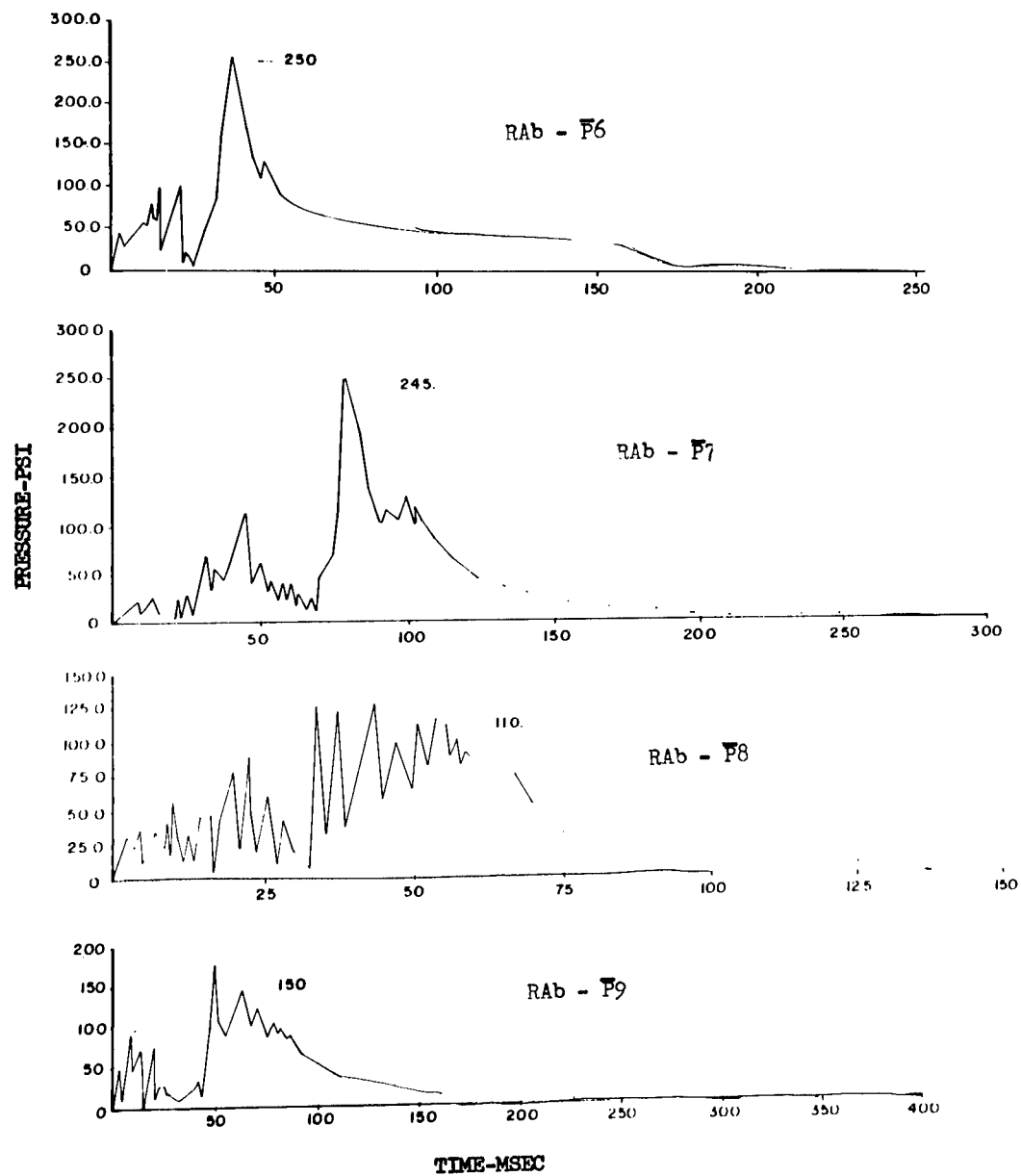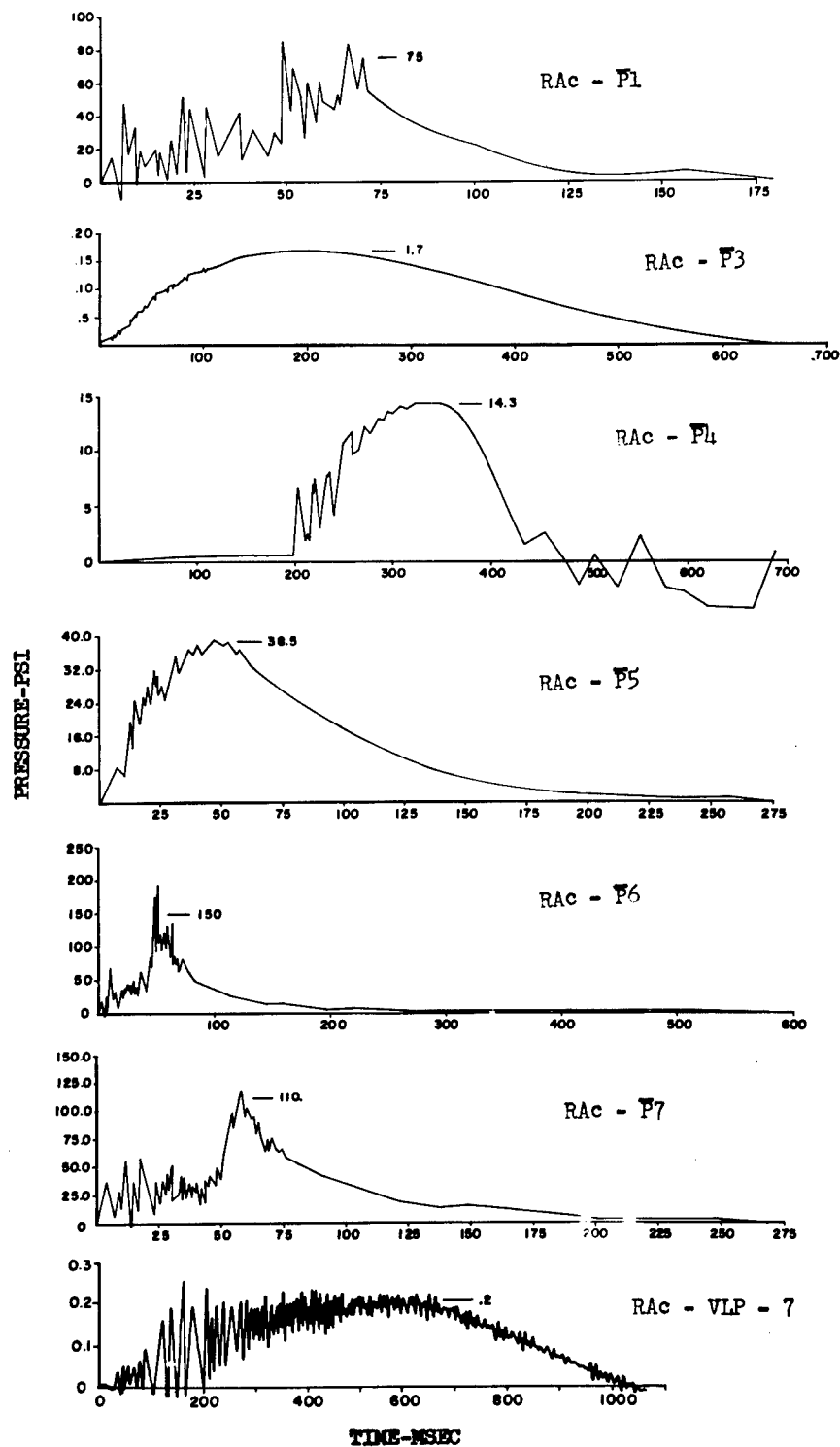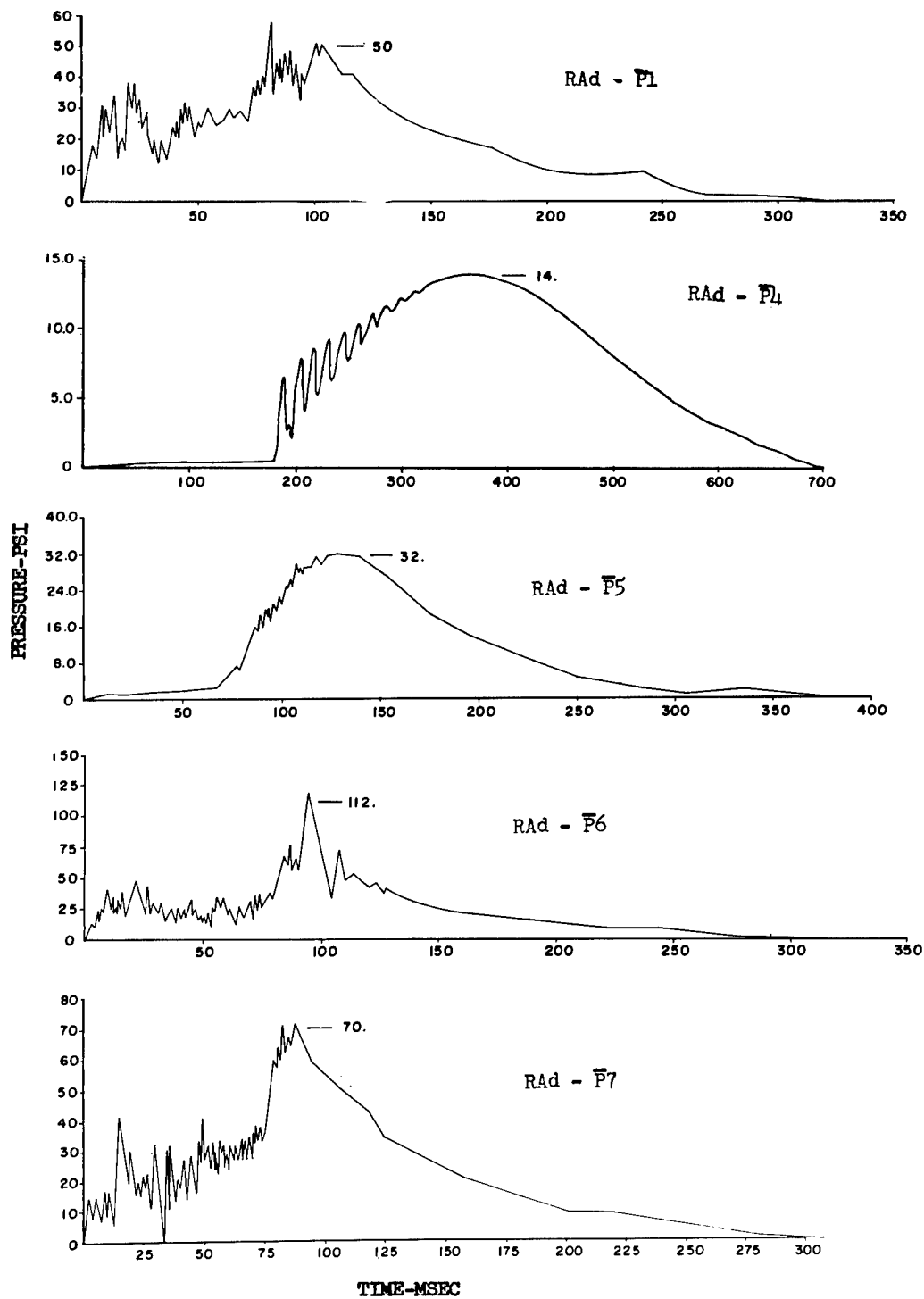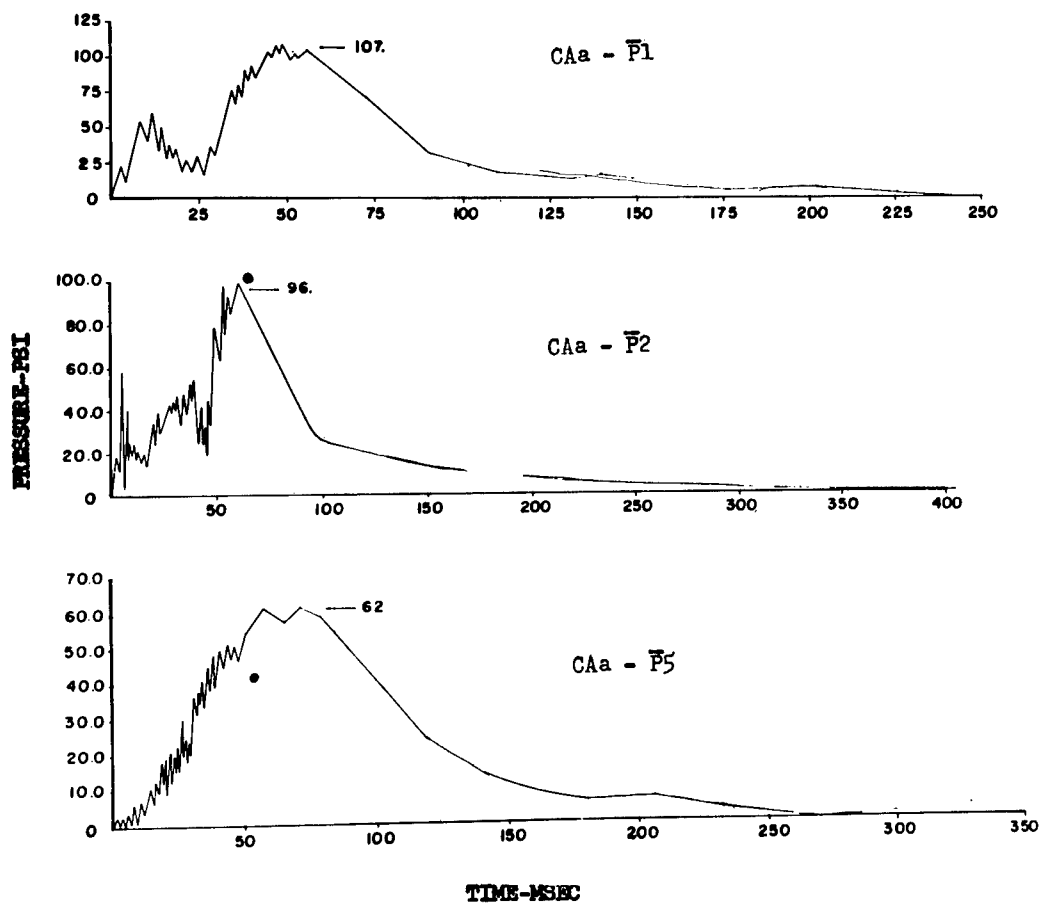
Fig. 3.104 — (Continued)

Fig. 3.104—(Continued)

153

Fig. 3.104—(Continued)

Fig. 3.104 — (Continued)

Fig. 3.104 — (Continued)

Fig. 3.104—(Continued)

Fig. 3.104—(Continued)

Fig. 3.104 — (Continued)

TIME - MSEC (Structure RAc)
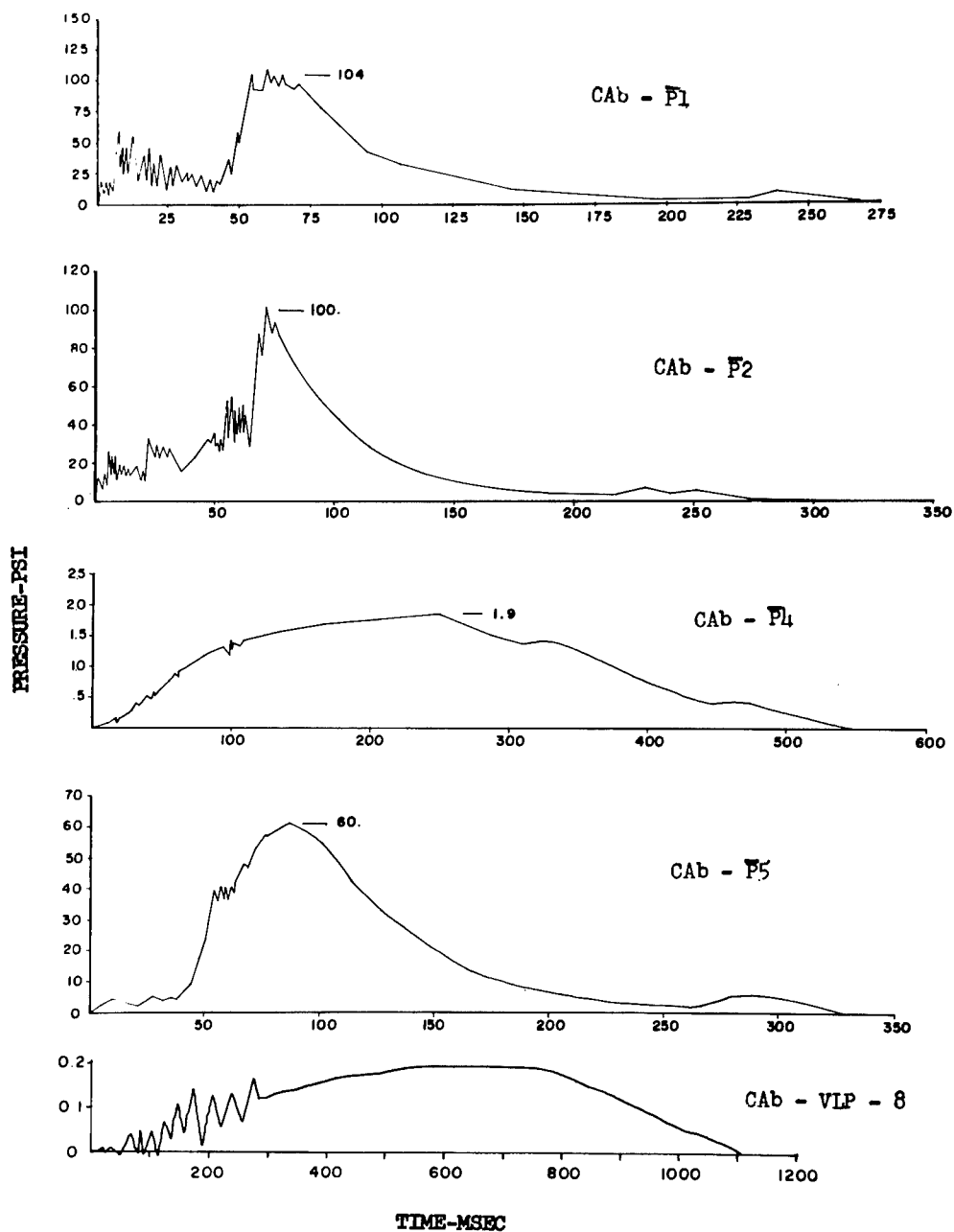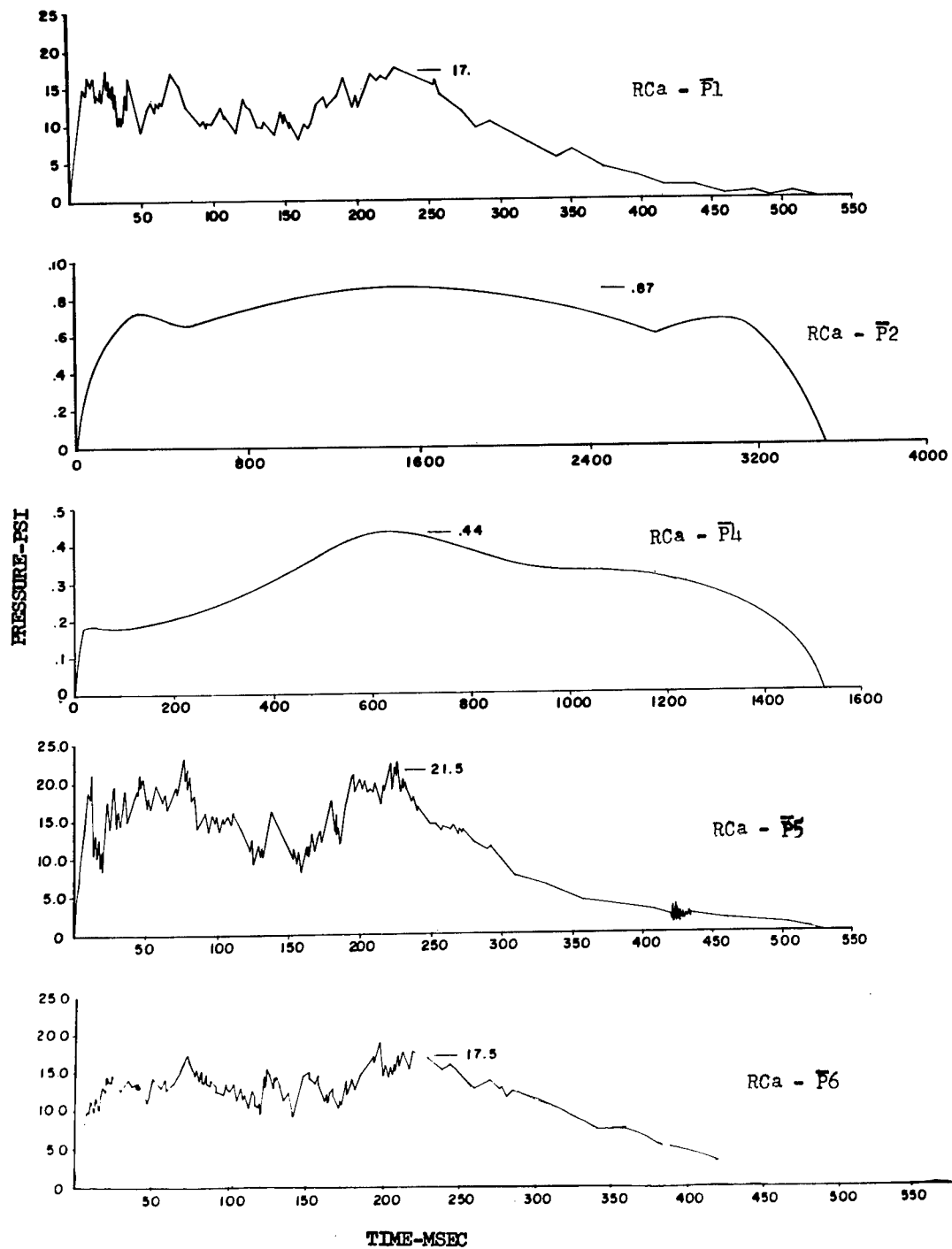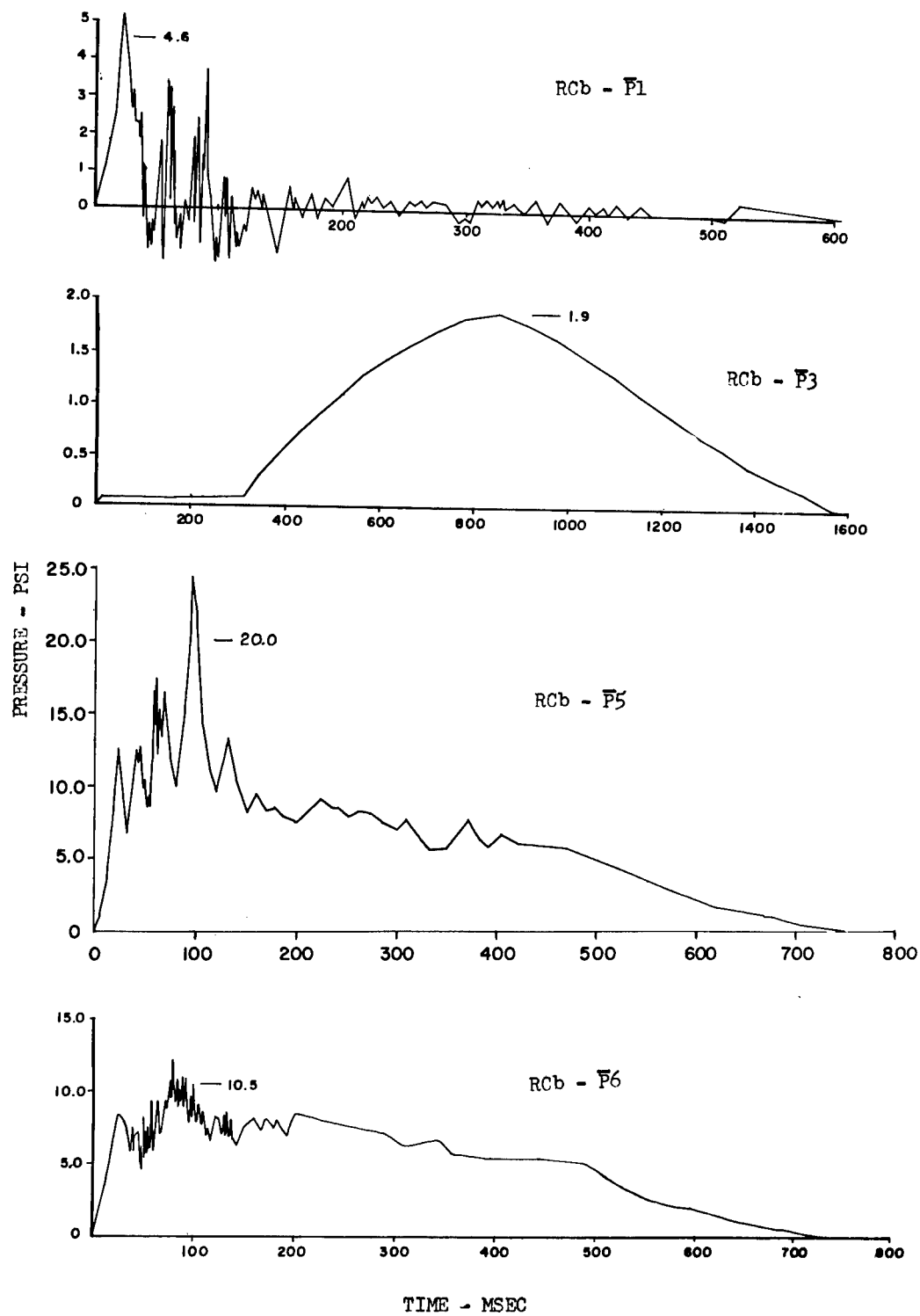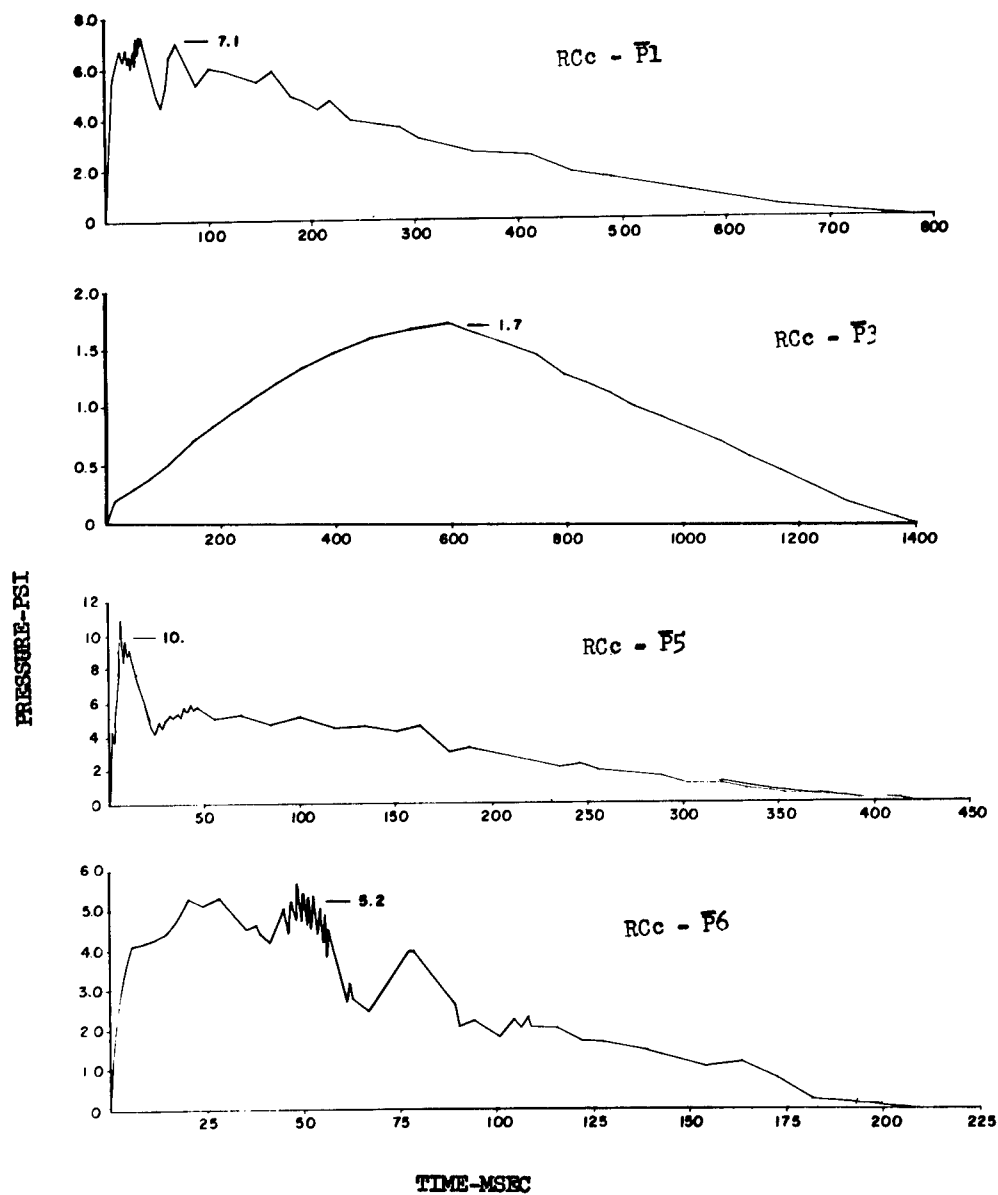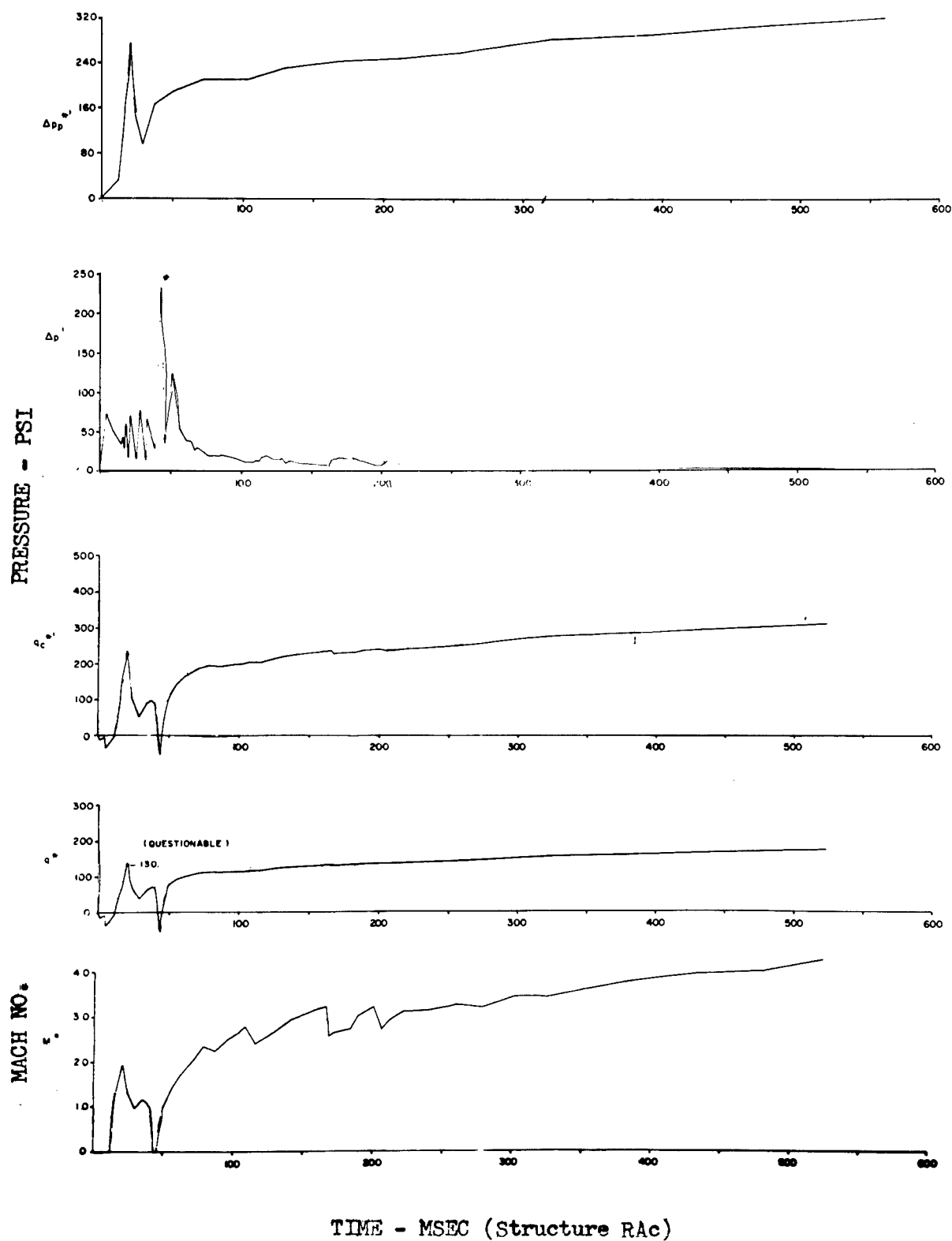
Fig. 3.105—Pressure, Mach number vs time; self-recording dynamic-pressure gauge records.

160

TIME — MSEC (Structure RCb)
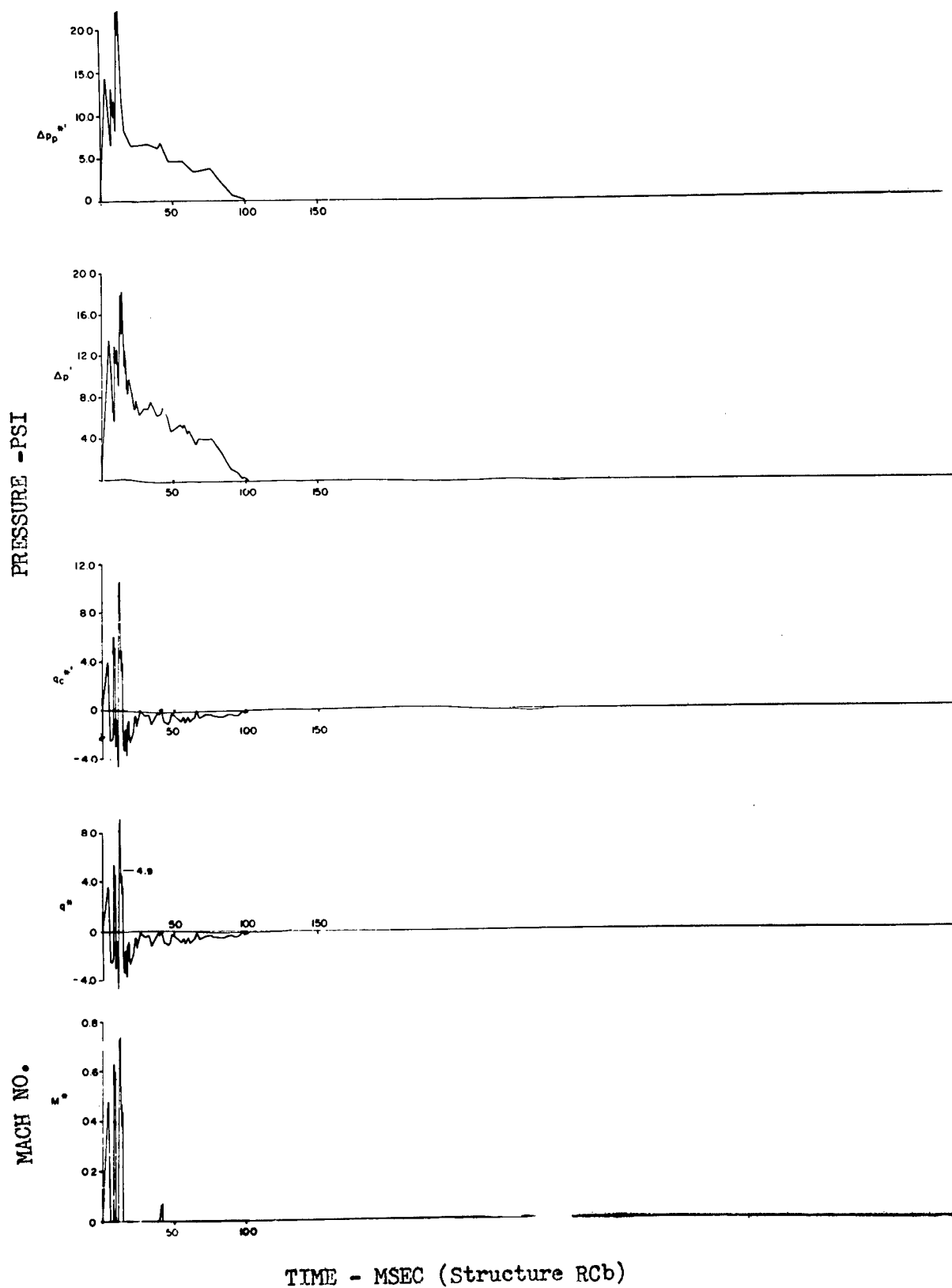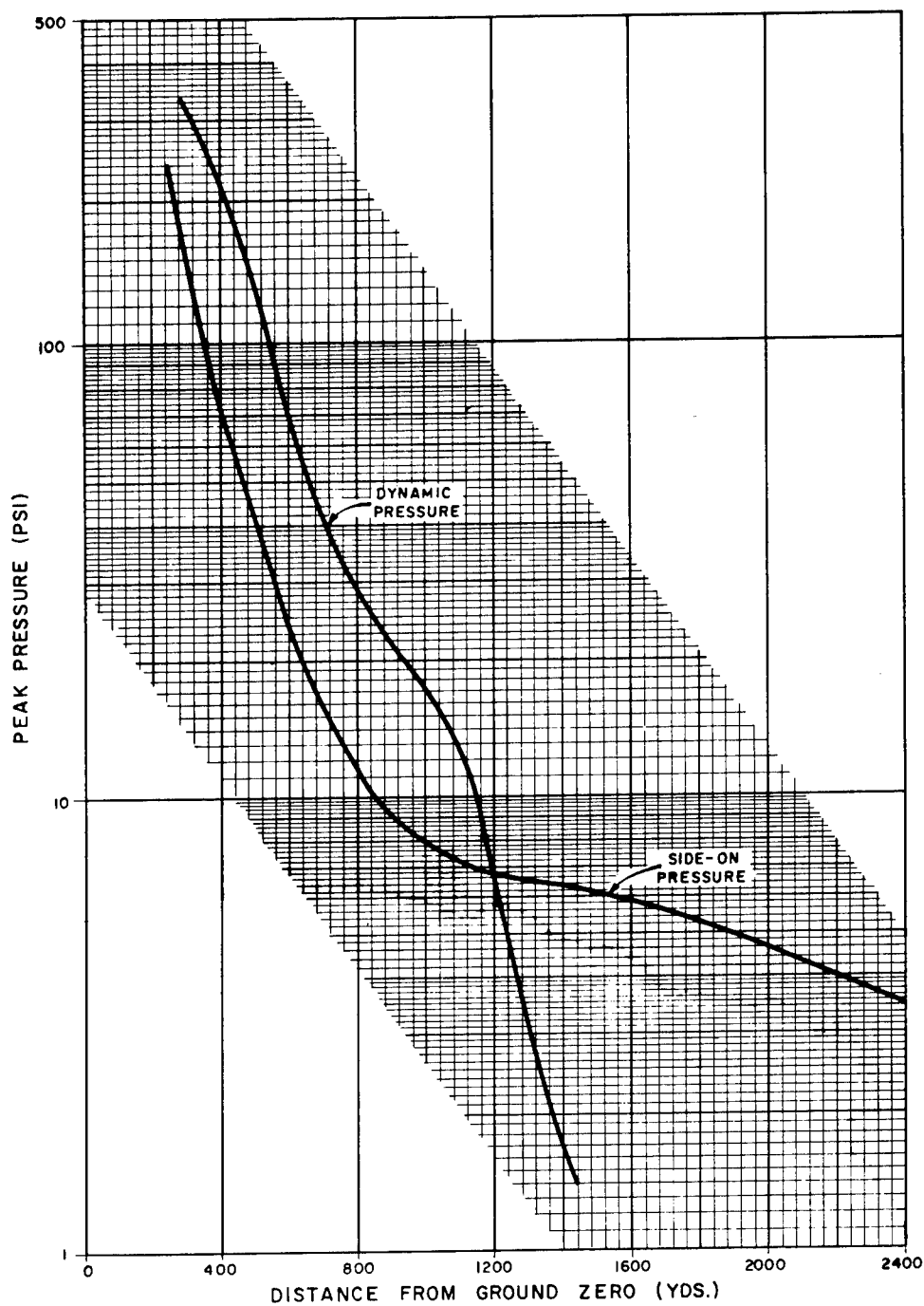
Fig. 3.105—(Continued)

Fig. 3.106—Blast-line pressure-distance curve.
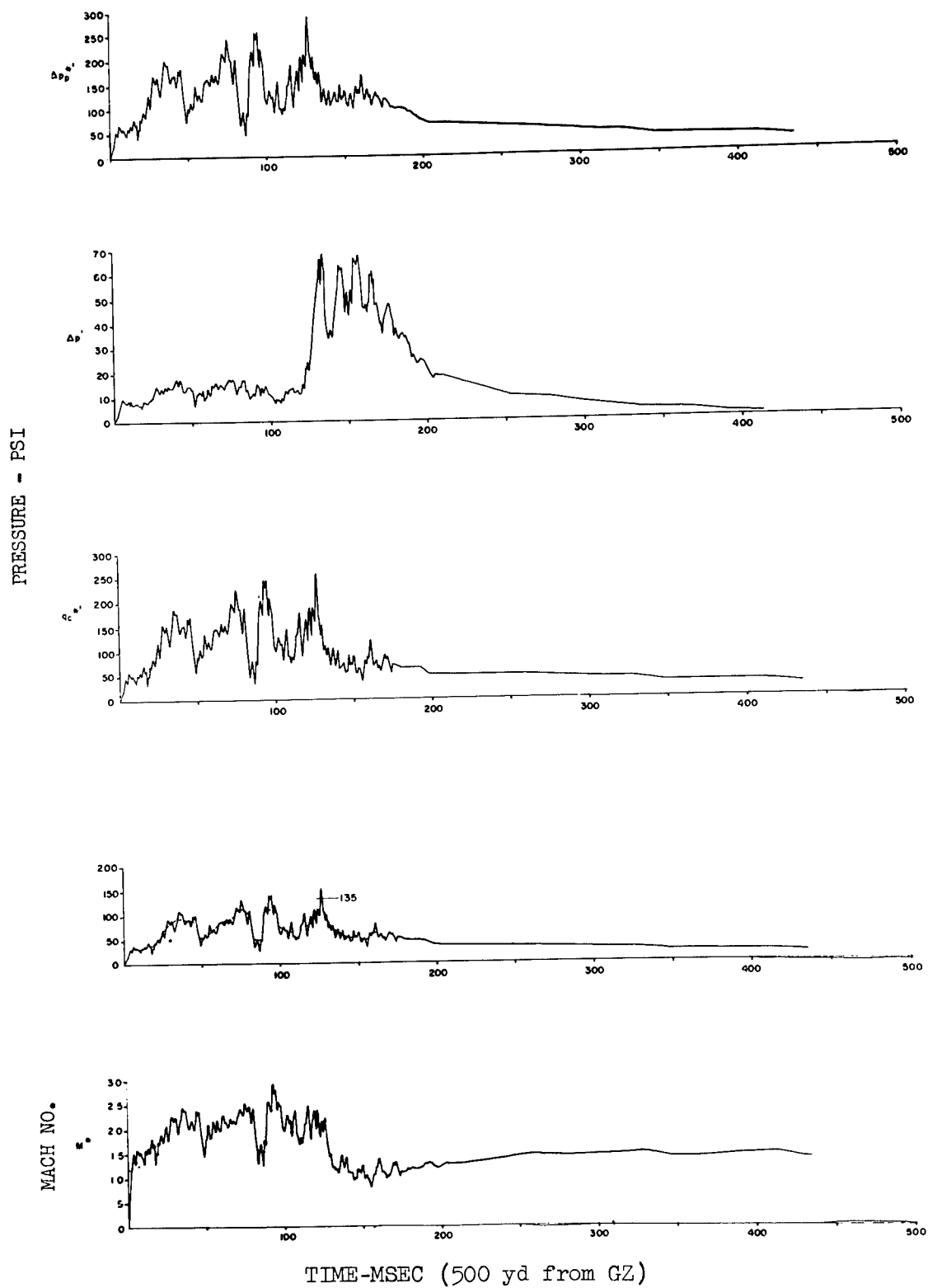
Fig. 3.107—Blast-line pressure, Mach number vs. time; self-recording dynamic-pressure gauge records.

163
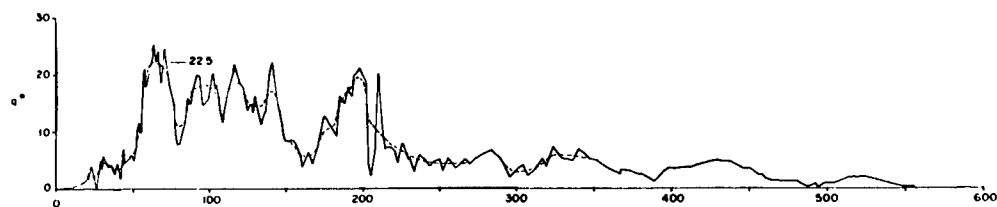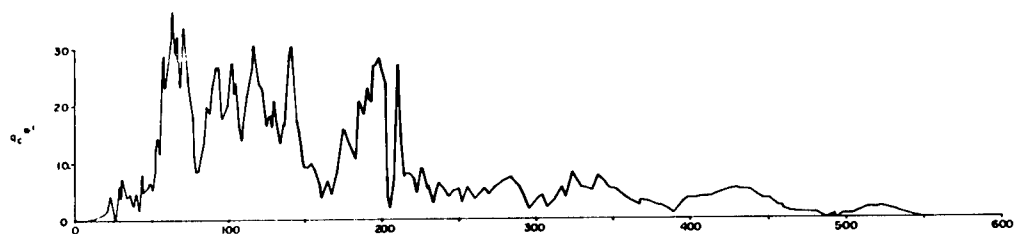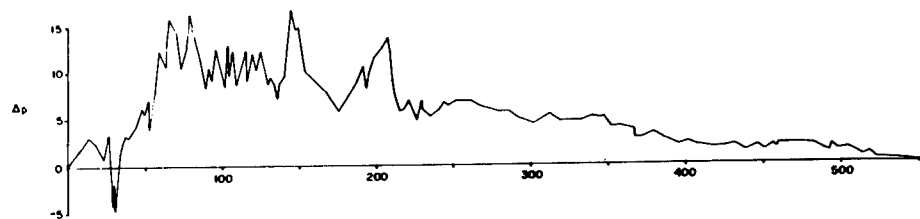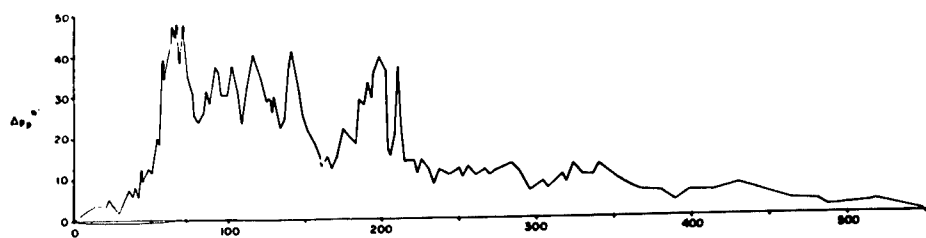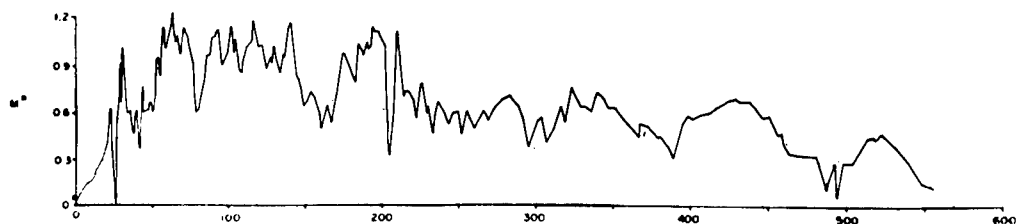
TIME-MSEC (863 yd from GZ)

Fig. 3.107—(Continued)

PRESSURE — PSI

MACH NO.

TIME-MSEC (981 yd from GZ)

Fig. 3.107—(Continued)

TIME-MSEC (1135 yd from GZ)
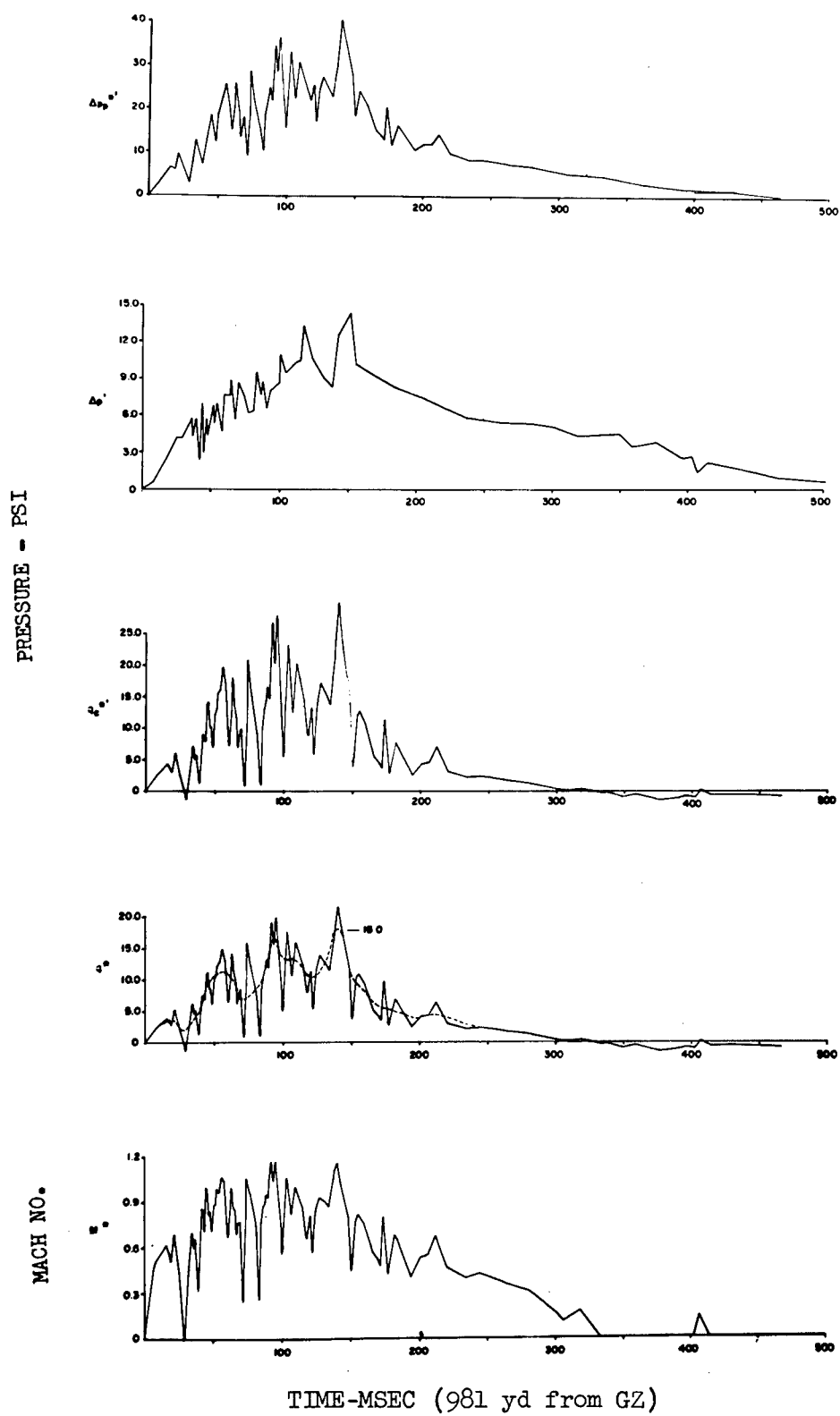
Fig. 3.107—(Continued)
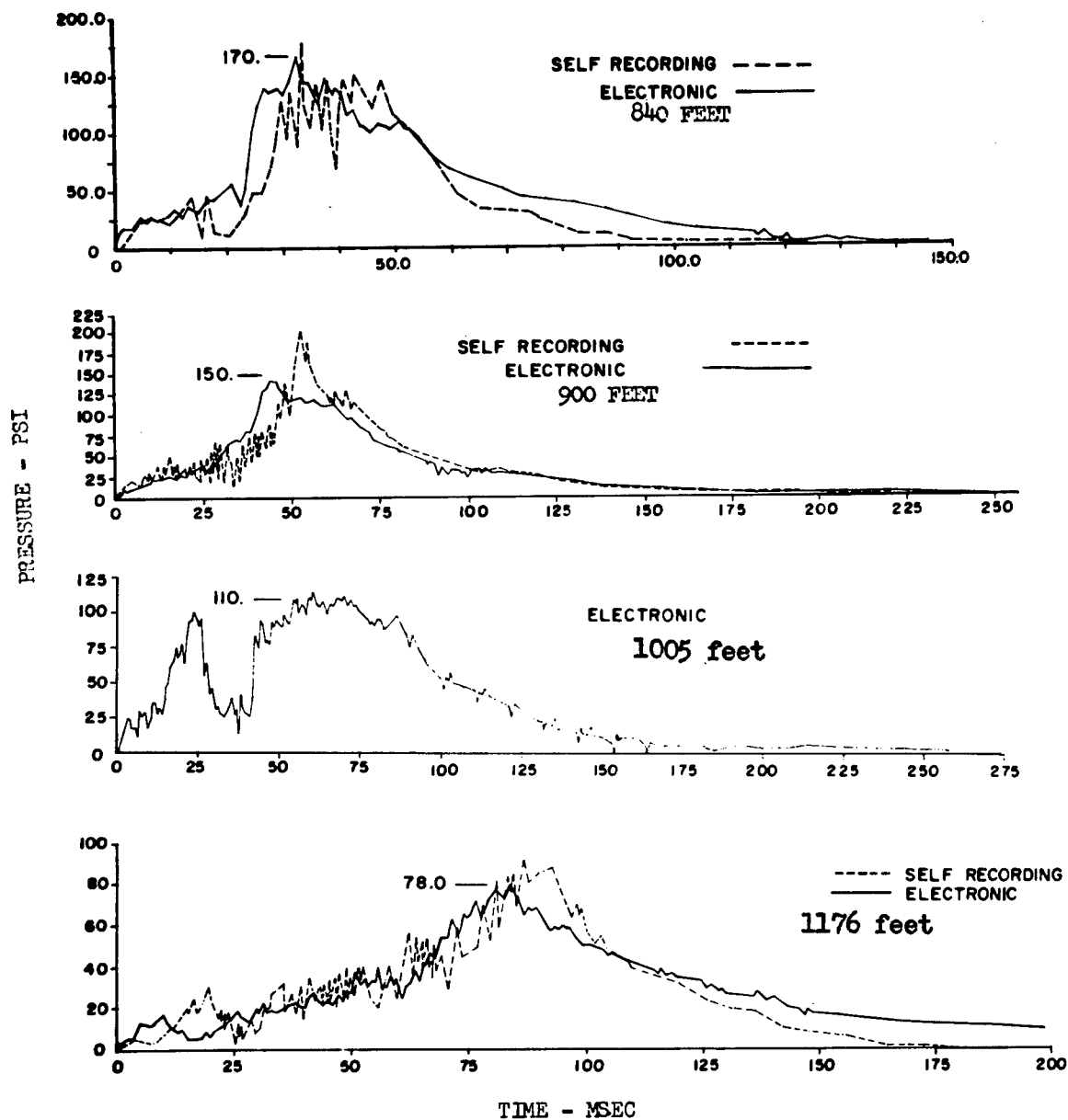
Fig. 3.108—Blast-line pressure-time; electronic and self-recording gauge records.
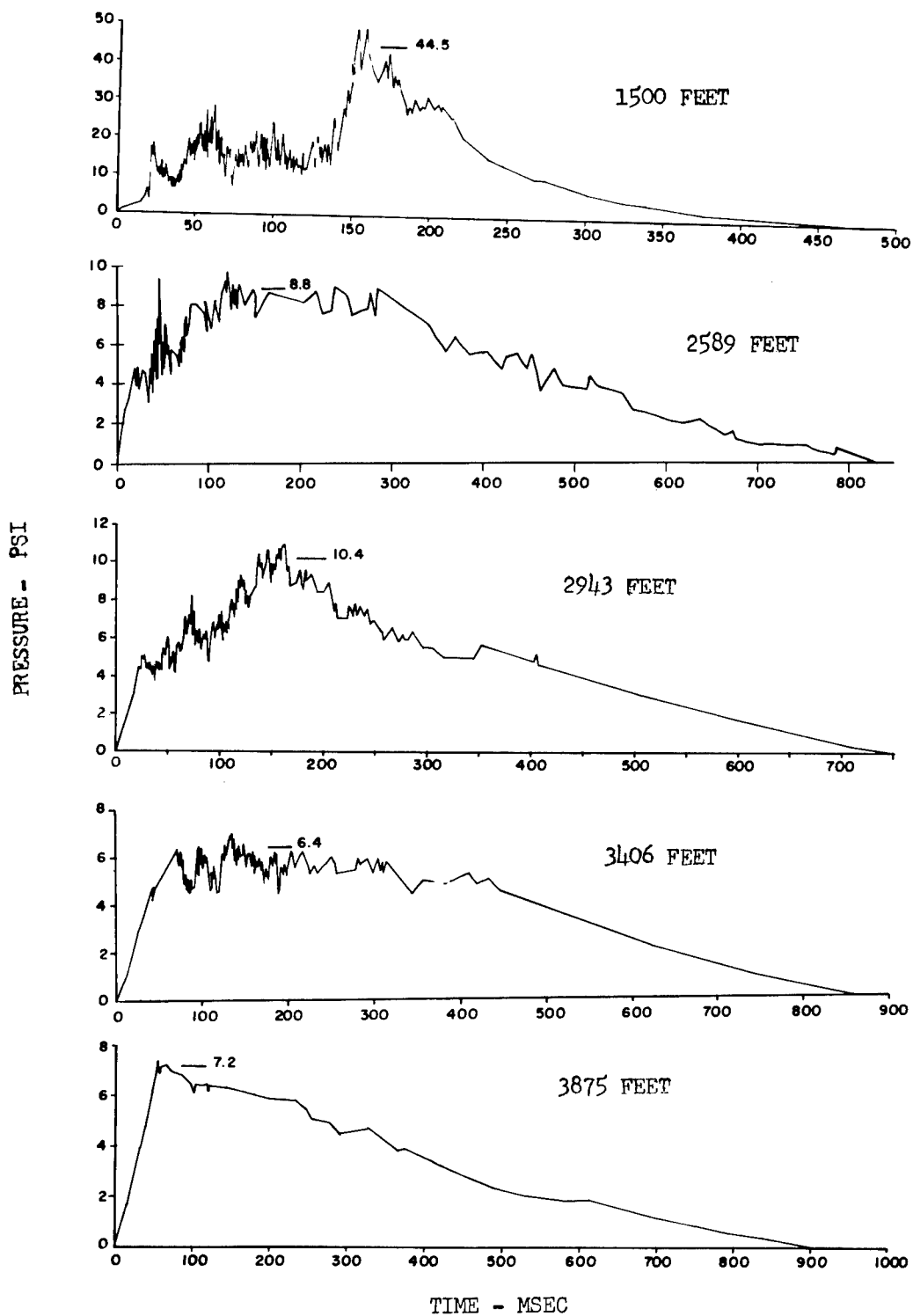
Fig. 3.109—Blast-line pressure-time; self-recording pressure gauge records.
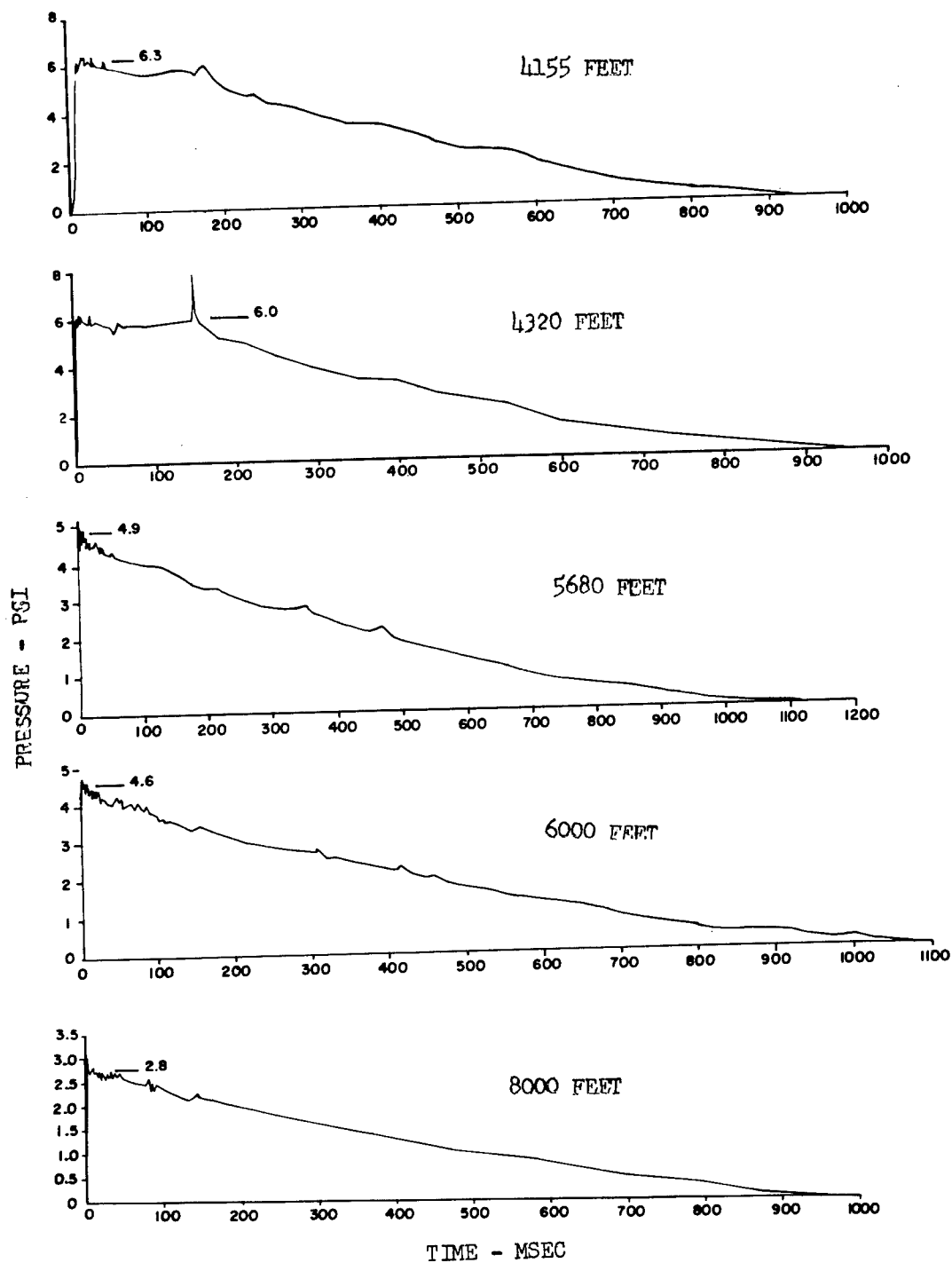
Fig. 3.109—(Continued)
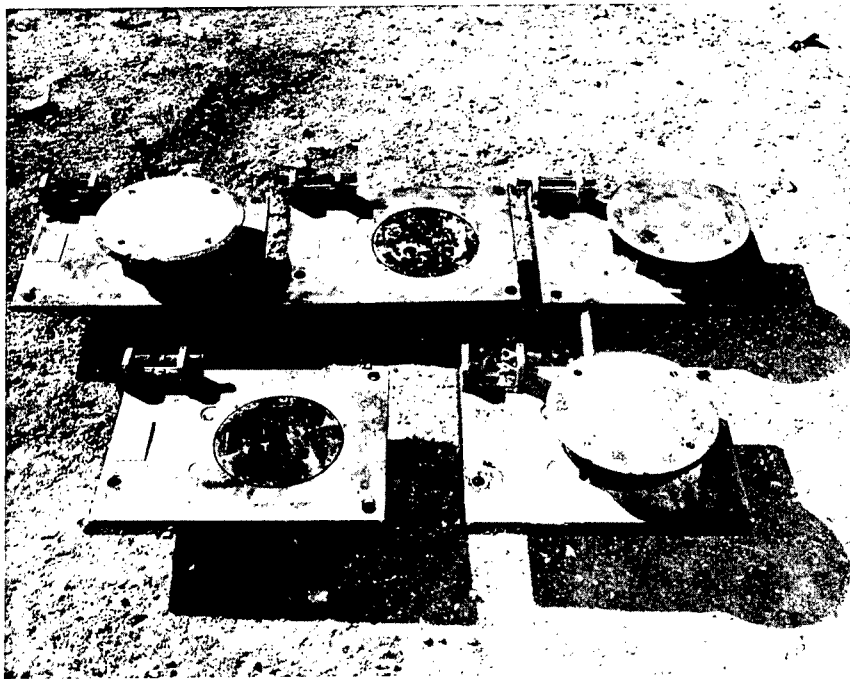
Fig. 3.110—German pressure gauges 1 to 5, following test.
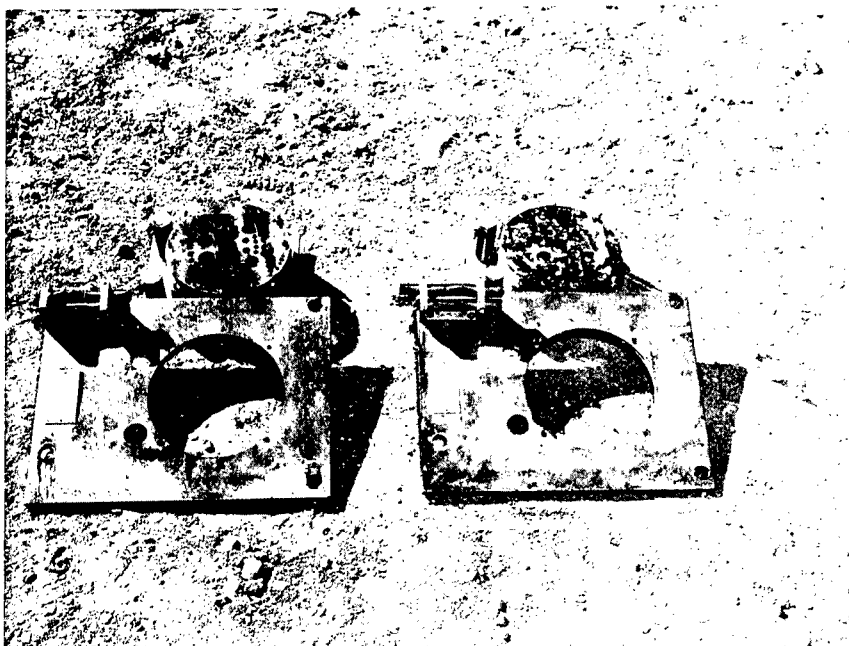
Fig. 3.111—German pressure gauges 1 and 4, following test.
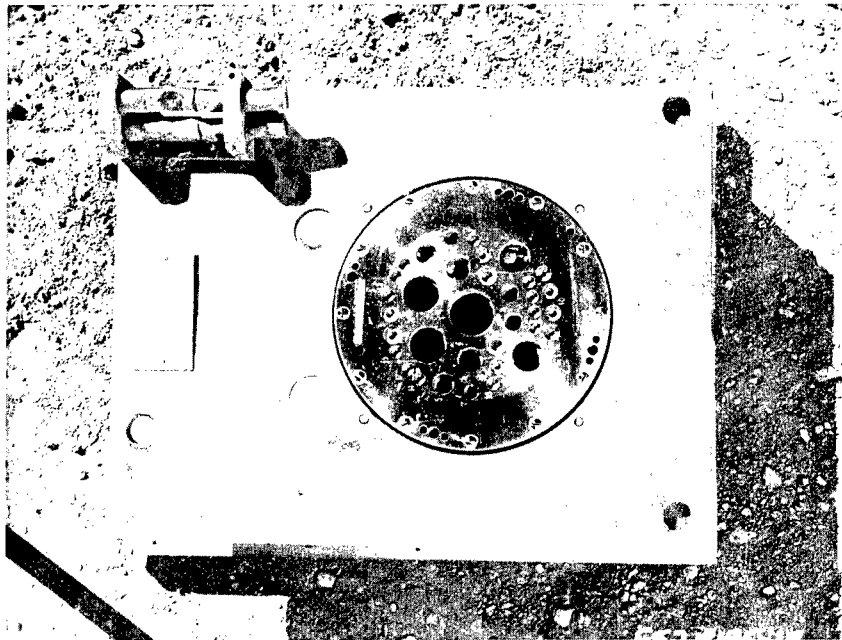
Fig. 3.112—Detail of German gauge No. 1.

Fig. 3.113—Detail of German gauge No. 2
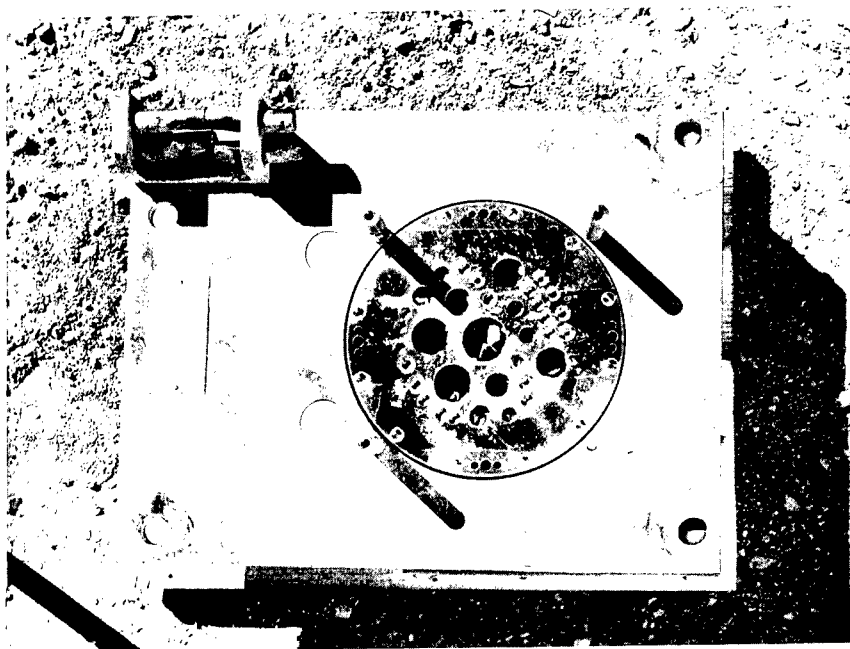
Fig. 3.114—Detail of German gauge No. 3.
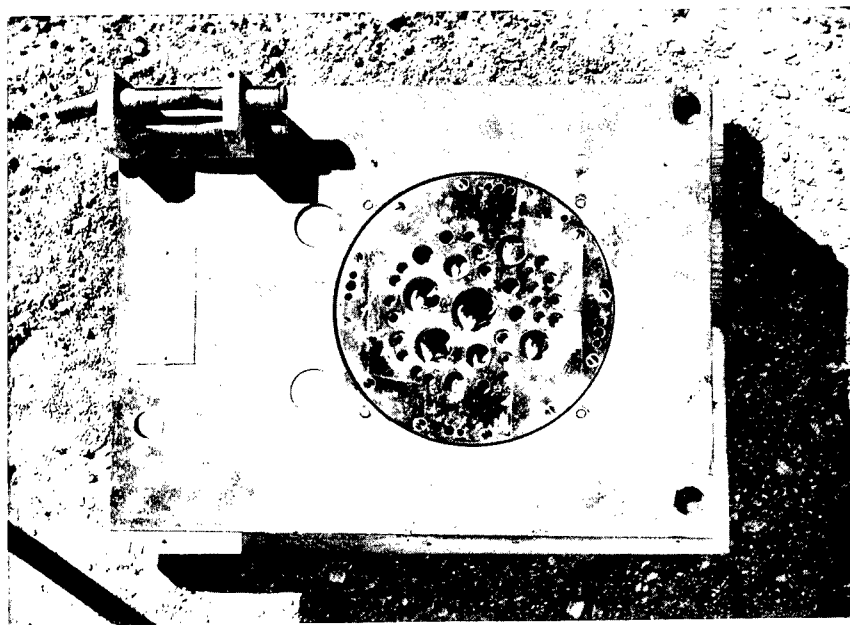
Fig. 3.115—Detail of German gauge No. 4.
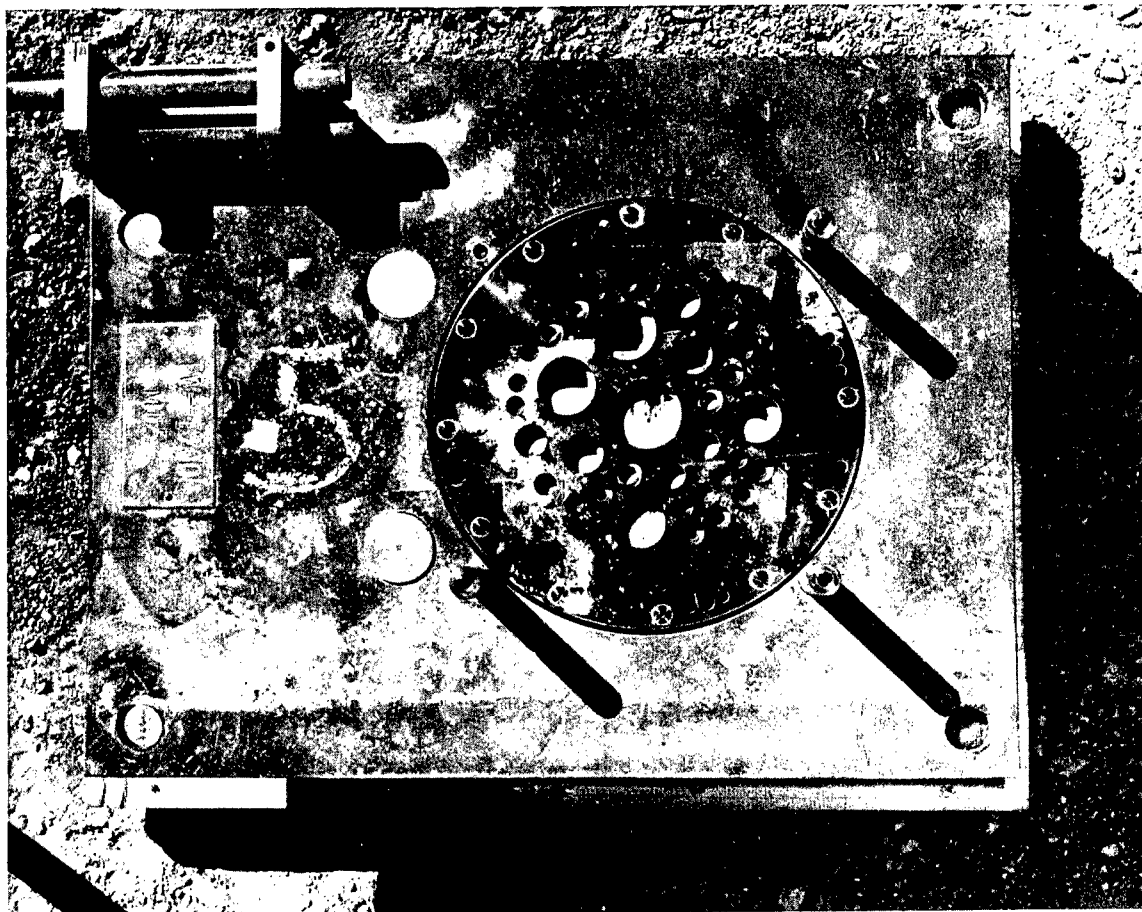
Fig. 3.116—Detail of German gauge No. 5.
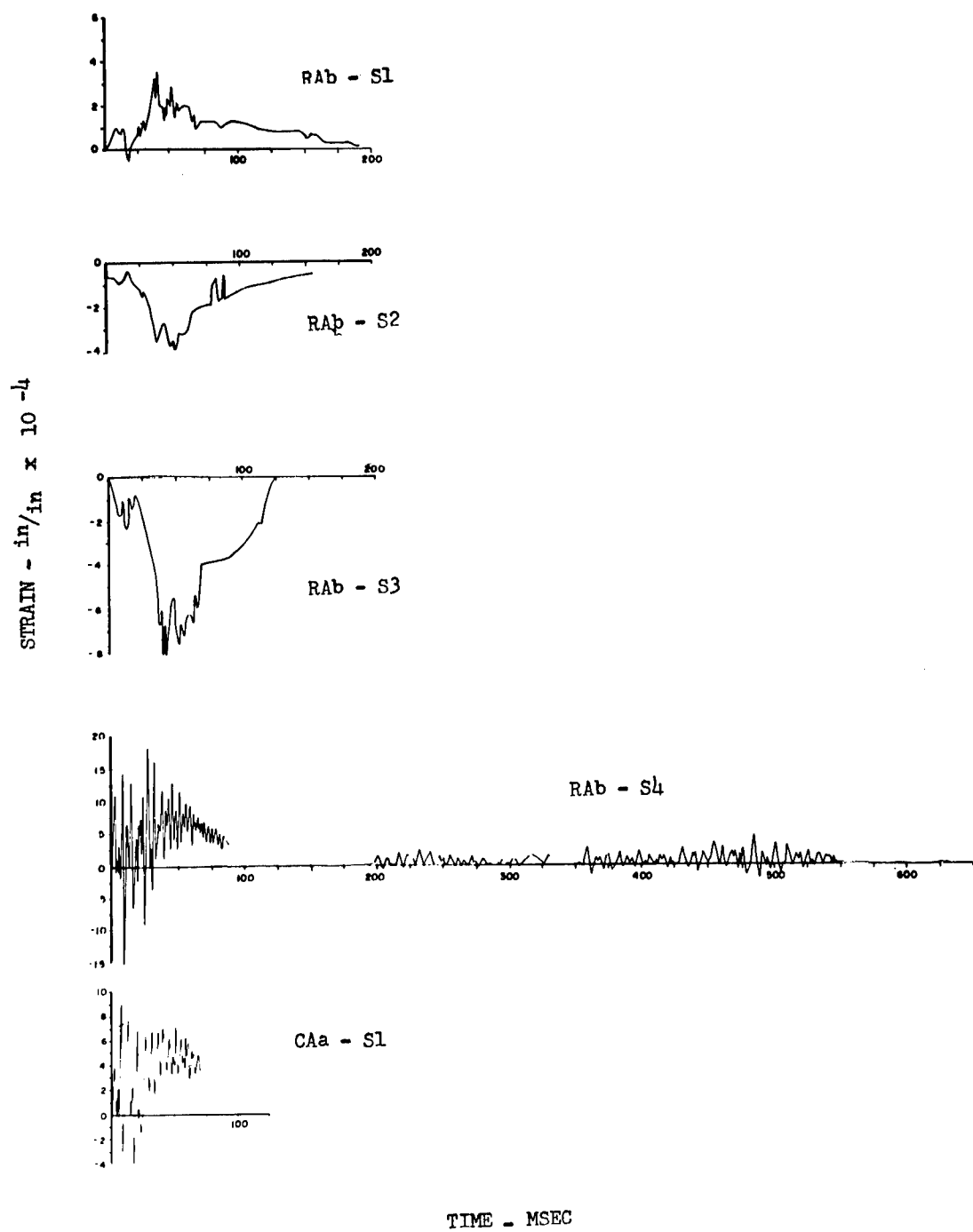
Fig. 3.117—Strain-time; electronic strain gauge records.
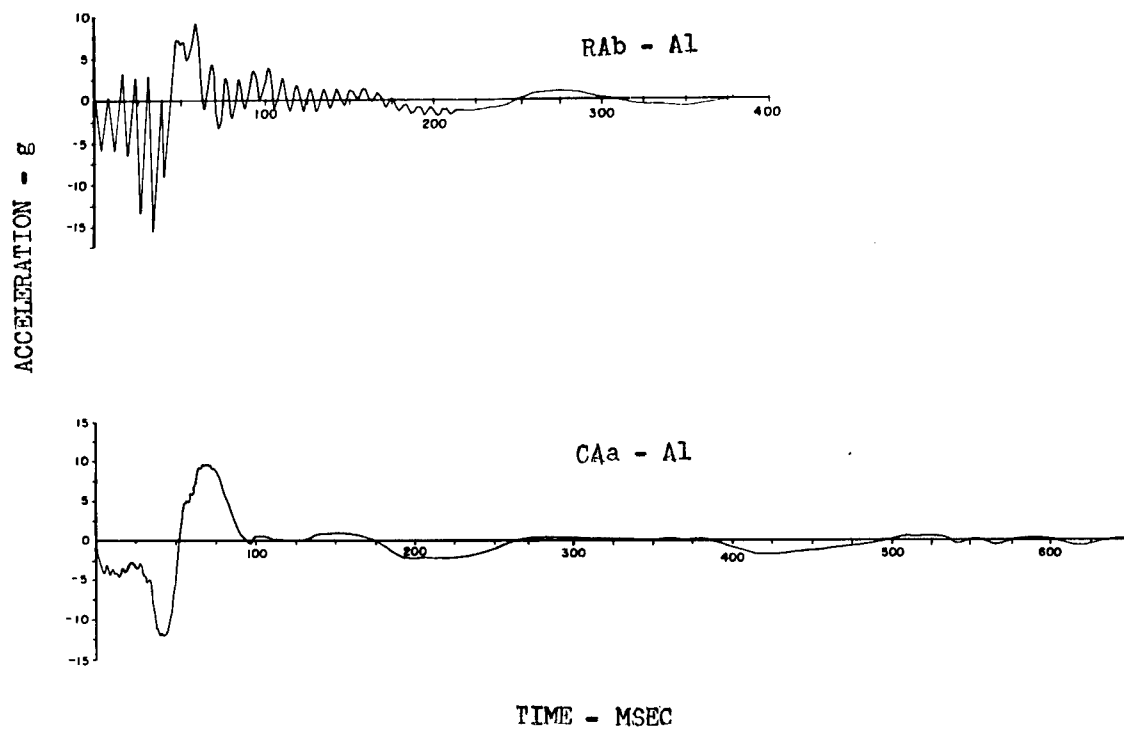
Fig. 3.118—Acceleration-time; electronic acceleration gauge records.
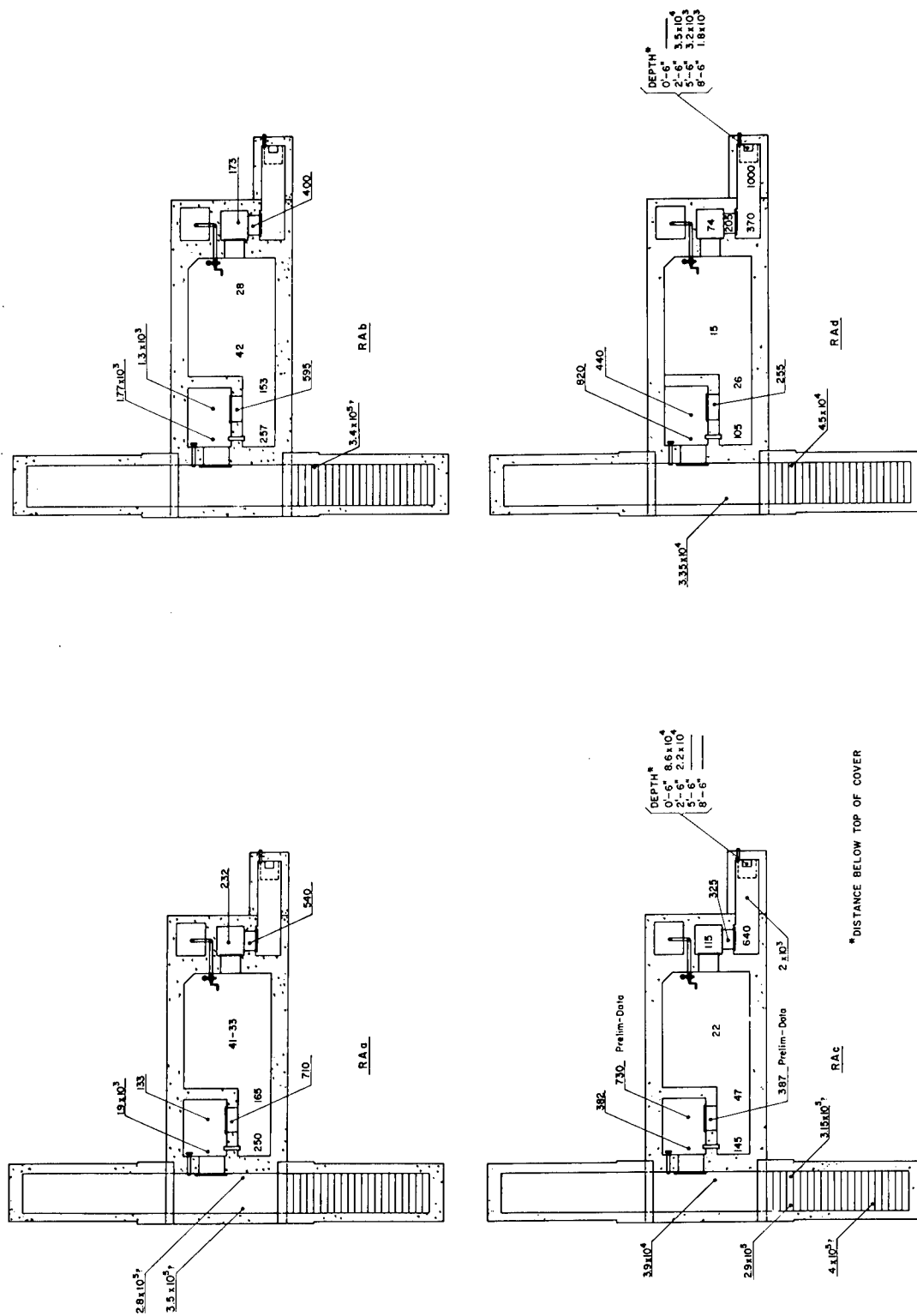
Fig. 3.119—Approximate total gamma dosages during first 52 hr after detonation (structure RA).

176
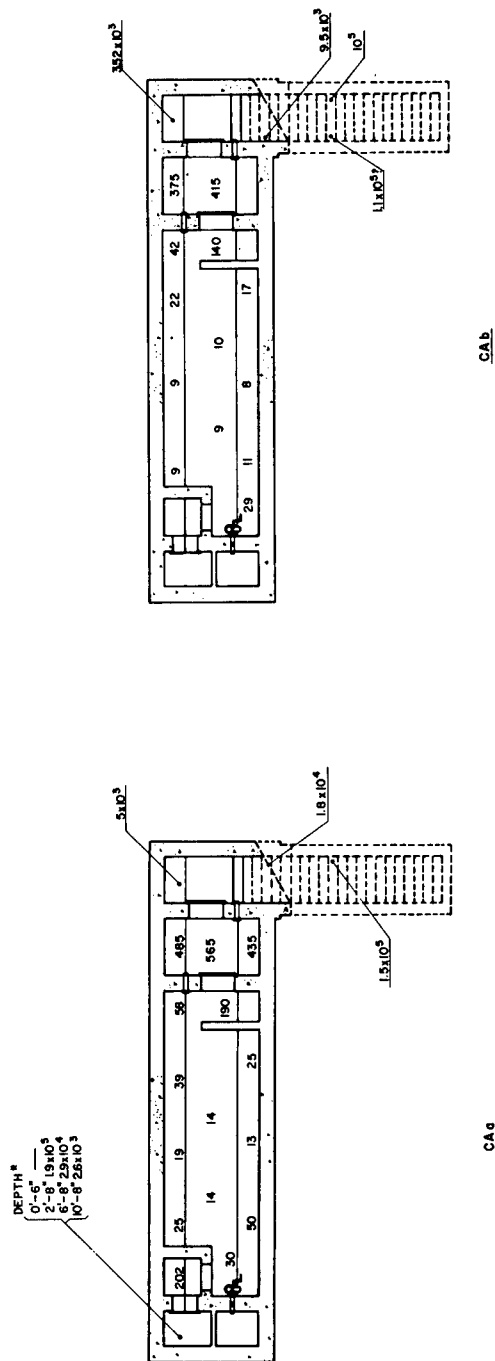
Fig. 3.120—Approximate total gamma dosages during first 52 hr after detonation (structure CA).

177
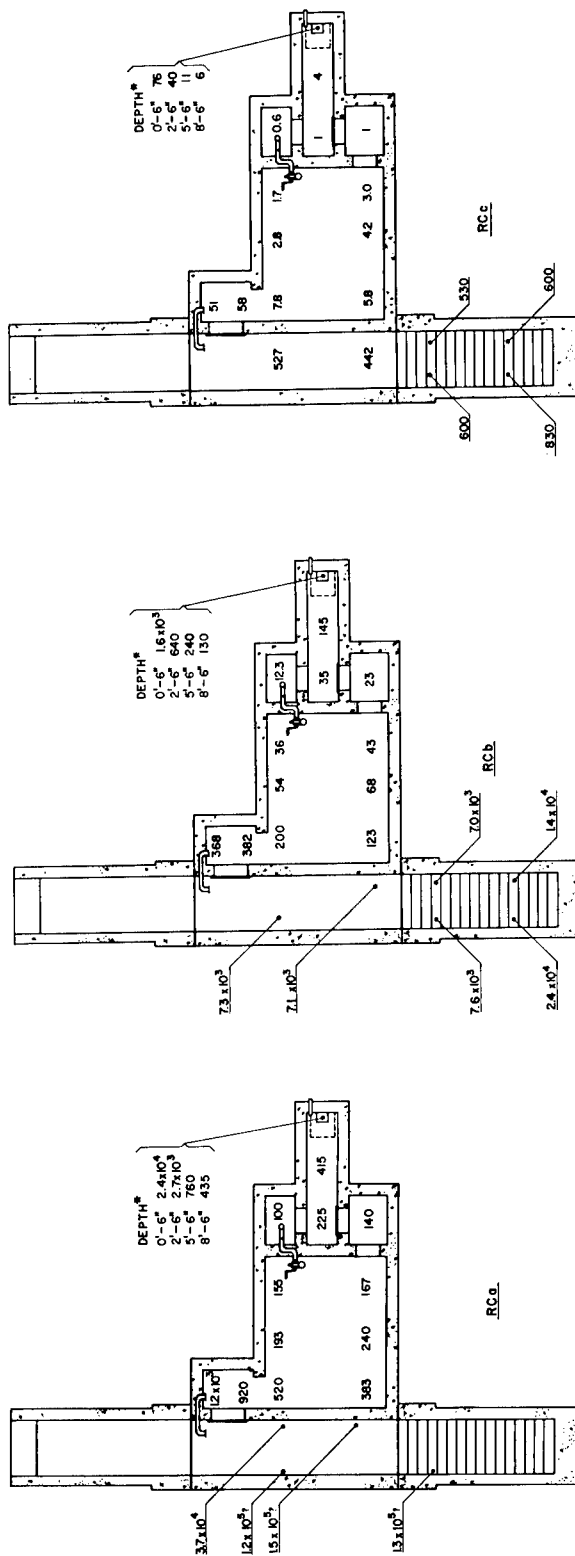
Fig. 3.121—Approximate total gamma dosages during first 52 hr after detonation (structure RC).
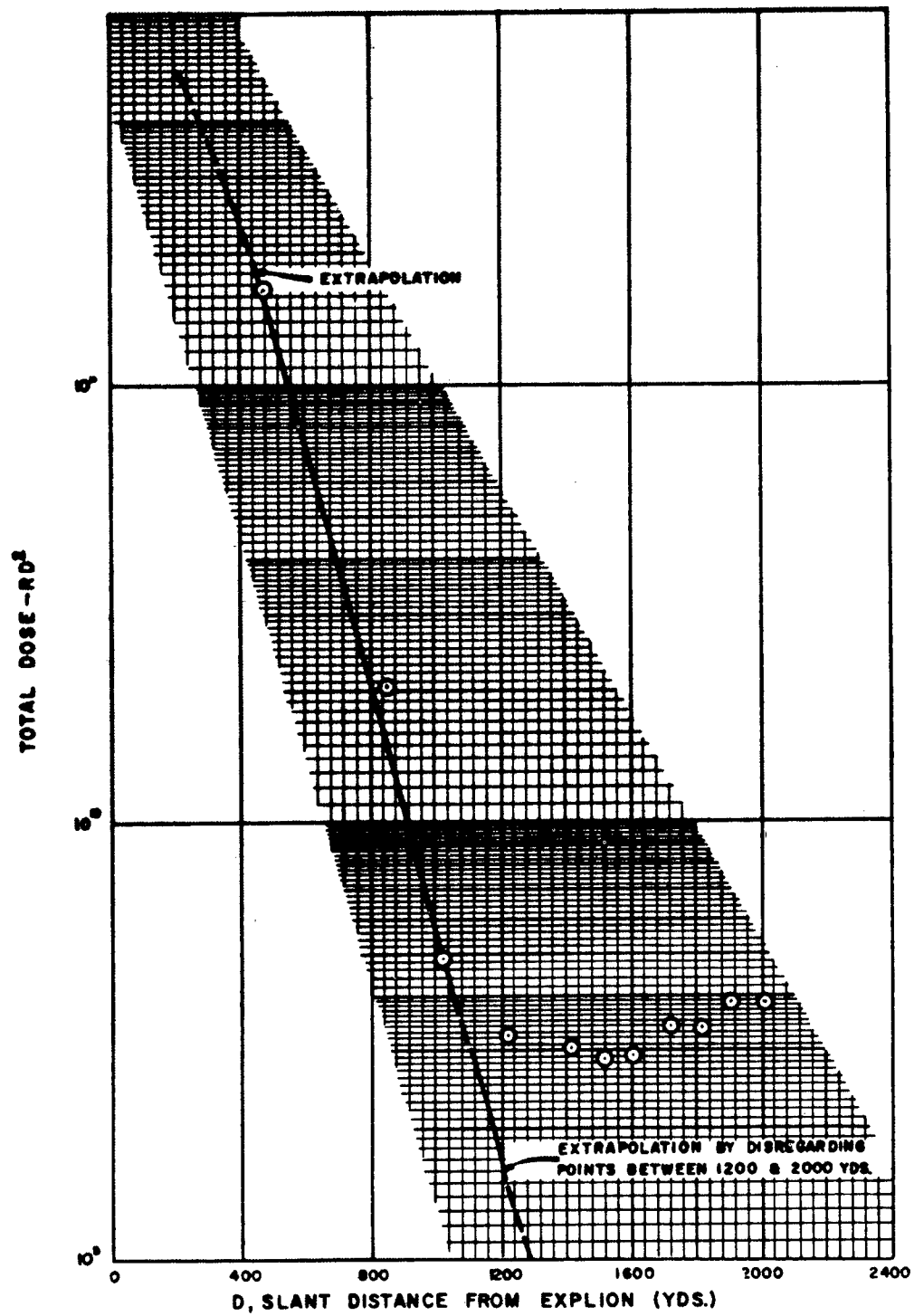
Fig. 3.122— Blast-line total gamma dose-distance curve.

179
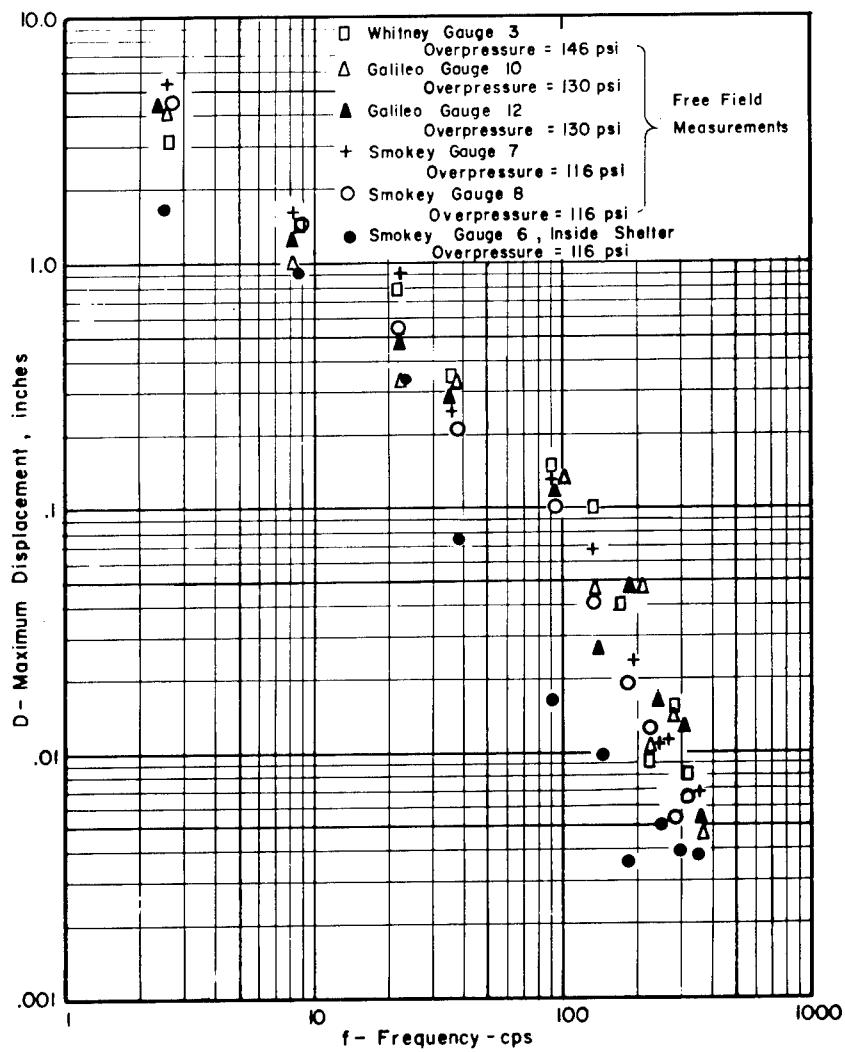
Fig. 3.123—Displacement-shock spectrum, vertical direction.
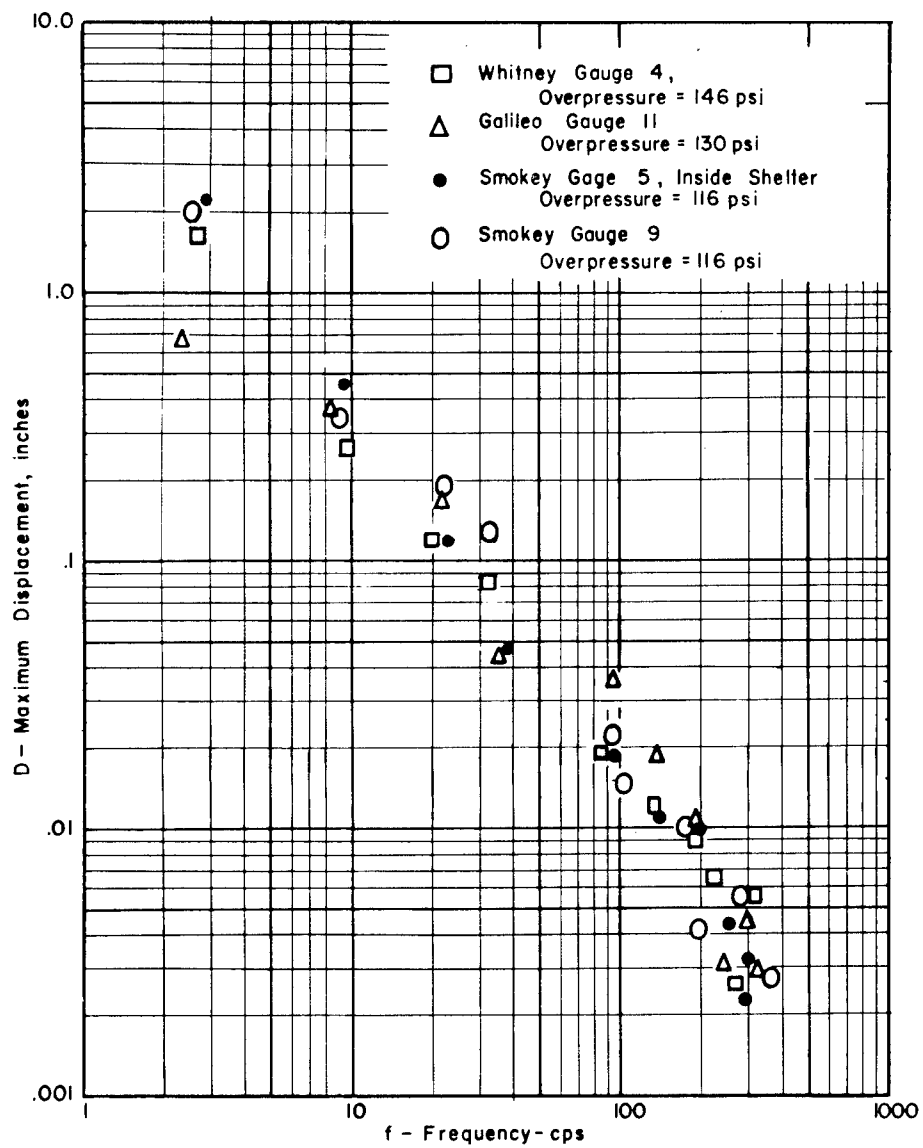
Fig. 3.124 — Displacement-shock spectrum, horizontal direction.
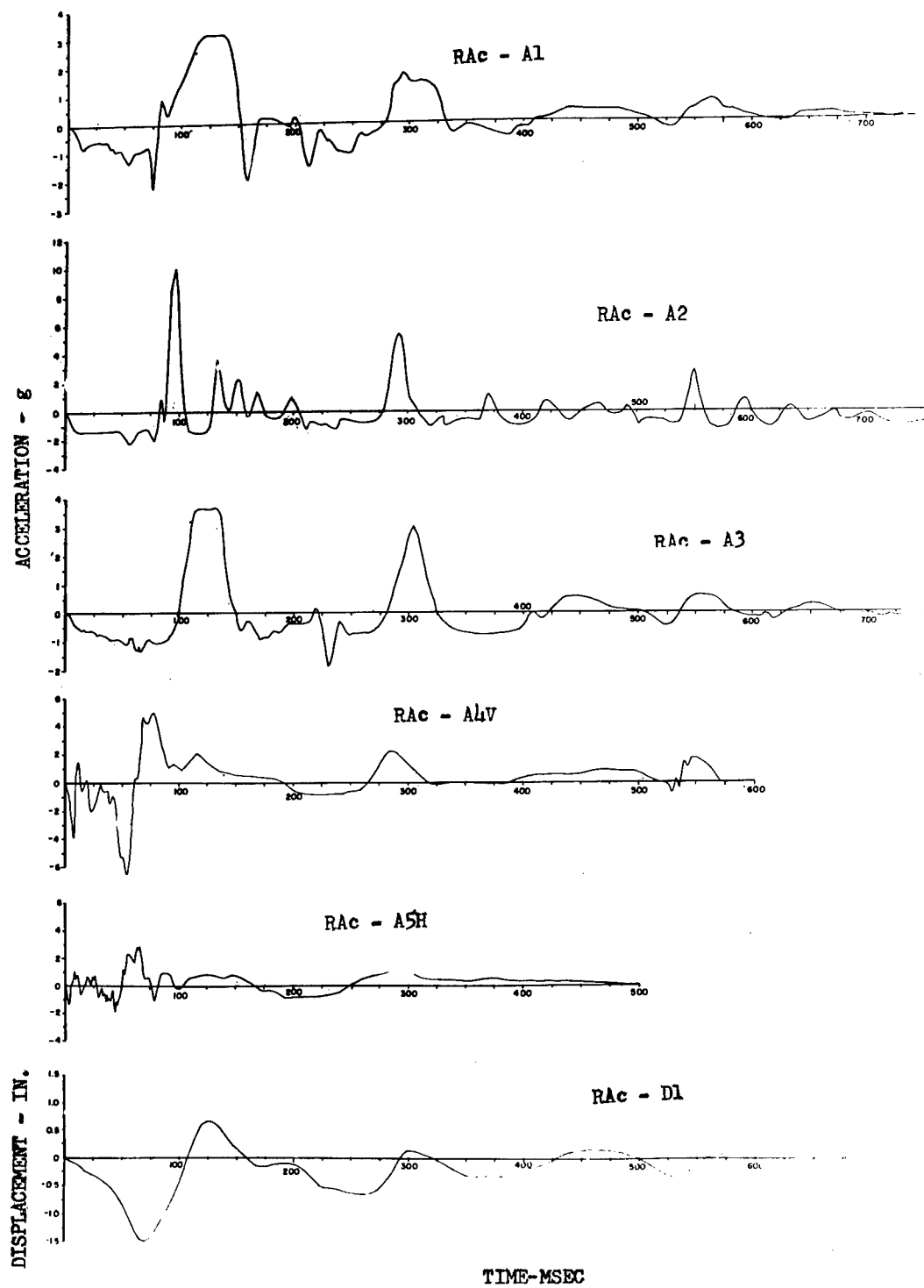
Fig. 5.125—Acceleration- and displacement-time, acceleration test gauge records.
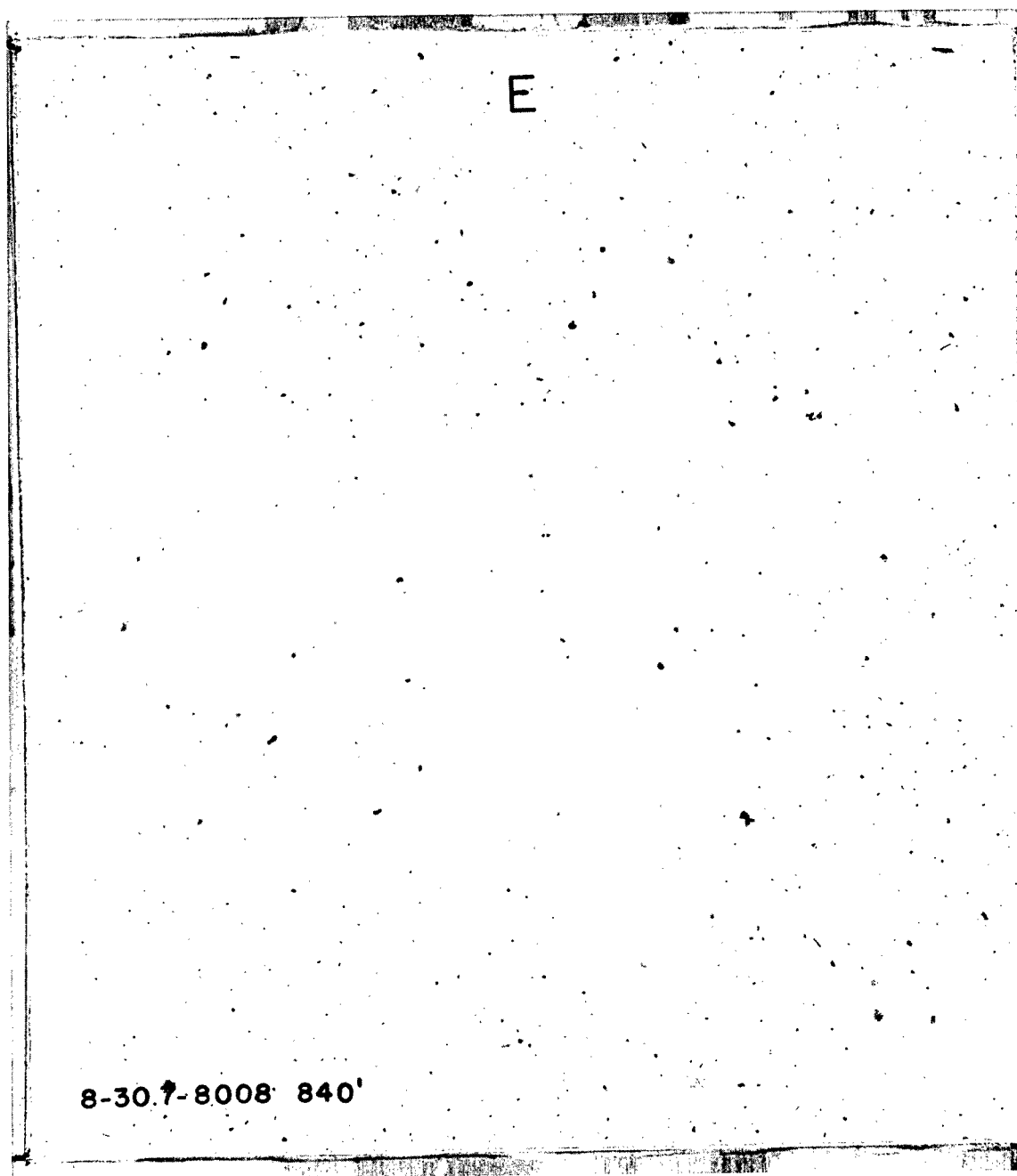
Fig. 3.126—Sticky-paper dust collector, type B (structure RAa).
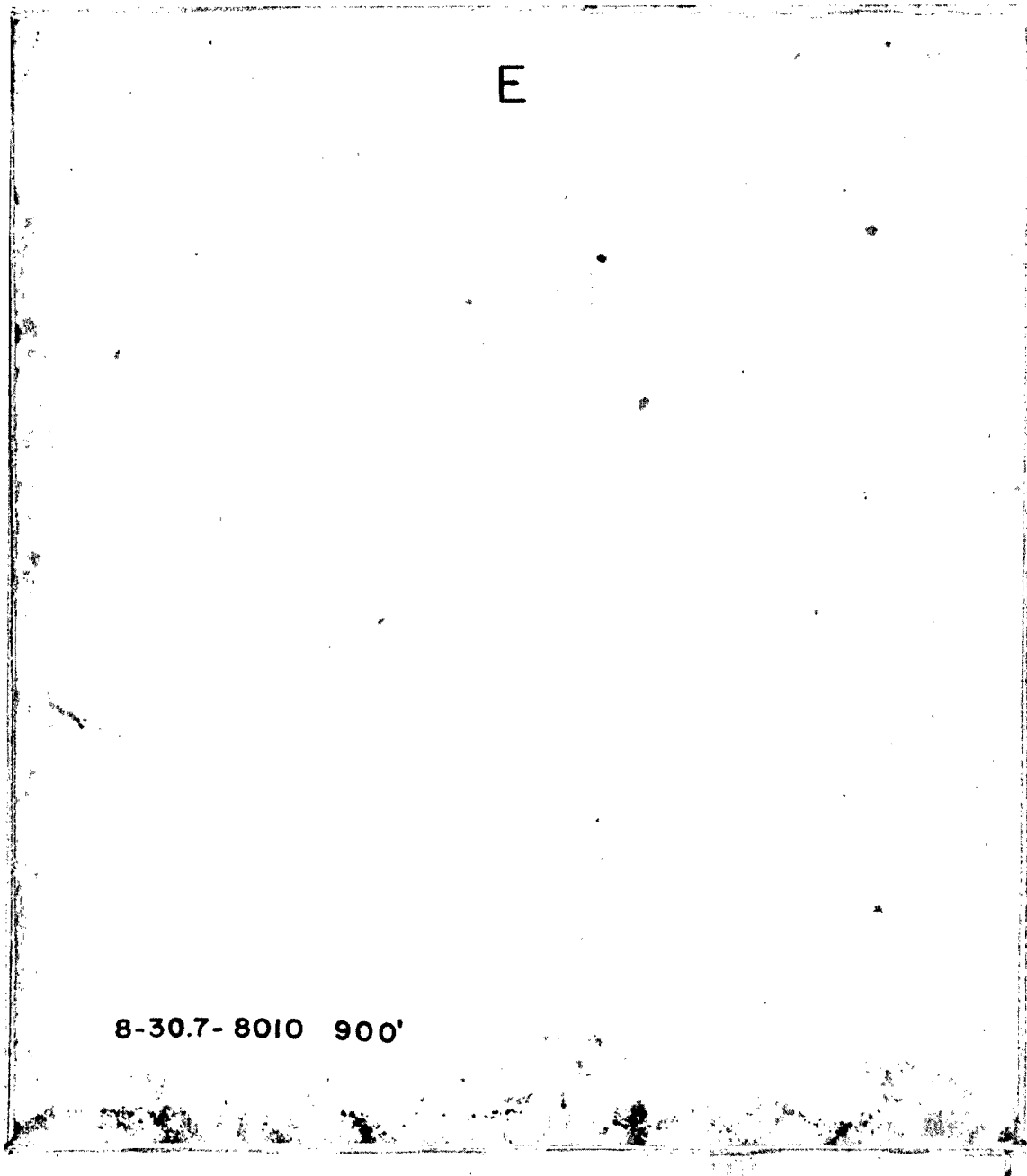
Fig. 3.127—Sticky-paper dust collector, type B (structure RAb).

E

8-30.7-8011 1005'
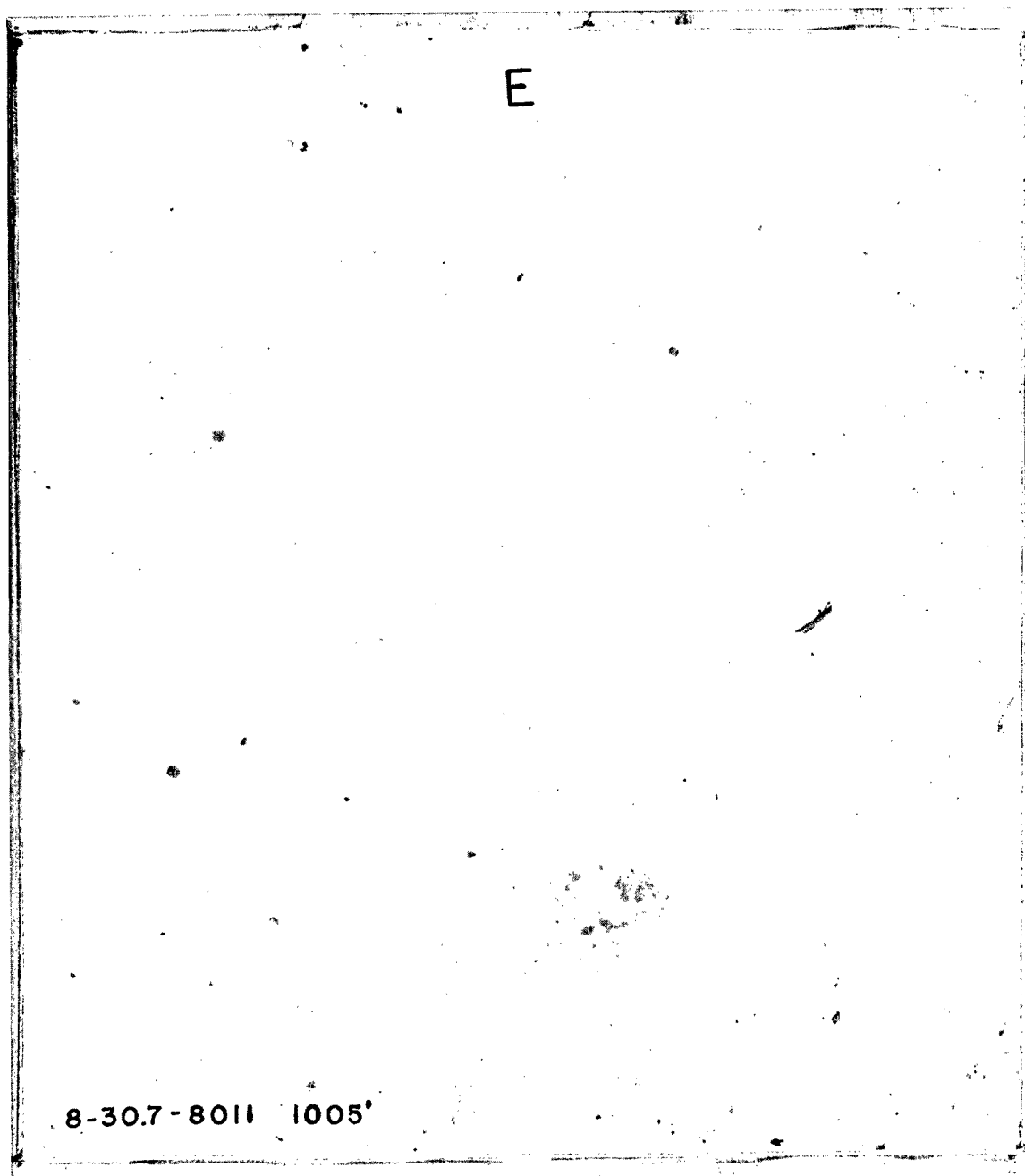
Fig. 3.128—Sticky-paper dust collector, type B (structure RAc).

E

8-30.7 - 8013 1176'
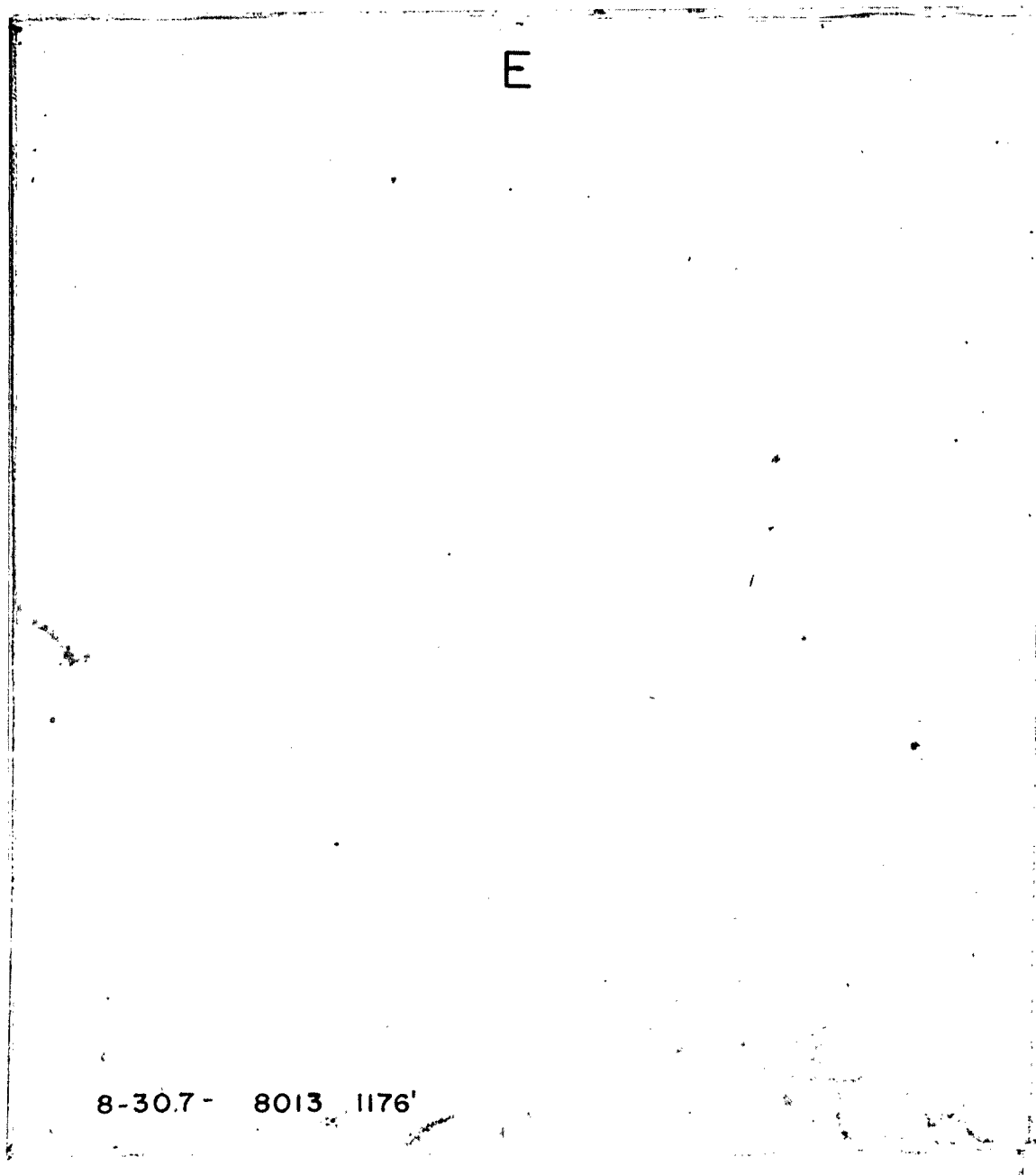
Fig. 3.129—Sticky-paper dust collector, type B (structure RAd).

LABORATORY CONTROL
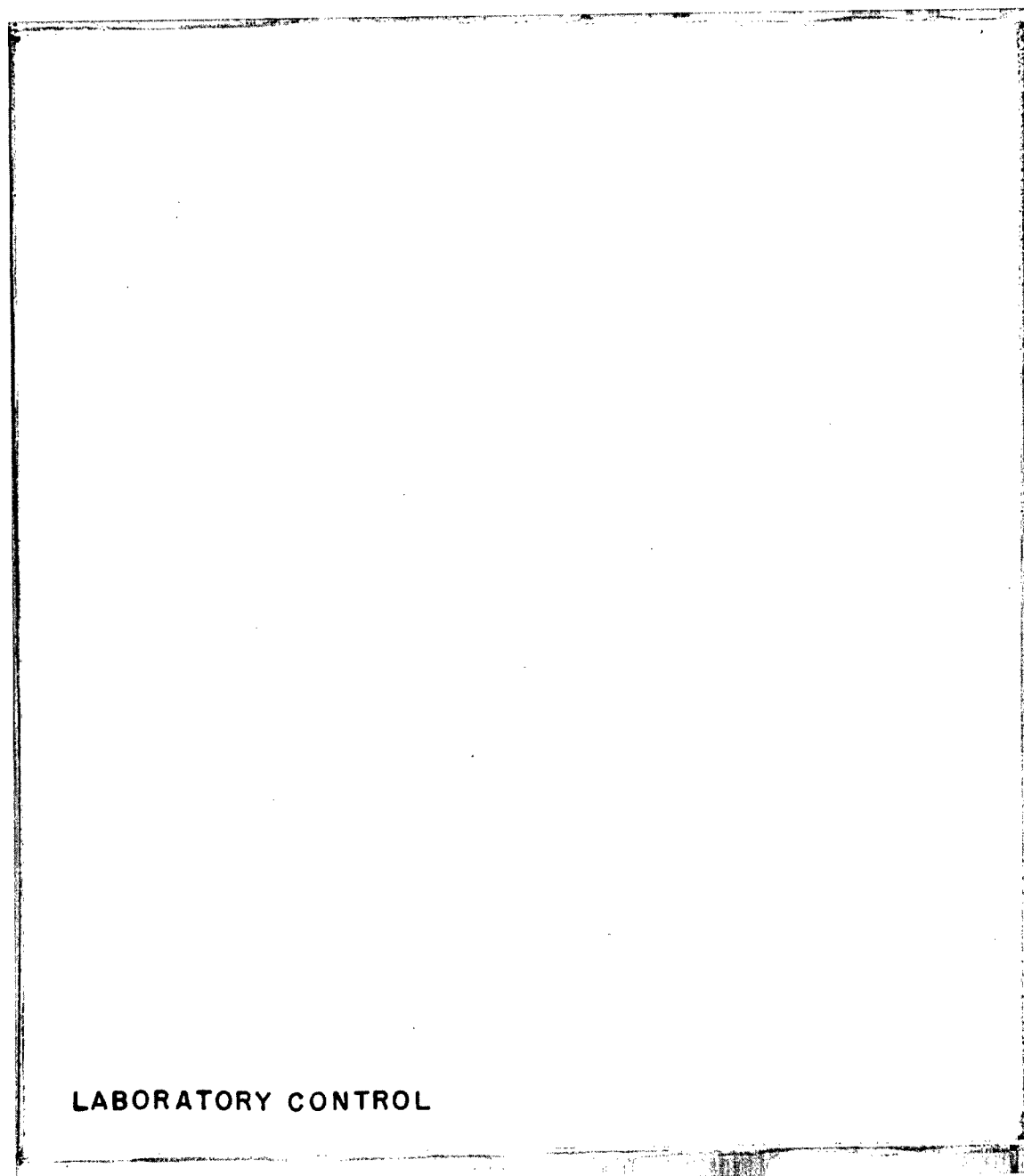
Fig. 3.130—Sticky-paper dust collector control.
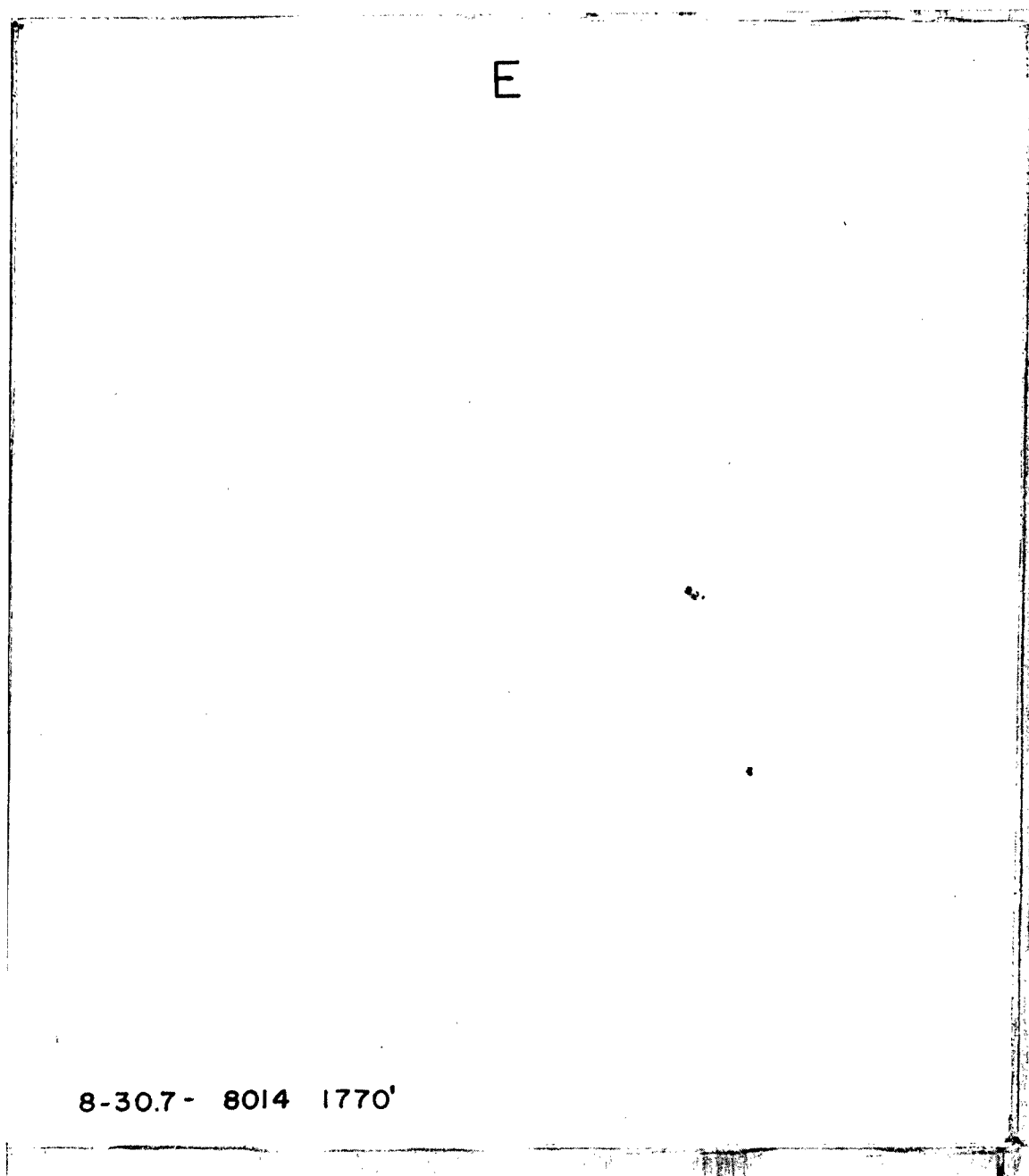
Fig. 3.131—Sticky-paper dust collector, type B (structure RCa).

E

8-30.7 - 8015 2430'
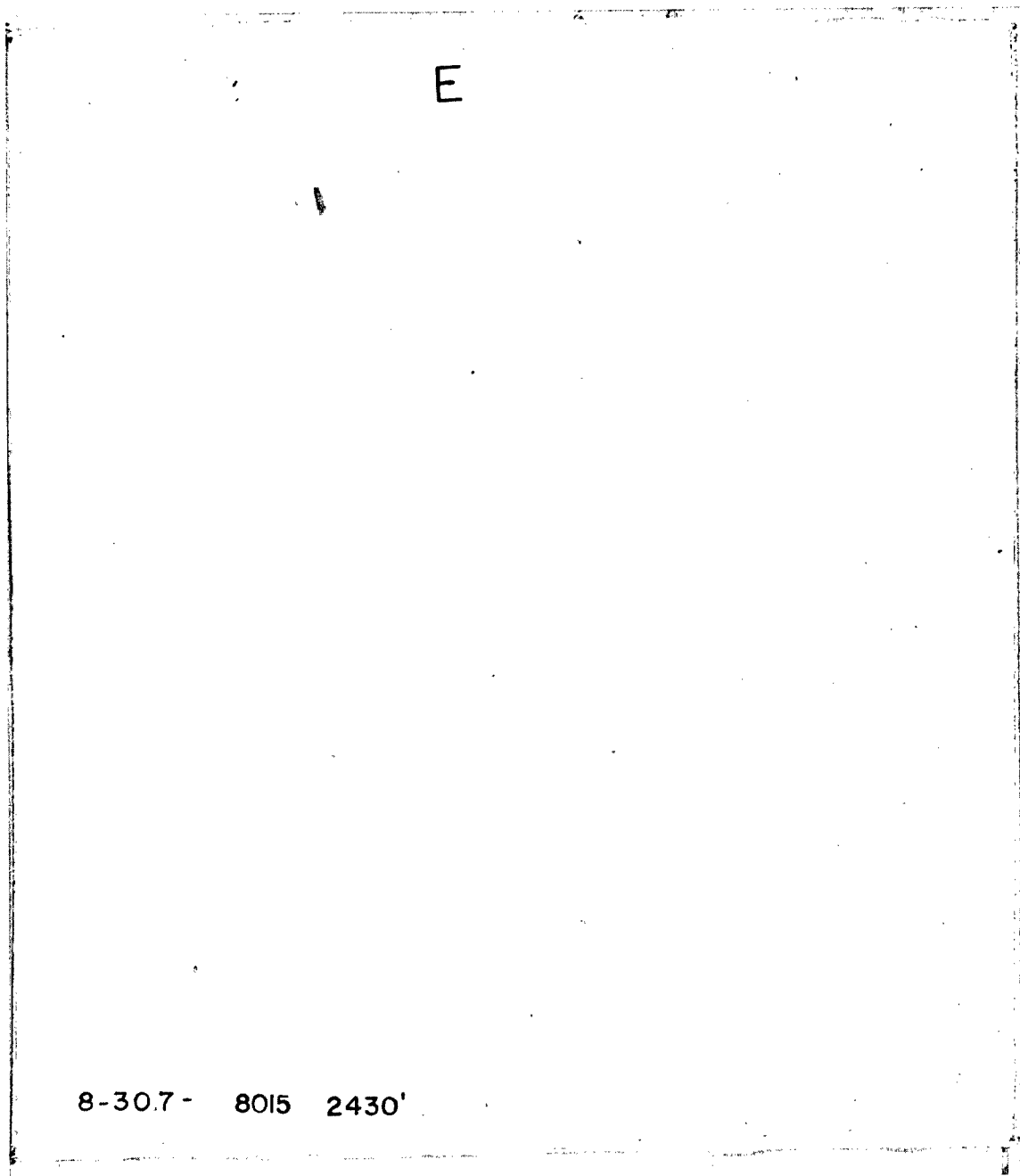
Fig. 3.132—Sticky-paper dust collector, type B (structure RCb).
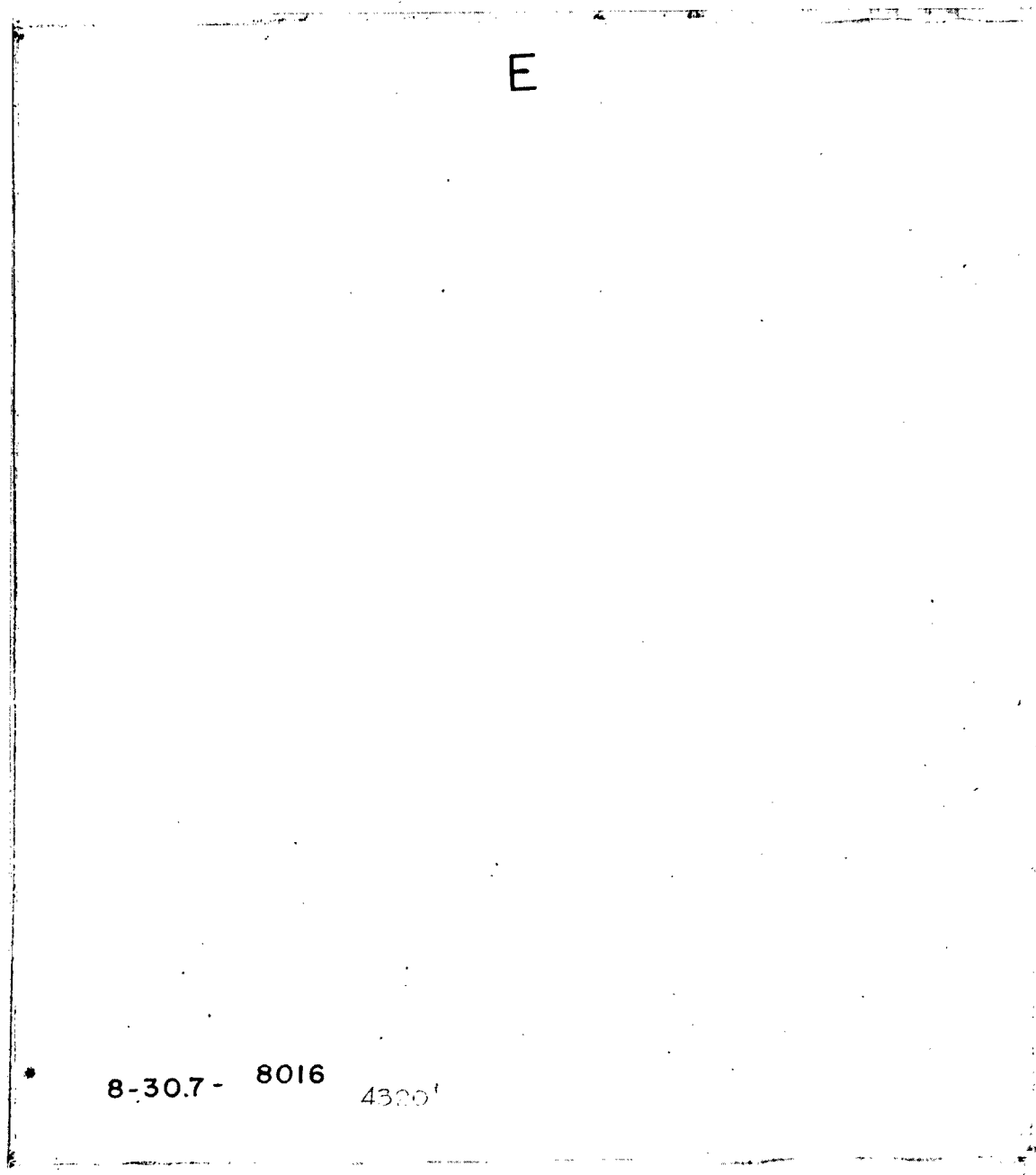
Fig. 3.133—Sticky-paper dust collector, type B (structure RCc).
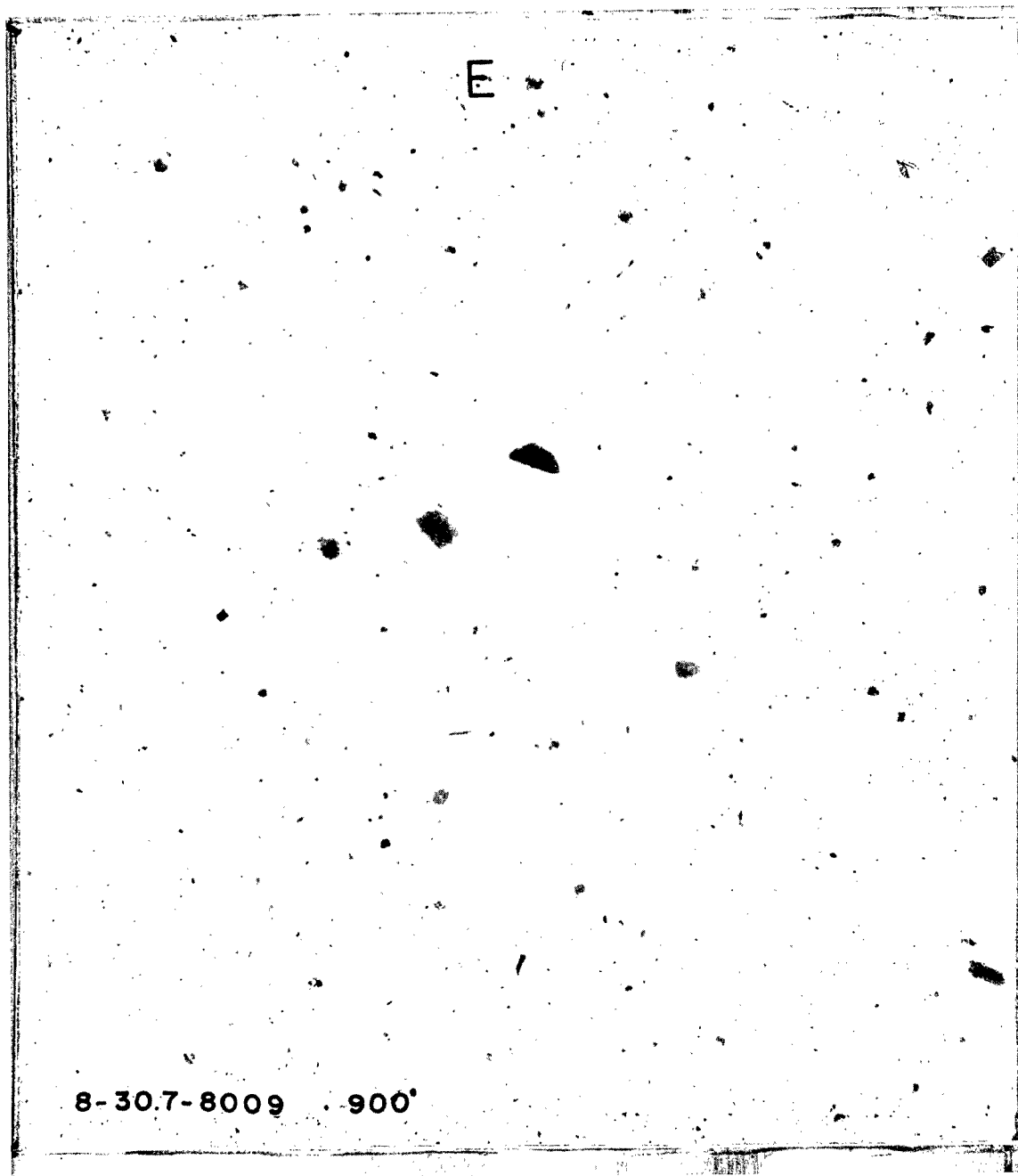
Fig. 3.134—Sticky-paper dust collector, type B (structure CAa).

E

8-30.7-8012 1005'
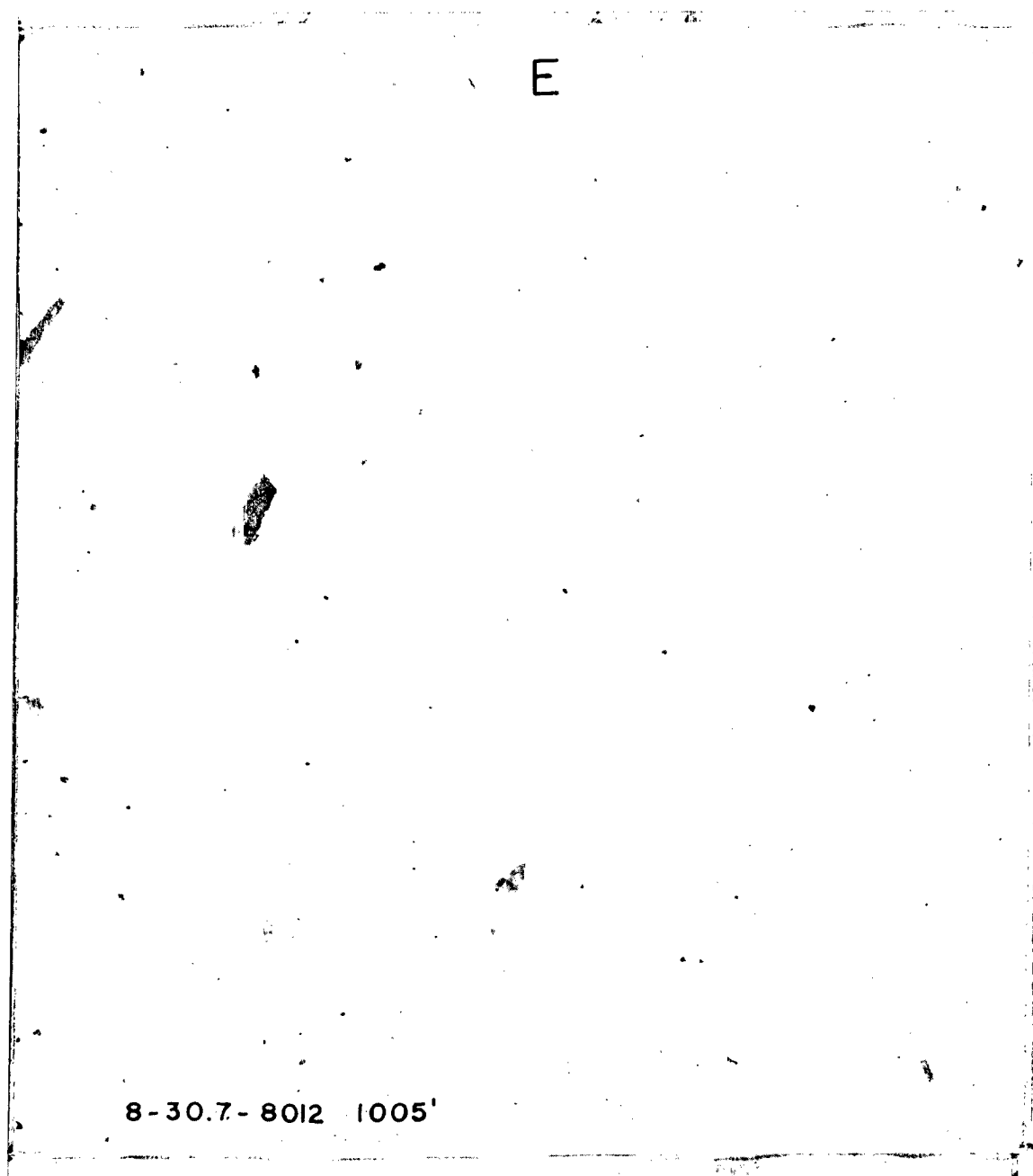
Fig. 3.135—Sticky-paper dust collector, type B (structure CAb).

Chapter 4

SUMMARY

4.1 GROUND AND STRUCTURE DISPLACEMENTS

The shock spectra data (Sec. 3.3) indicate substantial transient vertical and horizontal motions of both the free-field ground and the shelters. It is reasonable to assume that a part of these are permanent. This is substantiated by visual observations which indicated some differential movement between the main body and emergency exit of the structures tested. Comparison of preshot and postshot field location survey data has not been made since reliable postshot surveys have not been available up to the time of writing this report.

Review of the ground-shock spectra data indicates that the accelerations within structure RAc were about one-third to one-half the free-field values in both the radial and vertical directions.

4.2 EXTERNAL PRESSURE

As indicated by Fig. 1.4, the actual incident overpressure present at each of the seven pressure ranges where the structures were placed was lower than predicted. The highest peak pressures to which the RA, CA, and RC structures were exposed were approximately 28, 17, and 77 per cent higher, respectively, than the assumed design values.

4.3 INTERNAL PRESSURE

The overpressure in the interior of a structure is a function of the external pressure and duration, the interior volume of the structure, the size and configuration of the openings leading to the interior, and the type of blast closure employed. The ventilation systems as tested were just as they would be under actual blast conditions. That is, the natural ventilation was sealed, and the emergency ventilation, with sand filter, was open to the atmosphere and to the inside of the main chamber. The maximum overpressure recorded in the ventilation shaft of structure RAc was 14.3 psi, whereas the maximum overpressure in the combination ventilation shaft and emergency exit of structure CAb was 60.0 psi. Results of the VLP gauges placed in the main chambers of these two structures indicate that the maximum overpressure due to total leakage of the sand filter and overpressure flap valve was approximately 0.2 psi. All other gauges in the main body of the structures failed to produce a record. Gauges in the antechambers recorded maximum overpressure of 3.5 in structure RAb, 2.2 psi in RAc, and 0.87 psi in RCa.

4.4 STRUCTURAL DAMAGE

Very slight damage was sustained by the test structures in the shelter areas. Cracking was observed in all structures, but major damage occurred only to those portions exposed to

the shock wave, such as the entrances and the type RA and CA emergency-exit covers. A detailed description of the structural damage due to blast is given in Sec. 3.1.

A postshot dynamic analysis of the roof slab of shelter RAa is included as Appendix C of this report. This analysis utilizes current ultimate-strength theory and was performed using the material strengths as determined from test results, the reinforcement placement and structure dimensions as obtained from the as-built drawings, and the recorded incident pressure at the location of the structure as the loading. The analysis indicates that only minor cracking was expected and agrees with the actual postshot condition.

4.5 RADIATION

The West German Government assumed that the permissible level of the initial radiation within the structures placed at their design overpressure levels (structures RAc, CAb, and RCb) was to be 25 rem. No readings of the initial radiation were obtained as separate values, but Figs. 3.119 to 3.121 indicate the values for the total gamma dosage during the first 52 hr after the detonation at various points within all nine test structures. Structure RAc had radiation dosages equal to 145 r at the front wall (exposed to the exterior), 47 r by the interior corner of the antechamber, and 22 r at the center of the main chamber. Structure CAb had interior dosage values varying from 9 to 29 r, except directly behind the gastight door, where the dosage was 140 r. The interior dosages in structure RCb varied from a minimum of 36 r at the rear corner to a maximum of 382 r directly inside the main blast door.

The total gamma dosages on the blast line at various distances from GZ can be obtained from Fig. 3.122. The dosages indicated by this figure are greater than those presented in either "Effects of Atomic Weapons" or "Effects of Nuclear Weapons."

4.6 THERMAL EFFECTS

No residual thermal effects were apparent from visual observation. Instrumentation was not provided for obtaining thermal measurements.

4.7 DEBRIS AND DUST

The postshot photographs that were taken before the entranceways were cleaned indicate that deposited debris was comparatively light. The dust layer varied in thickness from approximately $\frac{1}{4}$ in. to a maximum of 2 in. at the higher pressure levels in places where drifting occurred. Some rubble was also present. Interior dust was not visibly discernible. From the results of Project 33.5, it has been suggested that dust, as it occurred in the structures studied, would not have been an immediate hazard to personnel.

Owing to the natural surface of the test area, it was difficult to ascertain the extent of the debris on the ground surface. All vertical or inclined surfaces facing GZ (ventilation projections, stairs, walls, etc.) were scoured by sand and debris carried by the blast wave. From other construction in the area, it was evident that above-ground projections that were broken off were deposited from 5 to 100 yd away from their original positions.

4.8 LIMITATIONS IN APPLICATION OF TEST RESULTS

Although the magnitude of the effects (overpressure vs. time, and thermal and nuclear radiation) is different for small nuclear weapons than for the large thermonuclear weapons now available and the physical environment at the Nevada Test Site is not typical of most populated areas, the data obtained from these weapons tests are very useful in estimating response and evaluating the parameters used in design. For this reason the records of blast overpressure, ground-shock motions, radiation, and other weapons effects are of prime importance. However, the results cannot be used directly for proof-test purposes except in special cases.

Appendix A

CONSTRUCTION

A.1 GENERAL

All work was done under contract to the U. S. Atomic Energy Commission. The contractor for the construction of the nine reinforced-concrete shelters was the Sierra Construction Company of Las Vegas, Nev. Reynolds Electric and Engineering Company supplied the concrete aggregate and miscellaneous work required to make the structures ready for the test. Holmes & Narver, Inc., provided over-all supervision and coordination as field representatives of the USAEC.

The FCDA and the West German Government were continuously represented at the site by an Ammann & Whitney field representative, who provided inspection and advisory service for the construction groups. This service was supplemented by visits to the site at critical times by the Project Officer.

Construction, in general, was geared to a very rapid time schedule. This schedule was closely adhered to despite the many difficulties that were experienced. The schedule called for a maximum of 75 calendar days, and work was scheduled to start on Apr. 6, 1957. Excavation was started on Apr. 8, 1957, and the backfilling was scheduled to be completed on June 20, 1957. The schedule, as indicated above, could not be completely adhered to because of problems that developed during the construction. These problems will be more fully defined in Secs. A.4.1 to A.4.7.

Figures A.1 to A.21 are photographs of the three basic shelter types at various stages of construction; the progress made on these rather complicated test structures is indicated by their dates of construction.

Deviations from the drawings and specifications are recorded in Figs. B.1.1 to B.4.2, as-built drawings. Tables A.1 to A.3 indicate the schedule adhered to during the construction phase of the operation.

A.2 MATERIALS

A.2.1 Concrete

Concrete was mixed at a central mixing plant operated by the Reynolds Electric and Engineering Company. The plant was a permanent batcher type installation and was located approximately 15 miles from the structures. The concrete was trucked to the structures by conventional transit-mix trucks. During the batching, the mixing water, as predetermined by the concrete-mix design, was added to the dry mix, and the concrete was mixed during transportation. The concrete was placed by the use of one or more of the three following methods: (1) by dumping into a $\frac{3}{8}$ or $\frac{1}{2}$ C.Y. bucket and placing by crane, (2) by dumping into tremies for wall pours, and (3) by placing directly with the use of concrete chutes. Hunt's paraffin-base curing compound was used to cure the concrete.

In general, a total of 133 standard 6- by 12-in. cylinders was taken from the structures for 7-, 28-, and 90-day tests; nine of these were lost during their shipment to the laboratory. Also, a total of twenty-seven $7\frac{7}{8}$-in. concrete cubes and fifty-two concrete test beams were tested. Two beams were ruptured during transit. The cubes were tested at 7 and 28 days, and concrete beams were tested at 28 and 90 days. In addition to the specimens tested, Schmidt concrete-hammer tests were used to check the uniformity of the concrete and to determine the correlation between the rebound values and the ultimate concrete strength of the structures.

The results of the concrete strength tests, as recorded for the concrete cylinders, beams, and cubes, are contained in Tables A.4 to A.6. Average results are summarized in Table A.7. The hammer-test results are given in Table A.8. Table A.9 gives the typical concrete-mix design used during construction.

A.2.2 Concrete Components

(a) *Cement.* Type II portland cement was used for the construction of the nine cast-in-place structures. Batching was by bulk.

(b) *Coarse Aggregate.* The coarse aggregate, $1\frac{1}{2}$-in. graded aggregate, was stockpiled at the batching plant. Owing to the handling procedure and transportation methods from the crusher, which were products of site conditions and the limited amount of time for construction, segregation of the aggregate was evident in the stockpile and batched concrete. Some aggregate was observed to have a maximum dimension ranging to $2\frac{1}{2}$ in.

(c) *Fine Aggregate.* The fine aggregate had additional wind-blown fines, not indicated in Table A.9, primarily because of the conditions at the site.

A.2.3 Concrete Forms

Wall and roof-slab forms for the seven rectangular structures consisted of $\frac{5}{8}$- and $\frac{3}{4}$-in. plywood panels. Some of this material had been used several times before being used on the German test structures and was then used as many as three times during construction of the test structures. The prefabricated interior and exterior formwork for the two circular structures was built from 1- by 6-in. planking. Stock for the studs was 2 by 4 in.

A.2.4 Reinforcing Steel

Reinforcing steel used in the nine test structures consisted of German-manufactured smooth round bars, as outlined in the specifications given in Sec. 1.4, and United States smooth round mild A 7 steel. The fabrication of the steel was subcontracted by Sierra Construction Company to Fontana Steel Company. All reinforcing steel was cut and bent at the site. The field fabrication shop was located near the concrete mixing plant, approximately 15 miles from the construction site. Flat-bed trucks hauled the fabricated reinforcement from the bending bench to the construction site. Although the bending operation was generally adequate, there are deficiencies between the actual construction and the original contract plans. None of these appear to have been critical in terms of the test results.

All deviations from the construction drawings of the fabrication and/or placement of the steel are shown in Figs. B.1.1 to B.4.2, Appendix B.

The yield and ultimate stresses and the percentage of elongation of 8-in. test specimens of the German and U. S. reinforcement used in construction and tested by Smith-Emery Company of Los Angeles, Calif., are given in Table A.10.

A.2.5 Structural Steel

The structural-steel components of the nine shelters consisted of doors, door frames, ventilation equipment, and miscellaneous accessories. All structural-steel items required for the construction were manufactured for, and supplied by, the West German Government. No damage in shipment from Germany was incurred by any of the structural-steel equipment. Some equipment was damaged after installation; this is described further in Secs. A.4.5 and A.4.6. All items were repaired before the test.

A.3 SOIL TESTS AND DESCRIPTION

The subsoil, upon visual investigation, was found to be a heterogeneous mixture of various sizes of sand and gravel particles with interstitial clay and silt; it may be loosely described as a calcinated conglomerate. The formation contained a cementing agent, apparently of calcium carbonate origin. The agent, in conjunction with the clay particles, produced a state of high consolidation. The soil condition described above was below 1 to $1\frac{1}{2}$ ft of typical desert top soil. The depth of the calcium carbonate mixture was of indefinite vertical extent.

Cross sections of the excavation were taken at all the structures to determine the dimension, shape, and peculiarities of cut; these are shown in Figs. A.22 and A.23.

In-place density tests were performed on pre- and postconstructional soil conditions that existed at the structures to evaluate the compaction achieved by the backfilling method.

The results of the tests are indicated in Table A.11.

A.4 CONSTRUCTION OF THE STRUCTURES THROUGH THEIR COMPONENT ITEMS

A.4.1 General

The following sections will deal essentially with the procedures used in construction of the component items of the structures and the conditions that existed at the completion of the construction phase of the operation. Also included in this section are all deviations from the drawings and specifications and any additions that were deemed necessary to complete the structures in a satisfactory manner.

A.4.2 Excavation

The predominant characteristic of the soil, with regard to the excavation, was its natural cementation. This characteristic made it virtually impossible to excavate using conventional back-hoeing equipment, and all existing soil had to be loosened by caterpillar-propelled rippers or explosive charges before removal by a caterpillar-drawn scraper, Figs. A.24 and A.25. Excavation was carried down from 3 to 6 in. below the elevation of the bottom of the lean base slab for all structures except RAb, which was inadvertently excavated $1\frac{1}{2}$ ft below the required grade. Required grade was obtained by backfilling, leveling, and compacting with the construction equipment. All additional excavation for the bottom of the seven emergency exit shafts was by hand.

A.4.3 Floor Slabs

The forms for the lean concrete working base and floor slabs of the nine German cast-in-place reinforced-concrete underground test structures were built as a single unit to the out-to-out dimensions given on the contract drawings. No preparation of the natural ground under the lean base took place. That is, kraft paper was not spread over the graded surface nor was this surface moistened prior to pouring of concrete. Reinforcing steel was then placed within the existing formwork directly over this lean concrete subbase slab. Concrete blocks of the required thickness were used to support the bottom layer of steel.

Because of the nature of the reinforcement in the three different types of structures, no special chairs were required to support the top mats. The rectangular type A and C structure floor slabs have a system of truss bars supported on small concrete blocks at the negative region of the steel. These supported truss bars in the positive region of the steel, together with stirrups spaced at 1 ft 8 in. on center, were sufficient to support the top mat reinforcement in its required positions. In the circular type A structures, the intricate pattern of reinforcement (including ties) dictated the placement of the top mat steel. The entire sequence of the placement of reinforcement for the walls and roof slab of the rectangular type A and C structures, as well as the barrel and crown reinforcement for the circular type A, is dictated by the pattern of reinforcement found in the floor slab.

Immediately prior to the pouring of the floor slabs of all the structures, the lean concrete working base was moistened to prevent excess absorption of moisture from the floor-slab concrete.

For the rectangular type A structure, the first pour consisted of the floor slabs of the landing, antechamber, main chamber, ventilation shaft, exit chamber, and 4-ft 7-in. section of the emergency-exit tunnel. The rectangular type C structures had the floor slabs of the antechamber, main chamber, exit chamber, ventilation chamber, and a 5-ft 3-in. section of the emergency-exit tunnel poured together. In the circular type A shelters, the floor slab from the emergency-exit end of the structure to the contraction joint by the fifth tread was poured initially.

Placement of reinforcement for all structures of the three different types was tedious and in many ways did not conform to U. S. standards.

Some deviations from the contract drawings therefore occurred, and these deviations can be found on Figs. B.1.1 to B.4.2.

A.4.4 Walls and Roof Slabs

As per the specific request of the German representative, the walls and roof slabs of the two types of rectangular shelters were poured monolithically. The cylinder, interior walls, emergency-exit shaft, and entrance to the contraction joint at the fifth tread of the circular shelters were poured as a unit.

In the rectangular type A shelters, the landing retaining wall, roof slab over the landing, the ventilation shaft, all interior walls, all exterior walls, and the roof slab up to the contraction joint between the structure and emergency-exit tunnel were poured as a single unit. Similarly, for the rectangular type C shelters, all interior walls, the front exterior wall, all exterior walls, and the roof slab for that portion of the structure from the contraction joint between the landing floor slab and front wall of the structure and the contraction joint by the emergency-exit tunnel were poured together. Rubber-tire tremies were used for pouring the lower portions of all walls for both types of rectangular shelters; concrete-chute placement was employed for accessible surfaces. Crane and bucket placement was used as required on all pouring operations.

The circular type A shelter had an entirely different type formwork and pouring arrangement than the rectangular structures. As previously stated, the interior and exterior cylinder forms were built using 1- by 6-in. planking. All exterior forms of the cylinder were carried up approximately 20 deg. past the horizontal diameter. Windows for pouring the lower half of the cylinder were cut in the exterior formwork on approximately 3-ft centers. The concrete was funneled through these windows and was vibrated in place.

Some difficulty was experienced in pouring shelter CAb owing to the stiffness of the concrete mix. The mix used was the same as that used for the rectangular type shelters. The concrete had approximately a 4-in. slump. It was found that with the equipment and facilities available the pouring operation was too slow using this slump. This difficulty was alleviated when pouring CAa by revising the concrete mix to allow a 6-in. slump. The cement content was increased by an amount sufficient to increase the strength by 500 psi. Then, to obtain a more fluid mix and also to bring the concrete strength below the maximum allowed by the German specifications, the proportions of the coarse and fine aggregate and the water-cement ratio, were manipulated to give a 6-in. slump. No difficulty was experienced in pouring the second circular shelter with the revised mix.

The second pour of the circular type shelter consisted of all interior walls, the combination ventilation and emergency-exit shaft, the cylinder, and the walls and roof of the stairs up to the contraction joint.

The entrance ramp and stairs and their respective interior and exterior retaining walls each had a contraction joint at their intersection with the main portion of the structure. Each entrance for the rectangular type A structures, consisting of a ramp and walls or stairs and wall, was poured as a unit together with the parapet wall on the roof slab over the landing. Although not indicated in Table A.2, a 4-in. working base of lean concrete was poured under each of the sections on natural ground. Rubber-tire tremies were used at such places where exces-

sive free fall of concrete would occur. The landing floor slab, landing retaining wall, and roof slab over the landing were poured with the main structure as per original design.

There was no roof slab over the landing of the three rectangular type C structures. The landing floor slab and the landing retaining wall of this type structure were poured in two separate pours. With the exception of the parapet wall over the landing, the pouring of the entranceways of the type C structures was identical to that for type A. That is, the walls and slabs were poured as a single unit by using a stiff mix and a minimum amount of vibration. The parapet retaining wall over the front wall of the shelter was used to hold back the 3 ft of earth cover over the main portion of the structure. The reinforcement in this wall was not detailed and fabricated as shown on the final contract drawings, and consequently provisions had to be made in the field to provide for continuity between the parapet and the interior ramp and stair retaining walls.

A.4.5 Emergency Exit

The emergency-exit tunnel and shaft for the type A rectangular structures are identical to the type C structures with one exception. The type C emergency-exit tunnel and shaft are also used as the ventilation shaft for the forced-air intake and, as such, have four 2-in. pipes located 8 in. below the top of the shaft to allow air to be drawn in from the outside. In contrast to this, the type A rectangular shelters have a separate ventilation stack and have no provisions for air to enter the emergency-exit shaft. Reinforcement and construction details are identical in other aspects.

In the circular type A structures the emergency exit is a vertical shaft that starts at the small blast door. This shaft is also used for air intake for the protected air supply.

A.4.6 Ventilation

No provisions were made in any of the nine shelters for natural pre- or postshot ventilation equipment. No difficulty was encountered in installing the protected ventilation equipment, except at the slip-joint junction between the duct from the sand filter and the air-reception boxes in the sand filter. These slip joints had a tendency to separate. In some cases the opposite was true, the fit was too tight and the parts had to be forced together. The cast-iron flange assembly on one ventilator motor was broken during installation but was fastened securely by large washers.

A.4.7 Doors

Both the large and small blast doors of the type A rectangular and circular shelters were installed and operated with no difficulty. The gastight doors exhibited no trouble in installation, but the operation of the locking mechanism for both the large and small type doors was very difficult if the mechanism was not given a minimum amount of maintenance.

The handle of the large gastight door in shelter RAd was broken off at one of the preshot trials. The point of failure was located where the circular section becomes square in order to engage the sliding locking bar. Replacement parts from an extra door were substituted, and the door functioned properly.

The rectangular type C shelters had a large blast door of a different type than the other shelters. While structurally adequate and of simple design, the latching mechanism did not allow for an easy engagement of the stationary lugs on the door frame. Shelter RCa was particularly difficult to close. Another construction difficulty arose with the size of the grout pocket recesses. As supplied by the West German Government, the door anchors required recesses 10 by 10 by 6 in. to accommodate them.

All emergency-exit hatch covers required eight grout pocket recesses, and such work was done in the field according to the revised drawings.

TABLE A.1—SCHEDULE OF CONSTRUCTION (1957)

Structure	Excavation (date)	Sub base			Floor slab				Walls and roof slab				
		Forms (date)	Concrete Date	Quantity	Forms (date)	Steel (date)	Concrete Date	Quantity	Interior forms (date)	Steel (date)	Exterior forms (date)	Concrete Date	Quantity
RAa	4/25	4/29	5/2	7	4/29	6/11	6/12	37	6/13	6/16	6/17	6/18	92
			4/29	5									
RAb	4/25	4/27	5/2	2	4/27	5/6	5/8	38	5/10	5/19	5/21	5/22	90
RAc	4/24	4/25	4/26	7	4/25	4/29	4/29	38	5/2	5/9	5/13	5/15	90
RAd	4/27	5/1	5/2	7	5/1	5/22	5/24	38	6/10	6/13	6/14	6/15	90
CAa	4/19	4/25	4/26	4	4/25	5/6	5/8	25	5/17	6/18	6/21	6/22	71
CAb	4/23	4/25	4/26	4	4/25	5/1	5/1	25	5/11	5/26	5/31	6/1	70
RCa	4/23	4/26	4/26	5	4/26	5/2	5/2	10	5/5	5/10	5/16	5/17	30
RCb	4/24	4/25	4/26	5	4/25	5/2	5/3	10	5/8	5/16	5/20	5/22	30
			5/3	2									
RCc	4/27	5/2	5/8	3	5/2	5/20	5/21	10	5/24	5/27	5/31	5/31	30

TABLE A.2—SCHEDULE OF CONSTRUCTION (1957)

| | Entranceways | | | | | Stairs | | | | | Entrance landing | | | |
| | Ramp | | | | | | | | | | Floor slab | | | |
Structure	Exterior form (date)	Steel (date)	Interior form (date)	Concrete Date	Concrete Quantity	Exterior form (date)	Steel (date)	Interior form (date)	Concrete Date	Concrete Quantity	Forms (date)	Reinforcement (date)	Concrete Date	Concrete Quantity
RAa	6/19	6/21	6/25	6/27	18	6/19	6/21	6/24	6/25	19		Poured with shelter		
RAb	6/11	6/15	6/17	6/18	18	6/11	6/15	6/17	6/17	19		Poured with shelter		
RAc	5/24	6/6	6/8	6/10	18	5/30	6/12	6/13	6/14	19		Poured with shelter		
RAd	6/18	6/24	6/25	6/27	18	6/17	6/20	6/21	6/22	19		Poured with shelter		
CAa						6/24	6/25	6/26	6/27	14		Poured with shelter		
CAb						6/11	6/13	6/14	6/14	13		Poured with shelter		
RCa	5/31	6/3	6/3	6/4	11½	5/31	6/3	6/3	6/4	12	5/6	5/11	5/13	6½
RCb	6/6	6/10	6/10	6/11	11	6/6	6/10	6/10	6/11	12	5/6	5/15	5/17	6½
RCc	6/8	6/12	6/13	6/14	11½	6/8	6/12	6/13	6/14	12½	5/22	5/24	5/25	6½

TABLE A.3—SCHEDULE OF CONSTRUCTION (1957)

| | Entrance landing | | | | | Emergency exit | | | | | | | | |
| | Front wall | | | | | Base slab | | | | Wall, roof, and shaft | | | | |
Structure	Interior form (date)	Reinforcement (date)	Exterior forms (date)	Concrete Date	Concrete Quantity	Forms (date)	Reinforcement (date)	Concrete Date	Concrete Quantity	Interior form (date)	Reinforcement (date)	Exterior forms (date)	Concrete Date	Concrete Quantity
RAa		Poured with shelter				6/18	6/21	6/22	3	6/23	6/24	6/26	6/27	6
RAb		Poured with shelter				6/14	6/15	6/17	3	6/18	6/19	6/20	6/21	7
RAc		Poured with shelter				6/12	6/13	6/14	3	6/15	6/16	6/16	6/17	7
RAd		Poured with shelter				6/17	6/20	6/21	3	6/23	6/24	6/24	6/25	6
CAa		Poured with shelter					None				None			
CAb		Poured with shelter					None				None			
RCa	5/14	5/16	5/16	5/17	11	5/10	5/14	5/16	2½	5/20	5/21	5/22	5/23	6½
RCb	5/18	5/20	5/21	5/21	11	5/13	5/15	5/17	2	5/23	5/30	5/31	6/3	7
RCc	5/26	5/27	5/30	5/31	11	5/24	5/27	5/31	2½	6/1	6/3	6/4	6/4	7

TABLE A.4—LABORATORY TEST RESULTS (CYLINDERS)

Structure	Members	Test results, psi		
		7 days	28 days	90 days
RAa	Floor slab	2140	3030	
		2190	3210	
		2200	3150	
	Walls and roof slab	3400	3610	4030
		3440	3540	4070
		3360	3360	4130
RAb	Floor slab	2100	2960	
		2130	3150	
		2100	3170	
	Walls and roof slab	2680	3430	5010
		2670	3560	4940
		2700	3450	5130
RAc	Floor slab	3260*	3750	
			3550	
			3500	
			3410	
			3650	
	Walls and roof slab	3420	3510	4090
		3530	3540	4140
		3570	3530	4150
RAd	Floor slab	3160	3490	
		3170	3460	
		3200	3400	
	Walls and roof slab	2650	2530	4230
		2570	3400	4070
		2590	3300	4410
RCb	Floor slab	2490	3330	
		2500	3300	
		2340	3340	
	Entrance wall	2220	3330	
	Walls and roof slab			4760
				4920
				4710
RCc	Floor slab	2190	3080	
	Entrance wall	2530	3270	
		2480	2960	
		2370	3010	
	Walls and roof slab	2850	3080	3580
		2470	3050	3370
		2370	3000	3500
CAa	Floor slab		3570	
			3800	
			3730	
			3700	
			3620	
			3850	
	Walls and crown	2890	3710	4680
		3360	3760	4480
		2480	3760	4160
CAb	Floor slab	3010	3100	
		2930	2750	
		3010	3050	
	Walls and crown	2710	3380	3890
		2680	3410	3910
		2680	3200	3890
RCa	Floor slab	2620	2940	
		2710	3100	
		2620	2950	
	Walls and roof slab	LIS†	LIS†	LIS†
		LIS†	LIS†	LIS†
		LIS†	LIS†	LIS†

*17-day test.
† LIS—lost in shipment.

TABLE A.5 — LABORATORY TEST RESULTS (CUBES)

| Structure | Members | Test results, psi | |
		7 days	28 days
RAa	Floor slab	2338	2843
		2251	2878
	ɔ	2266	2944
	Walls and roof slab	3276	3328
		3272	3176
		3200	3273
RAb	No results		
RAc	No results		
RAd	Walls and roof slab	2572	3768
		2580	3706
		2544	3362
CAa	Walls and crown	2909	3374
		2364	3280
		3146	3323
CAb	No results		
RCa	No results		
RCb	No results		
RCc	Entrance walls	2455	3146
			3547

TABLE A.6 — LABORATORY TEST RESULTS (BEAMS)

| Structure | Members | Test results, psi | |
		28 days	90 days
RAa	Walls and roof	547	609
		506	RIT*
		549	RIT*
RAb	Walls and roof	549	503
		538	483
		502	599
RAc	Walls and roof	215	400
		265	415
		290	385
RAd	Walls and roof	632	572
		597	632
		632	623
CAa	Walls and crown	517	601
		507	584
		542	620
CAb	Walls and crown	513	593
		576	635
		591	580
RCa	Walls and roof	381	495
		302	475
		293	515
RCb	Walls and roof	516	441
		461	489
		402	509
RCc	Walls and roof	415	530
		415	630
		525	600

*RIT—ruptured in transit.

TABLE A.7 — AVERAGE VALUES OF CONCRETE TEST DATA

	Structure								
	RAa	RAb	RAc	RAd	CAa	CAb	RCa	RCb	RCc
7 Days									
Cylinders (floor slab)	2177	2110	3260*	3176		2983	2650	2388†	2392†
Cylinders (walls and roof)	3400	2683	3506	2603	2910	2690			2430
Cubes (floor slab)	2285								2455
Cubes (walls and roof)	3249			2565	2806				
28 Days									
Cylinders (floor slab)	3130	3093	3572	3450	3711	2967	2997	3325†	3080†
Cylinders (walls and roof)	3503	3480	3526	3410	3743	3330			3043
Cubes (floor slab)	2888								3347
Cubes (walls and roof)	3259			3612	3326				
Beams (walls and roof)	534	529	257	620	522	560	325	459	451
90 Days									
Cylinders (walls and roof)	4076	5026	4126	4236	4440	3896		4796	3483
Beams (walls and roof)	609	528	400	609	602	603	495	479	586

*One test—17 days.
†Average of floor slab and entrance wall.

TABLE A.8 — CONCRETE-HAMMER TESTS (EQUIVALENT CYLINDER STRENGTH, PSI)*

Structure	Hammer No.	Wall facing GZ		Wall away from GZ		Roof slab		Floor slab	
		Preshot	Postshot	Preshot	Postshot	Preshot	Postshot	Preshot	Postshot
RAa	1	3200	2750	3150	3400	3700	4450	1800	1500
	2		5980		6040		6225		3720
RAb	1	3350	2750	3300	2750	3500	2400	1850	2400
	2		6160		6040		6350		5675
RAc	1	3300	2100	3350	2600	3400	2100	1350	2750
	2		4700		4340		6100		5000
RAd	1	3400	2400	3200	2400	3550	2600	1850	1650
	2		6600		6160		6350		3970
CAa	1	3200	1750	3150	1500	3800	2600	1750	1500
	2		5360		5650		6350		4030
RCa	2		5000		5500		5740		4760

*Hammer No. 1 supplied by Holmes & Narver, Inc. (No. 1639); hammer No. 2 supplied by FCDA.

TABLE A.9—TYPICAL CONCRETE-MIX DESIGN

Sieve size	Per cent passing U. S. standard sieve		
	Fine aggregate	Coarse aggregate	Combined
1.5 in.		100.0	100.0
¾ in.		59.0	76.4
⅜ in.		11.6	49.2
#4	100.0	1.4	43.3
#8	78.8		33.5
#16	57.0		24.2
#30	32.9		14.0
#50	17.9		7.8
#100	4.3		1.8
F. M.	3.091	7.280	5.498
Specific gravity (S. and S.D.)	2.47	2.665	

Mix design for one cubic yard of concrete is 3000 psi.
Absolute volume of aggregate in one cubic yard of concrete—19.73 cu ft.
Weight of one cubic yard batch of aggregate—3240 lb.

	Per cent	Batch wt., lb		Absolute vol., cu ft
Gravel			2000	12.03
Sand, dry	39	1188		7.70
Free water in sand, 6.2 gal	4.35	52		0.84
		1240	1240	
Water, added 28.5 gal			237	3.80
Cement, 5.5 sacks			517	2.63
			Total	27.00

Maximum slump = 5 in.

TABLE A.10— LABORATORY TEST RESULTS OF REINFORCEMENT

Type	Yield stress, psi			Ultimate stress, psi			Elongation,* %		
	Average	Low	High	Average	Low	High	Average	Low	High
8 mm	50,137	47,300	52,400	64,937	61,450	66,850	20.87	19.00	22.00
10 mm	49,737	47,550	51,750	63,562	60,650	66,650	20.50	20.00	21.00
12 mm	41,362	37,900	43,750	52,537	50,550	56,800	30.00	27.00	33.00
14 mm	42,812	41,100	44,200	62,325	56,200	66,100	28.62	27.00	32.50
16 mm	41,400	37,100	44,600	54,887	50,000	58,850	30.75	27.00	32.50
18 mm	43,425	41,700	45,850	57,837	57,150	58,750	31.25	30.00	32.50
20 mm	42,750	40,600	44,250	58,125	55,050	59,900	31.25	28.00	36.00
26 mm	40,937	40,100	42,800	54,725	52,600	56,100	30.88	29.50	33.00
$\frac{1}{2}$ in. ϕ	49,794			71,895			24.1		
$\frac{3}{4}$ in. ϕ	43,340			65,237			25.0		
1 in. ϕ	47,589			68,935			28.1		

*Per cent elongation for 8-in. specimen.

TABLE A.11 — IN-PLACE DENSITY TEST RESULTS

Structure	In-place density, lb/cu ft			Location of mid-height reading*
	Existing soil (av.)	Backfill at mid-height	Backfill at final grade	
RAa	111	115	112	North
RAb	111	Not taken	135	
RAc	113	118	130	North
RAd	113	115	122	South
CAa	111	112	115	Unknown
CAb	113	121	130	North
RCa	117	109	134	South
RCb	117	123	Not taken	South
RCc	117	118	130	South

*North, side of structure facing GZ; south, side of structure facing away from GZ.
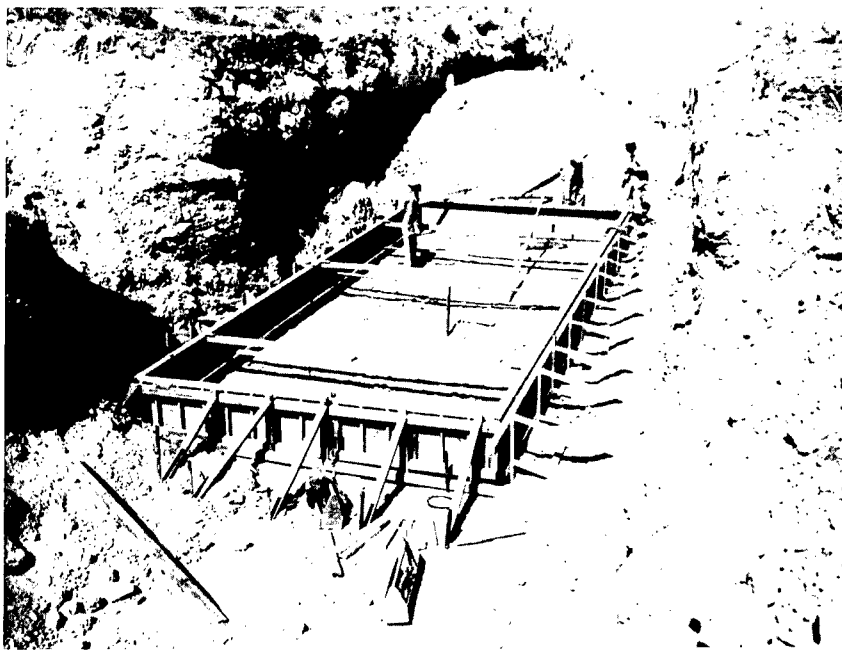
Fig. A.1—Erection of base-slab formwork (structure RA) (Apr. 25, 1957).
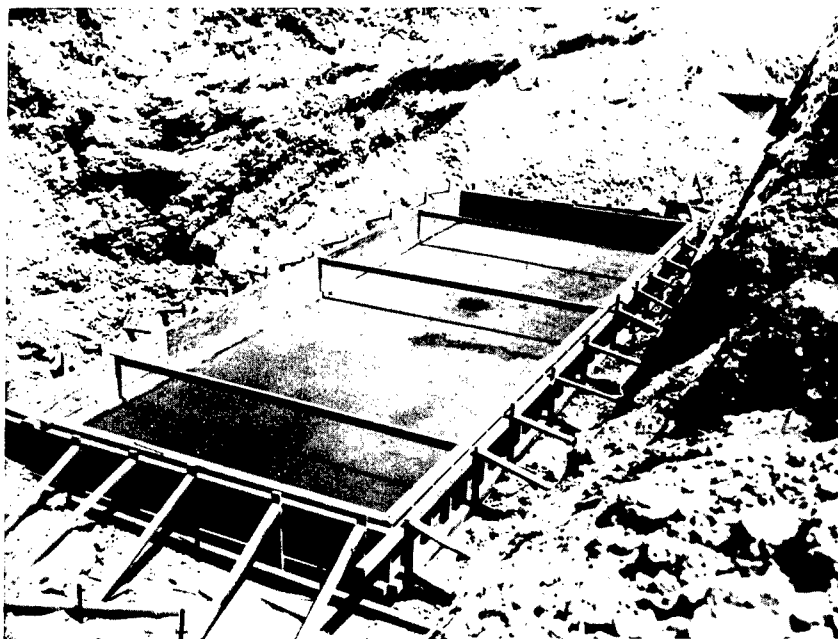
Fig. A.2—Sub-base concrete placement completed (structure RA) (Apr. 27, 1959).
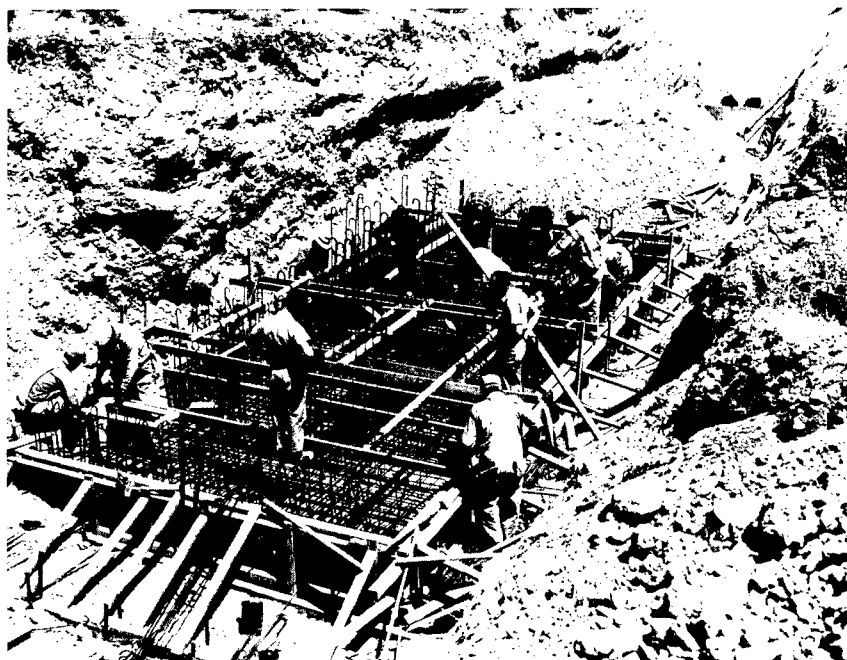
Fig. A.3—Placement of base-slab reinforcement (structure RA) (Apr. 28, 1957).
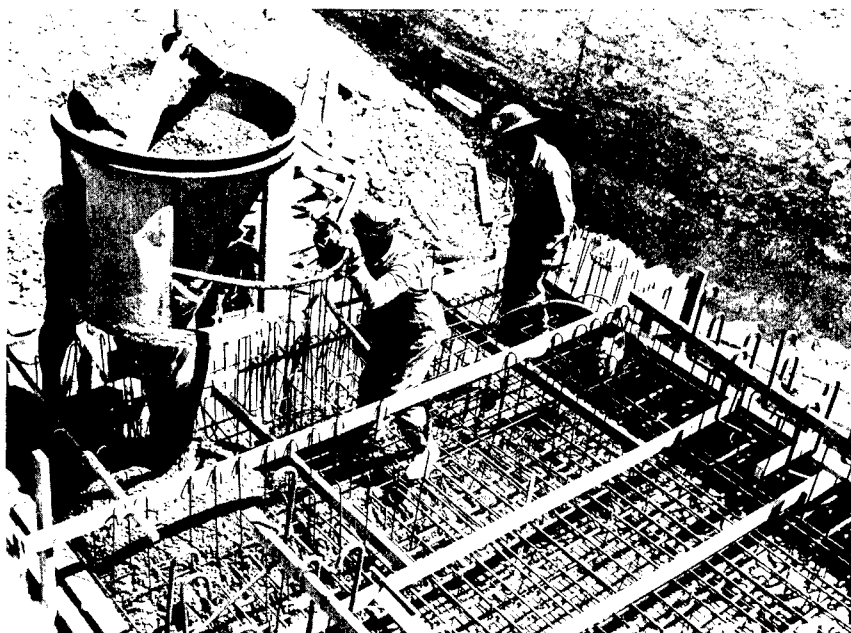
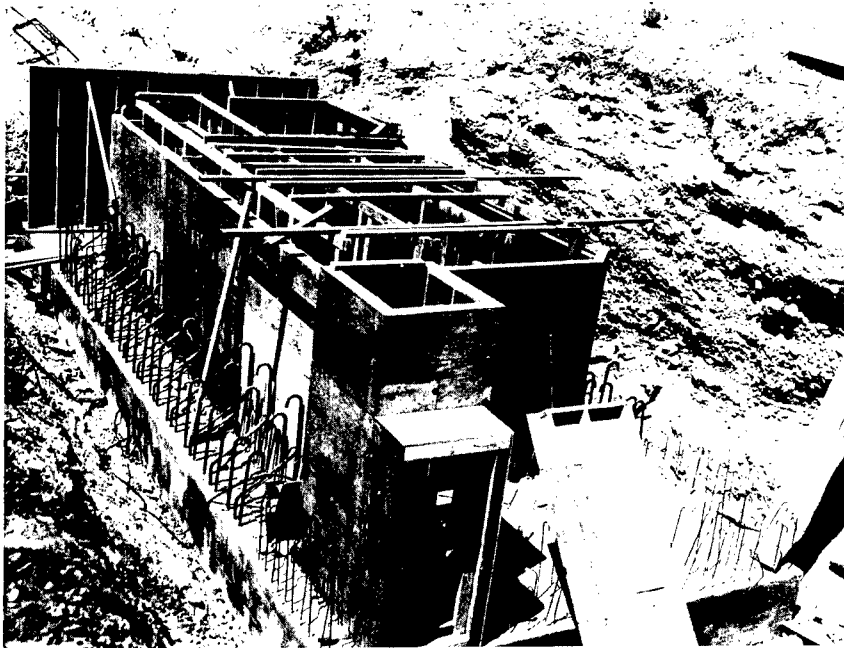Fig. A.4—Base-slab concrete placement (structure RA) (Apr. 29, 1957).

Fig. A.5—Partially erected wall and roof slab, interior formwork (structure RA) (May 1, 1957).
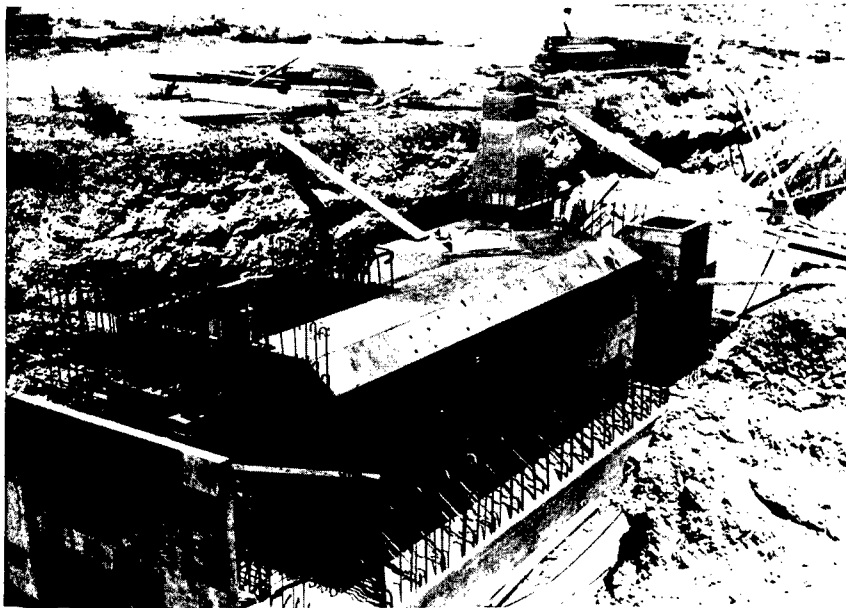

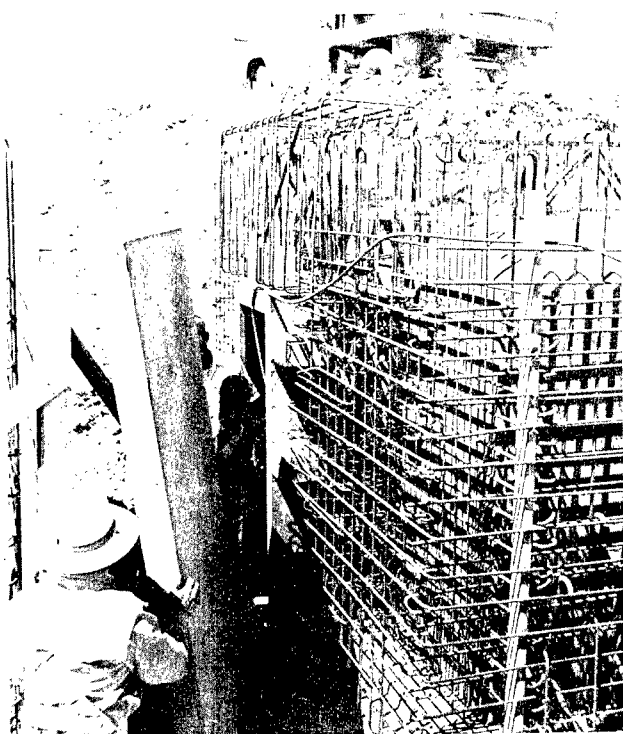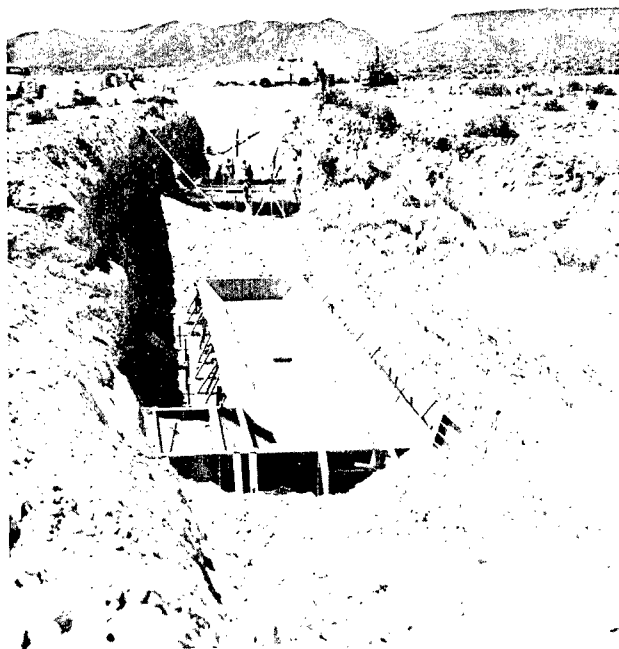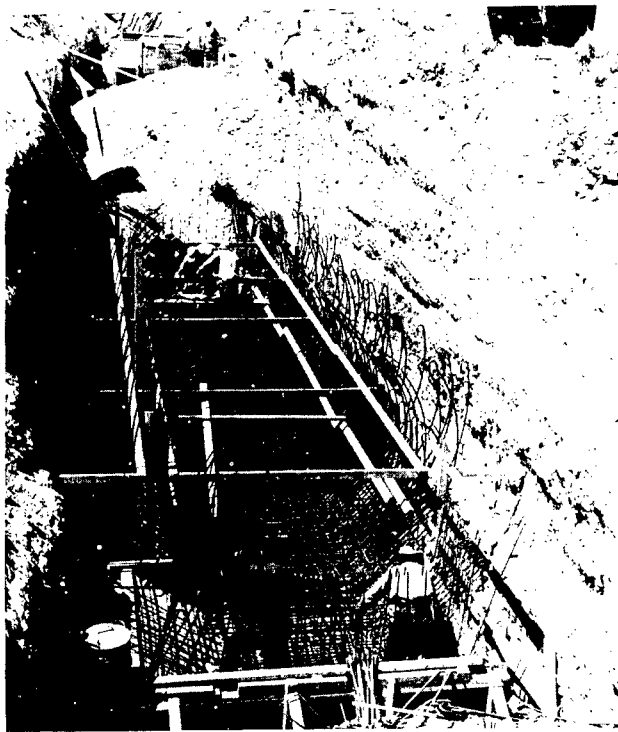Fig. A.6—Interior formwork erected; placement of wall reinforcement begun (structure RA) (May 3, 1957).

Fig. A.7—Erected formwork for entranceway walls and roof slab (structure RA) (May 4, 1957).

Fig. A.8—Detail of roof-slab reinforcement (structure RA) (May 8, 1957).
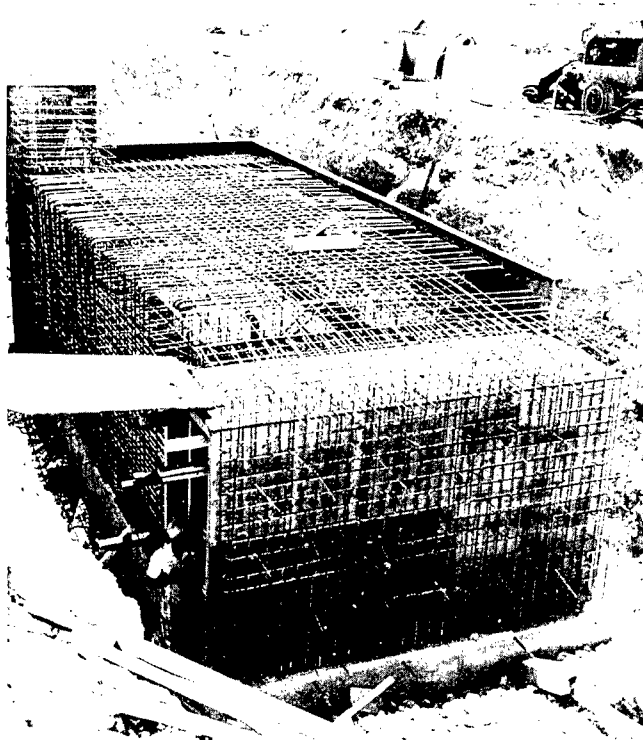
Fig. A.9—Wall- and roof-slab reinforcement placed; erecting exterior formwork (structure RA) (May 10, 1957).
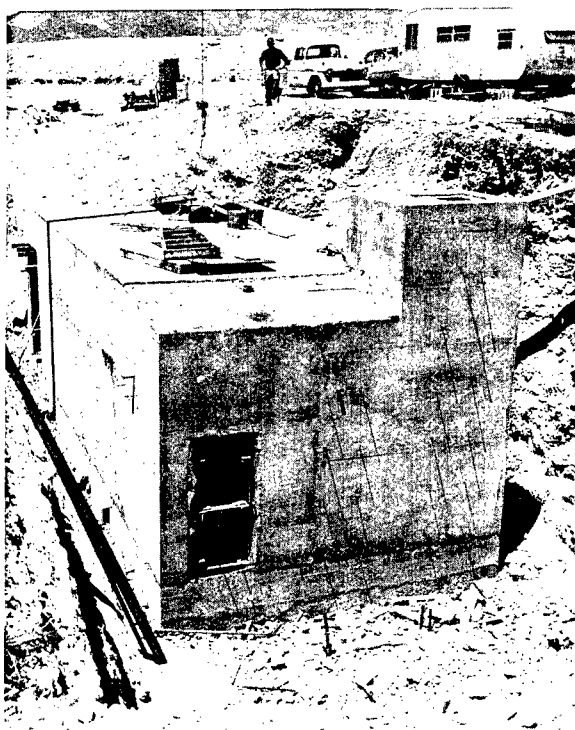
Fig. A.10—Main body of structure after removal of exterior formwork (structure RA) (May 20, 1957).

Fig. A.11—Erection of base-slab formwork (structure CA)
(Apr. 25, 1957).

Fig. A.12—Sub-base concrete placement completed (structure CA)
(Apr. 26, 1957).

Fig. A.13—Placement of base-slab reinforcement (structure CA)
(May 5, 1957).

Fig. A.14—Removal of base-slab formwork (structure CA)
(May 10, 1957).
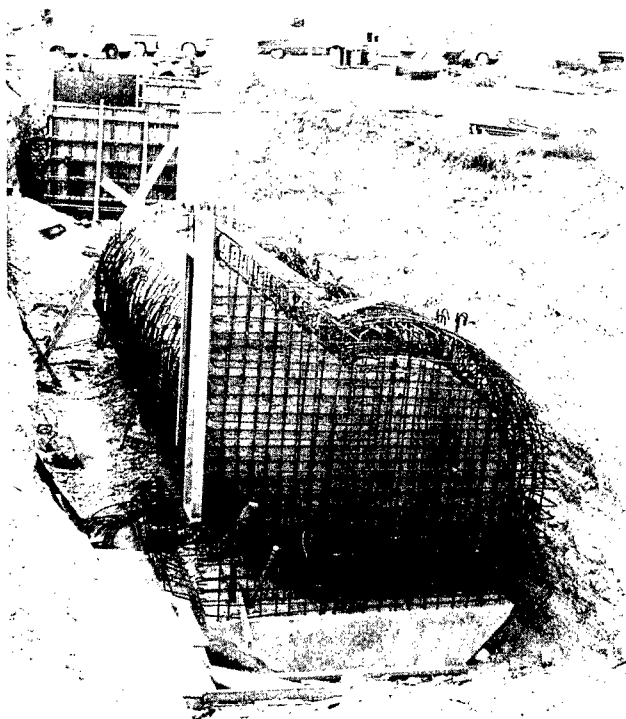
Fig. A.15—Interior formwork erected (structure CA) (May 22, 1957).
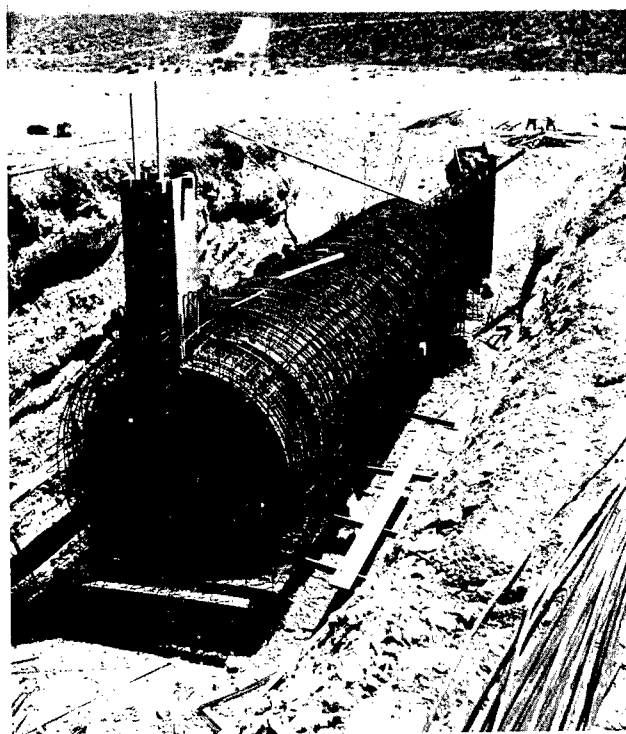
Fig. A.16—Reinforcement in place for main body of structure (structure CA) (June 18, 1957).

215

Fig. A.17—Structure immediately prior to concrete placement
(structure CA) (June 22, 1957).
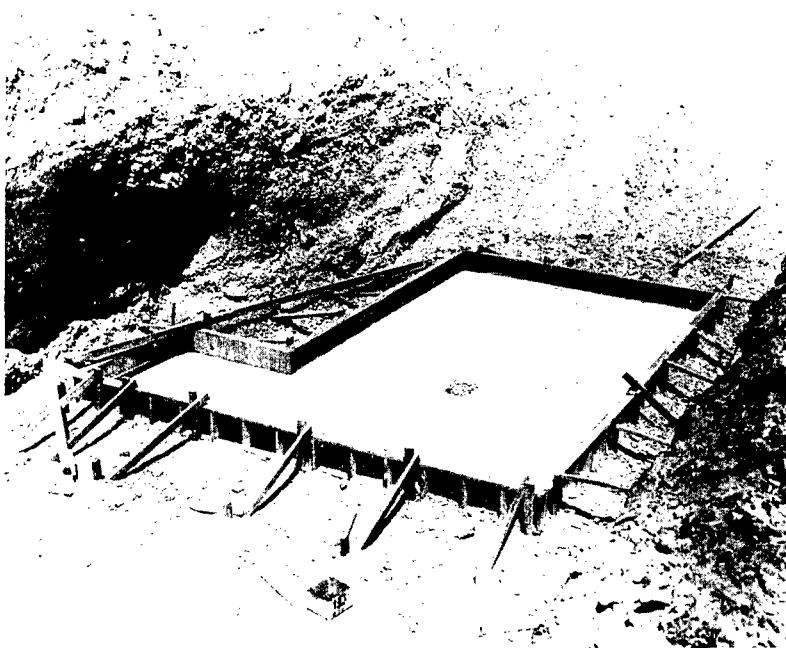
Fig. A.18—Base-slab formwork erected and sub-base concrete placed
(structure RC) (Apr. 27, 1957).
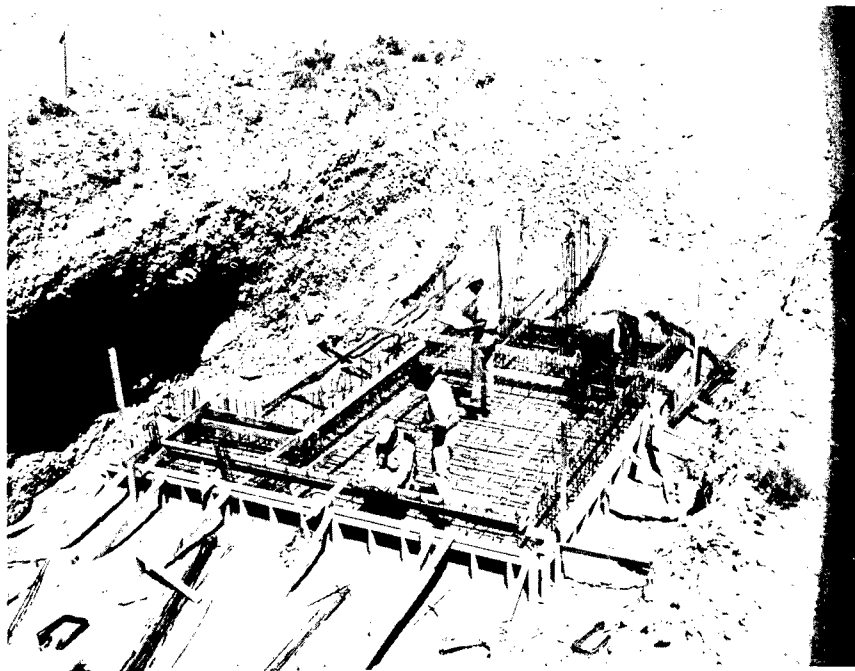
Fig. A.19—Placement of base-slab reinforcement (structure RC) (May 1, 1957).
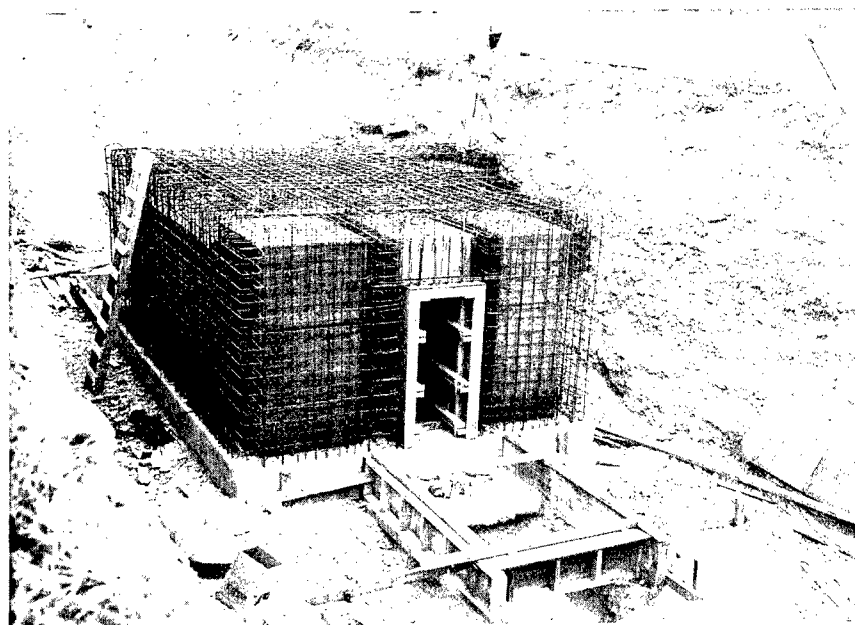
Fig. A.20—Wall- and roof-slab reinforcement in place (structure RC) (May 10, 1957).

Fig. A.21—Main body and emergency exit after removal of exterior forms (structure RC) (May 21, 1957).
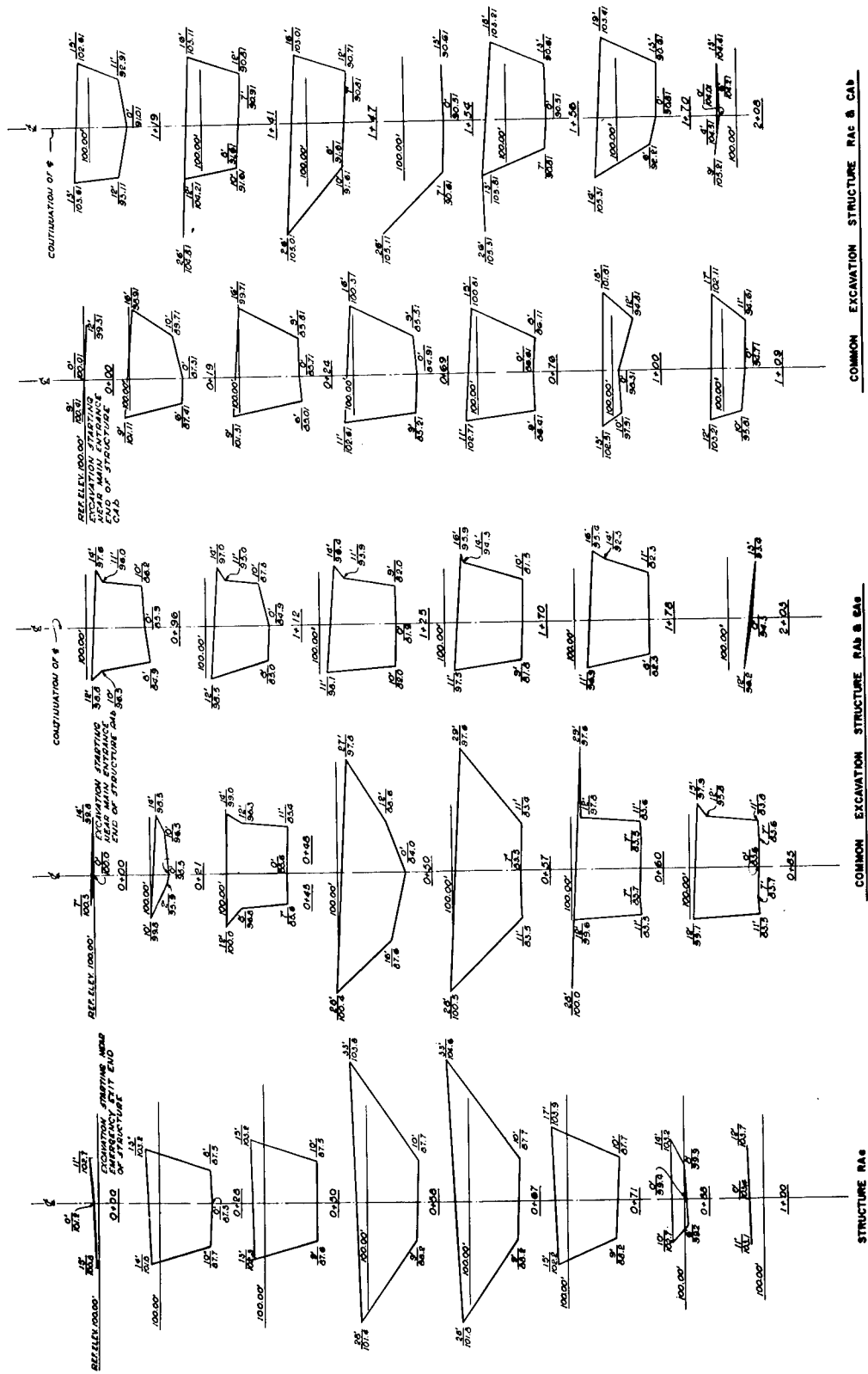
Fig. A.22—Excavation of structures RAa, RAb, CAa, RAc, and CAb.
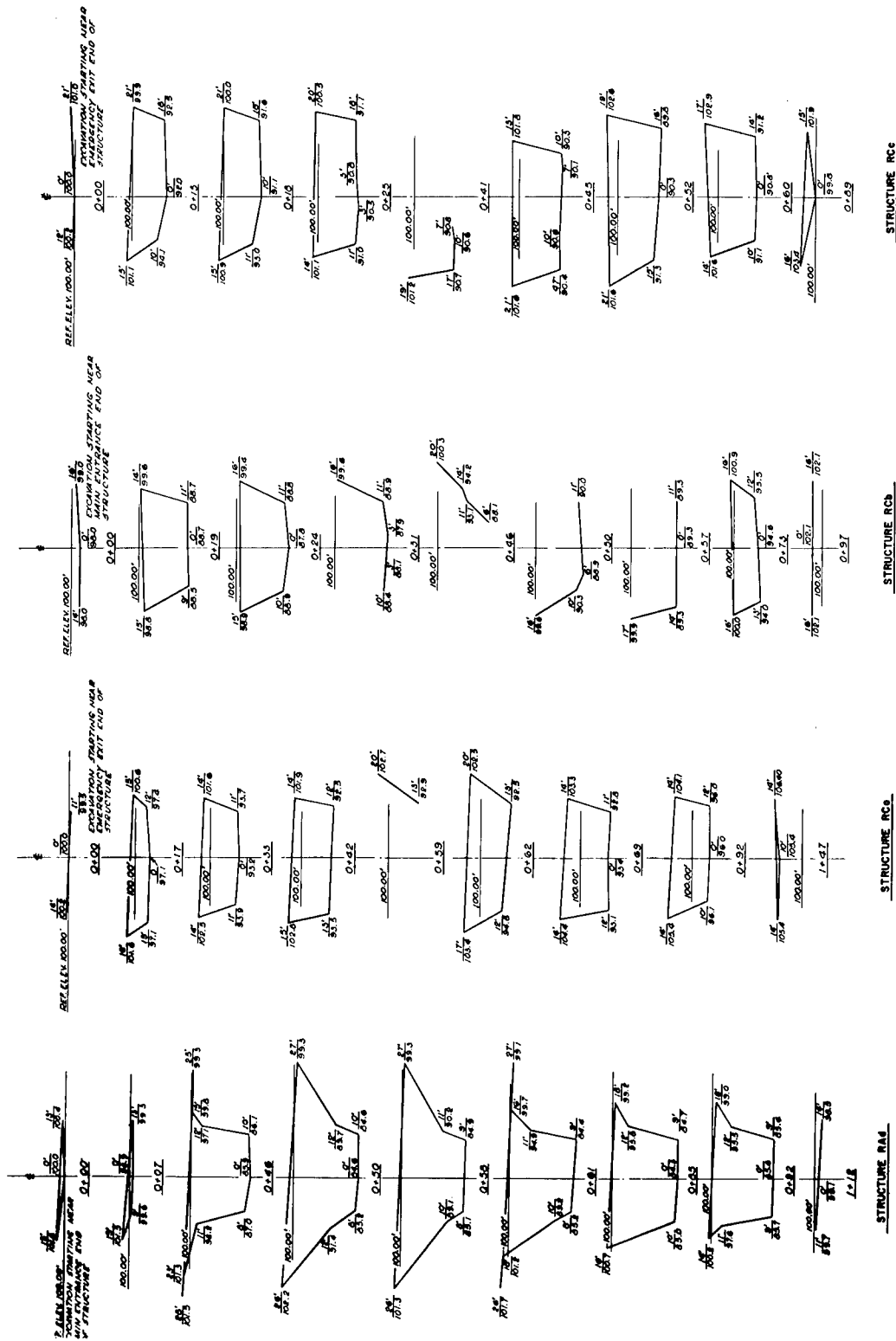
Fig. A.23—Excavation of structures RAd, RCa, RCb, and RCc.

Fig. A.24—Use of blade rippers during excavation.

Fig. A.25—Preparation of dynamite for tamping into drill holes.

Der Bundesminister Der Finanzen
Bonn Bundesbaudirektion
Bonn, Germany

UNDERGROUND PERSONNEL SHELTERS

Cast-in-place Reinforced Concrete

Title Sheet

Adapted By

Ammann & Whitney

Consulting Engineers

New York, N. Y.

DRAWING LIST

RECTANGULAR — TYPE A

1 DIMENSION PLAN & VENTILATION EQUIPMENT
2 REINFORCEMENT - PLANS, SECTIONS, & DETAILS
3 REINFORCING PLACEMENT DRAWING & BAR LIST

CIRCULAR — TYPE A

1 DIMENSION PLAN & VENTILATION EQUIPMENT
2 REINFORCING PLACEMENT DRAWING & BAR LIST

RECTANGULAR — TYPE C

1 DIMENSION PLAN & VENTILATION EQUIPMENT
2 REINFORCEMENT - PLANS, SECTIONS, & DETAILS
3 REINFORCING PLACEMENT DRAWING & BAR LIST

INSTRUMENTATION DRAWINGS

G1 — INSTUMENTATION LAYOUT
G2 — INSTUMENTATION MOUNTING DETAILS

LEGEND AND SYMBOLS

⑬- BAR MARK
NO. OF BARS AT EACH LOCATION
2 x 7 — 12ᴼ
DIA. OF BAR IN M.M.
NO. OF LOCATIONS AT WHICH BAR OCCURS

TA I —
TA IO — } DOOR LOCATIONS

SPACING OF BARS OF MARK INDICATED
EXTENT OF ALL BARS OF MARK INDICATED
⑬ - @ .5 2
BAR MARK
LOCATION OF BARS OF MARK INDICATED
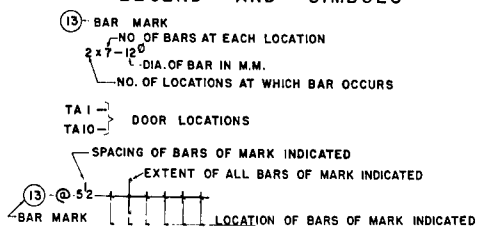
EQUIVALENT BAR DIAMETER	
DIAMETER IN M.M.	DIAMETER IN INCHES
8	.315
10	.395
12	.473
14	.552
16	.630
18	.710
20	.788
26	1.025

ABBREVIATIONS

ADD.	ADDITIONAL
@	AT
ALV	SAFETY VALVE
BOT.	BOTTOM
DIA.	DIAMETER
DN.	DOWN
HOR.	HORIZONTAL
JT.	JOINT
L	LEFT OR TOTAL LENGTH OF BAR
LONG.	LONGITUDINAL
M M	MILLIMETERS
O.C.	ON CENTER
OPP.	OPPOSITE
REINF.	REINFORCEMENT OR REINFORCING
R.	RIGHT
SECT.	SECTION
TRANS.	TRANSVERSE
UV	BLAST VALVE
VERT.	VERTICAL

Appendix B

AS-BUILT DRAWINGS

SECTION C-C

SECTION B-B

SECTION F-F

SECTION A-A

SECTION D-D

ELEVATION   SECTION

RECESSES FOR BLAST RESISTANT DOOR

ELEVATION   SECTION

BLAST RESISTANT DOOR

RECESSES

ELEVATION   SECTION

PLAN

INSIDE DOOR

ELEVATION   SECTION

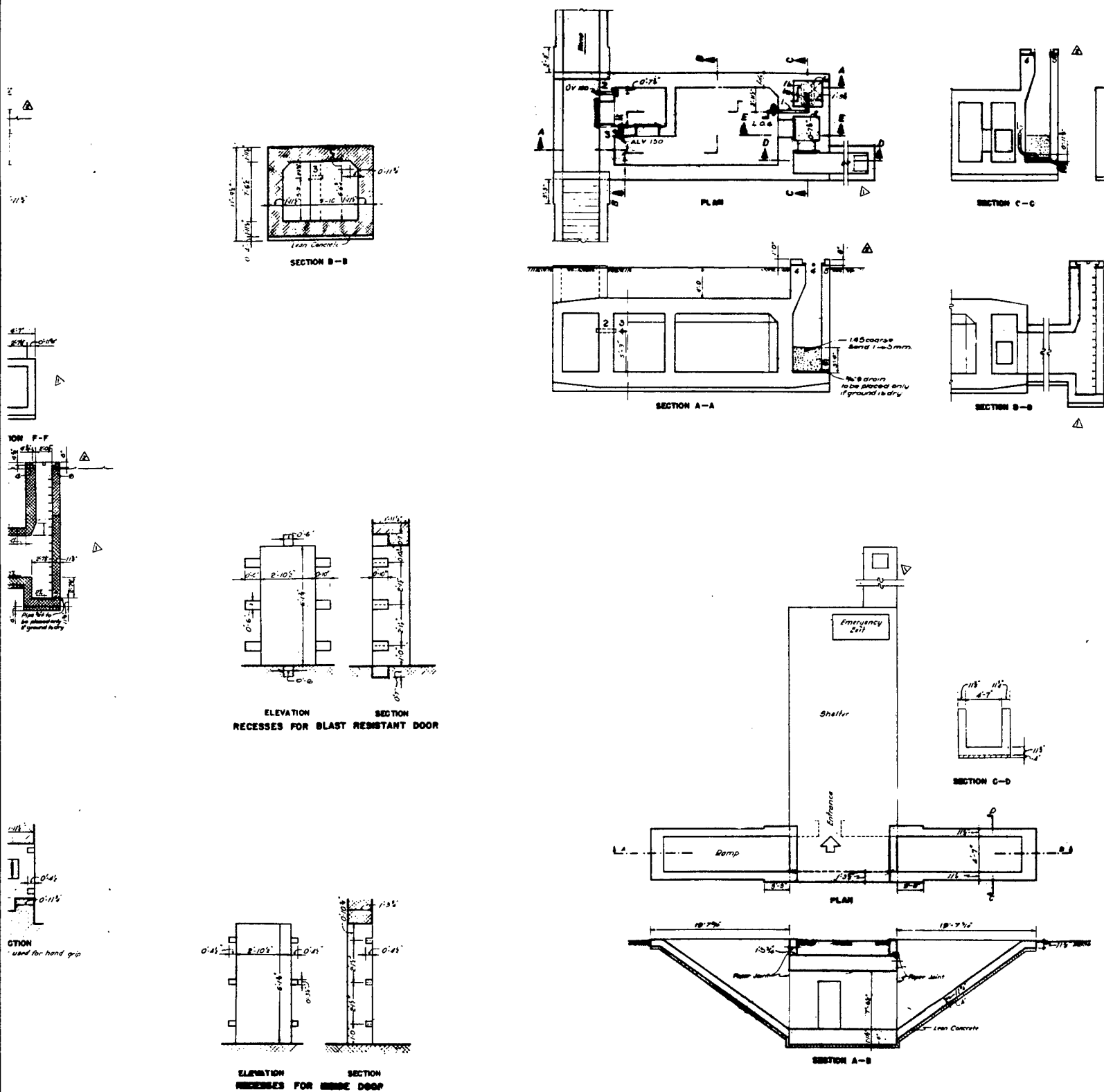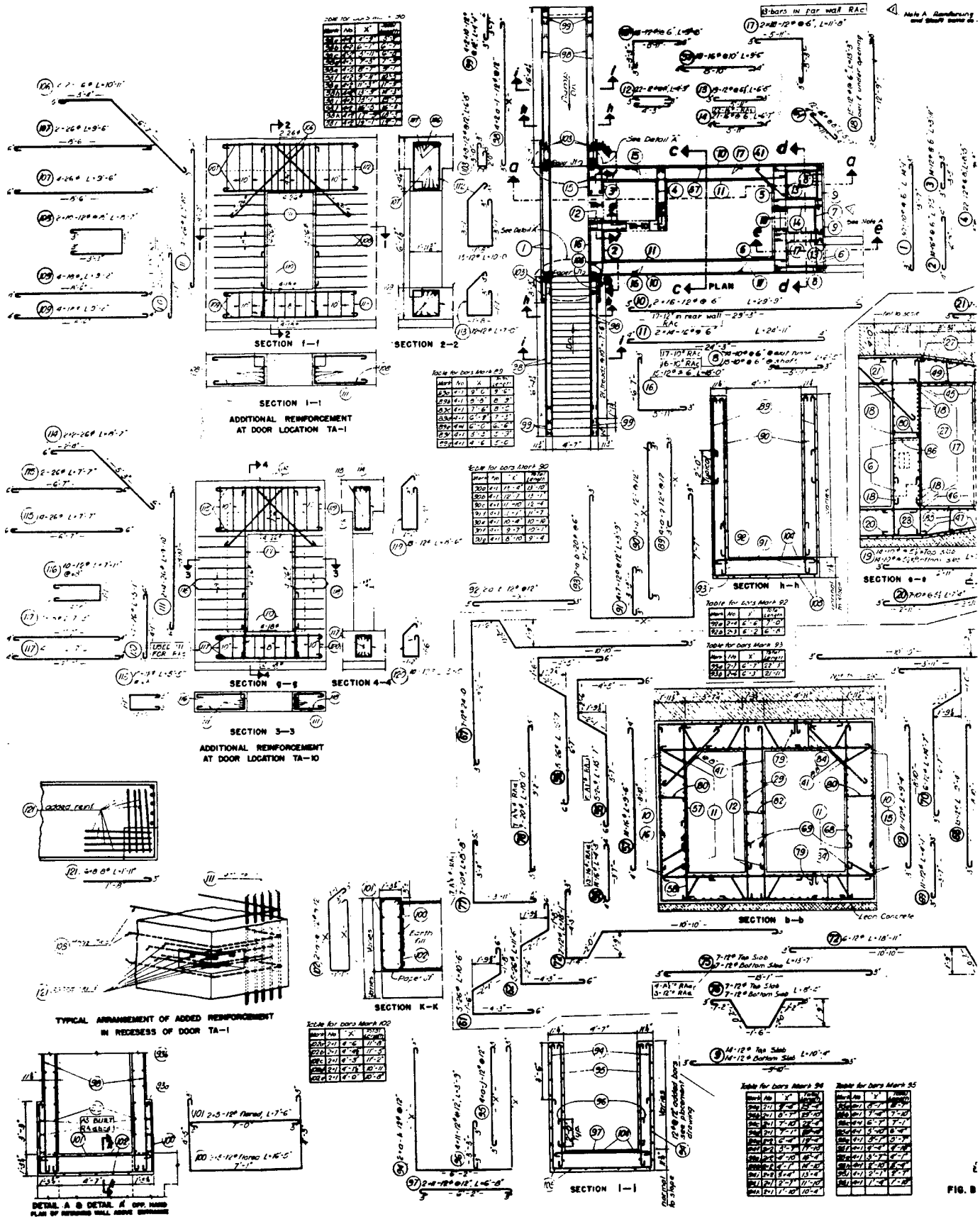RECESSES FOR INSIDE DOOR

Fig. B.1.1—Dimensions, plan, and ventilation equipm

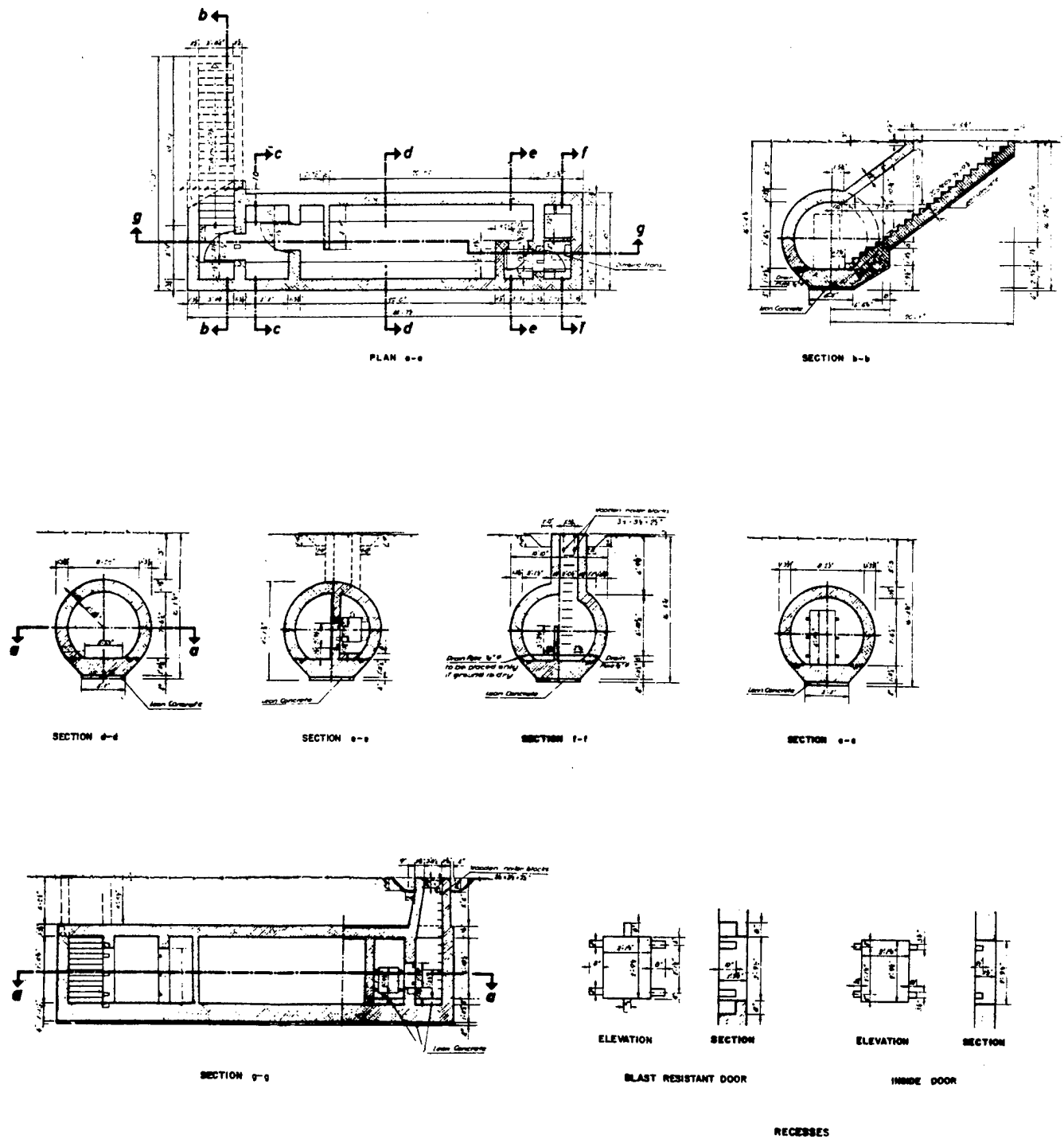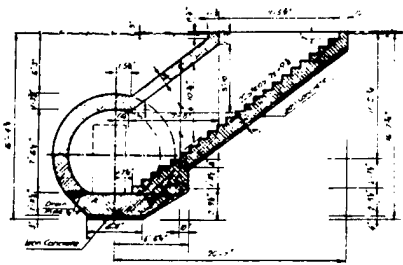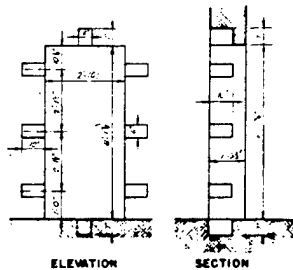Fig. B.1.1—Dimensions, plan, and ventilation equipment for type A cast-in-place rectangular shelter.

SECTION C—C   SECTION B—B

SECTION A—A   SECTION D—D   SECTION E—E

PLAN

SECTION C—D

Emergency Exit

Shelter

Entrance

Ramp

PLAN

SECTION A—B

-in-place rectangular shelter.

3

SECTION I—I
ADDITIONAL REINFORCEMENT
AT DOOR LOCATION TA-I

SECTION 2-2

SECTION g—g   SECTION 4-4

SECTION 3—3
ADDITIONAL REINFORCEMENT
AT DOOR LOCATION TA-IO

TYPICAL ARRANGEMENT OF ADDED REINFORCEMENT
IN RECESSES OF DOOR TA-I

DETAIL A & DETAIL A OPP. HAND
PLAN OF RETURNED WALL ABOVE ENTRANCE

SECTION K—K

SECTION 1—1

PLAN

SECTION h—h

SECTION o—o

SECTION b—b

Fig. B.1.2—Reinforcement plan (sections a

FIG. B.1.2

.1.2—Reinforcement plan (sections and details) for type A cast-in-place rectangular shelter.

A cast-in-place rectangular shelter.

3

Fig. B.1.3—Reinforcing placement and bar l

Fig. B.1.3—Reinforcing placement and bar list for type A cast-in-place rectangular shelter.

BAR LIST

SECTION T-T

SECTION U-U

SECTION V-V

SECTION W-W

tangular shelter.

RECTANGULAR SHELTER – TYPE A
CAST IN PLACE

3

PLAN a-a

SECTION b-b

SECTION d-d

SECTION e-e

SECTION f-f

SECTION c-c

SECTION g-g

ELEVATION   SECTION   ELEVATION   SECTION

BLAST RESISTANT DOOR   INSIDE DOOR

RECESSES

Fig. B.2.1—Dimensions, plan, and ventilation e

Fig. B.2.1—Dimensions, plan, and ventilation equipment for type A cast-in-place circular shelter.
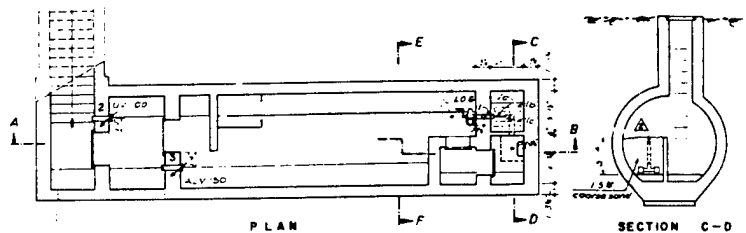
PLAN

SECTION C-D

ELEVATION A-B

SECTION E-F

ast-in-place circular shelter.

3
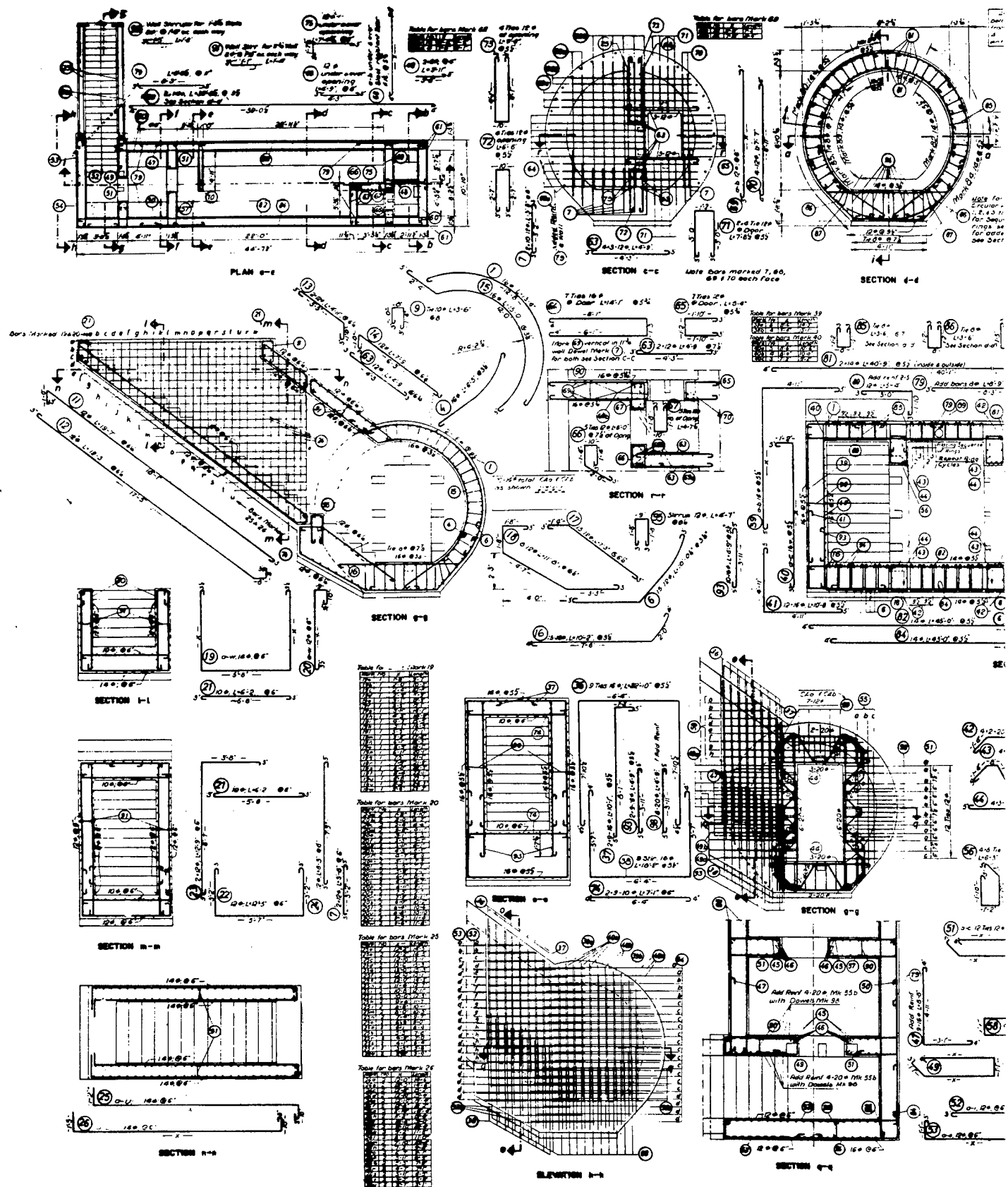
Fig. B.2.2—Reinforcement plan (sections and c

Fig. B.2.2—Reinforcement plan (sections and details) for type A cast-in-place circular shelter.

229

2

st-in-place circular shelter.

3

PLAN

SECTION A-B   SECTION C-D

SECTION E-F

SECTION E-E

Fig. B.3.1—Dimensions, plan, and ventilation

PLAN

SECTION E-E

SECTION A-A

SECTION F-F

SECTION B-B

SECTION C-C

SECTION D-D

ELEVATION   SECTION   ELEVATION
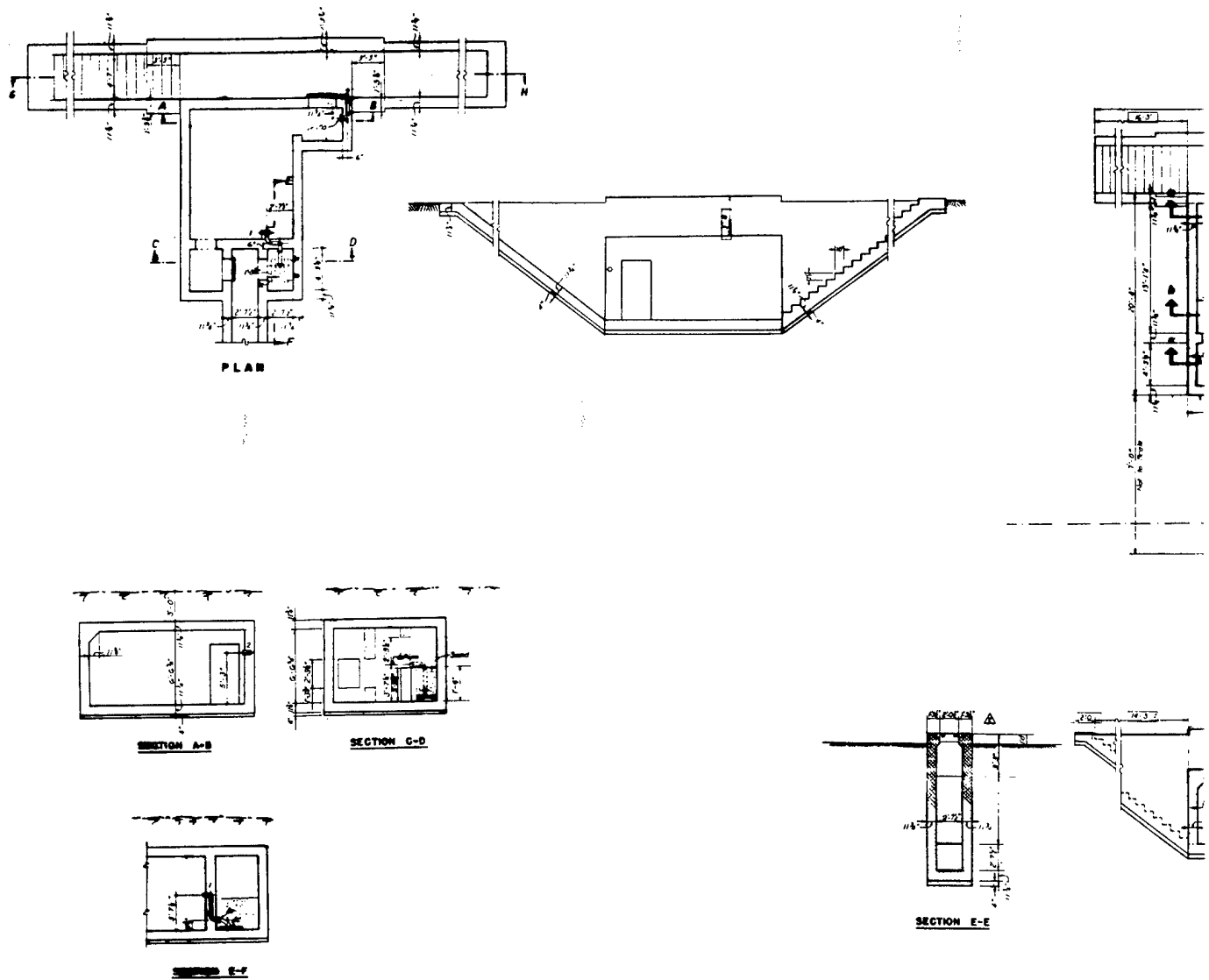
DOOR ON INSIDE   FL

RECESSES

RECESSES FOR EMERGEN
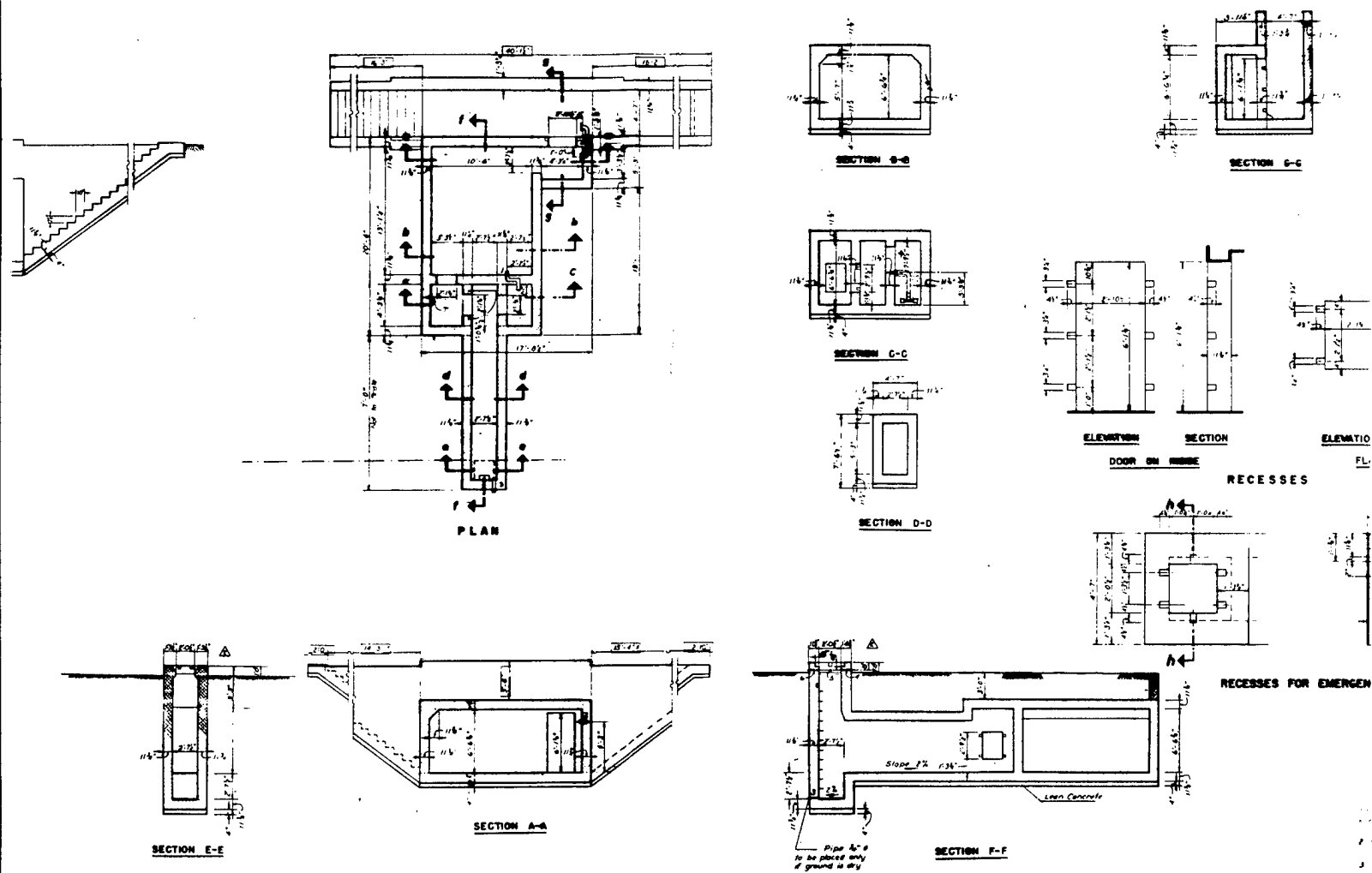
Fig. B.3.1—Dimensions, plan, and ventilation equipment for type C cast-in-place rectangular shelter.

SECTION B-B

SECTION C-C

SECTION C-C

SECTION D-D

ELEVATION   SECTION
DOOR ON INSIDE

ELEVATION   SECTION
FLAP ON INSIDE

RECESSES
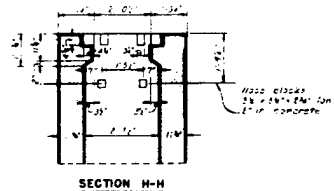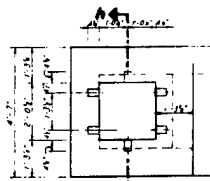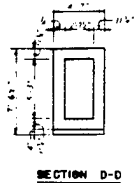
RECESSES FOR EMERGENCY EXIT

SECTION H-H

Slope 2%

Lean Concrete

SECTION F-F

Pipe to be
to be placed only
if ground is dry

cast-in-place rectangular shelter.

3

Fig. B.3.2—Reinforcement plan (sections a:

Fig. B.3.2—Reinforcement plan (sections and details) for type C cast-in-place rectangular shelter.

PART PLAN SHOWING ADDITIONAL
REINFORCEMENT AT DOOR OPENINGS
TO EMERGENCY EXIT

SECTION f—f

General Notes
1. Concrete
   a) Except as noted all concrete shall be stone concrete and have a minimum ultimate compressive strength of 88 days of 4260 psi
   b) The concrete for the setting bed steel have an ultimate compressive stress of 1700 psi
2. Aggregate sizes: see specifications
3. Reinforcing steel:
   a) For provision of reinf. steel see specifications
   b) Unless otherwise noted the substitution or use of bars other than those provided and indicated on drawings, may be made only with the approval of the contracting Engineer
   c) All detailing dimensions for reinforcement given are cut to cut dimensions
   d) Minimum lap distance for...

4. Concrete Cover for Main Reinforcement
   a) Walls – inside face – ½″
      outside – 1½″
   b) Floor slabs – top – ½″
      bottom – ½″
   c) Roof slabs – top – ½″
      bottom – ½″
   Required cover not... of cases
5. Contractor will provide concrete spacer blocks for obtaining required cover for all wall and slab reinforcement. These spacer blocks are to be spaced a maximum of 1′-8″ on center each way

As Built Notes
   1. All Reinforcement is per Revision No 2 not incorporated in structures
   2. For As Built Architectural Layout see...

ngular shelter.

AMMANN & WHITNEY
CONSULTING ENGINEERS
111–8TH AVENUE, NEW YORK, N.Y.

DER BUNDESMINISTER DER FINANZEN
BONN BUNDESBAUDIREKTION
BONN GERMANY

RECTANGULAR SHELTER — TYPE C
CAST IN PLACE
REINFORCEMENT-PLAN, SECTIONS & DETAILS

SHEET 2 OF 3

PLAN b-b
FLOOR SLAB

PLAN v-v
ROOF SLAB

SECTION s-s

SECTION u-u

SECTION p-p

KEY PLAN

SECTION t-t

SECTION r-r

Fig. B.3.3—Reinforcing placement an

Fig. B.3.3—Reinforcing placement and bar list for type C cast-in-place rectangular shelter.

PLAN $k_1 - k_1$

BAR LIST

SECTION n - n

SECTION o - o

SECTION m - m

SECTION l - l

N r - r

For Reinforcement Details
See Sheet 8

* Additional Bars for Shelter 'A'
(Exit Tunnel and Shaft)

As Built Notes

t-in-place rectangular shelter.

3

PLAN

SECTION A-A

SECTION B-B   SECTION C-C

SECTION E-E   SECTION D-D

CIRCULAR — TYPE A

PLAN

SECTION F-F

SECTION G-G

SECTION J-J   SECTION H-H

RECTANGULAR — TYPE C

Fig. B.4.1— Instrumentation mounting details for rectan

Fig. B.4.1—Instrumentation mounting details for rectangular types A and C and circular type A German protective shelters.

233

PLAN

SECTION K-K

SECTION L-L

SECTION M-M

SECTION N-N

SECTION P-P

SECTION Q-Q

RECTANGULAR—TYPE A

INSTRUMENTATION SUMMARY

SHELTER		PRESSURE LEVEL (PSI)	ELECTRONIC GAGES						SELF RECORDING		
			PRESSURE P	PRESSURE PS	DYN PRESS Q	DEFL D	ACTION ACCELERS A	STRAIN S	DYN PRESS Z	PRESS PR PS	SCRATCH GA S
CIRCULAR TYPE A	a	1985	4	3	—	2	1	1	—	3	—
	b	1385	—	—	—	—	—	—	—	3	—
RECTANGULAR TYPE A	a	2646	—	—	—	—	—	1	7	4	
	b	1985	3	4	—	2	—	1	9	—	
	c	1385	—	—	—	—	—	1	7	—	
	d	88c	—	—	—	—	—	1	5	—	
RECTANGULAR TYPE C	a	691	2	4	1	4	1	3	—	6	—
	b	14.7	—	—	—	—	—	—	—	2	—
	c	7.4	—	—	—	—	—	—	—	4	—

NOTES
1. Strain gages are to be attached to inside reinforcement spanning in short direction at sections shown
2. Four Electronic Free Field Pressure gages and four Self-Recording Free Field Pressure gages for same are to be located by B.R.L.
3. B.R.L will place all instrument cables (not conduits) install gages and provide all ditching required for same
4. Earth Pressure gages (Carlson type) must be calibrated by B.R.L after backfilling
5. Carlson type Pressure Gages ————— P
6. Wianco type Pressure Gages ————— R
7. Dynamic Pressure Gages ————— Q
8. B.R.L Deflection Gages ————— D
9. Acceleration Gages ————— A
10. SR4 Strain Gages ————— S
11. Self-Recording Pressure Gages ————— P
12. Self-Recording Dynamic Pressure Gages - Z
13. WES scratch Gages ————— S
14. All conduits to be 4" I.D. except as noted
15. See Sheet No. for Mount details
16. All conduits to have pull wires

AS BUILT
AS BUILT LOCATIONS ARE AS SHOWN ON FIGS 24 THRU ? ? INCLUSIVE OF
ITR REPORT 1454

and circular type A German protective shelters.

3

Fig. B.4.2—Instrumentation layout for rectangular t

Fig. B.4.2—Instrumentation layout for rectangular types A and C and circular type A German protective shelters.

DETAIL B   SECTION D-D

TYPICAL SECTION FOR CIRCULAR TYPE A SHELTER
NO SCALE

See detail A

Ball Joint

Scratch Gage Lengths			
Structure	Gage Mark	L	
Circular Type A			
Rectangular Type A	B₁₀	11'-10'±	7'-6'
	C₁₀	11'-10'±	7'-6'
	D₁₀	7'-1'±	7'-0'
	E₁₀	7'-2'±	5'-0'
Rectangular Type C			

Note
See Sh... ...ction of
Scratch Gages

PLAN

DETAIL C

See detail A

See dets 3

Ball Joint

NOTE
Scratch gage at floor
similar to scratch gage
at roof slab
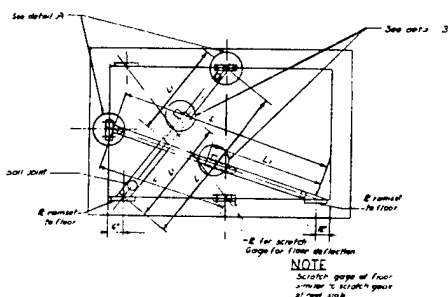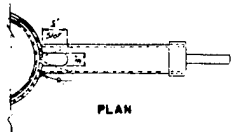
TYPICAL SECTION FOR SHELTERS
RECTANGULAR TYPE A
NO SCALE

W.E.S. SCRATCH GAGE

B WALLS
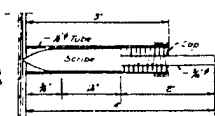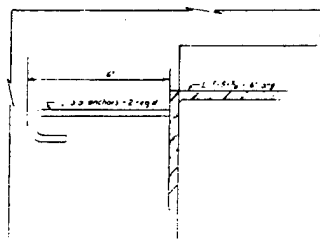
ACCELERATION GAGE MOUNT
HALF SCALE

PLAN

NTS

type A German protective shelters.
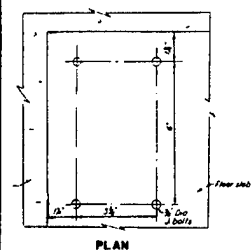
AMMANN & WHITNEY   DER BUNDESMINISTER DER FINANZEN
BONN BUNDESBAUDIREKTION
111- 8TH AVENUE, NEW YORK, N.Y.   BONN , GERMANY.

GERMAN PROTECTIVE SHELTERS
RECTANGULAR TYPE A&C,CIRCULAR TYPE A
INSTRUMENTATION MOUNTING DETAILS

APPROVED

SCALE
DRAWING NUMBER

SHEET G 2

3

Appendix C

ANALYSIS OF TYPE A RECTANGULAR STRUCTURE

C.1 GENERAL

The shelter was designed by German engineers for a static loading condition (Sec. 1.4).
Four shelters of this type were built at various pressure levels and tested during shot Smoky
of Operation Plumbbob. All four shelters withstood the effects of the blast with little or no
damage to the main body of the shelter. On the basis of the limited damage incurred, it was
deemed advisable to analyze the roof slab of this shelter type by the conventional ultimate-
strength theory to ascertain whether this method of analysis would substantiate the actual
damage sustained by this member.

C.2 BLAST LOADING

Shelter RAa was specifically analyzed. This shelter, placed closest to GZ (see Fig. 1.4),
was the most heavily loaded. The loading of this structure, for the purpose of analysis, was
the actual free-air pressure-time load as recorded at the location of this structure (Fig. C.1).
No attenuation due to the earth cover was assumed.

C.3 STRENGTH CRITERIA

The structure was analyzed for dynamic behavior by use of the ultimate-strength theory.
Compressive strength of concrete was 4000 psi and was determined as the average value
obtained from the 90-day test cylinders (preshot). Reinforcing steel was smooth round bars
sent from West Germany. The static unit stress at a yield of 43,800 psi was also the average
of values obtained from the test specimens. The increase in strength under dynamic loads was
taken into account with the use of dynamic increase factors obtained from Ref. 4 (see dynamic
analysis, Sec. C.8). The dynamic increase factors were determined as closely as possible, de-
pending on the rate of strain under the blast loading.

C.4 ANALYSIS

In general, the analyses of the various members of the structure which are exposed to the
blast consist in the solution of the equation of motion, $F - R = M_e \ddot{x}$, where F is the applied
blast force, R is the internal resistance of the structural member, M_e is the mass of an equiv-
alent single-degree-of-freedom system,[4] and $\ddot{x}$ is the acceleration of the mass.
This equation of motion can be readily solved by any of several numerical-integration[5]
methods. The numerical method illustrated in this appendix for the analysis of the roof slab of
the shelter is the Acceleration Impulse Extrapolation Method described in Ref. 4.

Poisson's ratio for reinforced concrete is usually taken to vary between 0.10 and 0.166. In this analysis, Poisson's ratio has been taken as zero. Previous experience has indicated that the effect of Poisson's ratio may be considered negligible over the entire range from elastic to plastic behavior of the structural member.

C.5 ARCHITECTURAL AND STRUCTURAL DRAWINGS

Architecturally, the shelter was constructed as shown in Chap. 1, Fig. 1.1. The as-built drawings shown in Appendix B, Figs. B.1.1 to B.1.3, show the actual reinforcement arrangement placed in the field. As is clearly indicated by these drawings, there is very little deviation from the original reinforcement details. No modifications other than those recorded on the as-built drawings were made to any of the constructed shelters.

C.6 NOMENCLATURE

A_s = area of steel
a = depth of compression block of the slab
b = width of the slab
d = distance from extreme compressive fiber to centroid of tension force in tensile reinforcement
E = modulus of elasticity
f_c' = static ultimate compressive unit stress of concrete
f_{dc}' = dynamic ultimate compressive stress of concrete
f_s = static unit stress of steel at yield
f_{ds} = dynamic unit stress of steel at yield
I_c = moment of inertia of cracked section
I_u = moment of inertia of uncracked section
K = stiffness of member
L_1 = clear span of member in short direction
L_2 = clear span of member in long direction
m = mass of the member
$M_{\mathfrak{C}}$ = moment at the centerline of the member
M_s = moment at the support of the member
n = ratio of modulus of elasticity of steel to that of concrete
r = unit resistance of the member
R = total resistance of the member
T = period of vibration of the member
ult = ultimate
x = deflection of the member

236
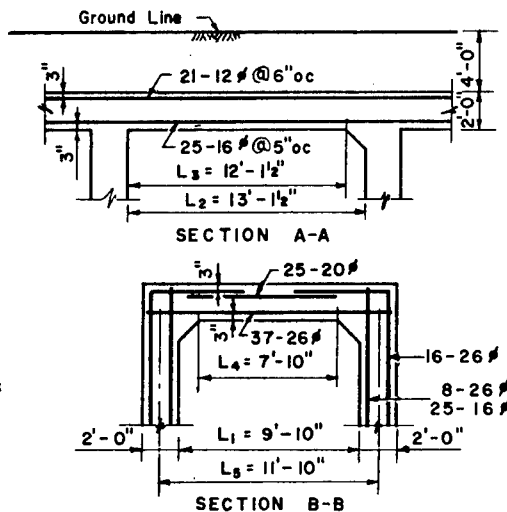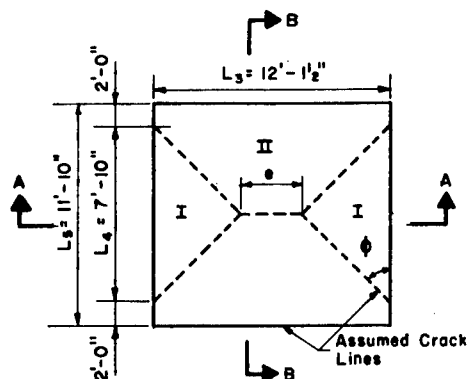
Note: The ultimate resistance of panel I is governed by the continuous portion of the slab. The ultimate resistance of panel II is governed by the moment capacity of the wall below the haunch. Assume the outer strips of panels I and II have one-half the moment and shear capacity of their respective midstrips.

f'_c = 4000 psi ⎫
f_s = 43,800 psi ⎭ Average values of test results

d = 24 in. − 3 in. = 21 in. ⎫
d' = 24 in. − 6 in. = 18 in. ⎭ Average values for both directions

ν = Poisson's ratio (for reinforced concrete) = 0

Reinforcement:

Diameter (mm)	Diameter (in.)
8	0.315
12	0.473
16	0.630
20	0.788
26	1.025

C.7 ULTIMATE STATIC RESISTANCE OF SLAB

C.7.1 Panel I

ϕ = 42° (by trial and error solution)

x = tan ϕ (3.92) = 3.53 ft

Positive reinforcement = $\dfrac{\pi}{4}$ $(0.630)^2$ $\dfrac{(12)}{5}$ = 0.75 sq in./ft

Negative reinforcement = $\dfrac{\pi}{4}$ $(0.473)^2$ $\dfrac{(12)}{6}$ = 0.35 sq in./ft
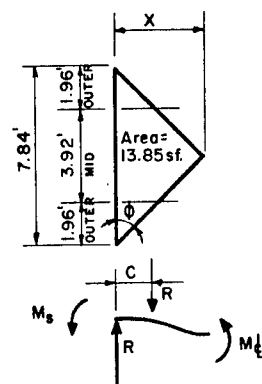
Negative-moment capacity (per foot):

$$a = \frac{A_s f_s}{0.85 b f'_c} \text{ (Ref. 1)} = \frac{0.35 \ (43.8)}{0.85 \ (12) \ (4)} = 0.376 \text{ in.}$$

$$M_{s \ ult} = A_s f_s \left(d - \frac{a}{2} \right) \text{ (Ref. 1)} = \frac{0.35 \ (43.8)}{12} \left(21 - \frac{0.376}{2} \right) = 26.6 \text{ kf/ft}$$

Positive-moment capacity (per foot):

$$a = \frac{0.75}{0.35} (0.376) = 0.805 \text{ in.}$$

$$M_{\text{¢ } ult} = \frac{0.75 \ (43.8)}{12} \left(21 - \frac{0.805}{2} \right) = 56.4 \text{ kf/ft}$$

237

Total positive and negative moments:

$$\sum M_{ult} = (M_s + M_\ell)\frac{3}{4}L_4$$

$$= (26.6 + 56.4)\,(0.75)\,(7.84) = 488 \text{ kf}$$

Total resistance of panel I:

$$R_{\Delta\,ult} = \frac{\sum M_{ult}}{c} = \frac{488}{(1/3)\,(3.53)} = 415 \text{ k}$$

Unit resistance of panel I:

$$r_{\Delta\,ult} = \frac{415}{13.85} = 30.0 \text{ ksf} = 208 \text{ psi}$$

C.7.2 Panel II

$$A_s^+ \text{ in slab} = \frac{37(1.025)^2\,(\pi)}{4} = 30.6 \text{ sq in.} = 2.34 \text{ sq in./ft}$$

$$A_s \text{ in wall} = \frac{16(1.025)^2\,(\pi)}{4} = 13.2 \text{ sq in.} = 1.00 \text{ sq in./ft}$$

$$A'_s \text{ in wall} = \frac{[8(1.025)^2 + 25(0.630)^2]\,(\pi)}{4} = 14.4 \text{ sq in.} = 1.10 \text{ sq in./ft}$$

Positive-moment capacity:

$$a = \frac{30.6\,(43.8)}{0.85(4)\,(12)\,(13.1)} = 2.5 \text{ in.}$$

$$M_\ell = 30.6\,(43.8)\left(21 - \frac{2.5}{2}\right) = 26{,}500 \text{ in k} = 2200 \text{ kf} = 181.5 \text{ kf/ft}$$

Negative-moment capacity: (section below wall haunch is critical)

Taking into account the effect of the axial load,

$$M_s = A_s f_s m + 0.85 f'_c\, aq\left(\frac{t}{2} - \frac{a}{2}\right) + A'_s f_s n \qquad \text{(Ref. 1)}$$

where A_s = tension reinforcement in the wall = 13.2 sq in.
   A'_s = compression reinforcement in the wall = 14.4 sq in.
   n = distance from centroid of compression steel to center line of wall = 0.75 ft
   m = distance from centroid of tension steel to center line of wall = 0.75 ft
   q = equivalent length of loaded area
   h = distance from center line of wall to centroid of panel
   t = wall thickness = 2 ft

$$a = -\frac{(2h - t)}{2} \pm \sqrt{h^2 - ht + \frac{t^2}{4} - \frac{A'_s f_y\,(h - n) - A_s f_y\,(h + m) - M_\ell}{0.425\,f'_c q}}$$

$$h = \frac{13.85\,(3.31) + 5.06\,(3.92)\,(3.96) + 24.24}{13.85 + 5.06\,(3.92) + 24.24}$$

238
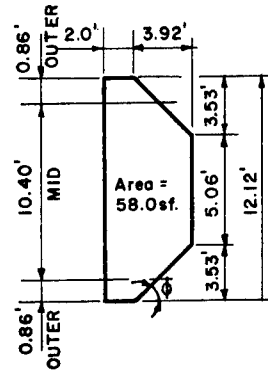
$$h = \frac{45.8 + 78.6 + 24.24}{13.85 + 19.8 + 24.24} = 2.57 \text{ ft}$$

$$q \approx 5.06 + \frac{3}{4}(12.12 - 5.06) = 10.36 \text{ ft}$$

$$a = -\frac{[2(2.57) - 2]}{2}$$

$$\pm \sqrt{(2.57)^2 - 2.57(2) + \frac{4}{4} - \frac{14.4\,(43.8)\,(2.57 - 0.75) - 13.2\,(43.8)\,(2.57 + 0.75) - 2200}{0.425\,(4.0)\,(10.36)\,(144)}}$$

$$a = 1.57 \pm \sqrt{6.60 - 5.14 + 1 - \frac{1150 - 1920 - 2200}{2520}}$$

$$a = 0.34 \text{ ft} = 4.08 \text{ in.}$$

$$M_s = 13.2\,(43.8)\,(0.75) + 0.85\,(4.00)\,(4.08)\,(12)\,(10.36)\left(\frac{2}{2} - \frac{0.34}{2}\right) + 14.4\,(43.8)\,(0.75)$$

$$M_s = 434 + 1431 + 473 = 2338 \text{ kf} = 193 \text{ k-ft/ft}$$

Total positive and negative moments:

$$\sum M_{ult} = M_s + M_{\mathcal{C}} = 2338 + 2200 = 4538 \text{ kf}$$

Actual total resistance of panel II:

$$R_{\triangle ult} = A_s' f_s - A_s f_s + 0.85\, f_c'\, aq$$
$$= 14.4\,(43.8) - 13.2\,(43.8) + 0.85\,(4.0)\,(0.34)\,(10.36)\,(144)$$
$$= 631 - 578 + 1725 = 1778 \text{ k}$$

Unit resistance of panel II:

$$r_{\triangle ult} = \frac{1778}{58.0} = 30.6 \text{ ksf} = 212 \text{ psi} \approx 208 \text{ psi}$$

Average unit resistance of total slab:

$$r_{av} = \frac{(1778 + 415)\,(2)}{(11.84)\,(12.12)} = 30.5 \text{ ksf}$$

Ultimate static resistance of total slab:

$$R_{ult} = (1778 + 415)\,(2) = 4390 \text{ k}$$

In the foregoing computations, the ultimate static capacity of the slab was computed. How-ever, the actual loads applied to the structure are dynamic in nature. Under this dynamic load, the capacity of the slab is considerably higher than the static capacity, depending on the time for the reinforcement to reach its yield point. To take this increase in strength into account, the static capacity may be increased by a dynamic increase factor. These factors may be obtained from Ref. 4 if the time for the reinforcement to reach yield is known. Since yielding of the reinforcement throughout the slab does not occur simultaneously, the dynamic increase factor will be different for each of the critical sections in the slab. For this reason, the static

resistance-deflection curve for the slab will be computed first; then, during the dynamic analysis, this curve will be modified by the dynamic increase factors applicable to each of the critical sections, depending on the time required for each of these sections to reach yield.

C.8 COMPUTATION OF STATIC RESISTANCE-DEFLECTION CURVE (Fig. C.2)

C.8.1 Yield of Negative Reinforcement of Panel I

Note: The member is considered fixed all around.

Panel I

$$\frac{L_3}{L_5} = \frac{b}{a} = \frac{12.12}{11.84} = 1.02$$

Negative moment of beginning of yield along edge

$$M_{S1} = 0.0518 \ \Delta r \ L_5^2 \ \text{(Ref. 2, p. 140)}$$

Unit resistance at first yield

$$\Delta r = \frac{M_{S1}}{0.0518 L_5^2} = \frac{26.6}{0.0518 \ (11.84)^2} = 3.66 \ \text{ksf} = 25.4 \ \text{psi}$$

Total resistance of slab at first yield

$$R_1 = 3.66 \ (11.84) \ (12.12) = 527 \ k$$

Positive moment at first yield

$$\frac{\Delta r \ L_5^2}{M_{\mathfrak{C}}} = 57.5 \ \text{(Ref. 2, p. 140)}$$

$$M_{\mathfrak{C}} = \frac{\Delta r \ L_5^2}{57.5} = \frac{3.66 \ (11.84)^2}{57.5} = 8.94 \ \text{kf/ft} < 56.4 \ \text{kf/ft}$$

∴ positive reinforcement has not yielded as yet.

Panel II

Negative moment at first yield

$$M_{S1} = 0.0530 \ \Delta r \ L_5^2 \ \text{(Ref. 2, p. 140)}$$

$$= 0.0530 \ (3.66) \ (11.84)^2$$

$$= 27.2 \ \text{kf/ft} < 193 \ \text{kf/ft}$$

∴ negative reinforcement has not yielded as yet.

Positive moment at first yield

$$\frac{\Delta r \ L_5^2}{M_{\mathfrak{C}1}} = 54.7 \ \text{(Ref. 2, p. 140)}$$

$$M_{\mathfrak{C}1} = \frac{3.66(11.84)^2}{54.7} = 9.39 \ \text{kf/ft} < 181.5 \ \text{kf/ft}$$

∴ positive reinforcement has not yielded as yet.

Properties of Slab at First Yield

$$E = 1000 \; f'_c = 4 \times 10^6 \; \text{psi (Ref. 3)}$$

Average percentage of reinforcement for the cracked moment of inertia

Average negative reinforcement $= p^- = \dfrac{1/2(0.35 + 1.00)}{12(21)} = 0.00268$

Average positive reinforcement $= p^+ = \dfrac{1/2(0.75 + 2.34)}{12(21)} = 0.00610$

Average per cent reinforcement $= \dfrac{0.00268 + 0.00610}{2} = 0.00439$

Average moment of inertia (Ref. 4)

$$n = 7.5, \; p_{av.} = 0.00439 \qquad \therefore F = 0.024$$

$$I_u = \frac{bt^3}{12} = \frac{12(24)^3}{12} = 13,800 \; \text{in.}^4$$

$$I_c = Fbd^3 = 0.024(12) \; (21)^3 = 2670 \; \text{in.}^4 \; \text{(Ref. 3)}$$

$$I_{av.} = \frac{13,800 + 2670}{2} = 8235 \; \text{in.}^4$$

Deflection at first crack

$$X_1 = \frac{q \; L_5^4}{E \; t^3} \; (0.0158); \quad t^3 = \frac{12 \; I}{b} = \frac{12(8235)}{12} = 8235 \; \text{cu in.}$$

$$X_1 = \frac{0.0158(25.4) \; (11.84 \times 12)^4}{4 \times 10^6 \; (8235)} = 0.00499 \; \text{in.} = 0.000416 \; \text{ft}$$

Stiffness

$$K_1 = \frac{R_1}{X_1} = \frac{527}{4.16 \times 10^{-4}} = 1.27 \times 10^6 \; \text{k/ft}$$

C.8.2 Yield of Negative Reinforcement of Panel II

Note: The member is assumed fixed on sides L_3 and pin supported on side L_5.

Panel II

Negative moment at beginning of yield along edge

$$\Delta M_{S2} = \frac{\Delta r_2 \; L_5^2}{14.2} \; \text{(Ref. 2, p. 236)}$$

$$\Delta M_{S2} = 193 - 27 = 166 \; \text{kf/ft}$$

$$\Delta r_2 = \frac{166(14.2)}{(11.84)^2} = 168 \; \text{ksf} = 117 \; \text{psi}$$

Positive moment at second yield

$$\Delta M_{\ell 2} = \frac{\Delta r_2 \, L_5^2}{34.4} \text{ (Ref. 2, p. 236)}$$

$$\Delta M_{\ell 2} = \frac{16.8(11.84)^2}{34.4} = 68.4 \text{ kf/ft}$$

$$M_{\ell 2} = 9.4 + 68.4 = 77.8 \text{ kf/ft} < 181.5 \text{ kf/ft}$$

∴ positive reinforcement has not yielded as yet.

Panel I

Positive moment at second yield

$$\Delta M_{\ell 2} = \frac{\Delta r_2 \, L_5^2}{65.4} = \frac{16.8(11.84)^2}{65.4}$$

$$\Delta M_{\ell 2} = 36.0 \text{ kf/ft}$$

$$M_{\ell 2} = 8.9 + 36.0 = 44.9 \text{ kf/ft} < 56.4 \text{ kf/ft}$$

∴ positive reinforcement has not yielded as yet.

Properties of Slab at Second Yield

Resistance of slab at second yield

$$\Delta R_2 = 16.8(12.12)\,(11.84) = 2415 \text{ k}$$

$$R_2 = R_1 + \Delta R_2 = 527 + 2415 = 2942 \text{ k}$$

Deflection of slab at second yield

$$\Delta X_2 = \frac{0.0234 \, \Delta r_2 \, L_5^4}{E \, t^3} \qquad \text{(Ref. 2, p. 236)}$$

$$\Delta X_2 = \frac{0.0234 \, (117) \, (1184 \times 12)^4}{4 \times 10^6 \, (8235)} = 0.0340 \text{ in.} = 0.00283 \text{ ft}$$

$$X_2' = X_1 + \Delta X_2 = 0.000416 + 0.00283 = 0.00325 \text{ ft}$$

Stiffness

$$K_2 = \frac{\Delta R_2}{\Delta X_2} = \frac{2.415 \times 10^3}{2.83 \times 10^{-3}} = 8.52 \times 10^5 \text{ k/ft}$$

C.8.3 Yield of Positive Reinforcement of Panel I

Note: The member is assumed as simply supported all around.

Panel I

$$\Delta M_{\ell 3} = \frac{\Delta r_3 \, L_5^2}{27.3} \qquad \text{(Ref. 2, p. 232)}$$

$$\Delta M_{\ell 3} = 56.4 - 44.9 = 11.5 \text{ kf/ft}$$

$$\Delta r_3 = \frac{11.5\ (27.3)}{(11.84)^2} = 2.24\ ksf = 15.6\ psi$$

Panel II

$$\Delta M_{\mathbb{C}3} = \frac{\Delta r_3\ L_5^2}{26.2} \qquad \text{(Ref. 2, p. 232)}$$

$$\Delta M_{\mathbb{C}3} = \frac{2.24(11.84)^2}{26.2} = 12.0\ kf/ft$$

$$M_{\mathbb{C}2} + \Delta M_{\mathbb{C}3} = 77.8 + 12.0 = 89.8\ kf/ft < 181.5\ kf/ft$$

$$\therefore \text{positive reinforcement has not yielded as yet.}$$

Properties of Slab at Third Yield

Resistance of slab at third yield

$$\Delta R_3 = 2.24\ (12.12)\ (11.84) = 322\ k$$

$$R_3 = R_2 + \Delta R_3 = 2942 + 322 = 3264\ k$$

Deflection of slab at third yield

$$\Delta X_3 = \frac{0.0506\ \Delta r_3\ L_5^4}{E\ t^3} \qquad \text{(Ref. 2, p. 232)}$$

$$= \frac{0.0506(15.6)\ (11.84 \times 12)^4}{4 \times 10^6\ (8235)} = 0.00985\ in. = 0.000821\ ft$$

$$X_3 = X_2 + \Delta X_3 = 0.00325 + 0.000821 = 0.00407\ ft$$

Stiffness

$$K_3 = \frac{\Delta R_3}{\Delta X_3} = \frac{3.22 \times 10^2}{8.21 \times 10^{-4}} = 3.93 \times 10^5\ k/ft$$

C.8.4 Yield of Positive Reinforcement of Panel II

Note: The member is assumed simply supported in one direction.

Panel II

Total static resistance of slab

$$R_4 = R_{ult} = 4390\ k$$

$$\Delta R_4 = 4390 - 3264 = 1126\ k$$

$$\Delta r_4 = \frac{1126}{(11.82)(12.12)} = 7.84\ ksf = 54.4\ psi$$

Resistance of Panel II

$$\Delta R_{4\triangle} = 7.84\ (58.0) = 454\ k$$

Reaction of unit mid-strip

$$\Delta R_{mid} = \frac{454}{10.36} = 44.0 \text{ k/ft}$$

Total load on unit mid-strip

$$W = 44.0 \ (2) = 88.0 \text{ k/ft}$$

Properties of Slab at Fourth Yield

Deflection of slab at fourth yield

$$\Delta X_4 = \frac{5 \ W \ L_5^3}{384 \ EI} \qquad \text{(Ref. 4)}$$

$$\Delta X_4 = \frac{5(88.0) \ (11.84 \times 12)^3}{384 \ (4) \ (10^3) \ (8235)} = 0.1005 \text{ in.} = 0.00838 \text{ ft}$$

$$X_4 = X_3 + \Delta X_4 = 0.00407 + 0.00838 = 0.01245 \text{ ft}$$

Stiffness

$$K_4 = \frac{\Delta R_4}{\Delta X_4} = \frac{1.126 \times 10^3}{8.38 \times 10^{-3}} = 1.35 \times 10^5 \text{ k/ft}$$

C.9 DYNAMIC ANALYSIS

Dead Load (Assume overburden = 100 pcf)

$$F_{dl} = R_{dl} = [0.15(2.0) + 0.10(4.0)] \ (11.84) \ (12.12) = 100.5 \text{ k}$$

Mass

$$\text{Panel I} = 2(13.85) \ [0.15(2.0) + 0.10(4.0)] \ (1/32.2) = 0.602 \text{ k-sec}^2\text{/ft}$$

$$\text{Panel II} = 2(58.0) \ [0.15(2.0) + 0.10(4.0)] \ (1/32.2) = 2.521 \text{ k-sec}^2\text{/ft}$$

$$\text{Total mass (m)} = 3.123 \text{ k-sec}^2\text{/ft}$$

Equivalent Mass

$$\text{Elastic, } m_1 = \left[0.610 + 0.156 \left(\frac{b}{a} - 1\right)\right] m \qquad \text{(Ref. 5)}$$

$$= [0.610 + 0.156 \ (1.02 - 1)] \ 3.123 = 1.92 \text{ k-sec}^2\text{/ft}$$

Elasto-plastic, m_3
(between second and
third yields)

$$= \left[0.630 + 0.160 \left(\frac{b}{a} - 1\right)\right] m \qquad \text{(Ref. 5)}$$

$$= [0.630 + 0.160 \ (1.02 - 1)] \ (3.123) = 1.97 \text{ k-sec}^2\text{/ft}$$

Plastic, m_5
(after fourth
yield)

$$= \frac{1}{2} \sum M_\Delta + \frac{4b - 3a}{6b - 4a} \sum m_\triangle \qquad \text{(Ref. 5)}$$

$$= \frac{1}{2} \ (0.602) + \frac{4(12.12) - 3(11.84)}{6(12.12) - 4(11.84)} \ (2.521)$$

$$= 0.301 + 1.290 = 1.59 \text{ k-sec}^2\text{/ft}$$

Elasto-plastic, m_2
(between first and
second yields)

≈ 1.95 k-sec^2/ft

Elasto-plastic, m_4
(between third and
fourth yields)

$= 0.68$ m   (Ref. 4)

$= 0.68 (3.123) = 2.12$ k-sec^2/ft

Summary of equivalent mass

$m_1 = 1.92$ k-sec^2/ft

$m_2 = 1.95$ k-sec^2/ft

$m_3 = 1.97$ k-sec^2/ft

$m_4 = 2.12$ k-sec^2/ft

$m_5 = 1.59$ k-sec^2/ft

Note: Assume that the dead load and the preliminary part of the pressure curve to t = 23.0 msec (time 0.00 of dynamic analysis) act as a static load.

Period

$$T = 2\pi \sqrt{\frac{m_1}{K_1}} = 2\pi \sqrt{\frac{1.92}{1.27 \times 10^6}} = 7.74 \times 10^{-3} \text{ sec}$$

$$\Delta t_{max} = \frac{T}{10} = 7.74 \times 10^{-4} \text{ sec}$$

Use time intervals of $\Delta t = 0.00025$ sec $< t_{max}$ (Ref. 4)

Static Load

$$F_{static} = F_{dl} + F_{pp} = 100.5 + 36(0.144)(11.84)(12.12)$$

$$F_s = R_s = 100.5 + 745 = 846 \text{ k} > 527 \text{ k}$$

Under the static load, the slab has undergone first yield and is in the elasto-plastic state between the first and second yields.

$$X_{static} = X_1 + (846 - 527) \times \frac{1}{K_2}$$

$$= 0.00042 + \frac{319}{8.52 \times 10^5} = 0.000790 \text{ ft}$$

Properties of Slab for Dynamic Analysis (static-load effects deducted)

Second yield:

$$\Delta R = R_2 - R_s = 2942 - 846 = 2096 \text{ k}$$

$$\Delta X = X_2 - X_s = 0.00325 - 0.0079 = 0.00246 \text{ ft}$$

$$K_2 = 8.52 \times 10^5 \text{ k/ft}$$

Third yield:

$$\Delta R = R_3 - R_s = 3264 - 846 = 2418 \text{ k}$$

$$\Delta X = X_3 - X_s = 0.00407 - 0.0079 = 0.00328 \text{ ft}$$

$$K_3 = 3.93 \times 10^5 \text{ k/ft}$$

Fourth yield:

$$\Delta R = R_4 - R_s = 4390 - 846 = 3544 \text{ k}$$

$$\Delta X = X_4 - X_s = 0.01245 - 0.00079 = 0.01166 \text{ ft}$$

$$K_4 = 1.35 \times 10^5 \text{ k/ft}$$

Note: These properties are for statically applied loads. They must be modified by dynamic increase factors in the dynamic analysis.

Analysis Constants

$$\Delta t^2 = (0.00025)^2 = 6.25 \times 10^{-8} \text{ sec}^2$$

$$\frac{\Delta t^2}{m_1} = \frac{6.25 \times 10^{-8}}{1.92} = 3.26 \times 10^{-8} \text{ ft/k}$$

$$\frac{\Delta t^2}{m_2} = \frac{6.25 \times 10^{-8}}{1.95} = 3.20 \times 10^{-8} \text{ ft/k}$$

$$\frac{\Delta t^2}{m_3} = \frac{6.25 \times 10^{-8}}{1.97} = 3.17 \times 10^{-8} \text{ ft/k}$$

$$\frac{\Delta t^2}{m_4} = \frac{6.25 \times 10^{-8}}{2.12} = 2.95 \times 10^{-8} \text{ ft/k}$$

$$\frac{\Delta t^2}{m_5} = \frac{6.25 \times 10^{-8}}{1.59} = 3.93 \times 10^{-8} \text{ ft/k}$$

Acceleration Impulse Extrapolation Method

This method will be used in the dynamic analysis as described in Ref. 4.

$$X_{n+1} = 2X_n - X_{n-1} + a_n (\Delta t)^2 \qquad \text{(Ref. 4)}$$

$$F = P(12.12)(11.84)(144) - 745 = 20.7 P - 745 \text{ k}$$

$$a_n = \frac{F_n - R_n}{m_e}$$

$$a_0 = \frac{1}{m_e}\left[\frac{F_0}{2} + \frac{F_1 - F_0}{6}\right] = \frac{1}{1.95}\left[0 + \frac{144}{6}\right] = 12.31 \text{ ft/sec}^2$$

$$X_0 = a_0 \Delta t^2 = 12.31 (6.25 \times 10^{-8}) = 0.770 \times 10^{-6} \text{ ft}$$

Maximum resistance of slab = 3235 + 846 = 4081 k (Table C.1)

Maximum deflection of slab = $[5295 + 790] \times 10^{-6} = 60.9 \times 10^{-4}$ ft (Table C.1)

Note: The resistance of the slab would vibrate about the load curve after the first reversal; therefore the maximum resistance will be produced at the first reversal of the slab. If damping

were in the analysis, the maximum resistance of the slab would be between 5 and 10 per cent less than that obtained above. Note further that the maximum resistance attained was considerably less than the plastic yield of the total slab and that the maximum deflection attained was only about $\frac{1}{12}$ in.

C.10 CHECK OF SHEAR (Ref. 6)

C.10.1 Diagonal Tension, Panel II

Note: For diagonal tension, the critical section is at a distance d from the interior edge of the haunch.

Check diagonal tension stresses at the maximum resistance of the slab.

t = 24 in.

d = 21 in. = 1.75 ft

x = 2 + 1.75 = 3.75 ft

R = 4081 maximum resistance of slab

$w = \dfrac{4081}{143.70} = 28.4$ ksf

$A_{tot} = A_1 + A_2 = 58.0$ sq ft

$A_2 = 5.06(2.17) + 2.17(2.17) (0.90)$

$= 15.24$ sq ft

$A_1 = 12.12(2.0) + \dfrac{12.12 + 8.96}{2} (1.75)$

$= 42.69$ sq ft

Total shear at d from support line (① − ①)

$V_T = 28.4(15.24) = 433$ k

Shear per foot

$V = \dfrac{433}{8.96} = 48.3$ k/ft

Actual unit shear

$v = \dfrac{48.3}{12(21)} = 192$ psi $= 3.04 \quad \sqrt{f_c'}$

C.10.2 Pure Shear, Panel II

Check pure shear in panel II at edge of haunch and face of wall at the maximum resistance of the slab.

247
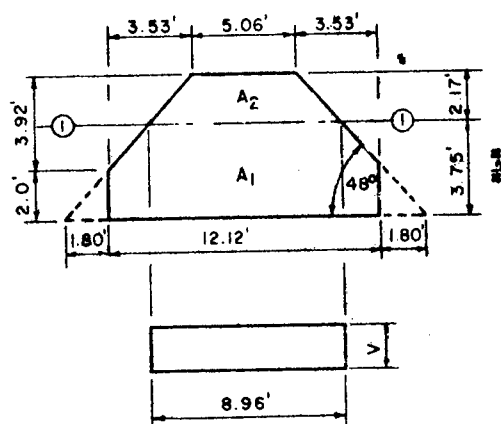
Pure Shear at Edge of Haunch

Total shear along edge of haunch at maximum resistance.

$$V_T = (58.0 - 24.24)\,28.4 = 958 \text{ k}$$

Shear per foot

$$2\left(\frac{V}{2}\right)(0.86) + 10.40\,V = 958 \text{ k}$$

$$11.26\,V = 958 \text{ k}$$

$$V = 85 \text{ k/ft}$$
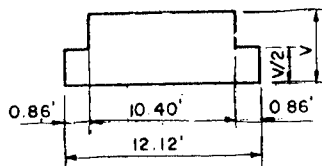
Actual unit pure shear

$$V = \frac{85}{12(21)} = 0.337 \text{ ksi} = 337 \text{ psi} = 0.0845\,f'_c$$

Pure Shear at Face of Wall

Total shear along face of wall at maximum resistance

$$V_T = (58.0 - 12.12)\,28.4 = 1300 \text{ k}$$

Shear per foot (shear distribution same as at edge of haunch)

$$11.26\,V = 1300$$

$$V = 155 \text{ k/ft}$$

Actual unit pure shear

$$V = \frac{115}{12(21 + 12)} = 0.290 \text{ ksi} = 290 \text{ psi} = 0.0725\,f'_c$$

Diagonal Tension, Panel I

Check diagonal tension at maximum resistance

$$A_T = 13.85 \text{ sq ft}$$

$$A_2 = \frac{3.95(1.78)}{2} = 3.52 \text{ sq ft}$$

$$A_1 = \frac{7.84 + 3.95}{2}(1.75) = 10.32 \text{ sq ft}$$

$$w = 28.4 \text{ ksf}$$
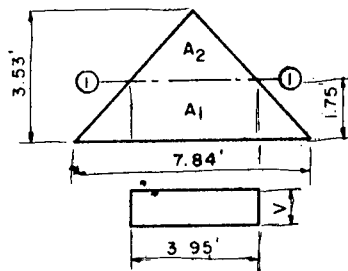
Total shear at d from support (line ① – ①)

$$V_T = 28.4\,(3.52) = 100.0 \text{ k}$$

Shear per foot

$$V = \frac{100.0}{3.95} = 25.3 \text{ k/ft}$$

Actual unit shear

$$V = \frac{25.3}{12(21)} = 0.1003 \text{ ksi} = 100.3 \text{ psi} = 1.59 \sqrt{f'_c}$$

REFERENCES

1. C. S. Whitney, Plastic Theory of Reinforced Concrete Design, Proc. Am. Soc. Civil Engrs., 66(10): 1749-1780 (1940).
2. Beton Kalender, 1958, Taschenbuch fur Beton- und Stahlbetonbau sowie die verwandten Facher—I, Teil.
3. Reinforced Concrete Design Handbook, Committee 317, American Concrete Institute, 2nd ed., 1955.
4. Engineering and Design, Design of Structures to Resist the Effects of Atomic Weapons, Principles of Dynamic Analysis and Design, Manual, U. S. Army Corps of Engineers.
5. C. S. Whitney, B. G. Anderson, and E. Cohen, Design of Blast-resistant Construction for Atomic Explosions, J. Am. Concrete Inst., 26(7): 589-683 (March 1955).
6. Current Ammann & Whitney criteria for the determination of ultimate shear requirements for beams and flat slabs.

TABLE C.1—DYNAMIC ANALYSIS

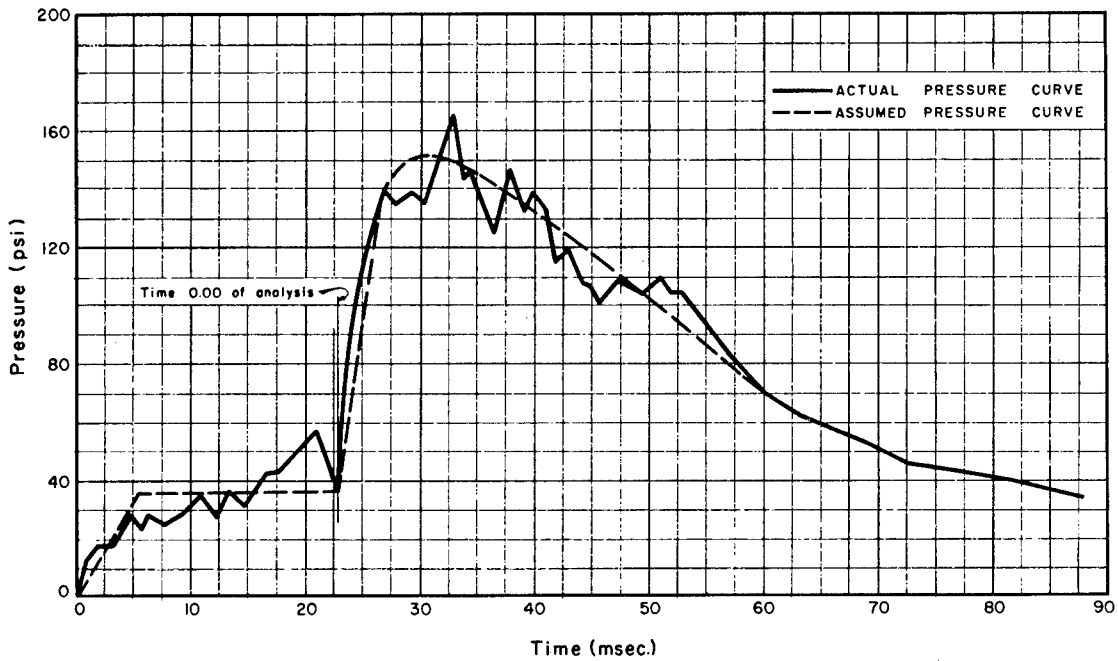| n	$t \times 10^4$, sec	F_n, k	R_n, k	$F_n - R_n$, k	$\Delta t^2/m \times 10^7$ ft/k	$A_n \Delta t^2 \times 10^6$ ft	$X_{n+1} \times 10^6$, ft	Remarks
0	0.0	0			0.320	0.770	0.770	$R_1 = 527$ k
1	2.5	144	1	143	0.320	4.576	6.116	$X_1 = 4.16 \times 10^{-4}$ ft } Fig. C.2
2	5.0	287	5	282	0.320	9.024	20.486	$K_1 = 1.27 \times 10^6$ k/f
3	7.5	432	17	415	0.320	13.280	48.136	Elasto-plastic
								DIF = 1.30 (Ref. 4)
								∴ The dynamic properties
								are for 2nd yield
4	10.0	578	41	537	0.320	17.184	92.970	$\Delta R = 2096\ (1.3)$
5	12.5	723	79	644	0.320	20.608	158.412	$= 2725$ k
6	15.0	871	135	736	0.320	23.552	247.406	$\Delta X = (1.3)\ (0.00246\ \text{ft})$ } See page
7	17.5	1005	211	794	0.320	25.408	361.808	$= 32.0 \times 10^{-4}$ ft } 245
8	20.0	1139	308	831	0.320	26.592	502.802	$K_2 = 8.52 \times 10^5$ k/ft
9	22.5	1293	428	865	0.320	27.680	671.476	
10	25.0	1445	572	873	0.320	27.936	868.086	
11	27.5	1590	740	850	0.320	27.200	1091.896	
12	30.0	1735	930	805	0.320	25.760	1341.466	
13	32.5	1858	1143	715	0.320	22.880	1613.916	
14	35.0	1980	1375	605	0.320	19.360	1905.726	
15	37.5	2064	1623	441	0.320	14.112	2211.648	
16	40.0	2147	1884	263	0.320	8.416	2525.986	
17	42.5	2195	2152	43	0.320	1.376	2841.700	
18	45.0	2242	2421	−179	0.320	−5.728	3151.686	
19	47.5	2266	2685	−419	0.320	−13.408	3448.264	Second yield
20	50.0	2292	2823	−531	0.317	−16.963	3727.879	For third yield
								DIF = 1.27 (Ref. 4)
21	52.5	2308	2932	−624	0.317	−19.781	3987.713	$\Delta R = 1.27\ (2418)$
								$= 3071$ k } See pages
								$\Delta X = 32.0 \times 10^{-4} + \dfrac{346}{3.93 \times 10^5}$ } 245 and 246
								$= 40.8 \times 10^{-4}$ ft
								$K_3 = 3.93 \times 10^5$ k/ft
22	55.0	2324	3035	−711	0.317	−22.539	4225.008	Third yield
								For fourth yield
23	57.5	2339	3091	−752	0.295	−23.794	4438.509	$\Delta R = 3544$ k } See page 246
								$K_4 = 1.35 \times 10^5$ k/ft
24	60.0	2352	3119	−767	0.295	−22.627	4629.383	
25	62.5	2363	3145	−782	0.295	−23.069	4797.188	
26	65.0	2366	3168	−802	0.295	−23.659	4941.334	
27	67.5	2368	3187	−819	0.295	−24.161	5061.319	
28	70.0	2370	3203	−833	0.295	−24.574	5156.730	
29	72.5	2381	3216	−835	0.295	−24.633	5227.508	
30	75.0	2391	3226	−835	0.295	−24.688	5273.598	
31	77.5	2401	3232	−831	0.295	−24.515	5295.173	maximum deflection
								$K = 1.27 \times 10^6$ k/ft
32	80.0	2397	3235	−838	0.295	−24.721	5292.027	
33	82.5	2393	3231	−838	0.295	−24.721	5264.160	
34	85.0	2389	3196	−807	0.295	−23.807	5212.486	
35	87.5	2385	3130	−745	0.295	−21.978	5138.834	

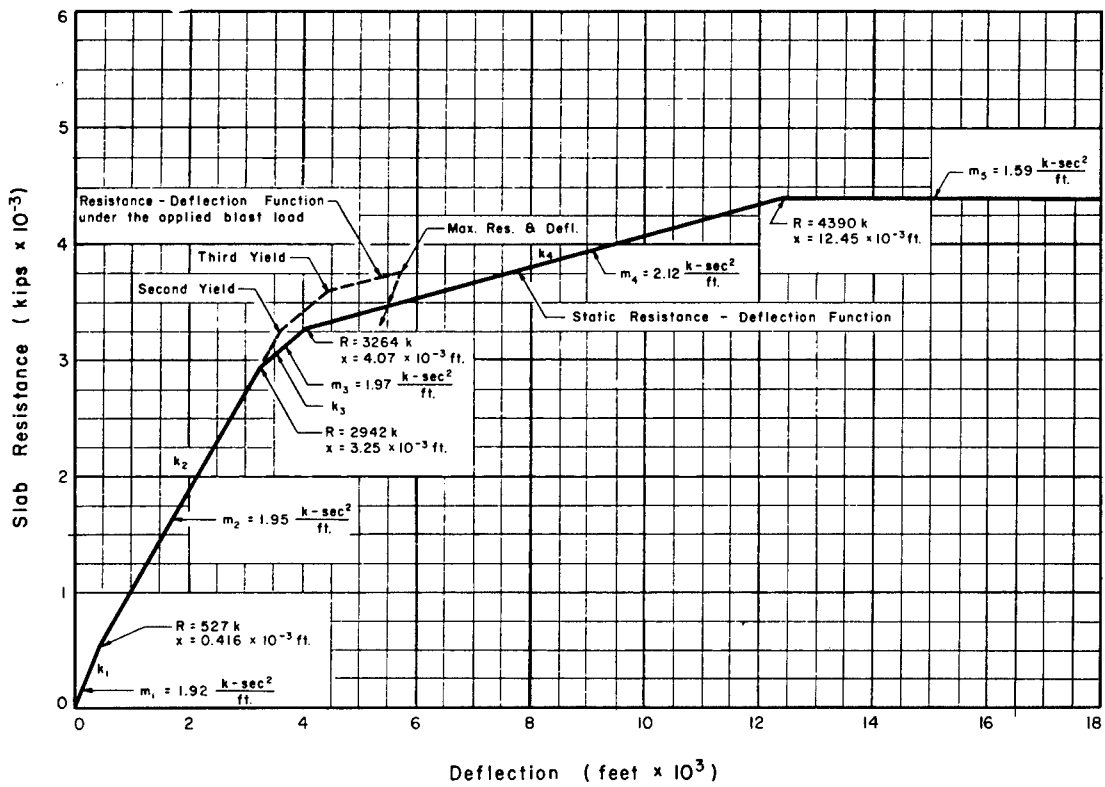Fig. C.1—Pressure-time curve.

Fig. C.2—Resistance-deflection curve.

251

Appendix D

FILM-BADGE MEASUREMENT TECHNIQUES *

D.1 GENERAL

On Operation Plumbbob film-badge dosimetry measurements were made primarily for the Civil Effects Test Group. In addition, some measurements were made for the Department of Defense, the Los Alamos Scientific Laboratory, Holmes & Narver, the Naval Radiological Defense Laboratory, and Edgerton, Germeshausen & Grier, Inc. Instrumentation was generally made to determine dose vs. distance (RD^2 vs. D) for a given event. Measurements were also made in shelters and in various other structures and test devices. Methods were essentially the same as those used on Operation Teapot (EG&G Report No. 1387). The controls required to ensure uniformity of measurements and the sensitometric problems encountered during the program are discussed in the following pages.

Four special types of film in two dental packets were used in making the measurements. The films used were Du Pont 502, 510, and 606, and Eastman SO-1112. An Eastman neutron-monitoring film was tried at the beginning of the operation, but use was discontinued because of extreme gamma darkening.

A 7-curie Co^{60} source was used to furnish irradiated controls for the interpretation of film badges used for each event. These badges were handled and processed with the field badges.

D.2 CALIBRATION

A Co^{60} gamma calibration system (shown in Fig. D.1) was arranged so that 10 badge assemblies were consecutively administered in three sets, logarithmically progressive exposures from 0.05 to 5×10^3 r. Table D.1 indicates the time of exposure, the dose rate, and the dose administered to the film. The readings listed in the table are accurate to 5 per cent.

Thirty badges were administered doses from 0.05 to 5×10^3 r; eighteen of the badge doses overlapped for standardization. Distances necessary to obtain the required doses with one exposure per series remained identical for each corresponding badge.

The source was placed in a cradle at one end of a calibration range table in such a manner that the center of the source beam passed through the center of the badges. The source was adjusted to the same position for each exposure so that, once the correct distances were established, they could be automatically reproduced each time.

Distances were determined with a 25-r Victoreen r-meter, which had recently been calibrated by National Bureau of Standards. Exposures were timed to obtain mid-scale readings for greatest accuracy. The badges were placed directly behind each other in a straight and level line away from the source; the calibrated positions were determined by use of identical dummy assemblies for attenuation. Total opening and closing time of the source was approximately 4 sec. This length of time could cause, at the most, a 2 per cent error on the 200-sec

---

*This information was extracted from Edgerton, Germeshausen & Grier, Inc., report No. 321 to the AEC.

exposures, and negligible error on all the others. It is believed an over-all accuracy of better than 5 per cent was maintained on administered doses.

Actual shot calibrations were made the morning of a shot on film badges that were assembled and handled with the field badges. All badges were developed together, with gray scales spaced at equal intervals throughout the reel. Ranges accurately covered by the dosimeter films were:

Du Pont 502	. 0.1 to 10 r
Du Pont 510	. 8 to 300 r
Du Pont 606	. 200 to 600 r
Eastman SO-1112	. 800 to 5×10^4 r

The Du Pont film packet is shown in Fig. D.2.

Owing to the accuracy limitations on administered doses, reading, and development, it was necessary to consider a total possible error of ±20 per cent. In addition, film irradiated in the field tends to darken beyond the density obtainable with gamma calibration alone. This is believed to be caused by some type of reciprocity failure, neutron effects (at closer range), thermal and pressure effects, or from secondaries. Finally, solar effects must be taken into consideration because film that has remained in the heat of the Nevada sun does not behave in the same way as fresh film.

D.3 FILM-BADGE HANDLING

Since each film badge consists of many parts, an assembly line was set up to handle exposed film efficiently. EG&G badge parts are: a lighttight package containing the film; a plastic box that serves as an electron diffuser; a special metal box made of a lamination of tin on the inside with lead on the outside, which functions as a filter to make the film energy-independent; a polyethylene bag to protect the badge against weather and contamination; and an identification tab (see Fig. D.2). The total assembly was then wrapped in aluminum foil for protection against thermal heat.

After recovery of the film badges from the field, the outside plastic cases containing the film and identification tab were then sorted and arranged numerically. The embossed film number and the number of films in each badge were listed on a loading order data sheet.

The next step was to arrange the film packets in numerical order in a special dispenser from which they were removed to be individually fastened together in the improved, more functional, edge-taping machine developed by EG&G for this purpose (Fig. D.3). After being taped on this machine, approximately 200 complete badges — or 800 pieces of film — could be assembled on a single reel and processed together. Although a single reel could contain more film, it was found this amount was the most convenient to handle.

When the processing operation had been completed, the density of each film was measured on a densitometer (Fig. D.4). Personnel working in pairs read the densities and simultaneously determined the equivalent roentgen exposures from the curves made from the calibration badges. The evaluated dosages were tabulated according to the proper film-badge number and transferred to the data sheets for analysis.

D.4 FILM PROCESSING

Because of the similarity between visible-light and gamma-radiation (short—wave length) sensitometry, precautions applicable to one must be applied to the other in the processing operation. In both cases the relation between exposure and developed density can be determined by means of a D — log E curve.

The shape of the curve is dependent upon the degree of development of the irradiated film in that, as development is increased, a given exposure will produce increasing values of density until the point is reached where density will be unaffected by a further increase in development. This point of complete development should theoretically be reached for optimum accuracy in sensitometric work. However, owing to the severe limitation which would be noticed in the

high-density range and to densitometer errors that may result from high-density readings, any advantages gained may be offset.

Although more control is required in the actual developing phase if development is not carried to completion, several advantages can be noticed from partial development of the film. A family of D − log E characteristic curves for different development times of a typical medium-speed emulsion is presented in Fig. D.5. The curve designated infinity represents development to completion. The curves of the incompletely developed films indicate that the range of exposures over·which the film is responsive is extended considerably, covering nearly two orders of magnitude beyond that exhibited by the completely developed film.

As can be seen from the figure, the maximum density that an incompletely developed film can attain is approximately 2.8. A further increase in exposure, rather than an increase in the density to the saturation point, produces a definite reduction of density, or a reversal in exposure response. This effect becomes more pronounced as development is decreased, until a point is reached where the reversal is minimized.

The curves for the incompletely developed emulsions indicate that two distinct slopes are present, and, as development is reduced, both slopes tend to become more nearly equal. The first slope of the curve is commonly referred to as the gamma of the D − log E curve.

Gamma initially increases very rapidly with an increase in development time; this rate subsequently becomes less, and finally levels off with no further change. This leveling point is known as gamma infinity, or complete development. The second slope region of the curve is less well defined because it is seldom a straightforward logarithmic response (Fig. D.6). Its average slope, however, exhibits considerably less change for different developing times than does the value of gamma.

D.5 PROBLEMS OF PROCESSING CONTROL

Fresh developer must enter the emulsion by diffusion. Once in the emulsion, the developer reacts with the exposed silver halides and forms complexes that must diffuse out of the emulsion before new developer can enter. Since the mild acid contained in the complexes retards development, violent action is often necessary to separate these acids from the surface. Once they have been removed, they diffuse throughout the developer and become neutralized or rendered inactive by components of the solution placed there to serve as such a buffer.

If a film being developed remains idle in the solution, the acid-retarding development will gradually be reduced by the buffer and development to completion can ultimately occur. However, when the film being processed is removed from the developer before complete development takes place, physical aid is necessary to remove the complexes from the emulsion surface. The method presently employed makes use of 10 double-squeegee wipers to provide agitation to the solution near the emulsion surface. This agitation is caused by the film moving past a series of 10 knife-like edges similar to soft-rubber windshield wipers. These blades are held in near contact with the emulsion surface and set up a turbulent flow pattern of developer as the film and a layer of developer move past them. This agitation system is designed so that there is little chance of damage to the film.

D.6 CONTROLLED PROCESSING OF RADIATION FILM BADGES

Figure D.6 is a plot of a comparison of two D − log E curves. The dashed line represents the response of several SO-1112 films subjected to a series of 400-μsec visible-light exposures; the solid line is the response curve of a series of calibrated Co^{60} exposures. Exposure values are given in arbitrary units. Although further experimental work must be performed before conclusive evidence can be drawn from the results of Fig. D.6, the similarity of the D − log E curve for the SO-1112 film indicates that white-light exposures may be used for process control of gamma-radiation exposures.

The development of SO-1112 emulsions was carried out to a high contrast in an effort to reduce the exposure-evaluation errors. With the contrast shown in Fig. D.6, the evaluation errors are ±3 per cent in the lower region of the curve and ±7 per cent in the upper slope region.

The resulting D – log E curves display a wide range in gamma-radiation exposure, especially in comparison to the accepted useful range produced as a result of development to completion.

D.7 PROCESSING PROCEDURE FOR PLUMBBOB FILM BADGES

Included with the cobalt calibration badges were several SO-1112 white-light standards. All badges were run through the taping machine and developed to a gamma of 1.3, as follows:
Emulsion type MF, No. 1112; MCS 5000; N.D. 1.3
Color: White
Developer: D-76, No. 4
Temperature: 70°F
Time: 2 ft 39 in., 10 double-squeegee wipers, used at $8\frac{1}{4}$ ft/min

The development gamma at the head of the series was 1.3 and at the tail was 1.29.

D.8 ANALYSIS

The reels of processed badges are mounted on rewinds and wound across the reading surface of an Ansco-Macbeth densitometer. Two central readings are made and recorded for each film. With the readings complete, the calibration films are first compared with previous runs, and then the shot films are compared with their calibration film. From the results of these comparisons, analysis charts and graphs can be drawn, and from these comprehensive summaries, the shot doses and the accuracy of the system can be determined.

TABLE D.1— FILM-BADGE CALIBRATION
(DOSE RATE: R/SEC)

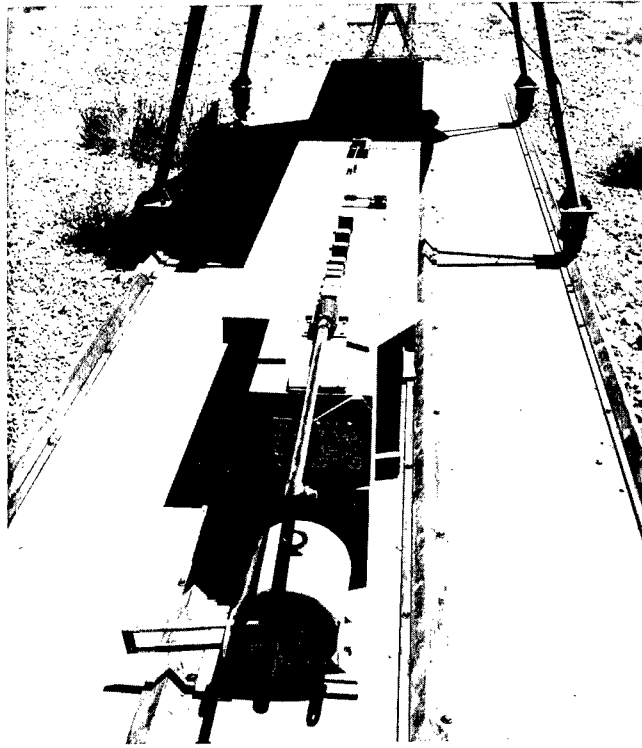| Administered dose, R	Time, sec		
	200	2×10^3	2×10^4
0.05	0.00025		
0.1	0.0005		
0.2	0.001		
0.5	0.0025	0.00025	
1	0.005	0.0005	
2	0.01	0.001	
5	0.025	0.0025	0.00025
10	0.05	0.005	0.0005
20	0.1	0.01	0.001
50	0.25	0.025	0.0025
100		0.05	0.005
200		0.1	0.01
500		0.25	0.025
10^3			0.05
2×10^3			0.1
5×10^3			0.25

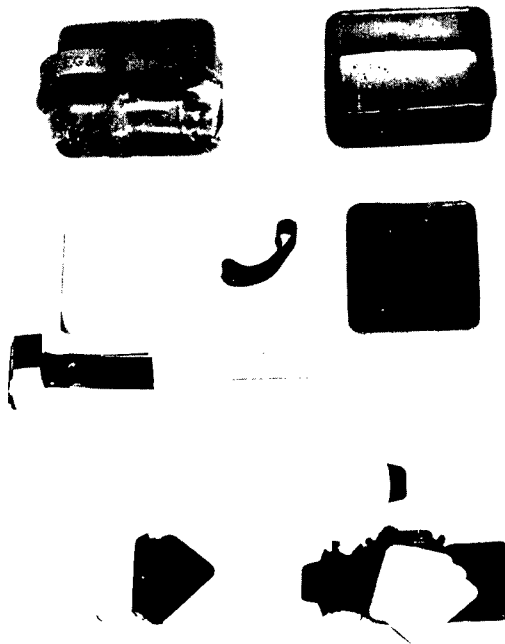Fig. D.1—Co^{60} gamma calibration system.

Fig. D.2—Du Pont film packet and EG&G film badge.

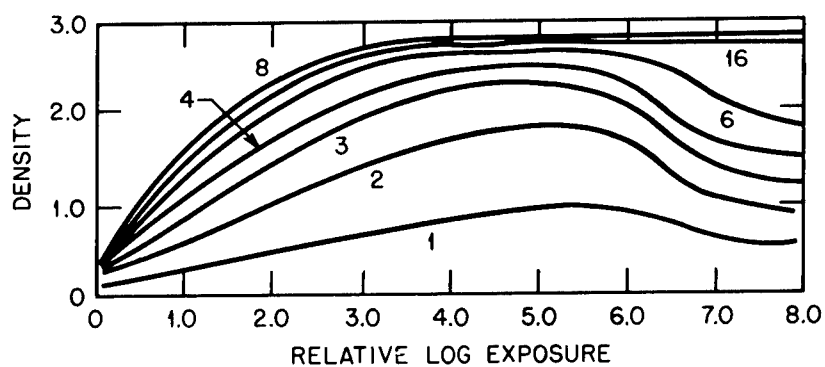Fig. D.3—EG&G taping machine.

Fig. D.4—Densitometer.

257

Fig. D.5—Effect of development time on the shape of the characteristic curve of a typical medium-speed film. (Mees, Theory of the Photographic Process, p. 261, The Macmillian Company, New York, 1952).
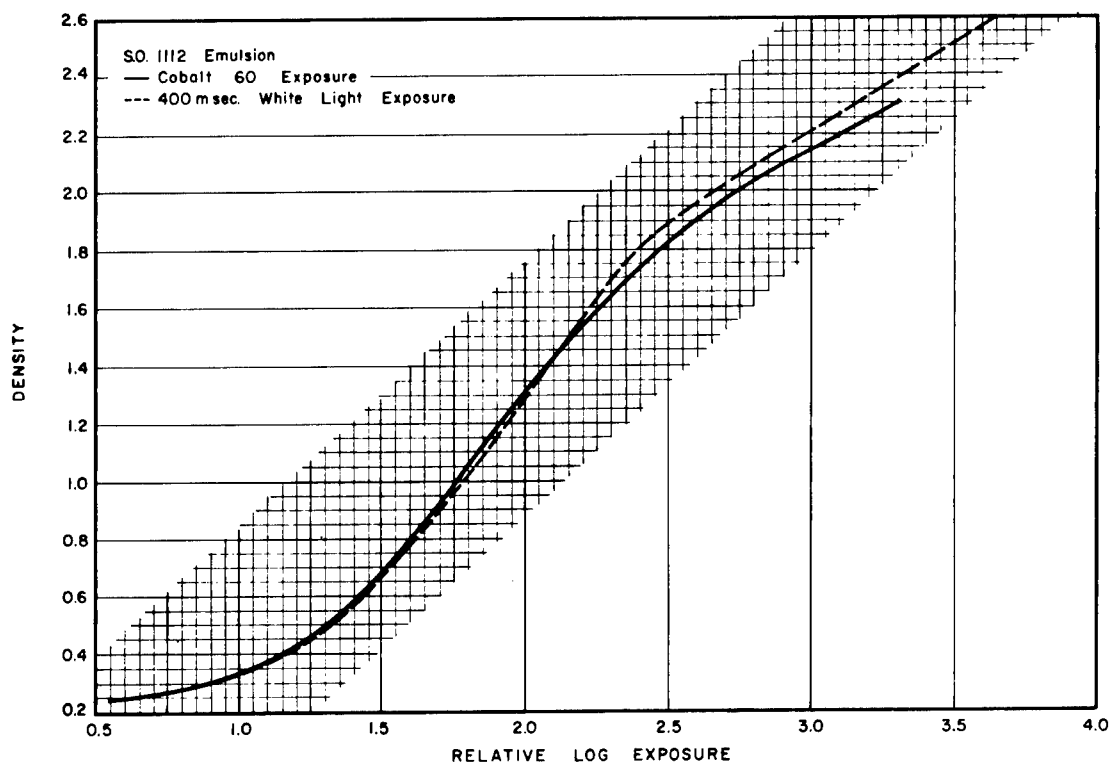

Fig. D.6—Comparison of white-light and gamma-radiation exposure densities.

LEGAL NOTICE